The CydDC transporter of *Escherichia coli*: investigating the impact of reductant export upon nitrosative stress, transcriptome/metabolome interplay, and host colonisation

PhD Thesis for the degree of PhD in Microbiology

Faculty of Sciences

School of Biosciences

University of Kent

Louise V. Holyoake

2016

Abstract

CydDC of *Escherichia coli* is an ABC transporter that exports cysteine and glutathione from the cytoplasm to the periplasm to maintain redox homeostasis; its loss elicits a pleiotropic phenotype and causes the periplasm to become 'over-oxidising'. In addition, the CydDC transporter is required for the assembly of cytochrome *bd*-I, a respiratory complex that provides tolerance to nitric oxide, a toxic radical produced by the host immune system in response to bacterial infection. The contribution of CydDC to nitric oxide tolerance and the pleiotropic phenotype of *cydDC* mutants implicates this exporter complex as a potential target for future therapies to combat *E. coli* infections. Indeed, given the rising incidence of multidrug-resistant bacterial infections, it is becoming increasingly important to develop novel strategies to combat infection. This thesis reports an investigation into the contribution of CydDC to NO tolerance, the relationship between CydDC expression and cytochrome *bd*-I assembly, adaptations resulting from loss of CydDC, and the requirement for CydDC for survival during infection.

To gain a better understanding of how CydDC expression influences cytochrome *bd*-I assembly, *cydDC* cells were grown in the presence of exogenous cysteine and/or reduced glutathione. This work demonstrates for the first time that addition of cysteine *and* glutathione (i.e. both CydDC substrates) is necessary for cytochrome *bd*-I assembly in a *cydDC* strain. *In vitro* growth curves utilising a nitric oxide donor show that CydDC-mediated reductant export contributes to the tolerance of nitric oxide (NO) both via permitting cytochrome *bd*-I assembly and through a mechanism independent of this respiratory complex. This work is consistent with a model whereby NO-reactive thiols (i.e. cysteine and glutathione) exported to the periplasm can diminish the levels of NO that can enter the cytoplasm.

The transcriptional response of *cydDC* mutants to exogenously added cysteine and glutathione was explored through microarray analysis in an attempt to gain a greater insight into the role of reduced thiol export to the periplasmic space. The addition of thiols affected genes involved in cell metabolism, respiration and led to the down-regulation of motility-related genes, providing insights into how the presence of CydDC substrates contribute to diverse cellular processes.

To investigate the contribution of CydDC to survival during infection, macrophage survival assays were performed along with an infection study using a mouse model of UTI (urinary tract infection). This work demonstrates that CydDC does not contribute to bacterial survival within NO-producing macrophage cells, and that loss

of CydDC has no significant effect on the ability to colonise the mouse lower urinary tract. We therefore conclude that while CydDC is important for cytochrome *bd*-I assembly and NO tolerance *in vitro*, it may not be a suitable drug target to combat pathogenic strains of *E. coli*.

Acknowledgements

During my PhD, I have been overwhelmed by the generosity of those who I have worked with, in giving their time, knowledge and support and I am truly grateful to so many people.

Foremost I would like to say a big thank you to my supervisor Mark Shepherd, it has been an honour to be his first Ph.D. student. I appreciate that he has always been willing to lend his time, ideas, and encouragement to make my PhD experience productive and stimulating. The enthusiasm he has for his research has been contagious and motivational for me, even during tough times.

I have really enjoyed my experience at the University of Kent and have found a community of people so willing to help and support one another. I am thankful to Ian Blomfield for his sagacious advice and for the many discussions that always left me with a lot to think about. Thank you to the members of the Shepherd, Blomfield and Robinson groups, affectionately known as the 'Shepblomson' group, which refers to Ami, Sara, Claudia, Charlie, Alex, Saranna, Bruno, Q and Aga, they have each been a source of friendship as well as good advice, encouragement and tea. I am indebted to Michelle for running my metabolite extraction samples through the NMR machine, for her subsequent help in the analysis of this data, as well as teaching me to crochet. I am thankful to Anna, my summer project student for performing yeast agglutination assays pictured in this thesis.

I appreciate the kindness of Robert Poole and his group, in allowing me to visit the University of Sheffield to use their equipment. I am particularly grateful to Lauren for her invaluable help in performing the microarray experiments discussed in this thesis, and to Matt for his advice and discussions concerning analysis of the microarray data.

The *in vivo* studies discussed in this thesis would not have been possible without the expertise and generosity of Mark Schembri and his group at the University of Queensland. I would particularly like to thank Kate for guiding me through the mouse infection studies as well as Maud and Asha for training me in the art of macrophage survival studies.

I am grateful to the University of Kent for funding my PhD, and to the Society of General Microbiology for funding my trip to the University of Queensland.

Lastly, I would like to thank my family for all their love and encouragement. For my parents and sister who have always supported me in my pursuits. I would like to thank James for his selflessness, patience, support and most importantly, his endless confidence in me. Thank you.

Presentations and Publications

Oral presentation:

15th- 18th March 2015: The European Federation of Biotechnology Conference, "Bacterial electron transfer processes and their regulation" Vimeiro Portugal.

Publications:

Holyoake, L. V., Poole, R. K. and Shepherd, M. (2015) The CydDC family of transporters and their roles in oxidase assembly and homeostasis. *Adv. Microb. Physiol.* **66**, 1-53.

*Sections of the introduction are reproduced from this review article.

Holyoake, L. V., Hunt, S., Sanguinetti, G., Cook, G. M., Poole, R. K. and Shepherd, M. (2016) CydDC-mediated reductant export in *Escherichia coli* controls the transcriptional wiring of energy metabolism and combats nitrosative stress. *Biochem. J.* **473**, 693-701

Abbreviations

1D-^{1}H NMR = 1-dimensional proton nuclear magnetic resonance

ABC transporter = ATP–binding cassette type transporter

B. abortus = *Brucella abortus*

BMM = Bone marrow-derived macrophage

Bp = Base pair

Ccm = Cytochrome *c* maturation

cDNA = (complementary) Deoxyribonucleic acid

CO = Carbon monoxide

cPTIO = 2-(4-carboxyphenyl)-4,4,5,5-tetramethylimidazoline-1-oxyl-3-oxide

CFU = Colony forming units

DEPC = Diethylpyrocarbonate

Dha = Dihydroxyacetone

dNTP = Deoxynucleoside triphosphate

DSS = 4,4-dimethyl-4-silapentane-1-sulfonic acid

DTT = Dithiothreitol

E. coli = *Escherichia coli*

Fim = Type 1 fimbriae

FRT = Flp recognition target

GSH = Reduced glutathione

GSSG = Glutathione disulphide

H_2O_2 = Hydrogen peroxide

IC_{50} = Half maximal inhibitory concentration

kDa = Kilodalton

k_{off} = Dissociation constant

LB = Luria Bertani medium

LMW = Low-molecular weight

MHz = Megahertz

MOI = Multiplicity of infection

MOPS = 3-(*N*-morpholino)-propanesulphonic acid

mRNA = (messenger) Ribonucleic acid

M. tuberculosis = *Mycobacterium tuberculosis*

nm = Nanometres

nM = Nanomolar

NO = Nitric oxide

NOC-12 = (1-hydrox-2-oxo-3-(N-ethyl-2-aminoethyl)-3-ethyl-1-triazene).

NOS = Nitric oxide synthase

OD = Optical density

$ONOO^-$ = Peroxynitrite

PBS = Phosphate buffered saline

PCR = Polymerase chain reaction

PMF = Proton motive force

Ppm = Parts per million

RNS = Reactive nitrogen species

RMPI = Roswell Park Memorial Institute

S. flexneri = *Shigella flexneri*

SDS- PAGE = Sodium dodecyl sulphate - polyacrylamide gel electrophoresis

SNP = Single nucleotide polymorphism

TCA = Tricarboxylic acid

UTI = Urinary tract infection

UPEC = Uropathogenic *E. coli*

X g = G force

Table of Contents

List of Figures

List of Tables

Supplementary Data

Chapter 1

Introduction

1.1 Maintaining redox homeostasis in the *E. coli* periplasm

The periplasm of *E. coli* is an oxidising environment that is subject to a fine balancing of the redox systems. Disulphide bonds are created in proteins between two cysteine residues by the oxidation of their thiol groups, resulting in the loss of two protons and two electrons (Figure 1-1). Disulphide bonds have a large impact upon the structure of proteins and are necessary for stability, enzymatic activity and resistance to proteolytic digestion. In *E. coli*, the introduction of disulphide bonds into extracytoplasmic proteins occurs in the periplasm where the oxidoreductase system DsbAB catalyses disulphide folding. In addition, the DsbCD isomerase system is required to rearrange non-native disulphide bonds as reviewed in (Raina and Missiakas 1997; Rietsch and Beckwith 1998).

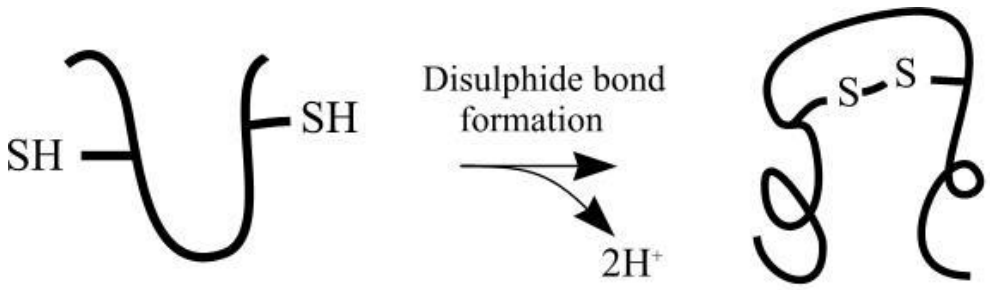

Figure 1-1. Formation of disulphide bonds

Within proteins disulphide bonds are created between two cysteine residues by the oxidation of their thiol groups, resulting in the loss of two protons and two electrons.

The 21 kDa periplasmic protein DsbA is a member of the thioredoxin superfamily, containing a classic CXXC motif (Collet and Bardwell 2002). In the disulphide bond oxidative folding pathway, oxidised DsbA catalyses the formation of disulphide bonds between cysteine residues of proteins located within the periplasm by accepting the proton and electrons from the protein thiol groups. DsbA is then re-oxidised by DsbB

(Bardwell *et al.* 1993; Missiakas *et al.* 1993), a membrane protein, anchored within the inner-membrane by four transmembrane helices. Once reduced, DsbB donates electrons to oxidised ubiquinone (Figure 1-3) which in turn transfers the electrons to respiratory complexes such as the *bd*-type oxidases (Bader *et al.* 1999). Mutations of *dsbA* or *dsbB* cause a pleiotropic phenotype, including sensitivity to some metal ions such as cadmium and mercury ions, alongside hypersensitivity to the reductant dithiothreitol (DTT), and benzylpenicillin (Missiakas, Georgopoulos and Raina 1993; Stafford, Humphreys and Lund 1999). The oxidising environment of the *E. coli* periplasm created by DsbAB promotes the formation of non-native disulphide bonds that result in the loss of protein activity. The disulphide bond isomerisation pathway catalysed by DsbCD is responsible for the reshuffling of incorrect disulphide bonds. DsbC also contains a CXXC motif, and is kept in a reduced state within the oxidising environment of the periplasm by the inner membrane protein DsbD (DipZ) (Collet and Bardwell 2002; Crooke and Cole 1995). DsbD in turn is reduced by the thioredoxin (TrxA)/thioredoxin reductase (TrxB) system in the periplasm (Figure 1-3).

Reduced low-molecular weight (LMW) thiols exported to the periplasm from the cytoplasm are believed to accompany the action of DsbAB and DsbCD, by providing reducing power. The inner membrane complex CydDC of *E. coli* has been shown to export reduced glutathione and cysteine to the periplasm. Messens *et al., (*2007) demonstrated that to maintain the redox potential of the periplasm at – 165mV, a combination of both the Dsb proteins and glutathione is required; deletion of *cydD* (or *gshA* required glutathione biosynthesis) increases the redox potential to -125mV. Thus glutathione does play a role in redox homeostasis of the periplasm, and is consequently predicted to play a role in disulphide folding as depicted in Figure 1-3. The combination of Dsb protein and reduced thiols in the periplasm, however, raises the question of how proteins and reduced thiols with opposing redox functions do not result in a futile cycle, i.e. what stops reduced glutathione reducing DsbA and vice versa? (Inaba 2008; Bader *et al.* 2001) suggest that cross talk between the oxidative DsbAB pathway and the DsbCD isomerisation pathway in the *E. coli* periplasm is prevented in a structural manner; DsbC has been shown to form a V-shaped homodimer [McCarthy, and Haebel, 2000; Heras et al., 2004] that creates a hydrophobic cavity that prevents interaction with DsbB and separates the oxidative and isomerisation pathways to prevent futile cycling.

Although DsbA can interact with GSH and cysteine, DsbA is believed to interact with proteins preferentially over small thiols such as GSH and cysteine (Frech *et al.*

1996); DsbA interacts with unfolded protein by both a covalent disulphide bond and non-covalent interactions within a putative polypeptide binding site of DsbA (Darby and Creighton 1995; Frech *et al.* 1996). This preferential oxidation of proteins over small thiol compounds would prevent futile cycling between reduced thiols exported to the periplasm via CydDC and DsbA.

1.1.1. *E. coli* reductant exporters

The *cydDC* operon of *E. coli* encodes an ABC-type transporter comprised of nonidentical subunits, which are located within the inner membrane (Figure 1-2). The CydDC complex was first identified because it is essential for the assembly of the cytochrome *bd*-I quinol oxidase (Georgiou, Hong and Gennis 1987; Poole *et al.* 1989). Assembly of *c*-type cytochromes and cytochrome b_{562} have also been shown to require CydDC (Poole *et al.* 1994; Goldman *et al.* 1996).

DTNB (5,5'-dithiobis-(2-nitrobenzoic acid) or Ellman's reagent) is a colourless compound that reacts rapidly with thiol groups to produce thionitrobenzoic acid that is yellow in solution and can be measured spectrophotometrically at 412 nm using an extinction coefficient of 14.15 M^{-1} cm^{-1}, comparing readings with a standard curve of a thiol containing compound such as cysteine allows the redox state to be measured (Riddles, Blakeley and Zerner. 1979). Treating wild type and *cydC* periplasmic fractions with DTNB showed that the normally oxidising environment of the periplasm is 'over-oxidising' in the absence of *cydC*, which first indicated that CydDC exports a reduced substrate to the periplasm (Goldman, Gabbert and Kranz 1996b). This later prompted the use of everted membrane vesicles to demonstrate that CydDC exports the thiol-containing amino acid cysteine (Pittman *et al.* 2002). French-pressure cell treatment was used to produce inside-out vesicles using either *E. coli orf299* mutants or isogenic *orf299, cydD* double mutants. An *orf299* deletion background was used because the product of this gene was thought to have a role in cysteine export (Daßler *et al.* 2000). It was shown that in *orf299*-derived vesicles, radio-labelled cysteine ([^{35}S] cysteine) is transported inwards in a manner dependent upon ATP (Pittman *et al.* 2002). In contrast, deletion of *cydD* eliminated cysteine transport even after ATP addition. Inclusion of sodium orthovanadate, an inhibitor of ABC-type transport systems, eradicated cysteine transport, with an uptake rate comparable for that seen for *cydD* mutants. It was therefore concluded that CydDC is responsible for the uptake of cysteine in everted

membrane vesicles, corresponding to active export of cysteine to the periplasm within intact cells.

Despite having an essential role in protein function, L-cysteine is toxic to cells, even at low concentrations in both eukaryotic and prokaryotic cells (Sørensen and Pedersen 1991). This may explain why *E. coli* strains lacking CydDC (and associated export of cysteine) are hypersensitive to cysteine, presumably accumulating higher cytoplasmic cysteine levels than wild type strains. Conversely, over-expressing CydDC increases resistance to cytotoxic levels of cysteine (Pittman *et al.* 2002), which is consistent with the hypothesis that cysteine is exported by CydDC. It is important to note, however, CydDC is not the only L-cysteine exporter found on the inner membrane of *E. coli*; EamA (YdeD), EamB (YfiK), and Bcr have also been shown to export L-cysteine (Daßler *et al.* 2000; Franke *et al.* 2003; Yamada *et al.* 2006). At the outer membrane, the TolC porin has also been shown to be important for tolerance to L-cysteine, and consequently is believed to play a role in release of L-cysteine from the periplasm into the medium either through passive or facilitated diffusion (Wiriyathanawudhiwong *et al.* 2009).

Ohtsu *et al.* 2010, suggest that cysteine in the periplasm participates in combating oxidative stress; the group showed that the oxidised form of L-cysteine, L-cystine is imported back into the cytoplasm of *E. coli* via FliY, a periplasmic L-cystine binding protein. They further showed that shutting of L-cysteine/L-cystine between the cytoplasm and periplasm is significantly induced at the transcriptional level in response to hydrogen peroxide but not by exogenous L-cysteine.

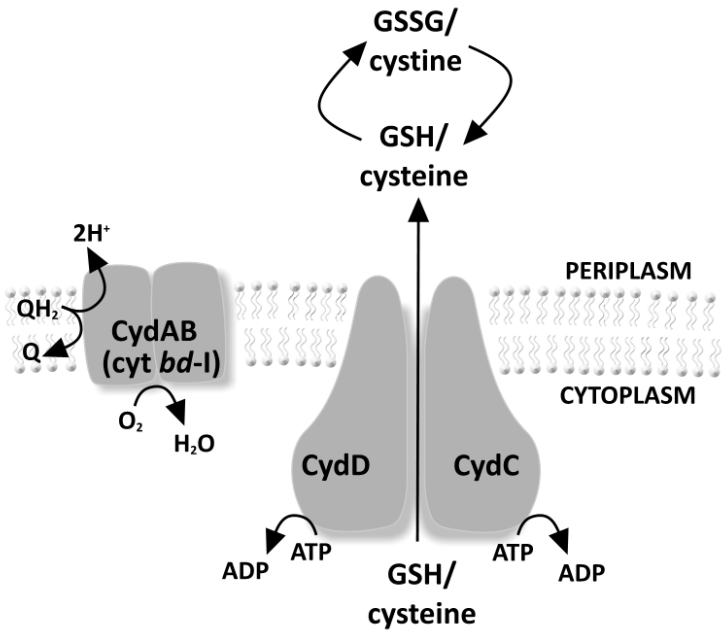

Figure 1-2. CydDC of *E. coli*

The heterodimeric complex CydDC exports the low-molecular weight thiols; reduced glutathione and cysteine from the cytoplasm to the periplasm. This process is dependent upon ATP hydrolysis. Loss of CydDC prevents the assembly of cytochrome *bd*-I (CydAB).

The tripeptide glutathione (L-γ-glutamylcysteinylglycine, GSH) is a major thiol-disulphide redox buffer. Modulation of the ratio of reduced to oxidised glutathione (glutathione disulphide, GSSG) influences different redox equilibria in different subcellular compartments such as the periplasm. By considering the similar properties of GSH and cysteine along with the characteristic broad specificity of ABC transporters, it was hypothesised that GSH is also a substrate for CydDC (Hosie and Poole 2001; Pittman, Robinson and Poole 2005). In everted membrane vesicles derived from wild type *E. coli*, no uptake of radio-labelled glutathione (GSH [^{35}S]) was seen before ATP addition. However, with a maximal rate of 3.8 nmol min^{-1}, GSH uptake was rapid after ATP addition. No GSH uptake was detected for the vesicles derived from the isogenic *cydD* mutant strain. Addition of sodium orthovanadate, an inhibitor of ABC-type transport systems, was shown to abolish GSH transport completely, proving that transport is dependent upon an ABC type transporter. GSH was therefore concluded to also be an allocrite of CydDC, and that transport of this redox active tripeptide is ATP-dependent. No uptake of oxidised GSH (GSSG) in wild type cells could be demonstrated in the presence or absence of ATP. The rate of reduced glutathione (GSH) uptake was positively correlated with the concentration of GSH added. It is important to

note that the uptake rate of GSH was approximately five times higher than that of L-cysteine for all equivalent concentrations of substrates added. While the evidence for CydDC-mediated GSH export is very strong, a later study reports that reduced glutathione is exported to the periplasm even in the absence of CydDC (Eser *et al.* 2009), suggesting that additional mechanisms exist for the export of GSH.

Once in the periplasm, GSH is expected to traverse the outer membrane via porin proteins, therefore GSH is expected to reach an equilibrium between the periplasmic space and growth media (Eser *et al.* 2009). *Escherichia coli* has been shown to excrete GSH into the growth medium during exponential and early stationary phase (Owens and Hartman 1986), and GSH has more recently been shown to be constantly cycled between cells and the external growth media in exponential phase (Smirnova, Muzyka and Oktyabrsky 2012). When cells advance further into stationary phase, glutathione in the periplasm is hydrolysed at the γ-glutamyl linkage by the periplasmic glutamyltranspeptide enzyme (GGT) (Suzuki, Hashimoto and Kumagai 1993; Suzuki, Kumagai and Tochikura 1987). The resultant cysteinylglycine and glutamic acid can then be imported into the cytoplasm where cysteinylglycine is subsequently cleaved into cysteine and glycine by aminopeptidases A, B, and N as well as dipeptidase D (Suzuki *et al.* 2001). Whole GSH is also imported from the periplasm via an ABC-type transporter, GsiABCD (YliABCD). It has been shown that this transporter and GGT enable *E. coli* to use GSH as a source of sulphur, cysteine and glycine (Suzuki *et al.* 2005; Suzuki, Hashimoto and Kumagai 1993). Oxidised glutathione has also been shown to be utilised as a source of glycine and cysteine via GGT (Suzuki, Hashimoto and Kumagai 1993).

1.1.2 Phenotypic characterisation of CydDC

Loss of CydDC results in a pleiotropic phenotype which includes the loss of periplasmic *c*- and *b*-type cytochromes (Goldman, Gabbert and Kranz 1996b; Poole, Gibson and Wu 1994); an increased sensitivity to high temperature, hydrogen peroxide (H_2O_2), azide, and Zn^{2+} ions (Delaney, Ang and Georgopoulos 1992; Goldman, Gabbert and Kranz 1996b; Poole *et al.* 1989); hypersensitivity to both benzylpenicillin (Pittman *et al.* 2005) and DTT (Goldman *et al.* 1996) and the inability to exit stationary phase at 37 °C under aerobic conditions (Siegele, Imlay and Imlay 1996). Exogenous addition of the known allocrites of CydDC has been shown to restore the survival and temperature-sensitive phenotypes of a *cydC* mutant (Goldman, Gabbert and Kranz 1996a), and it has been shown that exogenous cysteine can also re-establish cell motility, resistance to

benzylpenicillin and DTT and can partially restore the assembly of cytochrome *c* (Pittman *et al.* 2002). These observations highlight the multiple cellular roles for reductant export by CydDC. Interestingly, restoration of cytochrome *bd*-I assembly has not previously been observed in a *cydDC* mutant by the addition of either cysteine or GSH, and thus, the mechanism via which CydDC contributes to cytochrome *bd*-I assembly remains unclear.

Since both GSH and cysteine are low-molecular weight thiols that can participate in disulphide exchange, following their identification as CydDC substrates it was deemed likely that this ABC transporter would have an impact upon disulphide bond formation in the *E. coli* periplasm. It is striking that some phenotypes of the *cydD* mutant, including hypersensitivity to benzylpenicillin (Pittman *et al.* 2005) and DTT (Goldman, Gabbert and Kranz 1996b), are shared not only by mutants defective in the *dsbD* reducing pathway (Missiakas *et al.* 1995) but also by *dsbA* and *dsbB* mutants (Fabianek, Hennecke and Thony-meyer 2000). The similarity of phenotypes presumably relates both to the requirement of CydDC for cytochrome *bd*-I assembly which provides an electron sink for DsbB (Korshunov and Imlay 2010), as well as a more direct role for exported GSH and cysteine in disulphide reduction (Figure 1-3).

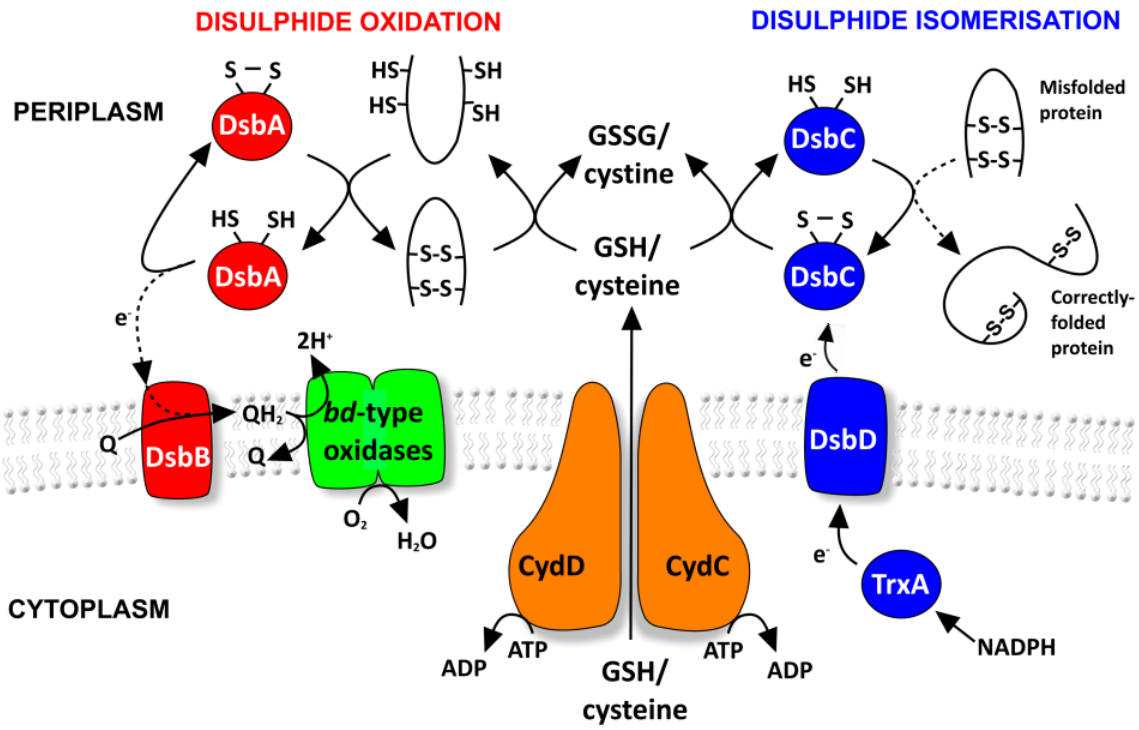

Figure 1-3. Disulphide folding within the *E. coli* periplasm

The oxidative folding pathway (DsbAB) and disulphide bond isomerisation pathway (DsbCD) work to ensure that proteins in the periplasm are correctly folded. Reduced glutathione (GSH) and cysteine exported to the periplasm via the ABC transporter, CydDC, influence the redox balance of the periplasm and are thus thought to impact upon disulphide folding. The *bd*-type oxidases that require CydDC for assembly act as an electron sink for DsbAB-mediated disulphide folding. Adapted from Holyoake *et al*. 2015.

1.1.3. Periplasmic machinery is perturbed by redox imbalance

The importance of periplasmic redox balance is highlighted by the pleiotropic phenotype observed for cells lacking CydDC, showing that a range of problems arise in cells that lack export of reduced low-molecular weight thiols to the periplasm. The correct folding required for structure and function of many proteins exported across the inner membrane rely upon the correct formation of disulphide bonds, and the absence of these bonds can result in protein degradation. Disruption of the periplasmic redox environment can therefore affect the functionality of a range of extracytoplasmic proteins including but not limited to; subunits of flagella needed for cell motility, *c*-type cytochromes involved in electron transfer, fimbrial subunits needed for cell adhesion, and secretion systems and other virulence factors required by pathogenic strains.

Motility in bacteria relies mostly upon flagella; supramolecular structures that extend from the inside of the cytoplasm to outside of the cell. The importance of redox homeostasis in motility is emphasised by the finding that deletion of *dsbA* or *dsbB* leaves many bacteria from different genera non-motile, due to the absence of functional flagella (Dailey and Berg 1993; Hayashi *et al.* 2000; Turcot *et al.* 2001; Agudo *et al.* 2004; Burall *et al.* 2004; Bringer *et al.* 2007; Coulthurst *et al.* 2008). It has been shown in *E. coli* that DsbA introduces an intramolecular disulphide bond within FlgI , a component of the P-ring protein of the flagella motor found in the periplasm (Figure 1-4) (Dailey and Berg 1993). In the absence of DsbA, FlgI is not folded correctly which is thought to prevent the incorporation of FliC, that makes up the filament, a major component of flagella. Mutation of *dsbA* has also been shown to abolish twitching motility in the pathogen *P. aeruginosa* (Ha, Wang and Jin 2003), a process that is important for the formation of biofilms in the cystic fibrosis lung.

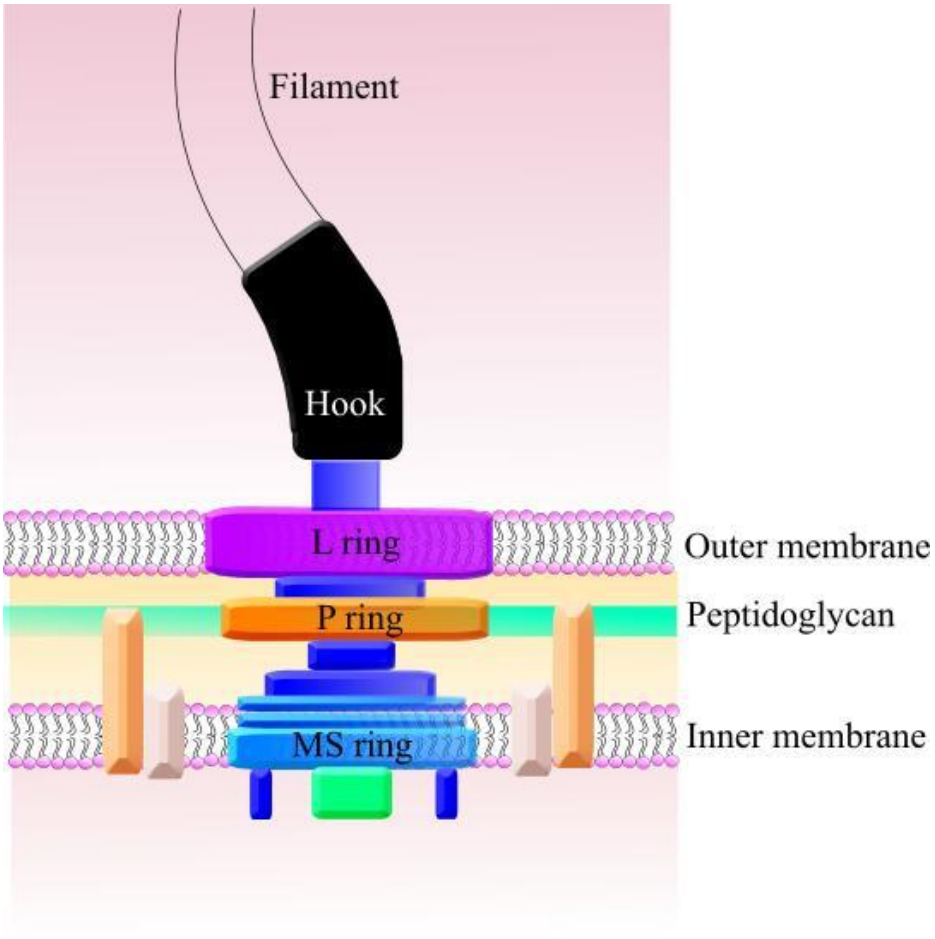

Figure 1-4. The structure of a flagellum

Schematic of flagella structure and its juxtaposition to the inner and outer cell membranes. Flagella are supramolecular structures that extend from within the cytoplasm to the outside of the cell. The motor includes the P-ring encoded by *flgI*. In the absence of DsbA, FlgI is not folded correctly which is thought to prevent the incorporation of FliC, that makes up the filament. (Adapted from Pallen and Matzke 2006)

In the *E. coli* periplasm, the cytochrome *c* maturation (Ccm) pathway catalyses the formation of *c*-type cytochromes. Central to this process is the ligation of haem to apocytochrome *c* by a covalent linkage between cysteine residues and the haem cofactor (Thöny-meyer and Kunzler 1997). Two thioether bonds link the thiol groups of two cysteine residues to the vinyl groups of the haem cofactor. The cysteine residues are located in a conserved CXXCH cytochrome *c* haem binding motif, with the histidine residue providing the axial ligand for coordination of the central haem iron.

As the maturation of *c*-type cytochromes occurs in the oxidising environment of the periplasm, redox control is important, as suggested by the requirement of the

disulphide bond (Dsb) machinery and thiol export by CydDC (Pittman *et al.* 2002; Poole, Gibson and Wu 1994). *In vitro* studies show that the ligation of haem to produce *c*-type cytochromes requires reducing power both to maintain the haem in the ferrous state, and also to avoid incorrect disulphide bonds forming with either of the cysteine residues within the CXXCH motif (Nicholson and Neupert 1989; Barker *et al.* 1995). Indeed, a disulphide bond between the two cysteines within the binding motif has been observed and shown to prevent haem ligation (Daltrop *et al.* 2002).

Cytochrome *c* synthesis is unique in that the polypeptide folds around the haem only after ligation (unlike other cytochromes where protein folding occurs before haem binding). The apocytochrome is delivered to the periplasm by the Sec system (Thöny-meyer and Kunzler 1997) in an unfolded state that is a more susceptible to DsbA-catalysed disulphide bond formation. The Ccm system therefore involves apocytochrome *c* thiol-reduction by a highly specific thioredoxin-like protein, CcmG (DsbE), which is limited to use in cytochrome *c* maturation (Fabianek *et al.* 1997; Monika *et al.* 1997). CcmG is in turn re-reduced by DsbD (Katzen and Beckwith 2000).

A wide range of bacterial virulence factors are both extracytoplasmic and disulphide-bonded, including proteins anchored to the cell surface needed for adhesion or cell motility, secreted proteins such as toxins and secretion systems. Systems that are paralogous to the Dsb proteins of *E. coli* exist in pathogenic strains of *E. coli* and in other bacterial species. The Dsb proteins and their homologs have been shown to be important in the correct folding of many virulence factors from a large variety of pathogens as discussed in depth in the following two review papers; (Łasica and Jagusztyn-Krynicka 2007; Heras *et al.* 2009).

During infection, the adhesion of bacterial pathogens to host cells is primarily mediated by fimbriae or pili, hair-like structures found on the cell surface. Several types of fimbriae have been described, mainly from Gram-negative bacteria (Fronzes, Remaut and Waksman 2008). Pathogen adherence is particularly important for strains of uropathogenic *E. coli* (UPEC) that are exposed to the hydrodynamic force of urine flow that can prevent bacterial colonisation. Early establishment of UPEC in the human urinary tract has been shown to require P fimbriae (Wullt *et al.* 2000), which are assembled via the chaperone-usher pathway. When P fimbrial subunits emerge through the inner membrane in a Sec-dependent manner, they are bound by PapD, a periplasmic chaperone that targets them to the outer membrane usher PapC. Which in turn directs fimbrial assembly and secretion to the bacterial cell surface (Thanassi and Hultgren 2000). DsbA permits the formation of an intramolecular disulphide bond within PapD,

folding the chaperone into its native confirmation and allowing binding to the P fimbrial subunits (Jacob-Dubuisson *et al.* 1994). The P fimbrial adhesin PapG, which recognises carbohydrate moieties on the host cell surface, also requires DsbA for the formation of an integral disulphide bond (Lund *et al.* 1987). In addition to the archetypal DsbABCD system, the pyelonephritis-causing CFT073 UPEC strain encodes an extended armoury of Dsb proteins (Sinha, Langford and Kroll 2004), with two paralogous disulphide bond systems; the DsbAB system, similar to that of *E. coli* K-12 and the DsbLI system (Grimshaw *et al.* 2008). A *dsbAB* deletion in CFT073, results in a lack of assembled P fimbriae and a severe attenuation of *E. coli* CFT073 in a mouse UTI model. Attenuation is likely to be a result of a combination of factors, for example, the deletion of *dsbAB* would not only affect P fimbriae formation but would also be detrimental to flagellum-mediated motility. DsbA is thought to play a key role in host adherence in a range of other Gram-negative pathogens including *Proteus mirabilis* (Burall *et al.* 2004), *Salmonella enterica* subsp. *enterica* serovar Typhimurium (Bouwman *et al.* 2003), enteropathogenic *E. coli* (EPEC) (Zhang, H. Z. & Donnenberg 1996) and *Vibrio cholerae* (Peek and Taylor 1992).

Toxins allow bacterial pathogens to promote their own growth by manipulating the host. Periplasmic redox homeostasis is required to ensure that bacterial toxins and the systems used to secret them are properly folded. Correct formation of the AB_5 toxins of *V. cholerae* and *E. coli* have been shown to require DsbA for disulphide bond formation and functionality (Yu, Webb and Hirst 1992; Okamoto *et al.* 1998).

Balance in the redox environment of the periplasm is also important for secretion systems. Ipa is an extracellular invasin of *S. flexneri*, that aids both bacterial uptake into host cells (Ménard, Sansonetti and Parsot 1993) and the subsequent spread to new host cells (Yu *et al.* 2000). In the absence of DsbA, Ipa cannot be secreted, because the outer membrane protein Spa32, involved in Ipa secretion is not folded correctly, and so Ipa proteins are confined to the periplasm (Watarai *et al.* 1995).

In summary, loss of DsbA and the resulting disruption to the redox homeostasis of the periplasm affects the folding and function of proteins involved in a range of functions including motility, adhesion and secretion. Periplasmic redox balance is therefore particularly important for pathogenic bacteria that rely upon multiple extracellular proteins for colonisation and survival within the host environment.

1.2 Transcriptional regulation of the *cydDC* operon

The CydDC complex is a heterodimer and was the first bacterial example of an ABC transporter that is comprised of non-identical subunits; the CydD and CydC protein sequences still however, have a 50% similarity and 27% identity and have similar hydrophobicity plots (Poole *et al.* 1993). Genes encoding ABC transporters are frequently found adjacent to genes encoding the transported substrate (Salmond and Reeves 1993). This however is more often the case for ABC transporters with an import function; probably for the reason that it is prudent for expression of importers to be co-ordinated with expression of enzymes required for catabolism of an incoming substrate, ensuring catabolism enzymes are only present when the relevant substrate is present. Immediately upstream of the *cydDC* operon is *trxB* gene, encoding thioredoxin reductase, an enzyme that supplies reducing power for the modulation of thiol redox state in the periplasm, which provided clues to the role in reductant export performed by CydDC. Despite the finding that *trxB* gene is not transcriptionally linked to *cydDC* (Cook, Membrillo-hernández and Poole 1997), looking at close relations of *E. coli* also found in the gammaproteobacter class reveals that *trxB* is consistenly found upstream of *cydDC*, this includes *Salmonella spp*., *Yersinia pestis*, *Vibrio cholerae*, *Shigella flexneri* and *haemophilus influenze*. This conservation is in agreement with the analysis perfomed by Cruz-Ramos *et al.* 2004 and indicates that it unlikely the close proximity of *trxB* to the *cydDC* operon is just due to chance. What advantage this proximity brings to gram-negative bacteria is unclear, however, this conservation of gene organisation disappears in Gram-positive organisms (Cruz-Ramos *et al.* 2004a).

To elucidate how expression of *cydDC* is regulated and to define a role for this ABC-type transporter, a *cydD-lacZ* transcriptional fusion was used to study the expression of *cydD* (Cook, Membrillo-hernández and Poole 1997). Initially, primer extension of a *cydD* messenger RNA (mRNA) transcript revealed a single transcriptional start site for *cydDC* 68 base pairs (bp) upstream of the translational start site. Northern blot analysis then confirmed that *cydDC* is transcribed as a polycistronic message independently of upstream gene *trxB.*

The expression levels of *cydD* in aerobically grown cells vary depending upon the growth phase. For example, *cydD-lacZ* expression during exponential phase was approximately 2.5 times higher than cells in stationary phase (Cook, Membrillo-hernández and Poole 1997). Cells grown anaerobically, however, displayed 5-fold lower *cydD-lacZ* activity compared to aerobically-grown cells, and this expression level was

unaffected by changes in growth phase. Antagonistic regulatory effects on *cydAB*, of ArcA (an activator) and FNR (a repressor) were subsequently demonstrated (Tseng *et al.* 1996), but neither mutation of *arcA* nor *fnr* had any significant effect on *cydD-lacZ* expression, consistent with the theory that *cydDC* and *cydAB* are independently regulated. Despite this, the observed changes in *cydD* expression between aerobically and anaerobically grown cells suggested that *cydD* is also regulated by oxygen tension. To investigate this, *cydD* transcription was measured at log phase under various oxygen tensions (Cook, Membrillo-hernández and Poole 1997). The level of *cydD-lacZ* increased as the efficiency of oxygen transfer rate increased in exponentially growing cultures, thus, demonstrating that *cydD* transcription is regulated by oxygen tension. Furthermore, mutations in *cydAB* did not affect expression of *cydD-lacZ*, and vice versa, expression of *cydA-lacZ* was unaffected by mutations in either *cydD* or *cydC*, indicating the regulation of the two operons is not coordinated, and that the structural cytochrome *bd*-I polypeptides are not required for *cydD* expression.

Periplasmic *c*-type cytochromes are only expressed in *E. coli* under anaerobic conditions in the presence of exogenous electron acceptors. Mirroring this regulation, expression of *cydD-lacZ* is elevated under anaerobic growth in the presence of the electron acceptors nitrate, nitrite or fumarate, when compared to anaerobically grown cells without alternative electron acceptors (Cook, Membrillo-hernández and Poole 1997). As *cydD* strains fail to synthesise periplasmic *c*-type cytochromes (Poole, Gibson and Wu 1994), this suggested an important role for *cydD* during anaerobic growth on nitrite and nitrate. Nitrate/nitrite-responsive gene expression in *E. coli* is mediated by a two-component system involving the DNA binding response regulators NarL and NarP. Mutations in *narL* alone or together with mutations in *narP* significantly reduced *cydD-lacZ* expression in the presence of nitrite or nitrate (Cook, Membrillo-hernández and Poole 1997). Expression of *cydD-lacZ*, however, was not as sensitive to *narP* mutations alone. Analysis of the promoter sequence for *cydD* led to the discovery of putative NarL binding sites that closely resemble the binding consensus sequence for NarL (Figure 1-5). Together, these data support an important role for CydDC in adaptive growth of *E. coli* because *cydDC* mutants lack both cytochrome *bd*-I that scavenges oxygen in microaerobic environments and periplasmic cytochrome *c* that is required for anaerobic growth on nitrite and nitrate.

Figure 1-5. The *cydDC* locus of *E. coli*

The CydDC ABC transporter is encoded by the *cydDC* operon, and *trxB* encodes thioredoxin. Putative NarL binding sites within the upstream *trx* gene control the nitrite/nitrate responsive expression of *cydDC*.

1.3 Structure and membrane topology of the CydDC complex

ATP-binding cassette proteins (ABC proteins) are well represented in both prokaryotes and eukaryotes. In *E. coli* the genes encoding these proteins are estimated to constitute 5% of the genome and are the largest paralogous family of proteins which can be further categorised into 10 subfamilies (Linton and Higgins 1998). Phylogenetic analysis sorted the CydD and CydC proteins into subfamily 6, alongside MsbA, a homodimeric lipid flippase involved in membrane biogenesis (Zhou *et al.* 1998). Regardless of function, all ABC transporters are composed of two transmembrane domains (TMDs) and two ATP binding domains, the members of subfamily 6 share the same organisation of these domains, with each transmembrane domain (TMD) being fused to one ATP binding domain. CydDC was first hypothesised to be an ABC protein when hydrophobicity analysis indicated that the N- terminal half of the CydD and CydC proteins consists of stretches of hydrophobic amino acids corresponding to 6 membrane spanning helices (Poole *et al.* 1993). Whereas the C-terminal half of the polypeptides were shown to be hydrophilic, containing ATP-binding sites. A later membrane topology study highlighted the similarity between the membrane topology of CydD and CydC, supporting the prediction that each of the proteins contains 6 TMDs. Protein fusions between CydD or CydC with alkaline phosphatase and *β*-galactosidase were able to demonstrate the presence of two major cytoplasmic loops, three minor periplasmic loops as well as the cytoplasmic location of the N- and C- termini of CydD and CydC (Cruz-Ramos *et al.* 2004b). Figure 6 shows a topography model of CydDC created using a recent modelling programme (Omasits *et al.* 2014), the findings are consistent with previous work. The model highlights the Walker A motif (also known as the P-loop), that interacts with bound nucleotide, the Walker B motif that coordinates magnesium ions and is essential for ATP hydrolysis, as well as the conserved histidine residue common to all ABC transporters, that hydrogen bonds with the gamma phosphate of ATP (Figure 1-6).

The stuctural properties of purified CydDC were analysed using electron microscopy (EM) alongside circular dichroism (CD) (Yamashita *et al.* 2014). Purified CydDC reconstituted in membrane lipids was used to generate two-dimensional crystals, which were subsequently analysed by electron cryomicroscopy, this showed that the protein is made of two non-identical domains, corresponding to CydD and CydC. The resolution was unfortunately low (30 Å) due to poor crystal order, thought to reflect a high conformational flexibility, which is also seen by other ABC type transporters, for

example in the x-ray crystal structure of the CydDC homologue MsbA (Ward *et al.* 2007).

Circular dichroism (CD) spectroscopy verified that CydDC is largely comprised of α-helices, and that the binding of haem has no significant affect upon the secondary structure. SDS-PAGE indicated a 1:1 ratio of CydD:CydC, and EM analysis of purified CydDC particles incubated with Ni-NTA-nanogold, demonstrated that each particle contained a single CydC subunit (only CydC was tagged during affinity chromatography of the CydDC complex).

ABC transporters utilise adenosine triphosphate (ATP) hydrolysis as the energy source to move substrates across cell membranes, often against a concentration gradient. There is a great diversity within ABC transporters in regards to function; working to either import or export a wide range of substrates (Higgins 2001), yet all contain two ATP binding domains that bind and hydrolyse ATP. These nucleotide binding domains (NBDs) are highly conserved and share motifs common to all ATPase proteins such as Walker A and B motifs, as well as motifs unique to ABC proteins including the signature sequence (LSGGQ) and a conserved histidine residue. This high level of conservation within NBDs suggests a common mechanism in the powering of substrate transport via ATP hydrolysis.

CydDC is a substrate exporter and thus has no substrate binding protein like the periplasmic proteins of importers. The binding of substrates to ABC transporters commonly induces their ATPase activity (Jones and George, 2004). Accordingly ATPase activity of CydDC was shown to be stimulated 3- to 4-fold by the addition of cysteine or GSH, however it is unknown exactly where these substrates bind (Yamashita *et al.*, 2014). Proteins related to CydDC, including the human P-glycoprotein and the bacterial Sav1866, are believed to receive their substrate from the lipid bilayer (Moussatova *et al.*, 2008). Transport of substrates is considered to be initiated by the binding of substrate causing a conformational change in the TMDs that is transmitted to the NBDs resulting in ATP hydrolysis.

The presence of haem in the form of hemin boosted thiol-stimulation of CydDC ATPase activity (Yamashita *et al.*, 2014). As haem transport to the periplasm has been shown to occur independently of CydDC, a regulatory role in CydDC thiol transport is expected for haem. Structural modelling has since located a putative haem-binding site on the periplasmic surface of CydDC (Shepherd, 2015).

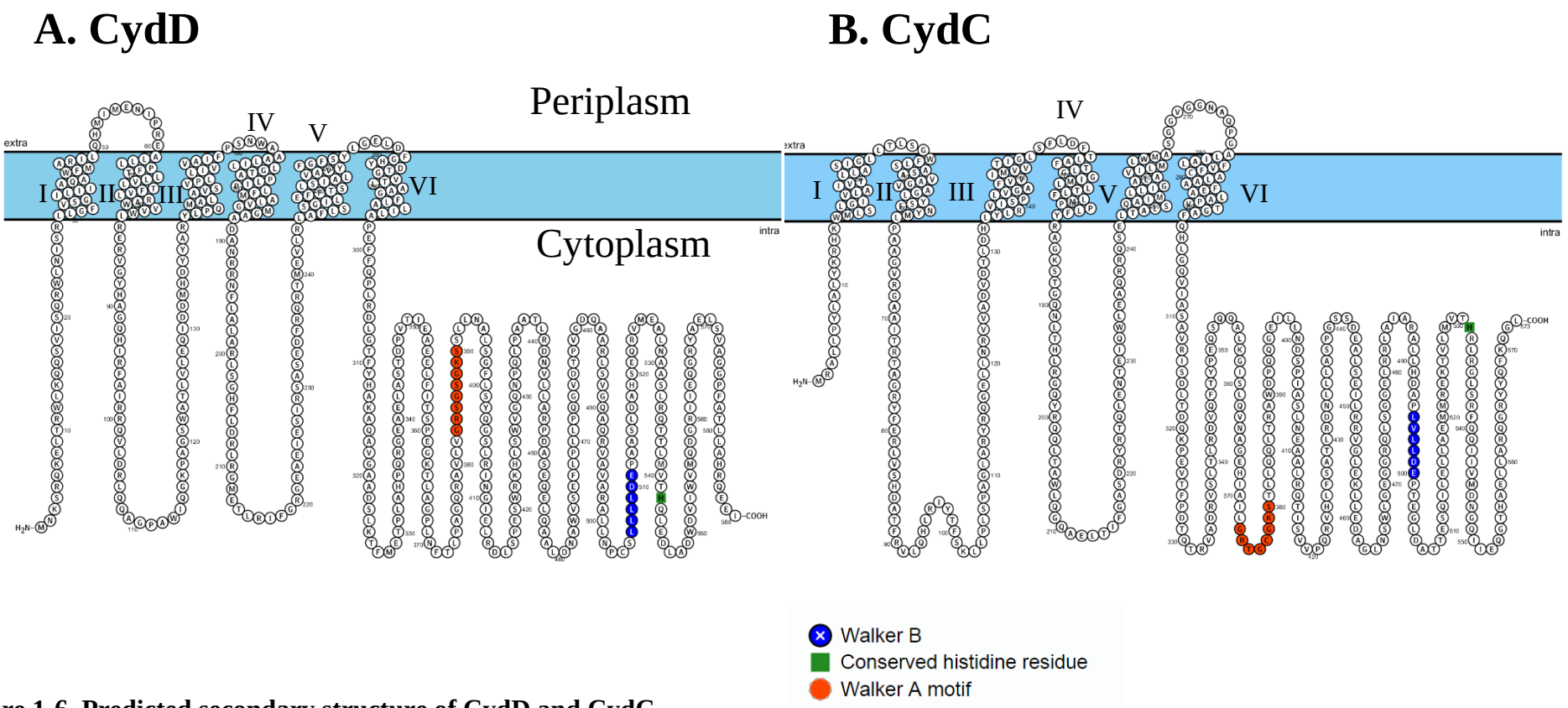

Figure 1-6. Predicted secondary structure of CydD and CydC

Secondary structure prediction was performed using the Protter online tool (v1.0) (Omasits *et al.* 2014). Transmembrane helices are numbered sequentially, Walker A motifs are shown in red, Walker B motifs are shown in Blue, and the conserved histidine residues of ABC transporter subunits (Linton and Higgins 1998) are shown in Green (His542 and His531 in CydD and CydC, respectively).

1.4. Role of CydDC in the formation of P-574, a novel haem compound

When *E. coli* cells are grown anaerobically, overexpression of the *cydDC* genes using a multi-copy plasmid elicits an increase in the levels of cytochromes *b* and *d*, and strikingly also results in the formation of a novel haem-containing molecule P-574 (Cook *et al.* 2002). This pigment has distinctive absorption characteristics at 574-579 nm and 448 nm in reduced *minus* oxidised spectra. Cells expressing P-574 appear reddish in colour, suggesting an overexpression of haem-containing proteins. The presence of P-574 is dependent upon haem biosynthesis as shown by the absence of P-574 in an *E. coli* strain auxotrophic for 5-aminolaevulinic acid (a precursor of haem biosynthesis) (Cook *et al.* 2002). In a *cydAB* mutant that is over-expressing *cydDC*, P-574 continues to be detected, thus eliminating the possibility that P-574 is a modified form of cytochrome *bd*-I (Cook *et al.* 2002).

Haem was originally thought to be the most likely substrate for CydDC as cytochrome *bd*-I subunits are detected in the membranes of *cydDC* mutants as apoproteins (Georgiou, Hong and Gennis 1987). The assembly of periplasmic cytochromes is also perturbed in this strain. The uptake, however, of radio-labelled haem into everted membrane vesicles is not affected by the deletion of *cydDC*, suggesting that haem is not exported by CydDC, instead entering the periplasm by another route which is as yet unknown (Pittman *et al.* 2002). Considering that CydDC exports the reduced low-molecular weight thiols glutathione and cysteine and that loss of the exporter leads to an over-oxidising periplasm, it is likely that the formation of P-574 in cells over-expressing CydDC results from a perturbation of redox balance in the periplasm. Cook *et al.* suggested that P-574 may be an intermediate or by-product of haem biosynthesis caused by a loss of redox balance in the periplasm (Cook *et al.* 2002). The authors further hypothesised that a derivative of haem biosynthesis could complex with the over-expressed polypeptides of CydDC. It has since been revealed, however, that P-574 is retained in a cut-off filter of only 50 kDa, indicating that this pigment is protein-bound, but not to the polypeptides of CydDC (Shepherd, Heath and Poole 2007). Furthermore, the majority of P-574 was shown to be located in the periplasm, rather than being membrane-bound like CydDC (Shepherd, Heath and Poole 2007). NikA, a haem-binding periplasmic protein involved in nickel uptake has been implicated in the formation of P-574; mutation of NikA significantly reduces the levels of P-574 seen in cells over-expressing CydDC.

1.5 The terminal oxidases of *E. coli*

The *bo′* and *bd*-type oxidases of *Escherichia coli* both catalyse the two-electron oxidation of ubiquinol by molecular oxygen within the cytoplasmic membrane, concomitantly generating a proton gradient across the membrane that can be utilised by bacterial cells to produce ATP for use as an energy source. A major phenotype of *cydDC* mutants is an inability to assemble the terminal resiratory oxidase cytochrome *bd*-I. The assembly of cytochrome *bo′* is thought to be independent of CydDC activity, and is the only functional respiratory oxidase in mutants lacking CydDC. Despite the presence of this alternative terminal oxidase, that can compensate for the loss of cytochrome *bd*-I, the two oxidases show variability in characteristics such as energy conservation and oxygen affinity that enable *E. coli* cells to adapt to their environment. This section discusses the alternative terminal oxidases of *E. coli* and highlights the significance of cytochrome *bd*-I deficiency.

1.5.1 Cytochrome *bo′*

In addition to generating a proton gradient via the vectorial translocation of protons that is linked to quinol reduction and oxidation, cytochrome *bo′* is also able to directly pump protons across the membrane (Puustinen, Finel and Haltia 1991) and has a H^+:e^- ratio of 2. The site of oxygen reduction in cytochrome *bo′* is a haem-copper binuclear oxygen-reactive centre, making it a member of the haem-copper superfamily of terminal oxidases (Anraku 1988) that have been extensively studied.

The *cyoABCDE* genes encode subunits I, II, III and IV of the cytochrome *bo′* complex and a protohaem farnesyltransferase (haem *o* synthase) respectively (Minghetti, Goswitz and Gabriel 1992; Saiki, Mogi and Anraku 1992). The assembly pathway for cytochrome *bo′* is an ordered process wherein subunits III and IV are assembled first, followed by subunit I, and finally subunit II (Stenberg, von Heijne and Daley 2007). CyoABC are homologous to the core subunits of the aa_3-type cytochrome *c* oxidase (Lemieux *et al.* 1992) both in terms of their primary sequence (Saraste, Sibbalda and Wittinghoferb 1988; Cotter *et al.* 1990) and structure (Gohlke, Warne and Saraste 1997; Abramson *et al.* 2000). A crystal structure of the entire cytochrome *bo′* terminal oxidase complex has been determined at a resolution of 3.5 Å (Abramson *et al.* 2000) and reveals 25 transmembrane helices with a ubiquinone binding site within the membrane domain of subunit I (Abramson *et al.* 2000). The entire complement of redox centres reside within the largest of the four subunits,

subunit I. A low-spin haem *b* associated with a copper ion (Cu_B) (Puustinen, Finel and Haltia 1991; Puustinen and Wikstrom 1991) is thought to act as an electron donor to reduce a binuclear centre composed of a high-spin haem *o* and another copper ion (Cu_B): this is where oxygen reduction takes place (Salerno, Bolgiano and Poole 1990). The assembly of cytochrome *bo′* is thought to be independent of CydDC activity, and is the only functional respiratory oxidase in mutants lacking CydDC.

1.5.2 Cytochrome *bd*-I

The terminal oxidase cytochrome *bd*-I is confined to the prokaryotic world and is well-characterised in *E. coli*. Unlike cytochrome *bo′*, cytochrome *bd*-I does not contain copper and so is not a member of the haem-copper oxidase superfamily. Instead, cytochrome *bd*-I utilises an unusual di-haem oxygen-reactive site (Rothery and Ingledew 1989; Junemann 1997; Borisov and Verkhovsky 2013). All known members of the *bd*-family use quinol as a substrate, receiving electrons commonly from either ubiquinol or menaquinol. A three dimensional structure has yet to be elucidated, existing data however, shows that cytochrome *bd*-I is a trimer of three integral membrane polypeptides, subunits I (CydA) and II (CydB) (Kita, Konishi and Anraku 1984) and CydX (VanOrsdel *et al.* 2013). Secondary structure prediction models suggest that CydA contains nine membrane-spanning helices, that CydB contains eight membrane-spanning helices (Osborne and Gennis 1999) and that CydX consists of just a single membrane-spanning helix. A large periplasmic loop between helices 6 and 7 of subunit I is involved in quinol binding and is consequently known as the 'Q loop' (Dueweket and Gennis 1991; Matsumoto *et al.* 2006; Mogi *et al.* 2006). Site-directed mutagenesis has revealed that two residues within the Q loop, Lysine-252 and Glutamate-257, are required for cytochrome *bd*-I oxidase activity (Mogi *et al.* 2006) and are thought to play a role in quinol binding. Shifts in 'reduced *minus* oxidised' spectra following Glu257 mutation indicate a close proximity of this residue to haem b_{558}, suggesting that Glu257 not only binds to quinol but also participates in electron transfer from quinol to haem b_{558} (Mogi *et al.* 2006).

Three haems are associated with the oxidase in a 1:1:1 stoichiometry per oxidase complex. Two of the haems are in a high-spin state (*d* and b_{595}) and are thought to form a di-haem active site where oxygen is reduced (Hill, Alben and Gennist 1993; Vos *et al.* 2000; Arutyunyan *et al.* 2008; Rappaport *et al.* 2010; Borisov and Verkhovsky 2013), and modelling of the excitonic interaction between haems *d* and b_{595}

has led to an estimated intermolecular distance of 10 Å (Arutyunyan *et al.* 2008). Despite the proximity and evidence for functional cooperation (Vos *et al.* 2000), doubt has been cast upon the existence of a di-haem active site as no spin coupling has been observed between the haems (Junemann 1997). The third haem cofactor is a hexacoordinate low-spin haem b_{558} located within subunit I that is responsible for quinol oxidation that supplies electrons to the di-haem site for the reduction of molecular oxygen to water.

In the absence of CydB, CydA is still integrated into the cytoplasmic membrane, and haem b_{558} is still incorporated but the high spin haems *d* and b_{595} are absent from the cytochrome subunits (Newton and Gennis 1991). In an attempt to explain this loss of haem groups, it has been suggested that the two high-spin haems are located at the interface between CydA and CydB subunits. Loss of *cydDC* abolishes haem cofactor incorporation into cytochrome *bd*-I but the CydAB polypeptides are still inserted into the membrane (Georgiou, Hong and Gennis 1987). Synthesis of this apo-cytochrome *bd*-I is also observed in haem-deficient cells (Calhoun, Newton and Gennis 1991), implying that haem insertion is the last step of cytochrome *bd*-I assembly.

Site-directed mutagenesis studies have been used alongside spectroscopic methods to reveal that highly-conserved histidine-186 and methionine-393 of CydA are axial ligands of b_{558} (Fang, Lin and Gennis 1989; Kaysser *et al.* 1995; Spinner *et al.* 1995). The positive charge of the conserved arginine-391 residue has a role in stabilising the reduced form of haem b_{558} and is required for oxidase activity (Zhang *et al.* 2004). Histidine-19 of CydA provides the essential axial ligand for b_{595} (Sun *et al.* 1996). Furthermore, an E99L mutation within CydA abolishes the haem *d* spectral signals (Bloch *et al.* 2009), supporting the idea that glutamate-99 could be the axial ligand to haem *d* (Mogi, Endou and Akimoto 2006).

Cytochrome *bd*-I contributes to the proton motive force (PMF) via the vectorial translocation of protons that is linked to quinol reduction and oxidation (Calhoun *et al.* 1993), but unlike cytochrome *bo′* is unable to directly pump protons (Puustinen, Finel and Haltia 1991) and is therefore considered, in bioenergetic terms, less efficient (H^+:e^- ratio = 1). All three haem cofactors appear to be located on the periplasmic side of cytochrome *bd*-I (Zhang *et al.* 2004), which poses the question of how protons are translocated across the membrane from the cytoplasm to the site of oxygen reduction that occurs on the periplasmic side. As the translocation of protons is unlikely to involve inter-haem transfer, conserved amino acid residues that can be reversibly protonated have been implicated, so far glutamates 99 and 107 within transmembrane helix III of

CydA have been suggested to partake in proton translocation (Osborne and Gennis 1999).

Despite having a reduced contribution to the PMF, cytochrome *bd*-I does facilitate aerobic respiration under conditions of low oxygen due to a very high affinity for oxygen: *bd*-I has a K_m of 3 ± 8 nM (D'mello, Hill and Poole 1996) compared to K_m values in the range of 0.016-0.35 µM for cytochrome *bo′* (D'Mello, Hill and Poole 1995). It is likely that the di-haem active site plays a role in this high affinity for oxygen (Borisov, Liebl and Rappaport 2002), promoting growth in microaerobic environments.

1.5.2.1 The *cydABX* genes

Until recently, cytochrome *bd*-I was generally believed to be comprised of two subunits encoded by *cydA* (subunit I) and *cydB* (subunit II) (Kranz and Gennis 1983; Green *et al.* 1988; Calhoun, Newton and Gennis 1991) located at 16.6 minutes on the *E. coli* genetic map (Bachmann 1990; Calhoun, Newton and Gennis 1991). The molecular weights of subunits I (57kDa) and II (43kDa) determined by sodium dodecyl sulphate-polyacrylamide-gel electrophoresis (SDS-PAGE) (Miller and Gennis 1983) are consistent with predicted masses calculated from the protein sequences (Green *et al.* 1988).

Two open reading frames, *ybgE* and *ybgT* are found at the 3' end of the *cydAB* genes which together are thought to form an operon (Figure 1-7) (Muller and Webster 1997). The 4 kDa YbgT protein was shown to co-purify with CydAB and is believed to be a part of the complex (VanOrsdel *et al.* 2013); *ybgT* has since been renamed *cydX*. Cells lacking CydX exhibit diminished oxidase activity which can be restored by the addition of *cydX* on a plasmid (VanOrsdel *et al.* 2013). Silver staining shows that CydX is present in stoichiometric amounts with CydA and CydB (Hoeser *et al.* 2014), confirming CydX as a third subunit of cytochrome *bd*-I. CydX is thought to be required for either the insertion or the stability of haem *d* and b_{595} that make up the di-haem active site of cytochrome *bd*-I; UV/visible difference spectroscopy revealed that the signals of haem *d* and b_{595} are lost when CydA and CydB are not accompanied by CydX. No role in cytochrome *bd*-I assembly/function has been identified for *ybgE*, with its deletion having no effect on phenotypes typically observed for *cydA* or *cydB* mutants (VanOrsdel *et al.* 2013).

Figure 1-7. The *cydABX* locus of *E. coli*

The cytochrome *bd*-I terminal oxidase is encoded by the *cydABX* genes. *ybgE* is thought to also form part of the operon but as of yet no role in cytochrome *bd*-I assembly/function has been identified.

Beyond *cydABX*, the two genes encoding CydDC are essential for assembly of functional cytochrome *bd*-I (Georgiou, Hong and Gennis 1987; Bebbington and Williams 1993; Poole *et al.* 1993; Poole, Gibson and Wu 1994). In its absence, CydA and CydB are still synthesised and inserted into the membrane, but the oxidase lacks haem groups essential for function (Georgiou, Hong and Gennis 1987). As discussed previously CydDC exports two low-molecular weight thiols, glutathione and cysteine, from the cytoplasm to the periplasmic space (Pittman *et al.* 2002; Pittman, Robinson and Poole 2005). However, exogenous addition of either of these thiols to a strain lacking CydDC does not restore cytochrome *bd*-I assembly, so the molecular mechanism via which CydDC contributes to cytochrome *bd*-I assembly remains unclear.

1.5.3 Cytochrome *bd*-II

Dassa *et al.* 1991 discovered an operon comprised of three genes upstream of *appA*, an acid phosphatase gene that is regulated positively in response to oxygen deprivation by AppR (KatF). The genes named *appC, appB and appX* are co-transcribed at a promoter, P2, just upstream of *appC*, whereas a second minor promoter P1 controls *appA* (Figure 1-8). The *appCBX* genes are regulated by oxygen in exactly the same way as *appA*. Support for the idea that AppC and AppB are implicated in oxygen metabolism was provided by the increased sensitivity to dioxygen phenotype of a *cyo cyd app* triple mutant (when compared to the *cyo cyd* double mutant) (Dassa *et al.* 1991).

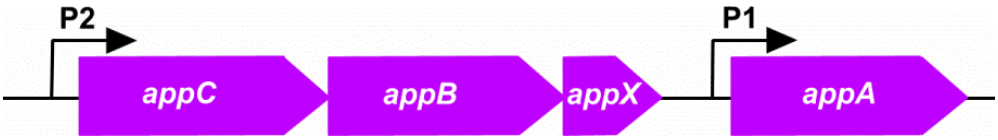

Figure 1-8. The *appCBX* locus of *E. coli*

The cytochrome *bd*-II terminal oxidase is encoded by the *appCBX* genes, downstream *appA* encodes an acid phosphatase enzyme. The *appCBX* genes are co-transcribed at a promoter, P2, whereas a second minor promoter P1 controls *appA*.

The newly discovered *appCB* genes were predicted to encode integral membrane proteins with striking sequence homology to CydA (60% similarity) and CydB (57% similarity) and with similar hydrophobicity profiles (Figure 1-9). To our knowledge, no CydD and CydC homologues with functions allied specifically to AppB and AppC assembly have been identified. The *appCB* gene products are also known as CbdAB (Sturr, Krulwich and Hicks 1996), AppBC, CyxAB or, most commonly now, cytochrome *bd*-II.

The cytochrome *bd*-II oxidase was at first considered to be nonelectrogenic (Bekker *et al.* 2009), but the ability of cytochrome *bd*-II to generate a proton motive force was later re-examined. It was shown via absorption and fluorescence spectroscopy along with oxygen pulse methods that in the steady-state, cytochrome *bd*-II can generate a proton motive force via a molecular mechanism identical to that in cytochrome *bd*-I (Borisov *et al.* 2011). With an estimated H^+/e^- ratio of 0.94 ± 0.18, the proton motive force generated by cytochrome *bd*-II is expected to be sufficient to drive ATP synthesis and transport of nutrients.

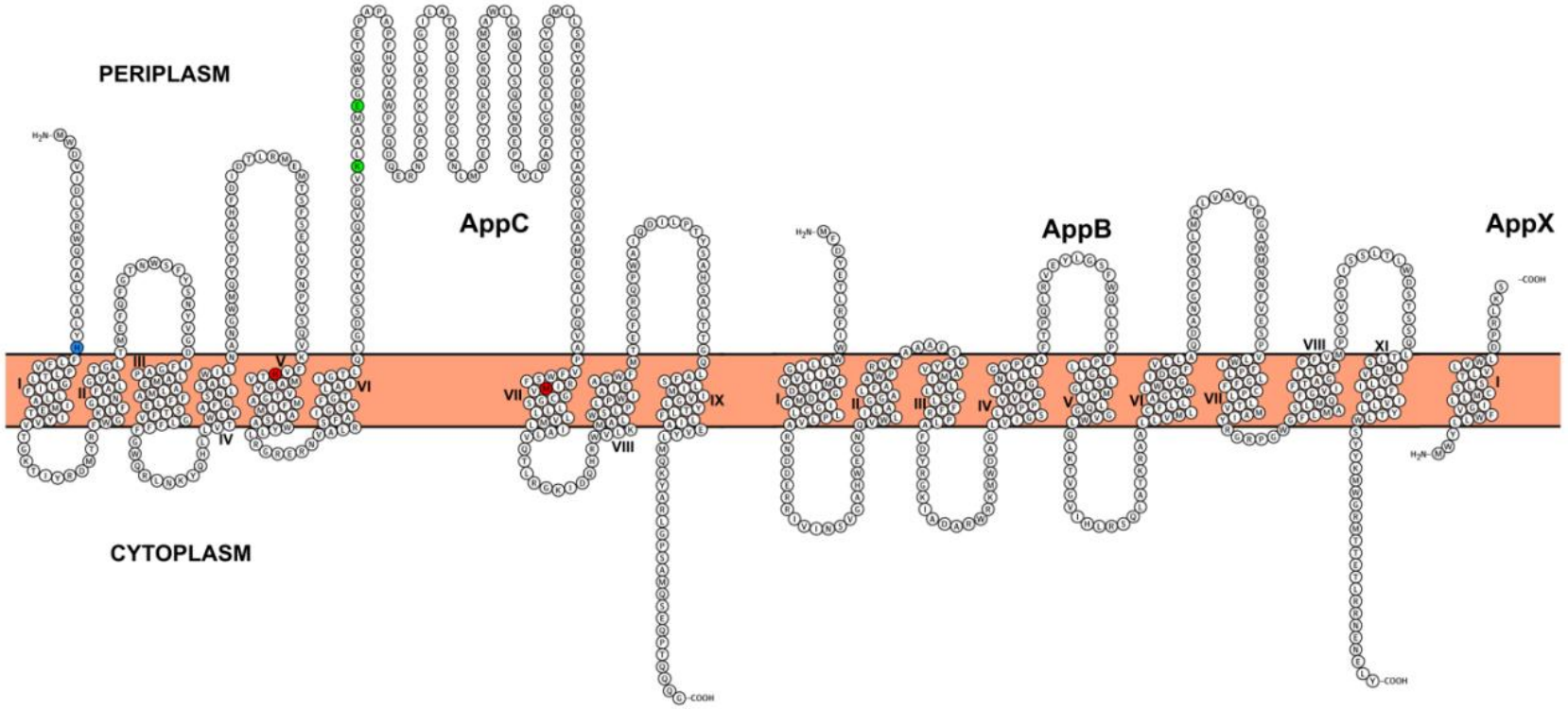

Figure 1-9. Predicted secondary structures of AppC, AppB, and AppX

Secondary structure prediction was performed using the Protter online tool (v1.0) (Omasits *et al.* 2014). Transmembrane helices are numbered sequentially, the haem b_{595} ligand (His19) is shown in blue, the haem b_{558} ligands (His186 and Met393) are shown in red, and the likely sites of quinol binding (Lys252 and Glu257) are shown in green.

1.5.4 Regulation of terminal oxidase expression

The respiratory chain of *Escherichia coli* is a complex branched array of modular components that are able to oxidise a wide variety of substrates, permitting bacteria to grow in a range of aerobic environments. The expression of cytochromes *bo′* and *bd*-I are controlled by different transcriptional regulators, and these complexes are expressed under different conditions. The regulation of cytochrome *bd*-II is lesser-studied, although the *appCB* operon is known to be induced under conditions of carbon and phosphate starvation and is under the control of RpoS and AppY (Atlung *et al.* 1997). The differential regulation of *cyo* and *cydAB* operons provides an insight into the roles of cytochromes *bo′* and *bd*-I in *E. coli*: cytochrome *bo′* has so far been shown to be more energetically efficient than cytochrome *bd*-I, but has a lower affinity for oxygen and is therefore less efficient than cytochrome *bd*-I in low oxygen environments. The regulatory mechanisms discussed below act to optimise the expression of the *bo′* and *bd*-I oxidases in response to changing respiratory requirements under varying oxygen tensions.

1.5.4.1 Regulation of the *cyo* and *cydAB* operons

LacZ-fusion experiments with cytochrome *bo′* and cytochrome *bd*-I revealed that in cells grown aerobically there are an estimated 304 molecules of cytochrome *bo′* and 204 molecules of cytochrome *bd*-I per cell compared to only two molecules of cytochrome *bo′* and 606 molecules of cytochrome *bd*-I per cell when grown anaerobically (Cotter *et al.* 1990). This difference in oxidase composition within the membrane illustrates the differential regulation of cytochrome *bd*-I and cytochrome *bo′* in response to oxygen tension.

Cytochrome *bo′* and cytochrome *bd*-I of *E. coli* are regulated by the combined action of FNR and the two-component system ArcAB (Gunsalus 1992). The fumarate and nitrate reductase regulator, FNR, is a global transcriptional regulator that orchestrates changes from aerobic to anaerobic metabolism at the transcriptional level (Unden *et al.* 1995; Becker *et al.* 1996; Beinert and Kiley 1999). FNR contains an oxygen-labile $[4Fe\text{-}4S]^{2+}$ cluster that controls protein dimerisation and site specific DNA binding. Oxygen is sensed via the assembly and disassembly of the $[4Fe\text{-}4S]^{2+}$ cluster (Green *et al.* 1996; Lazazzera and Beinert 1996; Beinert and Kiley 1999). When cells encounter a change from aerobic to anaerobic growth conditions, FNR is activated,

and subsequently binds to DNA at consensus sequences resulting in the modulation of gene expression (Lazazzera and Beinert 1996). In contrast, ArcAB is a two-component regulatory system comprised of a transmembrane sensor kinase (ArcB) and a cytosolic response regulator (ArcA). ArcB is activated by falling oxygen tensions and in turn phosphorylates ArcA, which functions at the transcriptional level, to activate the expression of *cydAB* and repress the expression of *cyoABCDE* (Iuchi *et al.* 1990; Fu, Iuchi and Lin 1991; Iuchi and Lin 1992). Expression of both aerobic and anaerobic respiratory pathway genes are controlled under microaerophilic conditions, ensuring a hierarchical pattern of gene expression in response to changes in oxygen availability (Tseng *et al.* 1996). Expression of cytochrome *bd*-I reaches a peak at an oxygen tension of approximately 2% (Tseng *et al.* 1996). At oxygen tensions lower than this FNR becomes activated and represses the *cyoABCDE* and *cydAB* operons, with the genes of the anaerobic respiratory pathway becoming activated (Cotter *et al.* 1990; Tseng *et al.* 1996). Repression of the *cydAB* genes by FNR is dependent upon ArcA (Cotter *et al.* 1990; Tseng *et al.* 1996; Cotter *et al.* 1997; Govantes *et al.* 2000), suggesting that FNR functions as an anti-activator by counteracting ArcA-mediated activation as opposed to direct repression of transcription (Tseng *et al.* 1996; Cotter *et al.* 1997; Govantes *et al.* 2000). Consequently, *cydAB* expression increases with falling oxygen tensions via ArcAB, until oxygen tension is low enough for FNR to suppress the effects of ArcAB. It has also been found that during shifts to anaerobic conditions or upon entry into stationary phase, changes in DNA supercoiling play a role in the induction of *cydAB* expression which is independent of ArcAB or FNR (Bebbington and Williams 2001).

The mechanisms above account for how cytochrome *bd*-I expression is regulated at lowering oxygen tensions, but does not fully explain how cytochrome *bo′* levels are higher than cytochrome *bd*-I at higher oxygen tensions. In highly aerobic conditions, the abundant histone-like protein, H-NS, represses *cydAB* expression resulting in diminished expression of *cydAB* under aerobic conditions (Govantes *et al.* 2000). H-NS is thought to decrease gene expression by causing localised changes to DNA that prevent RNA polymerase binding (Ueguchil and Mizuno 1993).

As well as adapting to low oxygen conditions, expression and membrane content of cytochrome *bd*-I has been shown to increase in response to a variety of stresses, including high temperature (Wall *et al.* 1992; Delaney *et al.* 1993), high pH (Avetisyan *et al.* 1991), high pressure (Tamegai *et al.* 2005) and the presence of protonophore-uncouplers (Armine V Avetisyan, Pavel A Dibrov, Anna L Semeykina, Vladimir P Skulachev 1991; Bogachev, Murtazina and Skulachev 1993; Bogachev *et al.* 1995).

Also, induction of cytochrome *bd*-I by heat shock and loss of PMF is dependent upon the ArcAB two-component system (Wall *et al.* 1992). In response to exposure of nitric oxide, anaerobically grown cells see a preferential induction of the cytochrome *bd*-I genes, but not of genes encoding cytochrome *bo'*; *cydA* and *cydB* were shown to be up-regulated by 3.9-fold and 3.2-fold, respectively. Similar results were seen in response to nitric oxide (NO) for cells growing aerobically, with the *cydA* and *cydB* genes being induced by 2.4-fold and 2.5-fold, respectively. This study reported an accompanying up-regulation of other FNR-repressed genes, suggesting that this response is likely due to an interaction between NO and the iron-sulphur cluster within FNR (Pullan *et al.* 2007): the iron-sulphur cluster is required for DNA binding and is inactivated upon NO exposure (Cruz-Ramos *et al.* 2002).

1.6 Nitric oxide stress in *E. coli*

Nitric oxide (NO) is a key signalling and defence molecule in biological systems which *Escherichia coli* encounters both as part of its own metabolism and during host infection. NO is produced by *E. coli* as an obligate intermediate of anaerobic denitrification; during which nitrate is reduced to nitrite, which is subsequently reduced to ammonia via a NO intermediate (Zumft 1997; Watmough *et al.* 1999). In eukaryotic cells and certain bacteria, nitric oxide is also produced via the oxidation of L-arginine by NO synthases (NOS) including inducible nitric oxide synthase (iNOS) (Cutruzzola 1999; Stuehr 1999; Elfering, Sarkela and Giulivi 2002). Host defence mechanisms such as neutrophils and activated macrophages (Fang 2004; Lundberg *et al.* 2004; Poole and Hughes 2000) utilise NO and associated reactive nitrogen species (RNS) as protection against invading bacteria. Nitric oxide has been shown to inhibit *E. coli* growth and respiration (Yu *et al.* 1997). The toxicity of NO and RNS in biological systems is due to their ability to react with a variety of cellular targets. Reactive nitrogen species are capable of causing damage to bacterial proteins, DNA and lipids. NO can affect terminal oxidases, thiol groups and metal centres such as iron sulphur clusters. To survive exposure to NO-mediated nitrosative stress, *E. coli* has evolved mechanisms to circumvent the harmful effects of NO. Various bacterial NO-detoxifying enzymes are contained within *E. coli* including the enzymes cytochrome *c* nitrite reductase (NrfA), flavohemoglobin (Hmp), and a flavorubredoxin (NorV). Alongside these enzymes, there are proteins that work to reverse the damage caused by NO such as the iron-

sulphur repair protein YtfE. These four NO protection mechanisms will now be discussed in more detail.

1.6.1. *E. coli* tolerance mechanisms against NO: Hmp

Flavohaemoglobins are comprised of two domains, a globin domain containing haem *b* and a ferredoxin-NADP reductase (FNR)-like domain that converts the globin into an NAD(P)H-oxidising protein with diverse reductase activities. In *E. coli*, *hmp* encodes a flavohemoglobin that is involved in the response to nitric oxide (NO) and nitrosative stress; The *hmp* gene is inducible under both aerobic and anaerobic conditions by nitrate, but is induced more efficiently by nitrite and NO (Poole *et al.* 1996).

The non-covalently bound haem of the globin domain has been shown to avidly bind NO *in vitro*. Sequential electron transfer from NAD(P)H to bound nitric oxide results in the reduction of NO to either nitrate under aerobic conditions or nitrous oxide under anaerobic conditions (Figure 1-10). Being one of the best-studied NO-defence mechanisms, the role of Hmp in NO detoxification was demonstrated by the finding that strains lacking Hmp are hypersensitive to NO and nitrosative stress. Hmp has been shown to be a virulence factor in *Salmonella* and other pathogens (Bang *et al.* 2006). Interestingly protection provided by Hmp appears to be more profound when grown aerobically than anaerobically (Gardner *et al.* 1998).

1.6.2. NorRVW

The nitric oxide reduction modulon *norRVW* is involved in the anaerobic or microaerobic reduction of NO to nitrous oxide (N_2O) (Gomes *et al.* 2002). The *norV* gene encodes a non-haem flavorubredoxin (Gomes *et al.* 2000; Vicente and Teixeira 2005; Gardner, Helmick and Gardner 2002) that has a di-iron centre and exhibits submicromolar affinity for NO (Tucker and D'autreaux 2004). NorV is associated with an NADH:(flavo)Rb oxidoreductase encoded by *norW* (Gardner, Helmick and Gardner 2002), which is rapidly reduced by NADH (but not NADPH) and transfers an electron to oxidised NorV to support multiple turnovers of NorV-mediated NO reduction (Figure 1-11) (Vicente *et al.* 2007).

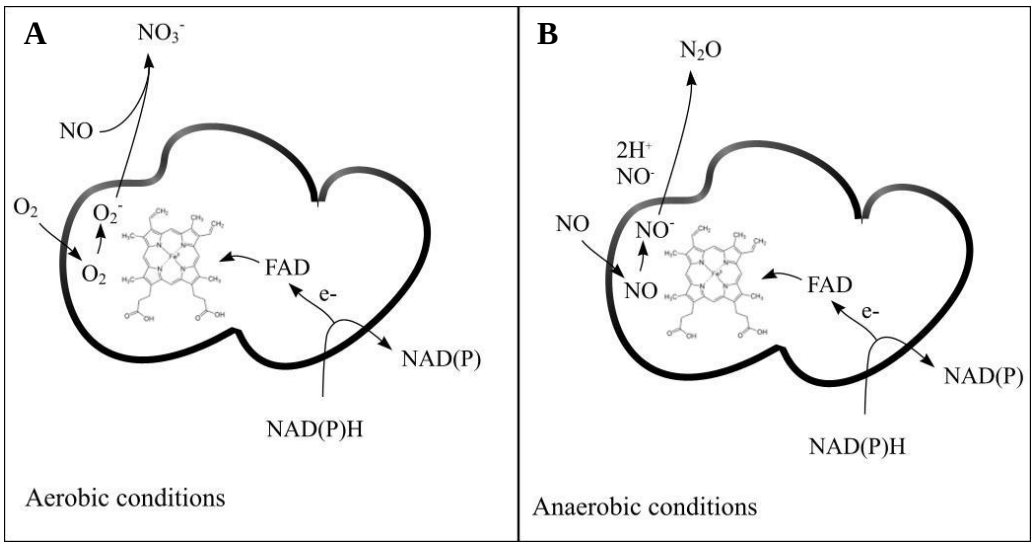

Figure 1-10. Electron transfer within Hmp leading to the reduction of NO

Hmp is depicted with the globin domain containing the haem prosthetic group at the left of the protein. Electrons are transferred from NAD(P)H to FAD and then to the haem group. **A** Under aerobic conditions O_2 is reduced to form a superoxide anion, subsequent oxygenation of NO leads to the formation of NO_3- presumably via a peroxynitrite intermediate that is not shown. **B** Under anaerobic conditions the ferrous haem reacts directly with NO to form a nitrosyl species, electron transfer to NO results in N_2O via an NO_2 intermediate which is not shown. Figure adapted from Poole and Hughes 2000.

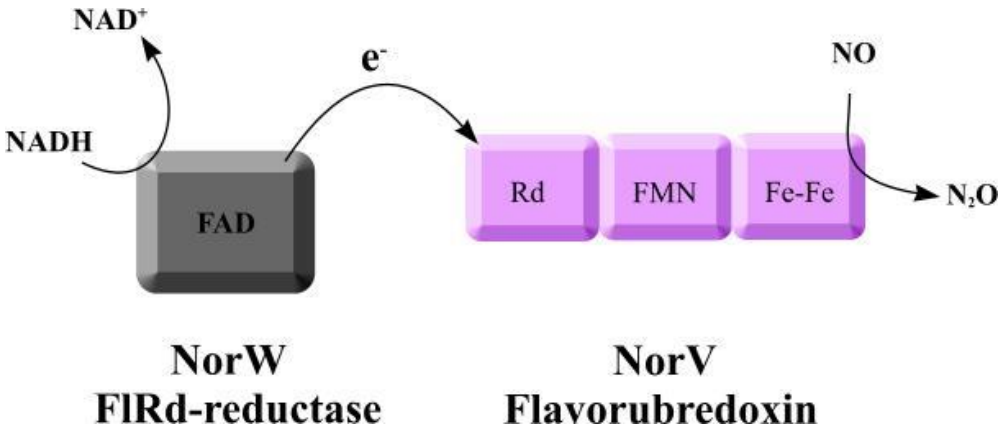

Figure 1-11. NorVW couples NADH oxidation to NO reduction

The flavorubredoxin NorV reduces nitric oxide to nitrous oxide. The flavorubredoxin reductase (FlRd-reductase) NorW then re-reduces NorV using NADH as an electron donor. NorV of *E. coli* contains three domains: a metallo-β-lactamase-like domain which contains the non-haem di-iron centre (Fe-Fe), a flavodoxin-like domain, containing one FMN moiety and a C-terminal module with a rubredoxin-like centre. Figure adapted from Vicente *et al*. 2007.

The *norVW* genes are regulated by an NO-responsive transcription factor NorR. NorR is formed of three domains, a GAF domain which contains a mononuclear non-haem iron that binds nitric oxide, a central AAA domain with ATPase activity and a DNA binding domain at the C-terminal of the protein (Gardner, Gessner and Gardner 2003; Justino *et al.* 2005; D'Autréaux *et al.* 2005). NorR is thought to respond only to NO (Spiro 2006), becoming activated by the reversible formation of a mononitrosyl complex which consequently stimulates the ATPase activity to initiate transcription of *norV* (Figure 1-12) (D'Autréaux *et al.* 2005).

Deletion of *norV* elicits a sensitivity to NO under anaerobic conditions (Gardner, Helmick and Gardner 2002). Despite this, the rate of NO reduction remains similar to the parental strain. Deletion of *hmp* alongside *norV* however results in a clear defect in anaerobic metabolism of NO (Justino *et al.* 2005; Vine and Cole 2011). NorV has been shown to contribute to the survival of EHEC within macrophages, and is considered a virulence factor of EHEC (Shimizu *et al.* 2012). This finding reinforces the identity of the flavorubredoxin and its accompanying reductase as a factor used by *E. coli* in the protection from host-derived NO. Baptista *et al.* (2012) used electron paramagnetic resonance (EPR) experiments to show that exposure to oxidative stress at the same time as nitrosative stress inhibits NorR, by preventing NO binding, a requirement for flavorubredoxin activation. This is of importance in the context of infection as macrophage cells use a combination of nitrosative and oxidative stress to combat pathogenic bacteria. Survival of *E. coli* was studied within activated murine macrophages; this showed that the contribution of NorV to survival within macrophages depends upon the stage of macrophage infection. An initial oxidative burst inhibits NorR as revealed by the lack of protection observed at the early stage of macrophage infection (Baptista *et al.* 2012).

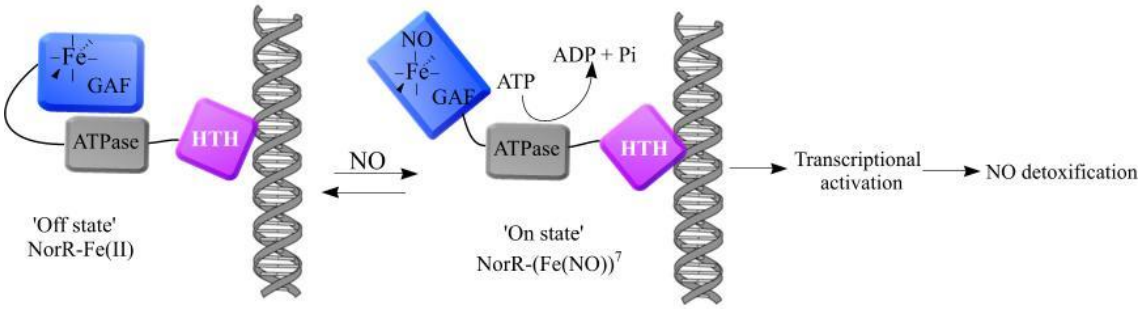

Figure 1-12. Schematic of NorR and the proposed mechanism of transcriptional activation

The schematic includes the three domains of NorR; the C-terminal helix-turn-helix (HTH) DNA binding domain, the ATPase domain and the N-terminal GAF domain containing a non-haem iron centre. In the 'off state' NorR contains a ferrous iron ion, but in the presence of nitric oxide a mononitrosyl complex is formed which activates NorR to an 'on state' with ATPase activity that is coupled to the activation of *norV* transcription. For the purpose of clarity NorR is depicted as a monomer. Figure adapted from D'Autréaux *et al*. 2005.

1.6.3. NrfA and the detoxification of NO

The periplasmic cytochrome *c* nitrite reductase, NrfA, of *E. coli* is a homodimer of approximately 110 kDa that contains ten *c*-type haems; five per monomer. This respiratory enzyme is expressed under anoxic or microaerobic growth conditions in the presence of nitrate and nitrite (Darwin *et al.* 1993; Rabin and Stewart 1993). NrfA (Nitrite Reduction by Formate) catalyses the respiratory six electron reduction of nitrite to ammonium (Poock *et al.* 2002) but importantly can also catalyse the five electron reduction of nitric oxide to ammonia (van Wonderen *et al.* 2008). The reduction and therefore detoxification of NO by NrfA suggests a protective role against NO. Consistently, under anaerobic conditions strains lacking NrfA have been shown to have a much greater sensitivity to NO (Poock *et al.* 2002).

The consumption of NO by NrfA under anaerobic conditions was demonstrated *in vivo* by Poock *et al.* using a Clarke-type oxygen electrode polarised to detect nitric oxide. To prevent complications in studying the contribution of NrfA to NO metabolism Poock *et al.* used a mutant strain of *E. coli* with a deletion of *nirA* which encodes a cytoplasmic sirohaem nitrite reductase (Harborne *et al.* 1992). This enzyme also reduces nitrite to ammonium and would also be switched on under anaerobic or microaerobic conditions. NO consumption was compared between a *nrfA* mutant and its parental

strain (*nirA*$^{-}$). The parental strain reduced NO at maximum rate of 300 nmol NO mg protein^{-1} min^{-1}. However, nitric oxide consumption could not be detected when measured in a *nrf- nirA*$^{-}$ strain (Poock *et al.* 2002). Taken together this demonstrates a role for NrfA in tolerance to nitrosative conditions.

E. coli has multiple routes for detoxifying nitric oxide. In changeable environments *E. coli* can be exposed to, particularly for pathogenic *E. coli*, it is likely that these different mechanisms, rather than being functionally redundant will be important for different conditions faced by bacteria. NrfA, for example, is particularly well suited to NO removal as it is located in the periplasm and so can detoxify NO before reaching targets within the cytoplasm. Also as NrfA is expressed under anoxic or micro-oxic growth conditions, NrfA is likely to be active in the oxygen limiting conditions experienced within the host.

1.6.4 Iron-sulphur cluster repair

Among cellular targets of nitric oxide cytotoxicity are a group of proteins that contain iron–sulphur clusters. Iron-sulphur (Fe-S) clusters are a ubiquitous prosthetic group that underpin a diverse range of protein functions and fundamental life processes including electron transfer (Cooper 1999). NO can bind to the iron of iron-sulphur clusters to form an iron-sulphur nitrosyl complex and thus inhibit the catalytic role they play in proteins (Butler, Glidewell and Li 1988). Some propose that nitrosative stress limits activity of Fe-S proteins by the release of iron from clusters, however more research is needed to prove this (Drapier 1997).

Also known as RIC (Repair of Iron Centres), *Escherichia coli* YtfE is a di-iron protein that has been shown to enable *E. coli* to cope with nitrosative and oxidative stress by repair of iron sulphur clusters (Todorovic *et al.* 2008; Justino *et al.* 2006; Justino *et al.* 2005). YtfE was first associated with nitrosative stress protection when a DNA microarray experiment showed a 55-fold increase in *ytfE* mRNA when treated with NO (Justino *et al.* 2005). Mutation of *ytfE* was later shown to elicit a sensitivity to nitric oxide (Justino *et al.* 2005), and to reduce activity of iron-sulphur cluster proteins under nitrosative stress (Justino *et al.* 2006). Furthermore in the absence of YtfE, nitrosative damage to Fe-S clusters is accelerated (Justino *et al.* 2007).

In wild type *E. coli*, once sources of nitrosative or oxidative stress are eliminated, a recovery in activity of iron-sulphur cluster proteins, aconitase B and fumarase A is seen.

Strains lacking *ytfE* however do not demonstrate this recovery of activity. Furthermore, addition of purified holo-YtfE to *ytfE* mutant extracts, has been shown to restore the activity of fumarase and aconitase to rates similar to wild type. This demonstrates that YtfE is able to repair nitrosative damage to Fe-S clusters.

1.6.5 Role for cytochrome *bd*-I in NO tolerance

Alongside protein thiol groups and iron sulphur clusters, NO can bind to haem proteins including cytochromes *bo′* and *bd*-I of *E. coli*. In response to NO exposure, a transcriptomic study reported elevated expression of the *cydAB* operon encoding cytochrome *bd*-I, which suggested that this terminal oxidase may have a role in tolerance to nitrosative stress (Pullan *et al.* 2007). Gene knockouts were performed in *E. coli* so that cells lacked either the genes encoding cytochrome *bo′* or cytochrome *bd*-I; growth and respiratory rates were then assessed for these respiratory mutants in response to NO (Mason *et al.* 2009). Cells that possessed cytochrome *bd*-I were shown to have a higher IC_{50} (half maximal inhibitory concentration) value for NO than cells with cytochrome *bo′*, revealing a reduced sensitivity of cytochrome *bd*-I to NO. Recovery rates of respiration were also studied by inhibition with NO, which was subsequently removed by the fast-reacting NO scavenger cPTIO. The recovery rate is thought to be equivalent to the rate of NO dissociation from the oxidases (Sarti *et al.* 2000), so a fast rate of recovery for cytochrome *bd*-I (cells in which cytochrome *bo′* was not present) suggested a rapid k_{off}(NO) for this terminal oxidase, complementing previous *in vitro* work (Borisov *et al.* 2004). The cytochrome *bd*-I recovery rate translated to an NO dissociation rate of 0.163 s^{-1}, similar to that of fully reduced purified cytochrome *bd*-I (Borisov *et al.* 2007). This rate of dissociation is faster than that observed for the majority of haem-proteins (Cooper 1999), and more than five times faster than for cytochrome *bo′* (Mason *et al.* 2009), which explains how cytochrome *bd*-I is able to support aerobic respiration in the presence of NO.

NO is thought to bind at the haem *d* cofactor, as absorption spectroscopy revealed that addition of NO to reduced cytochrome *bd*-I of *E. coli* or *Azotobacter vinelandii* shifts the absorption peak of ferrous haem *d* from 629nm to 641nm, yielding a ferrous iron–NO adduct (Borisov *et al.* 2004). Also a linear relationship between oxygen concentration and IC_{50} of NO (Mason *et al.* 2009) shows that the two gases are in competition with each other, implying that they have the same binding site. If NO-

mediated inhibition of cytochrome *bd*-I is due to binding at haem *d*, a faster rate of NO dissociation will facilitate competing oxygen to bind to haem *d*, so that aerobic respiration can continue in the presence of NO.

The superoxide anion generated by macrophages can combine with nitric oxide to produce peroxynitrite ($ONOO^-$), which is thought to be at high concentrations within the host. Production of $ONOO^-$ is particularly prominent in phagosomes once microbes have been engulfed. Peroxynitrite is a strong nucleophilic oxidant, which can cause damage to DNA, lipid oxidation, protein modifications and ultimately cell death (Pacher, Beckman and Liaudet 2007). Cytochrome *bd*-I in turnover with oxygen has been shown to not only resist $ONOO^-$ damage, but to be capable of rapidly metabolising $ONOO^-$ (Borisov *et al*. 2015), and is thought to be the first example of an enzyme that can metabolise $ONOO^-$ within *E. coli*. A temporary inhibition of cytochrome *bd*-I oxidase after $ONOO^-$ addition has been attributed to generated nitric oxide, as oxygen consumption levels were comparable to those observed when cells were treated with nitric oxide.

1.7 *bd*-type oxidases in the context of bacterial pathogenicity

With a high affinity for oxygen, expression of *bd*-type oxidases is advantageous to bacteria that colonise microaerobic niches at the sites of infection. The host immune system imposes oxidative and nitrosative stresses to combat microbial infections. Cytochrome *bd*-I expression is induced in *E. coli* in the presence of nitrosating species, which suggests a protective role especially in the context of pathogenesis. Indeed, *bd*-type oxidases are expressed in a number of bacterial pathogens such as *Listeria monocytogenes* (Larsen *et al.* 2006), and even anaerobic pathogens such as *Bacteroides fragilis* (Baughn and Malamy 2004). For some pathogens the *bd*-type terminal oxidase is so vital for survival during host colonisation, that it's loss has been shown to attenuate virulence, this is the case for both *Salmonella* (Turner *et al.* 2003) and group B *Streptococcus* (Yamamoto *et al.* 2005).

Brucella abortus (*B. abortus*) is a Gram-negative species that can multiply within macrophage cells and subsequently spread throughout the host. This intracellular pathogen modifies gene expression rapidly to adapt to the hostile environment of macrophage cells. *B. abortus* preferentially utilises a *bd*-type oxidase during intracellular replication (Loisel-Meyer *et al.* 2005). A transposon mutant of *cydB* was

found to have attenuated survival within murine macrophages. Subsequently, *Brucella* cells lacking the oxidase were also shown to be highly attenuated in the mouse model of infection (Endley, Murray and Ficht 2001). The diminished survival of this pathogen is likely to be connected to an inability to cope with the oxidative stress; presented both by the macrophage and due to a build-up of oxidative radicals from the disrupted electron transport chain (Endley, Murray and Ficht 2001). The oxygen-scavenging nature of *bd*-type cytochromes is thought to not only support bacterial survival within low oxygen conditions of phagocytes (James *et al.* 1995), but also doubles up to provide an anti-oxidant function by reducing intracellular oxygen levels (Rezaïki *et al.* 2004). As previously discussed, the role of cytochrome *bd*-I in NO tolerance, as shown for *E. coli* (Mason *et al.* 2009), is also a likely contributing factor to *Brucella* survival through resistance to macrophage-derived nitrosative stress. Other intracellular pathogens, such as *Shigella flexneri* (*S. flexneri*), exhibit a positive correlation between expression of a *bd*-type oxidase and virulence (Way *et al.* 1999), and *Mycobacterium tuberculosis* (*M. tuberculosis*) displays a transient up-regulation of a *bd*-type oxidase during the transition from acute to chronic infection of mouse lungs (Shi *et al.* 2005). With a clear role in virulence of human pathogens, a notable observation is that *bd*-type oxidases are restricted to the prokaryotic world and these respiratory complexes are therefore potential drug targets: in fact studies to find inhibitors have already begun (Mogi and Kita 2009; Mogi *et al.* 2009).

1.8 CydDC in the context of bacterial pathogenicity

The export of reduced low-molecular weight thiols by CydDC plays a role in periplasmic redox balance, and so, is likely to impact upon bacterial virulence. Loss of CydDC in *E. coli* creates a pleiotropic phenotype, including an inability to synthesise functional cytochrome *bd*-I. As discussed above, cytochrome *bd*-I plays a key role in the adaptation of pathogenic strains within the host. It is not known whether deletion of *cydDC* elicits the loss of *bd*-type oxidase assembly in all Gram-negative species, but the major focus of non- *E. coli* research on CydDC has been on a general contribution to bacterial virulence.

The intracellular pathogen, *S. flexneri* depends upon survival within host cells during pathogenesis (Sansonetti *et al.* 1991). Cellular infection, intracellular survival and spread of *S. flexneri* can be studied *in vitro* by infecting confluent monolayers of mammalian cells and comparing the size of resulting bacterial plaques within this cell

monolayer. Disruption of *cydC* was shown to result in impaired pathogenesis as demonstrated by a reduced plaque size when compared to wild type cells (Way, Borczuk and Goldberg 1999). Survival within the monolayer was then determined by counts of bacterial cells recovered from the monolayer, after six hours a reduction in cell count was observed for *cydC* mutant cells, suggesting that a reduction in cell viability is, at least in part, accountable for the small plaque size in the absence of CydDC (Way, Borczuk and Goldberg 1999). In a mouse intranasal model, the lethal dose was 100-fold higher for a *cydC* mutant when compared to that required of wild type cells. As a *cydC* mutant was shown to have only a baseline level of cytochrome *d*, which corresponds to minimal levels of a *bd*-type oxidase, the authors of this study suggest that the reason for reduced virulence of a *cydC* mutant in *S. flexneri* is a lack of cytochrome *bd-I* (Way, Borczuk and Goldberg 1999).

CydDC is also thought to play a role in the virulence of *M. tuberculosis* and has been studied by using a mouse model of infection: bacteria are introduced to the mouse lung, resulting in an acute phase of infection followed by a chronic phase. Expression of the *cydC* gene transiently increases during *M. tuberculosis* infection of a mouse lung, which is thought to correspond to the transition from the acute to chronic phase that is observed in the mouse model. However, up-regulation of the *cydB* gene is even more dramatic than *cydC*, suggesting that CydDC and *bd*-type oxidase structural genes are both up-regulated to enhance oxidase assembly required for pathogen adaptation (Shi *et al.* 2005). Disruption of *cydC* results in a decreased survival in mice during the transition to chronic infection, providing evidence that CydDC is required for adaptation to conditions within the host (Shi *et al.* 2005).

Virulence of *B. abortus* was found to be significantly attenuated in mice when *cydC* was disrupted by a transposon insertion (Truong *et al.* 2014). The same mutant also displayed heightened sensitivity to respiratory inhibitors and a reduced ability to survive and replicate within murine macrophage and HeLa cells. These findings indicate that CydDC confers upon *B. abortus* an ability to cope with the low oxygen availability and environmental stresses associated with intracellular growth. Although one might assume that the role of CydDC during *B. abortus* pathogenesis is to permit synthesis of cytochrome *bd*-I, it is interesting to note that a *B. abortus cydB* mutant can survive up to 8 weeks in a mouse model, compared to only 3 weeks for a *cydC* strain. This work supports a role for CydDC beyond the synthesis of *bd*-type oxidases that can facilitate survival within the host environment.

1.9 Hypotheses and project aims

The overarching goal for this work is to gain a deeper understanding of the role of CydDC in *E. coli*. This includes analysing the changes that occur in the cell when CydDC is absent, with particular attention to one of the most important phenotypes of a *cydDC* mutant; the loss of functional cytochrome *bd*-I.

Since cytochrome *bd*-I contributes to NO tolerance by virtue of a fast dissociation rate, it was hypothesised that CydDC would also have a role in NO tolerance due to the requirement of CydDC for cytochrome *bd*-I functionality. In addition to this, the CydDC substrates GSH and cysteine are thiols that can react with incoming NO, so it was also anticipated that CydDC might provide a greater contribution to NO tolerance than cytochrome *bd*-I alone. A major aim was to assess the relative contribution of CydDC and cytochrome *bd*-I to NO tolerance.

The majority of *cydDC* mutant phenotypes can be restored by one of the two known substrates of CydDC, reduced glutathione or cysteine. Phenotypes that can be complemented in this way include loss of motility, the sensitivity to dithiothreitol and benzylpenicillin as well as the absence of holocytochrome *c* and periplasmic cytochrome b_{562}. The restoration of cytochrome *bd*-I, however, has not been shown in the presence of either reduced glutathione or cysteine at a range of concentrations. Due to the promiscuous nature of ABC-type transporters, it was hypothesised that additional unknown substrates may exist for CydDC that are required for cytochrome *bd*-I assembly. Alternatively, it was hypothesised that the export of both cysteine *and* glutathione is required for cytochrome *bd*-I assembly. A major aim was to identify conditions that could complement the loss of cytochrome *bd*-I in a *cydDC* mutant, and then, to gain insights into the physiological changes induced under these conditions via performing transcriptomic analyses.

If CydDC is indeed important for tolerance to NO, one would expect that this transporter would have a substantial role in bacterial pathogenesis as loss of CydDC would not only elicit NO sensitivity, but would also perturb the redox environment of the periplasm leading to a detrimental effect on the folding of extracytoplasmic virulence factors. It was therefore hypothesised that CydDC would be important for colonisation of the host by pathogenic strains. Hence, another major aim of this work was to evaluate the role of CydDC during *in vivo* survival of clinical isolates using macrophage survival assays and a mouse infection model.

Chapter 2

Materials and Methods

2.1 Bacteriological methods

2.1.1 Bacterial strains, plasmids and oligoncleotides

E. coli strains and plasmids as used in this study are listed in Table 2-1. Oligonucleotides used in this study are listed in Table 2-2.

***E. coli* Strain**	**Characteristics**	**Reference or source**
AAEC554	MG1655 *fimB+ fimE+ fimL1*; invertible element locked on	McClain & Blomfield, 1993
BGEC487	MG1655 Δ*fim* Δ*lac* Ω[*sacB* -Kan^{R}]; Afim	Kulasekara & Blomfield, 1999
MS2	MG1655; *Escherichia coli* K-12	Bachmann 1996
MS1	CFT073; UPEC wild type pyelonephritis strain	Welch *et al.* 2002
MS5	CFT073 but harbouring pKD46	MS1180 from Prof. Mark Schembri
MS10	EC958; UPEC wild type belonging to clonal group sequence type 131, CTX-M-15, CMY-23	Totsika *et al.* 2011
MS13	MG1655 *cydAB*::Km	MS3666 from Prof. Mark Schembri
MS14	MG1655 *cydDC*::Cm	MS3671 from Prof. Mark Schembri
MS15	MG1655 *cydAB*::Cm	MS3672 from Prof. Mark Schembri

MS16	ST131 EC958 *cydAB*::Cm	MS3673 from Prof. Mark Schembri
MS17	CFT073 *cydAB*::Cm	MS3684 from Prof. Mark Schembri
MS52	BW25113 F^-, Δ(*araD-araB*)567, Δ*lacZ*4787(del)::*rrnB*-3, LAM^-, *rph*-1, Δ(*rhaD-rhaB*)568, *hsdR*514	Keio collection- Baba *et al.* 2006
MS53	BW25113 *cydB*::ΩKm	Keio collection- Baba *et al.* 2006
MS54	BW25113 *cydD*::ΩKm	Keio collection- Baba *et al.* 2006
MS115	CFT073 *cydDC*::Cm	This work
MS271	ST131 EC958 *cydDC*::Cm. MS19 with pKOBEG removed	MS3924 from Prof. Mark Schembri
MS336	MG1655 *cydAB- cydDC*::Cm	This work
MS3899	EC958 type 1 enriched	Prof. Mark Schembri
MS3907	EC958*cydAB*::Gm type 1 enriched	Prof. Mark Schembri
MS6016	EC958*lac*::*mkate*-Cm type 1 enriched	Prof. Mark Schembri
MS6110	EC958*cydDC*::Gm type 1 enriched	Prof. Mark Schembri
Plasmids		
pCP20	*FLP*$^+$, Ts replicon, Amp^R, Cm^R	Cherepanov and Wackernagel 1995
pKD3	Cm^R flanked by FRT sites	Datsenko and Wanner 2000
pKD4	Km^R flanked by FRT sites, Amp^R	Datsenko and Wanner 2000
pKD46	λ-Red recombinase plasmid Ts replicon; Amp^r	Datsenko and Wanner 2000
pKOBEG	λ-Red recombinase, Ts replicon, araC, arabinose-inducible, Gm^R	Chaveroche, Ghigo and D'Enfert 2000

Table 2-1 *E. coli* strains and plasmids

Name	5' - 3' Sequence	Use	Direction
P1	TCGTTTTGCCGGATTATGGG	For checking *fim* switch orientation	Forward
P2	AGTGAACGGTCCCACCATTAACC	For checking *fim* switch orientation	Reverse
pMS35	AACGGCAACATCATTCTGCACACCAA	Mutagenesis primer for *cydDC*, anneals 500bp upstream of *cydD* start codon	Forward
pMS36	GCTCATCTTCACGCCAGACTTCAAT	Mutagenesis primer for *cydDC*, anneals 500bp downstream of *cydC* stop codon	Reverse
pMS3	TCGCCAGGCCATTACATCTG	*cydDC* fwd screening primer, anneals 200 bp upstream of *cydD* start codon.	Forward
pMS4	GGATGGGGTCGCCTGGAGAA	*cydDC* rev screening primer, anneals 200 bp downstream of *cydC* stop codon	Reverse
pMS9	TAAGGATTTTGCGGCGTAAT	*cydAB* fwd screening primer, anneals 200 bp upstream of *cydA* start codon	Forward
pMS10	CCATCACGAAGGAAAGCGCC	*cydAB* rev screening primer, anneals 200 bp downstream of *cydB* stop codon	Reverse

Table 2-2 of Oligonucleotide sequences

2.1.2 Chemicals and water

Reagents were purchased from Sigma or Melford (unless otherwise stated). Nutrient agar, yeast extract and tryptone were purchased from Oxoid. Distilled-deionised water was used throughout this work. Milli-Q water was used wherever a greater level of purity was necessary. For RNA work milli-Q water was used, however, it was essential that it had been treated with diethyl pyrocarbonate (DEPC) prior to use.

Media and solutions of a volume in excess of 50 ml were sterilised by autoclaving at 121^{o}C at 15 psi (pound-force per square inch) for 15 minutes. Antibiotic stock solutions and solutions with a volume of less than 50 ml were filter-sterilised using Millipore filters with a pore size of 0.22 μm.

2.1.4 Oligonucleotide sequences

Oligonucleotides (Table 2-2) were designed and then checked using OligoCalc: Oligonucleotide properties calculator to ensure no secondary structure is present within each oligonucleotide and that G/C content is appropriate. Oligonucleotides were produced by MWG-biotech.

2.1.5 Media and buffer solutions

2.1.5.1 Acetonitrile buffer extraction solution

For metabolite extraction, an extraction solution was made. Acetonitrile and $Na^{+}K^{+}$ buffer (pH 7.4) were mixed together in equal volumes. $Na^{+}K^{+}$ buffer was made by mixing 10 ml 0.1 M NaH_2PO_4 with 40 ml 0.1 M K_2HPO_4 and pH was checked.

2.1.5.2 Defined medium

Defined media (Flatley *et al.* 2005) contained 4g K_2HPO_4, 1g KH_2PO_4, 1g NH_4Cl, 0.01g $CaCl_2$, 2.6g K_2SO_4, 5g glycerol per litre (52 mM) supplemented with 0.1% (w/v) casamino acids and 10ml trace elements.

Trace elements solution was prepared by dissolving 5g Na_2EDTA in 800ml milli-Q water, the pH was adjusted to between pH7.0- 8.0. The following were then added; 0.5g $FeCl_2.6H_2O$, 0.05g ZnO, 0.01g $CaCl_2.2H_2O$, 0.01g $CoNO_3.6H_2O$, 0.01g H_3BO_3 and 0.01g ammonium molybdate. Milli-Q water was used to make up to 1 litre before filter sterilisation of the solution.

1 M $MgCl_2$ stock was added just before use of the media at a final concentration of 1 mM/ml.

2.1.5.3 Luria Bertani medium

Luria Bertani medium (LB) medium contained 10g tryptone, 5g yeast extract and 10g NaCl per litre. pH was adjusted to 7.0 using NaOH (Sambrook and Russel, 2001).

2.1.5.4 MOPS (3-(*N*-morpholino)-propanesulphonic acid) buffer

To prepare a 50x stock solution one litre of DEPC water contained 0.2 M MOPS (pH 7.0), 20 mM sodium acetate anhydrous and 10 mM EDTA (pH 8.0). The MOPS was first added to 700 ml DEPC-H_2O and pH adjusted to 7.0. The sodium acetate was then added to this solution, followed by EDTA which had been dissolved in a small volume of DEPC-H_2O and adjusted to pH 8.0. The total volume was then made up to 1l before filter sterilising using a Millipore 0.45 μm filter and stored away from light due to the light sensitive nature of MOPS.

2.1.5.5 MOPS minimal media (Neidhardt, Bloch and Smith 1974)

A 10x stock of MOPS was made by mixing 83.72g MOPS and 7.17g tricine in 300 ml milli-Q water, to this 10 M KOH was added dropwise until a pH of 7.4 was reached. Water was added to make a volume of 440 ml before the addition of 10 ml 0.01M $FeSO_4.7H_2O$. The following were then added; 50 ml 1.9 M NH_4Cl, 10 ml 0.276 M K_2SO_4, 0.25 ml 0.02 M $CaCl_2.2H_2O$, 2.1 ml 2.5 M $MgCl_2$, 100 ml 5 M NaCl, 0.2 ml micronutrient stock and 387 ml autoclaved milli-Q water. The 10x stock of MOPS was then filter sterilised and aliquoted into flacon tubes as 50 ml portions.

The micronutrient stock used to make 10x MOPS was made by adding 0.009g ammonium molybdate, 0.062 H_3BO_3, 0.018g $CoCl_2$, 0.006g $CuSO_4$, 0.040g $MnCl_2$, 0.007g $ZnSO_4$ to 50ml milli-Q water.

MOPS minimal media was made by mixing 5 ml 10x MOPS stock with 0.132M K_2HPO_4 in 50 ml milli-Q water. pH was adjusted to 7.4 by adding 10 M NaOH dropwise. The resulting solution was filter sterilised and stored at 4°C for up to one month. Before use glucose was added at a final concentration of 40 mM.

2.1.5.6 M9 minimal media

1 litre of 5x stock of M9 salts contained; 80.24g $Na_2HPO_4.2H_2O$, 15g KH_2PO_4, 2.5g NaCl and 5g NH_4Cl. M9 media contained 200 ml 5 x M9 salts, 2 ml filter sterilised 1 M $MgSO_4$, 100 µL filter sterilised 1M $CaCl_2$, 20 ml filter sterilised 20% glucose and 778 ml autoclaved water.

2.1.5.7 Potassium phosphate buffer (pH7.4)

0.1M potassium phosphate buffer (pH7.4) was made by mixing 802 ml of 0.1 M K_2HPO_4 and 198 ml of 0.1M KH_2PO_4 and checking final pH.

2.1.5.8 SOB media

To make SOB media, 20g tryptone, 5g yeast extract, 0.584g NaCl and 0.186g KCl were added to 990ml milli-Q water and autoclaved. Once cooled 10ml filter sterilised 2M Mg^{2+} stock was added.

2.1.5.9 SOC media

To prepare SOC media, 20g tryptone, 5g yeast extract, 0.584g NaCl and 0.186g KCl were added to 970ml milli-Q water and autoclaved. Once cooled 10ml filter sterilised 2M Mg^{2+} stock was added and 20ml 1M glucose stock.

2.1.5.10 Yeast extract-peptone-glycerol media (YPG)

YPG media contained per litre milli-Q water; 10g bacto yeast extract (Difco), 20g bacto peptone (Difco), and 30 ml glycerol.

2.1.6 Media supplements

2.1.6.1 Antibiotics

Media were supplemented, where indicated, with ampicillin (125 µg/ml), kanamycin (25 µg/ml), chloramphenicol (25 µg/ml), gentamycin (20 µg/ml) or tetracycline (10 µg/ml).

2.1.6.2 Casamino acid solution

A 10% (w/v) stock solution of casamino acid solution was prepared by the addition of dried casamino acids to water and was then filter sterilised using a 0.22μm Millipore filter.

2.1.6.4 Nutrient agar

One litre of medium contained 15g dried nutrient agar.

2.1.6.5 Tris buffers

All Tris buffers contain Trizma base and the resulting buffer was adjusted to the desired pH using 1M HCl.

2.1.7 Culture conditions

Cultures were typically grown at 37^{o}C in LB at an initial pH of 7.0 (Sambrook and Russel, 2001). Cultures were inoculated with 1% (v/v) using an overnight starter culture. Agar plates were inverted and incubated overnight at 37^{o}C.

Aerated cultures were grown by shaking at 180 rpm in conical flasks containing one-tenth of their own volume of medium.

2.1.7.1 Measuring culture optical density

Culture optical density at 600 nm was measured using a Shimadzu UV-1800 spectrophotometer in cells with a 1 cm path length.

2.1.7.2 Preparing *E. coli* glycerol stocks

0.75 ml 50% autoclaved glycerol was pipetted up and down within a fresh cryotube vial to make the glycerol more viscous, 0.75 ml stationary phase culture was then added and strains stored at -80^{o}C

2.1.8 NOC-12 growth curves

2.1.8.1 NOC-12 Preparation

Growth curves were carried out using NOC-12 (Calibochem), a donor of nitric oxide. NOC compounds are relatively stable NO-amine complexes that spontaneously release NO. NOC-12 is a relatively slow releaser of NO with a half-life of 100 minutes at 37ºC, pH 7.4. In this work NOC-12 was dissolved in 80 mM sodium phosphate buffer (pH 8.0) and prepared immediately before use. The 80 mM phosphate buffer (pH 8), was made by mixing 46.6 ml 80 mM Na_2HPO_4 with 3.4 ml 80 mM $NaH_2PO_4.H_20$. The buffer was pH checked before being filter sterilised, aliquoted and stored at 4ºC. A range of NOC-12 concentrations between 0.1 mM and 0.75 mM were used to ensure an effect on growth would be observed.

2.1.8.2 Bacterial growth in the presence of NOC-12

Initially bacterial strains used were from the Keio collection (Datsenko and Wanner 2000). Stationary phase cultures grown in defined medium (Flatley *et al.* 2005) as described in Section 2.1.5.2 and supplemented with 0.1 % casamino acids and antibiotics where appropriate were used to inoculate fresh defined medium (Flatley *et al.* 2005) which was aliquoted as volumes of 200 µl into 96-well plates. Cells were grown at 37ºC, 200 rpm in a plate reader (SPECTROstar nano) with growth measured every 30 minutes at OD_{600} for 25 hours. Freshly prepared NOC-12 at a volume to give the desired final concentration was added to wells after an hour and a half of growth. In control wells where NOC-12 was not added, 80 mM sodium phosphate buffer (pH 8.0) was added to compensate for the reduction in OD_{600} of test wells and to ensure no growth affect by the buffer.

2.1.9 Yeast Agglutination assay

A quick method for investigating the expression of Type 1 fimbriae. Yeast strain BY4741 (Flatley *et al*. 2005) was grown at 30ºC 180 rpm to stationary phase in 10 ml YPG media in a 50 ml falcon tube. The culture was then pelleted at 3500 rpm for 5 minutes at 4ºC and re-suspended in 1ml MOPS, aliquoted in 100 µl and stored at 4ºC until needed.

For the assay 10 µl yeast solution was mixed with 10 µl of *E. coli* sample (in stationary phase after growing at 37ºC overnight) on a microscope slide and left for 5 minutes. The mixture was analysed using a light microscope (Leica MZ 75). A consistent zoom was used to collect all samples. Images were saved at maximum resolution.

2.2 Genetic methods

2.2.1 Isolation of plasmid DNA

Plasmid DNA was isolated from bacterial strains using a Wizard Plus SV 'miniprep' DNA purification kit (Promega). The manufacturers' instructions were followed for use with a centrifugation. All centrifugation and filtrations were carried out at room temperature. Following the initial pelleting of overnight cultures in an Eppendorf centrifuge 5418 at 6,000 x *g* for 10 minutes, all centrifugation steps were carried out in an Eppendorf 5415R microcentrifuge at 13,000 rpm (maximum speed).

2.2.2 Polymerase chain reaction (PCR)

For colony PCR, a colony was diluted in 50 µl sterile water, and 1 µl of this was used as a DNA template in the reaction. A typical reaction contained within a 50 µl volume; 300 nM (1.5 µl of a 10 µM stock) of each primer (forward and reverse), 1 µl of ready mixed 10 mM dNTPs, 5 µl 10x PCR buffer, and sterile distilled water (roughly 39.5 µl) was used to make the end volume 50 µl. Finally 0.5 µl Taq polymerase was added to the mix and PCR tubes were transferred to a Techne progene PCR machine. The PCR programme used was one cycle of 94ºC for 4 minutes, then 35 cycles of 94ºC for 15 seconds, 55ºC for 30 seconds and 72ºC with a time depending on the length of PCR product required and polymerase enzyme used. A final elongation at 72ºC for 7 minutes for one cycle finished the PCR reaction.

2.2.3 DNA electrophoresis on agarose gels

Electrophoresis was performed in a gel apparatus at a constant voltage of 120 V in 1 x TAE buffer (a 1:50 dilution of a 50 x TAE stock solution consisting of 242g Trizma base, 57.1 ml glacial acetic acid and 100 ml 0.5M NaEDTA (pH 8.0) per litre giving final concentrations of 40 mM Tris-acetate and 1 mM NaEDTA as described in

Sambrook and Russell (2001)). Gels were composed of 1 % agarose dissolved in 1 x TAE buffer, and 1 µl of 6x loading dye (New England Biolabs) was mixed with 5 µl of sample before being added to gel wells. A 1 kb ladder (Promega) was resolved on each gel to determine the size of sample DNA fragments. When the concentration of samples was also required, hyperladder 1 (Bioline) was used instead. Gels were stained in 100 ml water with 5 µl ethidium bromide, rocking for 30 minutes before visualising bands on a UV box.

2.2.4 λ-Red mutagenesis

The procedure described by Datsenko and Wanner in 2000 was used to replace the *cydDC* operon of *E. coli* CFT073 with an antibiotic resistance cassette. Recombination between the genome and a PCR product was achieved using the phage λ-Red recombinase system, which is synthesised under the control of an arabinose inducible promoter on an easily curable, low copy number plasmid pKD46.

2.2.4.1 *cydDC* gene knockout in CFT073 background

A PCR product was amplified using primers pMS35 and pMS36 with a K-12 *cydDC*::Cm strain used as a template to produce a fragment consisting of the chloramphenicol cassette flanked either side by 500 bp of the sequences before and after the *cydDC* operon. This PCR product was then concentrated and purified by excision on an agarose gel before being introduced into CFT073 cells via electroporation.

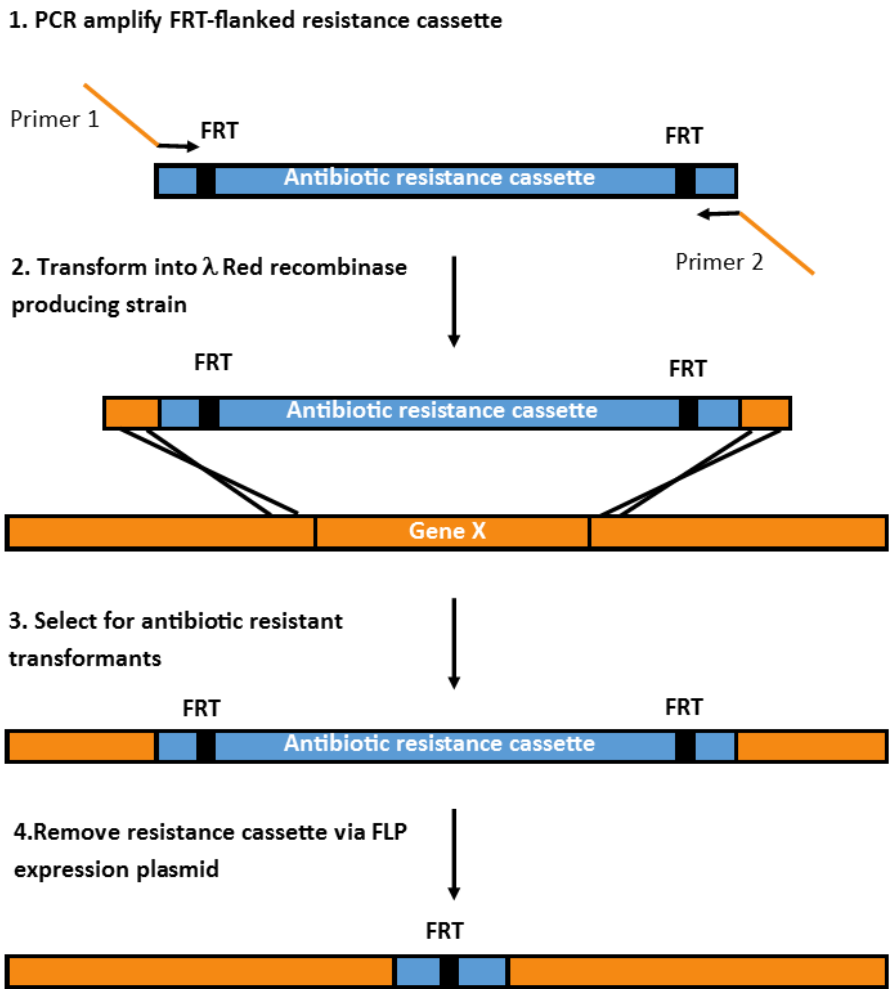

Figure 2-1. λ-Red mutagenesis
Strategy used to disrupt gene sequence using λ-Red recombinase expression. **1**. Primers (pMS35 and pMS36, Table 2-2) were designed to produce, via PCR, a DNA fragment encoding the chloramphenicol resistance cassette flanked by 500 bp regions homologous to areas flanking gene X (orange). **2**. DNA fragment was transformed into cells expressing λ-Red recombinase to encourage recombination between the DNA fragment and the genome. **3**. Transformants were selected on antibiotic plates. **4**. The resistance cassette of transformants was excised by the plasmid-encoded FLP recombinase which acts upon the FRT (FLP recognition target) repeats that flank the resistance gene.

2.2.4.2 Preparation of electro-competent cells

Competent cells were made using a recipient strain (MS5) containing the temperature sensitive plasmid pKD46 (Amp^R) that comprises the λ-Red recombinase to enhance recombination between the PCR product and the genome. In a 250 ml conical flask containing 50 ml SOB media supplemented with ampicillin and 20 mM arabinose, recipient strain cells were grown at 28°C, 180 rpm until an OD_{600} between 0.4- 0.8 was

reached. From this point on the cells were kept cold. Cells were transferred to chilled 50 ml falcon tubes and spun at 3000 x g at 4ºC for 10 minutes. Supernatant was removed and the pellet was re-suspended in 5 ml ice-cold 10% glycerol by gently pipetting up and down with cut 1ml pipette tips. Cells were washed in 10% ice-cold glycerol in this way three more times before being re-suspended in a final volume of 200 µl 10% ice-cold glycerol, this was kept on ice until it was used in electroporation.

2.2.4.3 Transformation by electroporation

The concentration of PCR product was measured via nanodrop to determine the volume needed to add 1000 ng of DNA. This calculated volume was then placed into a chilled 2 mm electroporation cuvette. Then 50 µl of competent cells were added and the cuvette tapped to ensure the mix moved to the bottom of the cuvette. The electroporator was set to 2.45kV with a resistance of 200 Ω and a capacity of 25 µF, the cuvette was then placed into shocking chamber for pulsing.

1 ml SOC media was added immediately to aid cell recovery and cell mix was transferred to a 1.5 ml Eppendorf tube and incubated at 37ºC 180 rpm for one hour. Cells were then plated onto chloramphenicol LB plates to select for transformants. Resulting colonies were checked by colony PCR using primers pMS3 and pMS4.

2.2.5 Sequencing of DNA

DNA samples were sequenced by Source Bioscience and were then examined and aligned using the sequence analysis program BioEdit (7.2.5).

2.2.6 Curing of Chlorampenicol resistance cassette

To create the *cydDC cydAB* double mutant used in microarray experiments, a single mutant needed to be cured of the resistance cassette so that a second deletion could be detected.

This process required the pCP20 plasmid (Table 2-1) which encodes a flippase enzyme (FLP) for removal of the antibiotic resistance cassette. pCP20 is ampicillin and chloramphenicol resistant and also shows temperature-sensitive replication and thermal induction of FLP synthesis, so growth was performed at 28ºC (Baba *et al*. 2006).

2.2.6.1 Preparation of competent cells (Brachmann *et al*. 1998).

Cells were grown in 10ml LB overnight at 37ºC, 28 µl of this culture was then used to inoculate 28 ml pre-warmed LB (37ºC) and then incubated shaking at 37ºC until an OD_{600} of ~0.48 was reached. A volume of 3.75 ml warm sterile 100% glycerol was added drop-wise to cells while swirling to aid mixing. Cells were then chilled on ice for 10 minutes before pelleting at 4ºC 4000 rpm. The supernatant was removed and the pellet was re-suspended in 25 ml ice-cold magnesium chloride solution (freshly made before use from 2.5 ml 1M $MgCl_2$, 3.75 ml sterile 100% glycerol made up to 25 ml with milli-Q water). Cells were pelleted again for 8 minutes at 4ºC 3800 rpm before being re-suspended in 6.25 ml ice-cold T-salts solution (freshly made before use by mixing 1.5 ml sterile 100% glycerol, 0.75 ml 1M $CaCl_2$, 0.06 ml 1M $MgCl_2$, made up to 10 ml with milli-Q water). Cells were pelleted one last time for 6 minutes 4ºC 3600 rpm before being re-suspended in 1.25 ml ice-cold T-salt solution. Cells were aliquoted into 100 µl volumes into pre-cooled Eppendorf tubes and stored immediately at -80ºC. Cells were left at -80ºC overnight before being used.

2.2.6.2 Transformation with plasmid

100 µl of competent cells were mixed with 2 µl plasmid solution, this mixture was then incubated on ice for 30 minutes before being heat shocked at 42ºC for 30-60 seconds in a heat block. A volume of 1 ml SOC medium was then added immediately to cells to aid recovery, before incubating for a further one hour, shaking (180 rpm) in a water bath at 28ºC. A volume of 200 µl was plated onto ampicillin Luria Bertani (LB) plates to select for pCP20. Ampicillin resistant colonies were then grown for 3 hours in LB at 42ºC, plated out onto plain LB plates and further grown overnight at 42ºC to ensure removal of the pCP20 plasmid. Colonies were picked and streaked onto LB, LB-ampicillin and LB-kanamycin plates. Colonies that could only grow on LB plates were expected to be cured of the kanamycin resistance cassette as well as the pCP20 plasmid, and so were grown and glycerol stocked. The removal of the cassette was then checked by PCR.

2.2.7 Microarray analysis

All reagents were prepared using milli-Q water treated with 0.1% DEPC stirring overnight to remove RNases that may degrade RNA. After overnight treatment, DEPC milli-Q water was autoclaved to eliminate toxicity. The microarrays detailed in this

work were carried out using a 'Two-Colour Microarray-Based Prokaryote Analysis" by Agilent Technologies, Inc. 2009. All solutions described in Section 2.2.7.6 were obtained from Agilent Technologies, unless otherwise stated.

2.2.7.1 Growth conditions

Strains used in the microarrays had an MG1655 background. Starter cultures (10 ml) were grown to stationary phase in LB with chloramphenicol (25 µg/ml), 0.5 ml was used to inoculate 50 ml of defined chemostat medium supplemented with 0.1% (w/v) casamino acids. Cells were grown in triplicate in 250 ml conical flasks at 37ºC 180 rpm.

2.2.7.2 Sampling and RNA stabilisation

Once an OD_{600} of 0.4 was reached, 30 ml of culture was removed and added to 187.5 µl chilled phenol and 3.56 ml chilled ethanol and immediately mixed by vortex for 5 seconds. After incubating on ice for 5 minutes, samples underwent centrifugation at 5500 x *g* (7000 rpm) for 5 minutes at 4ºC. Supernatant was removed and remaining pellet was stored at -80ºC.

2.2.7.3 RNA isolation

RNA was isolated from pellets using a Qiagen 'RNeasy Mini Kit' according to the manufacturer's instructions. Sample pellets were thawed on ice then re-suspended in 200 µl of TE buffer containing lysozyme (1mg/ml) and vortexed for 10 seconds followed by an incubation at 25ºC shaking (180 rpm) for 5 minutes. RLT buffer (700 µl) containing β-mercaptoethanol (10 µl/ml) was added before vigorous vortexing and the addition of 0.5ml 100% ethanol. Mixed by pipetting, the lysates were applied to RNeasy Mini columns placed in a 2ml collection tube, then centrifuged for 15 seconds at 10,000 rpm and the flow through was discarded. Buffer RW1 (350 µl) was added to the column, followed by centrifugation for 15 seconds at 10,000 rpm, the flow through was discarded. To remove DNA a mixture of 10 µl DNaseI and 70 µl buffer RDD was added directly onto the RNeasy silica gel membrane and incubated at room temperature for 15 minutes. After digest, buffer RW1 (350 µl) was added to the column and a further 5 minute room temperature incubation before centrifugation for 15 seconds at 10,000rpm. Both the flow through and collection tube were discarded. Transferred to a fresh 2ml collection tube, the column was washed twice with 500 µl buffer RPE. The column was transferred to a fresh, RNase free 1.5 ml Eppendorf tube, 30 µl of RNase

free water was pipetted directed onto the RNeasy silica gel membrane before centrifugation at 10,000 rpm for 1 minute. To increase RNA yield, the eluate was replaced onto the membrane with a 1 minute pause before repeating the centrifugation at 10,000 rpm for 1 minute. A volume of 2 µl of the RNA was aliquoted while the rest was stored at -80^{o}C.

2.2.7.4 RNA determination

The concentration of RNA was determined using a Nanodrop ND-1000 UV-VIS spectrophotometer accompanied with programme ND-1000 version 3.1.2. After blanking the instrument with 2 µl nuclease free water, 2 µl of RNA sample was added to the pedestal, and its concentration and purity measured. The ratio of OD_{260} /OD_{280} should be around 2, if lower, this may suggest contamination from protein and the sample would have been discarded, this however was not necessary.

2.2.7.5 Complementary DNA (cDNA) synthesis

For each sample, 12.3 µl RNA (16 µg) was incubated in a PCR block with random primers (5 µg) at 72^{o}C for 10 minutes and then chilled on ice for a further 10 minutes. For cDNA synthesis, primed RNA was added to a reaction mix consisting of 6 µl 5x first strand buffer (Invitrogen), 3 µl 0.1M DTT (Invitrogen) 0.6 µl 50x dNTP master mix (0.1 mM dATP, dGTP, dTTP and 0.05 mM dCTP) (Roche) and 2.9 µl nuclease free water (Qiagen). Samples were then taken into a dark room, and treated with 2 µl of either Cy3 or Cy5 dye (with a technical repeat for each, where the dyes were swapped.) Superscript III (1.5 µl 200U μl^{-1}) was added to each sample followed by 5 minutes incubation at 25^{o}C. Samples were then taken from dark room for an overnight incubation in a PCR machine at 50^{o}C. RNA was hydrolysed by addition of 15 µl freshly prepared 0.1M NaOH and incubation at 72^{o}C for 10 minutes. To neutralise samples, freshly prepared 15 µl 0.1M HCl was added. The labelling reactions were clean up using a QIAquick PCR purification kit (Qiagen) according to manufacturer's instructions. Buffer PB (without pH indicator) was added to samples at a volume ratio of 5:1 and inverted to mix. The mix was then transferred to a spin column in a 2 ml collection tube and centrifuged for 1 minute at 10,000 rpm. The flow through was discarded and the column was washed twice with 750 µl buffer PE. To ensure the removal of all liquid, the column was replaced into the same collection tube and centrifuged for a further 1 minute at 10,000 rpm. For cDNA elution, the column was

transferred into a fresh nuclease free 1.5 ml Eppendorf, 50 µl of nuclease free water was applied to the centre of the membrane and centrifuged for 1 minute at 10,000 rpm. To measure concentration of single stranded cDNA, 1.5 µl of labelled cDNA was denatured by heating to 95ºC for 5 minutes. cDNA was quantified by using a Nanodrop ND-1000 UV-VIS spectrophotometer version 3.2.1 against a nuclease-free water blank. Samples were suitable for hybridisation if the yield was over 400 ng.

2.2.7.6 Hybridisation of labelled cDNA to array slides

An appropriate volume of each cDNA was calculated to give a final concentration of 400 ng. 400 ng of Cy3- labelled cDNA was added to 400 ng of Cy5-labelled cDNA for each dye swap, the total volume was then made up to 20 µl using nuclease free water. Samples were boiled at 100ºC for 2 minutes, then placed onto ice for 2 minutes before being placed at room temperature for a further 2 minutes. Samples were centrifuged briefly to collect condensation from around the edge of the tubes. Ensuring that no air bubbles were introduced to the mixture, 5 µl 10x blocking agent and 25 µl GEx hybridisation buffer were added to make a final volume of 50 µl. The samples were centrifuged for 1 minute at 13000 rpm before loading onto slides.

A clean gasket slide was placed into the Agilent SureHyb chamber base with the 'Agilent' label facing upwards. 40 µl of hybridisation sample was slowly dispensed onto the gasket, ensuring that the tip of the pipette did not directly touch the slide. The array was then placed 'active side' down onto the SureHyb gasket slide so that the slide went over the gaskets flat, preferably with no air bubbles as this would hinder hybridisation. The SureHyb chamber cover was then placed onto the sandwiched slides and clamped together. The assembled chamber was then placed into a hybridisation oven set to 65ºC, rotating at 10 rpm for 17 hours.

The array-gasket sandwich was removed from the hybridisation chamber and submerged in wash buffer 1 at room temperature. The sandwich was prised open. The exposed array slide was then transferred to fresh buffer 1 in a dish with a magnetic stirrer to stir the buffer for 1 minute. The array slide was then transferred to a dish containing pre-warmed buffer 2 (37°C), and the buffer was stirred for 1 minute. The slide was then scanned immediately (to minimise the impact of environmental oxidants

on signal intensities) in an Agilent DNA microarray scanner. Data was extracted using Agilent software ready for analysis in GeneSpring (v13.1).

2.2.7.7 Data analysis of Microarrays

The average signal intensity and local background correction were obtained using GeneSpring software (v13.1). The mean values from each channel were transformed and normalised using the Lowess method to remove intensity-dependent effects in the $\log_2$ (ratios) values. The Cy3/Cy5 fluorescent ratios were calculated from the normalised values. Biological experiments, were carried out twice and dye-swap analysis performed on each experiment providing four technical repeats, two from each biological experiment. Genes differentially regulated ≥2 fold and exhibiting *P*-values of ≤0.05 (by means of *t*-test) were defined as being statistically and differentially transcribed.

2.2.7.8 Modelling changes in transcription factor activities that result from exogenous addition of GSH and cysteine

Mathematical modelling of the microarray data was carried out using TFinfer version 2.0 (Shahzad Asif *et al.* 2010). This open access programme is based on a state space model and enables the activity of transcription factors to be inferred from gene expression data obtained from microarray experiments. The complete transcriptomic data-sets obtained from GeneSpring were used for the analysis; therefore no limitations with regard to gene expression level were enforced prior to the application of TFinfer.

Data was input alongside a null hypothesis consisting of zeros, the output data from TFinfer was then compared to this null hypothesis 'data'. Transcription factors with a difference between the null data set larger than 2 were considered significant.

TFinfer cannot assign whether activity of transcription factors is up or down, so this has to be corrected manually. To do this information on transcription factor function was obtained from Ecocyc and RegulonDB, this involved looking at the genes with each TF regulon and finding out if the TF acts as a repressor or activator of transcription. Fold-changes of genes within the regulons of significant transcription factors were looked at in the raw data to see if fold-changes were positive or negative, and depending upon whether the TF is an activator or repressor, activity signs could be determined, for example; if a transcription factor acts as a repressor to genes with a positive fold-

change, it can be concluded that the transcription factor activity is reduced, and a negative sign is manually placed in front of the change in activity value.

2.3 Biochemical methods

2.3.1 CO difference spectra

10 ml LB cultures (with appropriate antibiotics) were grown at 37ºC and 180 rpm overnight. Overnight cultures were then used to inoculate 100 ml LB in 250 ml conical flasks. Cells were grown to stationary phase at 150 rpm 37ºC. Two 45 ml samples were taken from each conical flask and cells were harvested at 4000 rpm for 10 minutes at 4ºC before being re-suspended in 1 ml 0.1 M potassium phosphate buffer (pH 7.4). Further dilutions were made where required to generate appropriate cell densities for whole cell 'CO reduced' *minus* 'reduced' spectra (i.e. CO difference spectra) to be recorded.

A custom-built SDB4 dual wavelength scanning spectrophotometer was used (Sambrook, Fritsch and Maniatis. 1989) to obtain CO *minus* reduced difference spectra (400nm- 700nm) at room temperature. The whole cell samples were first reduced with sodium dithionite and scanned, then bubbled with CO gas for five minutes before being scanned again. Each reduced reading was then subtracted from the corresponding 'CO reduced' reading to give a CO difference spectrum.

2.4 ^{1}H NMR metabolomics

2.4.1 Growth of cells

4 ml of stationary phase culture was used to inoculate 400 ml defined medium (Flatley *et al.* 2005) supplemented with 0.1 % casamino acids in 2 litre flasks. Six flasks for wild type, six flasks for *cydD*. Cells were grown at 37ºC 180 rpm to emulate the microarray growth conditions.

2.4.2 Metabolite extraction

Cells were harvested at an OD_{600} of 0.4 by centrifugation (6000 rpm 5 minutes 4°C) and the supernatant was decanted. The cell pellet was washed three times with 1 ml of ice-cold phosphate buffered saline (PBS), and cells were then snap frozen with liquid nitrogen and stored at -80ºC until metabolite extraction. Frozen samples were

homogenised in 600 µl ice-cold acetonitrile buffer extraction solution (Section 2.1.5.1). Homogenates were then snap frozen in liquid nitrogen and subjected to three rounds of freeze-thaw cycles with vigorous pipetting and vortexing. Samples were then sonicated on ice with two seconds pulse/two seconds rest for 99 cycles. Sonicated samples were centrifuged for 10 minutes at 12000 rpm 4ºC, and the supernatant collected. The remaining pellet was re-suspended in 500 µl acetonitrile extraction solution and vortexed for further metabolite extraction, and the resultant supernatant was pooled with that from the first extraction. The supernatants were condensed using a vacuum desiccator to remove acetonitrile, and samples were then stored at -80^{o}C until NMR analysis.

2.4.3 Proton NMR data collection

Samples were dissolved in a mixture of 590 µl deuterated water (D_20) and 10 µl 6 mM DSS (4,4-dimethyl-4-silapentane-1-sulfonic acid) (added as an internal standard to calibrate the chemical shift). After centrifugation for 2 minutes at 14000 rpm to clear any debris, 550 µl of this mixture was pipetted into NMR tubes (5 mm outer diameter) for 1D (one dimensional) proton NMR spectroscopy.

All spectra were recorded at 37°C on a UnityINOVA 600 MHz NMR spectrometer (Varian Inc, Palo Alto, CA, USA). All spectra were referenced to DSS at 0.00 ppm. Spectra were recorded over 32768 points, 512 transients and a spectral width of 8004.8 Hz. An acquisition time of 2.047 seconds and a relaxation delay of 1.5 seconds were used. This produced a total experimental time of 31 minutes that enabled efficient and fast data acquisition with minimal effects resulting from relaxation. Areas beneath peaks were integrated to provide a measure of metabolite abundance.

2.5 *In vivo* methods

2.5.1 Mouse UTI studies

Mouse infection experiments (Roos *et al.* 2006) were performed as competition experiments; wild type and mutant bacteria were mixed in equal cell numbers before introducing into the bladders of mice transurethrally. This allowed the virulence of *cydDC* mutants to be directly compared with the wild type cells. For this experiment 15 mice were used.

Urine was collected from female C57BL/6 mice (aged between 8-10 weeks) 24 hours prior to microbial infection to identify mice with pre-existing conditions. Mice found to have a combination of $5x10^2$ CFU bacteria and $2x10^5$ white blood cells/ml were excluded from the study.

Strains EC958*lac*::*mkate*-Cm type 1 enriched (MS6016, wild type) and EC958*cydDC*::Gm type 1 enriched (MS6110, Table 2-1) were cultured statically at 37°C overnight in 100 ml LB broth in 500 ml flasks, (two flasks for each strain). Stationary phase cells were harvested in 50 ml falcon tubes and were centrifuged at 9,000 x *g* for 6 minutes at 20°C, washed twice with 30 ml phosphate-buffered saline (PBS), re-suspended in 25 ml PBS and samples of the same strains were combined, harvested and finally re-suspended in approximately 1 ml of PBS. Strains were diluted/concentrated so that 1 ml concentrated cell suspension had an OD_{600} =100 (10 µl/ 990 µl dilution has an OD_{600} of 1). A 400 µl volume of wild type cells was mixed with 400 µl of the mutant strain cells in an Eppendorf with 8 µl Indian ink at a final concentration of 1%. From this mix, 200 µl was taken to perform colony counts on and the remaining bacterial sample was supplied for mouse infection.

To document exact numbers of CFU in the inoculum supplied for mouse infection, a 10-fold dilution series of the bacterial suspension was performed in PBS. Dilutions down to 10^{-9} were plated out; 10^{-9} dilution was spotted in triplicate of 20 µl and 10^{-8} and 10^{-7} dilutions were spotted in triplicate of 5 µl volumes. Colony counts were performed the next day

For mouse infection; mice were anaesthetised by brief inhalation exposure to isoflurane, and the periurethral area was sterilised by swabbing with 10% povidone-iodine solution, this was then subsequently removed with PBS. Mice were catheterised by inserting a

sterile Teflon catheter device directly into the bladder through the urethra, 30-40 µl PBS containing a mixture of wild type and mutant *E. coli* with 1% India ink (to visualise inocula at autopsy) was instilled transurethrally into the bladder using a 1 ml syringe attached to the catheter. The catheter was removed after inoculation and the mice were then returned to cages for recovery. At 24 hours post-infection urine samples were collected and mice were euthanised, bladders and kidneys were removed aseptically to be weighed and homogenised in PBS using sterile ball bearings and a tissue lyser.

Serial 10-fold dilutions to 10^{-9} were made (in PBS) of urine and homogenised tissue samples (bladder and kidney), and 5 µl volumes were spotted in triplicate onto LB, LB- chlorampenicol and MacConkey agar plates. Plates were incubated overnight to allow bacterial growth. The next day bacterial colonies were counted including the number of white (EC958*lac*::*mkate*-Cm type 1 enriched) and red colonies (EC958*cydDC*::Gm type 1 enriched) on MacConkey plates and the results analysed using Prism software.

2.5.2 Macrophage survival assay

Hemapoietic stem cells were harvested from C57BL/6 mice as previously described by Tushinski *et al*. 1982 with 1 x 10^4 U/ml recombinant human CSF-1 (colony stimulating factor-1) to promote differentiation into bone marrow-derived macrophage (BMM) cells. BMMs were maintained in RPMI 1640 (Roswell Park Memorial Institute 1640 medium) (Invitrogen, Carlsbad CA, USA) supplemented with GlutaMAX-I (Invitrogen), 10% heat inactivated foetal calf serum (Invitrogen), 20 U/ml penicillin and 20 µg/ml streptomycin (Invitrogen). Once differentiated into macrophages, cells were harvested, and using a haemocytometer, cell counts were performed to achieve approximately 200,000 BMM cells per well in three 24-well plates. The three plates were set up in tandem as shown in Figure 2-2, and the macrophage cells they contained were harvested at different times post infection to allow for three time point measurements of infection. Cells were left to adhere to wells overnight in antibiotic-free RPMI 1640 medium at 37ºC 5% CO_2. The next day, BMMs were infected at a multiplicity of infection (MOI) of 10, so there would be a ratio of 10 bacterial cells per macrophage cell.

	1	2	3	4	5	6
A	WT – EC958	WT – EC958	WT – EC958	Control		
B	EC958 *ΔcydAB*	EC958 *ΔcydAB*	EC958 *ΔcydAB*			
C	EC958 *ΔcydDC*	EC958 *ΔcydDC*	EC958 *ΔcydDC*			
D						

Figure 2-2. Layout of 24-well plate used for macrophage survival assay
The layout used to fill three 24-well plates used per macrophage survival assay. Control well contained BMMs cells without bacteria. Other wells contained wild type EC958 (3899), EC958*cydAB* (MS3907) mutant and EC958*cydDC* (MS6110) mutant cells as depicted.

All three plates were taken out of the incubator after 30 minutes of the BMMs being infected, any bacteria which had not been taken up by macrophages were killed by washing and replacing media with gentamycin-containing (200 µg/ml) media. To determine the uptake of bacteria into macrophage cells at this time, one of the three 24 well plates, known as the 'uptake' plate had the antibiotic media removed and cells were washed with antibiotic free media. Macrophage cells were lysed open by replacing the media with 500 µl 0.01% triton X-100, left to incubate for 5 minutes at room temperature, then pipetted with vigour. This released the bacteria from within the macrophage cells. Only the macrophage cells were disrupted at this concentration of triton X-100 as prokaryotic *E. coli* cells which have two membranes surrounding the cells are more robust. Bacterial loads (CFU/ml) were then quantified via serial dilution (10^{-1} to 10^{-7}) and spotting in triplicate onto Luria Bertani (LB) agar plates. Plates were then incubated overnight. The survival of intra-macrophage bacteria were determined by counting cell colonies released from macrophage cells.

After two hours the number of bacterial cells were counted from one of the remaining 24-well plates. These two plates are called 'survival' plates, as they allow the number of intra-macrophage bacterial cells to be counted once uptake into macrophages has been stopped by the addition of antibiotics to the media which kills extra-macrophage cells. After 24 hours of infection, the third 24-well plate was taken from the incubator and the number of intracellular bacteria were counted.

2.5.2.1 Type 1 fimbrial phase switch promoter PCR

When the *fim* switch invertible element is in the 'on' orientation, *fimA* is transcribed and fimbriae are produced by cells. This PCR reaction is a diagnostic tool to determine which orientation the *fim* switch is in. Each PCR is run in duplicate. 1 µl of stationary phase culture is used as template and added to 2.5 µl 10x NEB Taq buffer, 1 µl 5 mM dNTP, 0.25 µl 25 µM primer P1 (Table 2-2), 0.25 µl 25 µM primer P2 (Table 2-2), 20.88 µl milli-Q water and finally 0.125 µl NEB Taq polymerase. PCR reactions were incubated at 94ºC for 2 minutes followed by 35 thermal cycles of 94°C (1 minute), 55ºC (1 minute), 72ºC (1 minute). Samples of each PCR reaction were digested with HinfI in NE buffer overnight at 37ºC. Digested and undigested samples were then resolved on a 2% agarose gel.

As shown in Figure 2-3A, HinfI-digested PCR products produce bands of 130 bp and 511 bp when the switch is in the 'on' orientation and bands of 230 bp and 411 bp when in the 'off' orientation. A combination of the four bands seen in Figure 2-3B, shows that there is a mixture of cells in the 'on' and 'off' orientation within a population. For mouse and macrophage assays, this PCR and subsequent digest were used to check that strains have similar expression levels of type 1 fimbriae.

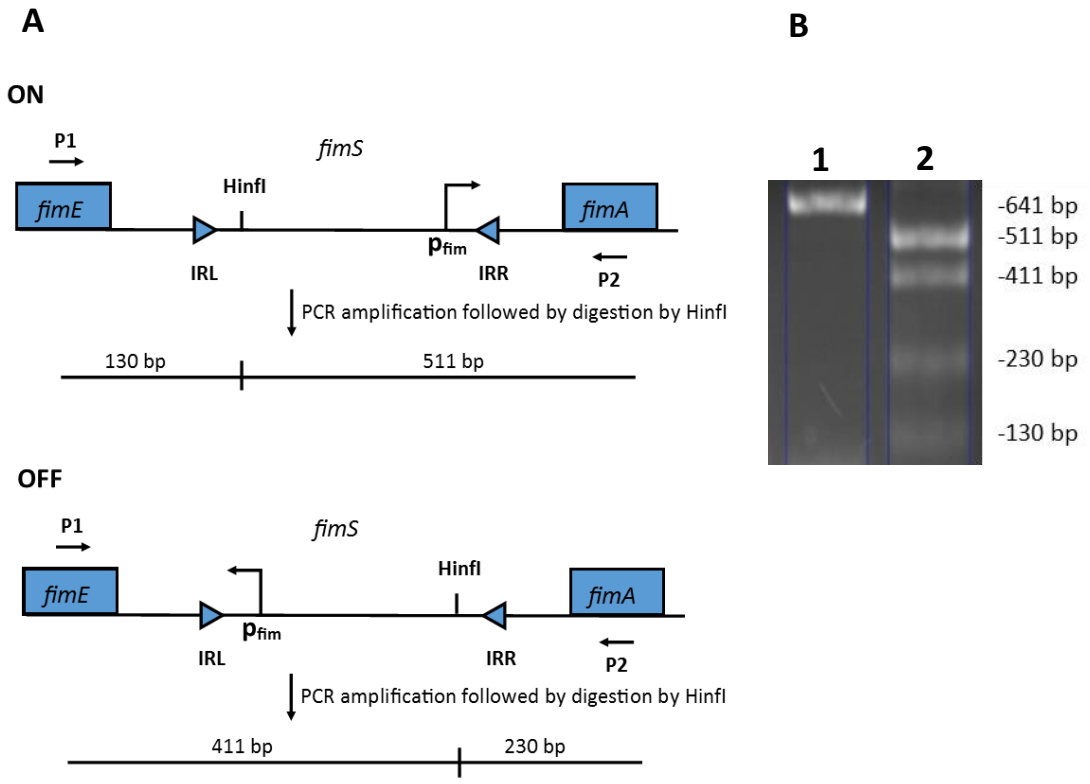

Figure 2-3. Digestion of PCR product indicates orientation of *fim* switch
A schematic diagram of PCR-amplified *fim* switch (*fimS*), depicts that in the 'on' orientation HinfI digestion produces DNA of 130 bp and 511 bp but when the switch is inverted (i.e. off), products of the HinfI digest are changed to 411 bp and 230 bp. **B** Visualisation of bands produced after digestion with HinfI on an agarose gel. Lane 1 shows an uncut DNA fragment and lane 2 shows HinfI digested fragments, displaying a mixture of 'on' and 'off' orientated *fim* switches as indicated by the presence of all four fragment sizes.

Chapter 3

Characterisation of the *cydDC* phenotype: NO tolerance, cytochrome *bd*-I assembly, and metabolic adaptations

Summary

Consistent with previously reported data, the work herein demonstrates that loss of cytochrome *bd*-I elicits sensitivity to NO. As CydDC is required for the assembly of this respiratory oxidase it was expected that a mutant of CydDC would be as sensitive to NO as a cytochrome *bd*-I mutant. A *cydD* mutant was not only sensitive to NO but was more sensitive than a cytochrome *bd*-I (*cydB*) mutant, suggesting that CydDC provides additional NO tolerance beyond the role of cytochrome *bd*-I. It was then hypothesised that additional CydDC-mediated protection against NO toxicity was provided by the presence of cysteine and glutathione in the periplasm which are exported by this transporter: these thiols are known targets of NO that could hinder the diffusion of this toxic radical into the cytoplasm. To test this hypothesis, exogenous glutathione and cysteine were added to the growth medium of *cydDC* cells, which alleviated the level of NO-sensitivity to a level resembling that of a cytochrome *bd*-I mutant. This suggests that CydDC-mediated reductant export contributes to protection against NO toxicity both by permitting the assembly of cytochrome *bd*-I and by a more direct mechanism (i.e. by reacting with incoming NO).

It is intriguing that many of the phenotypes of a *cydDC* mutant can be corrected by the addition of cysteine or glutathione to the growth medium (Pittman *et al.* 2002; Pittman, Robinson and Poole 2005), except cytochrome *bd*-I synthesis, that cannot be restored by the addition of glutathione or cysteine alone. Herein, it is demonstrated for the first time that addition of both glutathione *and* cysteine is necessary to restore the assembly of cytochrome *bd*-I. To further investigate the pleiotropic *cydDC* phenotype, the metabolome of wild type cells was compared to that of *cydD* cells through 1D-^{1}H NMR analysis. This showed that loss of CydDC leads to changes in metabolite levels including; the elevation of L-methionine and fumarate along with the reduction of succinate, D-mannitol, acetate and NAD. The only metabolite with peak intensities that are significantly different between the two strains above the 99% level after an unpaired *t*-test was performed was betaine, with an increase in *cydD* cells. These data complement existing *cydD vs.* wild type microarray data, and provide molecular insights into the role of CydDC.

3.1 Introduction

To combat infection, the mammalian immune system releases NO, a free radical that is toxic to invading bacteria (Fang 2004; Lundberg *et al.* 2004; Poole and Hughes 2000). *E. coli* has two well-characterised terminal oxidases of aerobic respiration; cytochromes *bo′* and *bd*-I. Both catalyse the two-electron oxidation of ubiquinol by molecular oxygen within the cytoplasmic membrane but differ with respect to the efficiency of proton translocation and pattern of expression (Ingledew and Poole 1984). Mason *et al.* (2009) have also shown that these respiratory oxidases differ in their tolerance to NO; cytochrome *bd*-I activity is more resistant to nitric oxide than cytochrome *bo′* due to a fast NO dissociation rate, permitting oxygen reduction to continue in the presence of NO. As cytochrome *bd*-I has a very high affinity for oxygen (D'mello, Hill and Poole 1996) and is maximally expressed under microaerobic conditions (Tseng *et al.* 1996), it is expected that pathogenic bacteria rely upon this terminal oxidase for respiration within the oxygen limiting environment of the host. This role as oxygen scavenger, taken together with the tolerance to NO, cytochrome *bd*–I has been linked to the virulence of certain bacterial pathogens. In fact, a range of bacterial pathogens have been shown to express *bd*-type oxidases including *Listeria monocytogenes* (Larsen *et al.* 2006), *B. abortus* (Loisel-Meyer *et al.* 2005), *Bacteroides fragilis* (Baughn and Malamy 2004) and *S. flexneri*. Furthermore, *bd*-type terminal oxidases have been observed to be so vital to pathogen survival during host colonisation that the loss of this oxidase results in attenuation of virulence of some pathogens including *Salmonella* (Turner *et al.* 2003) and group B *Streptococcus* (Y. Yamamoto *et al*. 2005). The connection between virulence and cytochrome *bd*-I is discussed further in section 1.6.5.

A significant phenotype of *cydDC* mutants is their inability to assemble cytochrome *bd*-I (Bebbington and Williams 1993; Georgiou, Hong and Gennis 1987; Poole, Gibson and Wu 1994; Poole *et al.* 1993). Given that the deletion of cytochrome *bd*-I has been shown to elicit sensitivity to NO (Mason *et al.* 2009), it is expected that *cydDC* mutants will also be sensitive to NO due to an inability to assemble functional cytochrome *bd*-I. The experimental approaches in this chapter are designed to test this hypothesis by using the NO-donor molecule NOC-12 to impose nitrosative stress upon a series of *E. coli* knockout strains. In addition, spectroscopic tools and metabolomics are used to gain further insights into the *cydDC* phenotype.

3.1.1 Nitric oxide releasing compound NOC-12

NOC-12 is a nitric oxide-amine complex that can spontaneously release nitric oxide under physiological conditions without the need for a cofactor. Decomposition of NOC-12 is elicited by protonation of the oxygen of the NO group and results in the release of two molecules of NO per molecule of NOC-12 (Hrabie *et al.* 1993), the release rate of the second NO molecule is much slower than that of the first (Figure 3-1). NOC-12 has a similar structure to two other NO releasing compounds; NOC-5 and NOC-7 but with a much longer half-life of NO release. The benefits of using NOC compounds is that their NO generation is simpler than other classical NO donors, such as GSNO, and the by-products are thought not to interfere with cell physiology. Decomposition of NOC compounds is faster in acidic solutions (Aga and Hughes 2008); stock solutions were therefore prepared in an 80mM sodium phosphate buffer (pH 8). Temperature also affects the half-life of NOC-12, at pH7 37°C the half-life of NOC-12 is 100 minutes, reducing the temperature to 22°C extends the half-life to 327 minutes (Hrabie *et al.* 1993).

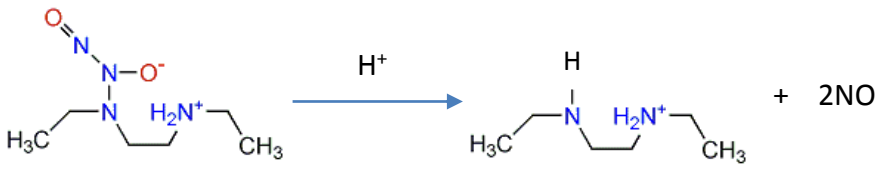

Figure 3-1. Nitric oxide release from NOC-12

The reaction scheme above shows how the protonation of NOC-12 leads to the release of two nitric oxide molecules. It is thought that the release rate of the second NO molecule is much slower than the first.

3.2 Results

3.2.1 Loss of functional CydDC elicits sensitivity to nitric oxide

To investigate whether the loss of CydDC would elicit sensitivity to nitric oxide, growth curves for wild type (MS52), *cydD* (MS54), and *cydB* (MS53) K-12 Keio strains (Table 2-1) were performed using a plate reader as described in section 2.1.8. Following the addition of NOC-12, growth was inhibited for a finite period after which growth resumed, probably due to adaptation of the cells and/or depletion of the NOC-12 (Figure 3-2). As expected, this 'lag time' appears to be dependent upon the concentration of NOC-12 used. One way to directly compare the inhibition by NOC-12 across the three strains is to look at the time taken to reach a particular OD_{600} value (e.g. an OD_{600} of 0.1 is used in Figure 3-3). Since normal growth rates are observed following the lag time, it was not sensible to calculate doubling times as a measure of NO sensitivity. After the addition of 0.1 mM and 0.2 mM NOC-12 the difference in time taken for wild type cultures to reach an OD_{600} of 0.1 is very small. Wild type growth remained unaffected in the presence of 0.1 mM NOC-12, with growth comparable to that in the absence of NOC-12. This indicates that wild type cells are able to adapt to this level of nitrosative stress. However, addition of NOC-12 in the absence of cytochrome *bd*-I or CydDC increases the time taken to reach an OD_{600} of 0.1 by one hour or 3 hours, respectively. This suggests that the protection from NO in wild type cells is compromised in the absence of these two protein complexes. Growth of wild type cells is inhibited when the concentration of NOC-12 is increased to 0.5 mM, suggesting that at this concentration, CydDC and cytochrome *bd*-I of wild type cells are not able to completely protect against the detrimental effects of NO.

The loss of cytochrome *bd*-I has previously been shown to elicit sensitivity to NO (Mason *et al.* 2009), and consistently with this, mutation of *cydB* in the Keio strain elicits sensitivity to NO. Since the assembly of cytochrome *bd*-I requires CydDC (Georgiou, Hong and Gennis 1987), mutation of *cydD* would be expected to also elicit NO sensitivity, which the current work clearly demonstrates (Figures 3-2 and 3-3). When the growth inhibition at equivalent NOC-12 concentrations is compared between the *cydB* and *cydD* mutants, growth of the *cydD* mutant is more sensitive than the *cydB* mutant. This result demonstrates that CydDC provides protection against NO, and furthermore, suggests an additional CydDC-mediated NO-tolerance mechanism beyond that of cytochrome *bd*-I assembly.

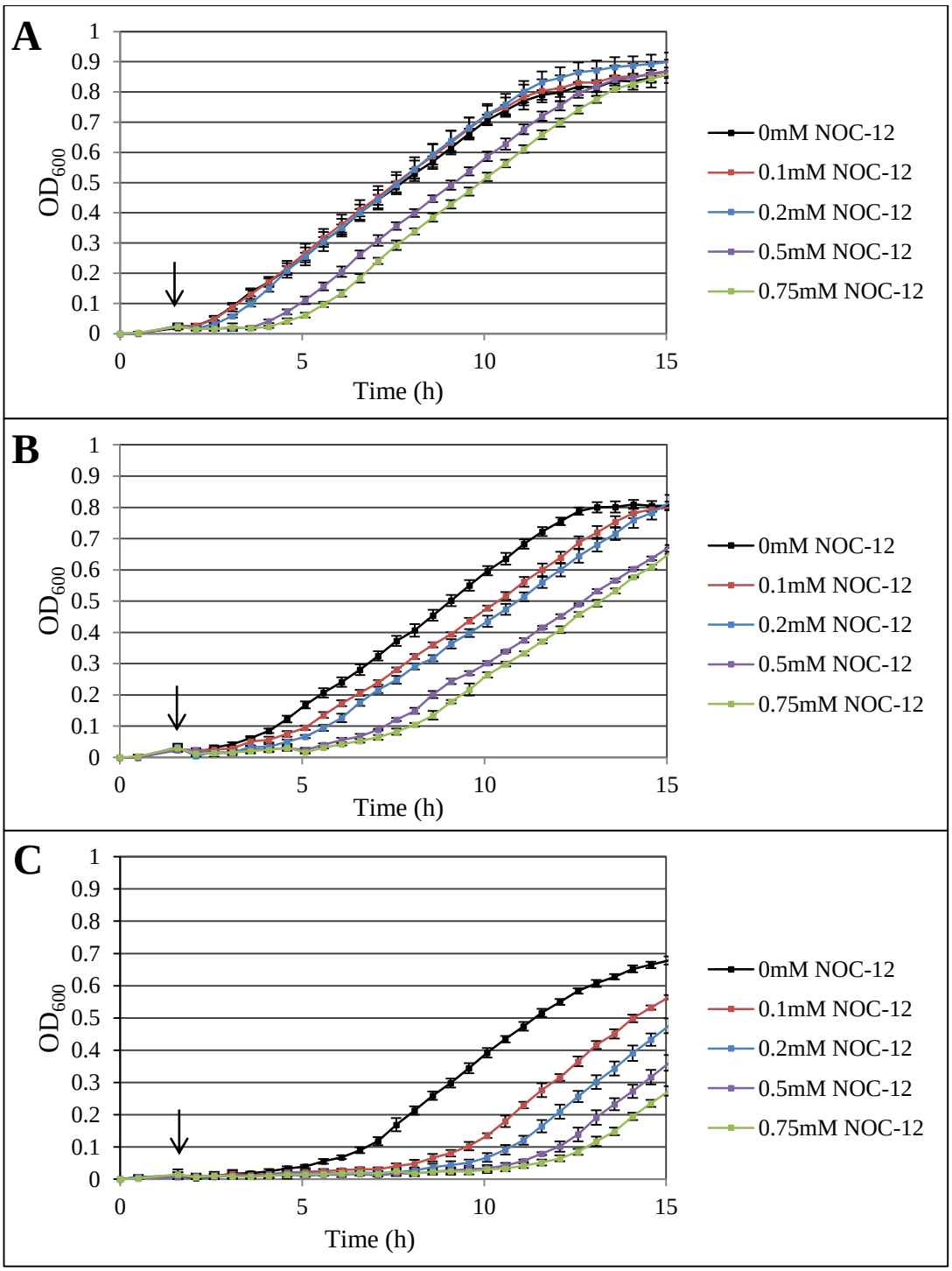

Figure 3-2. Mutation of *cydB* and *cydD* elicits sensitivity to NO in *E. coli*

Cultures of wild type (MS52)(**A**), *cydB* (MS53)(**B**) and *cydD* (MS54)(**C**) *E. coli* Keio strains were grown under aerobic conditions, and various concentrations of NOC-12 were added after 1.5 h: black, no NOC-12 control; red, 0.1 mM; blue, 0.2 mM; purple, 0.5 mM; green, 0.75 mM NOC-12. Error bars represent standard deviations of three technical repeats.

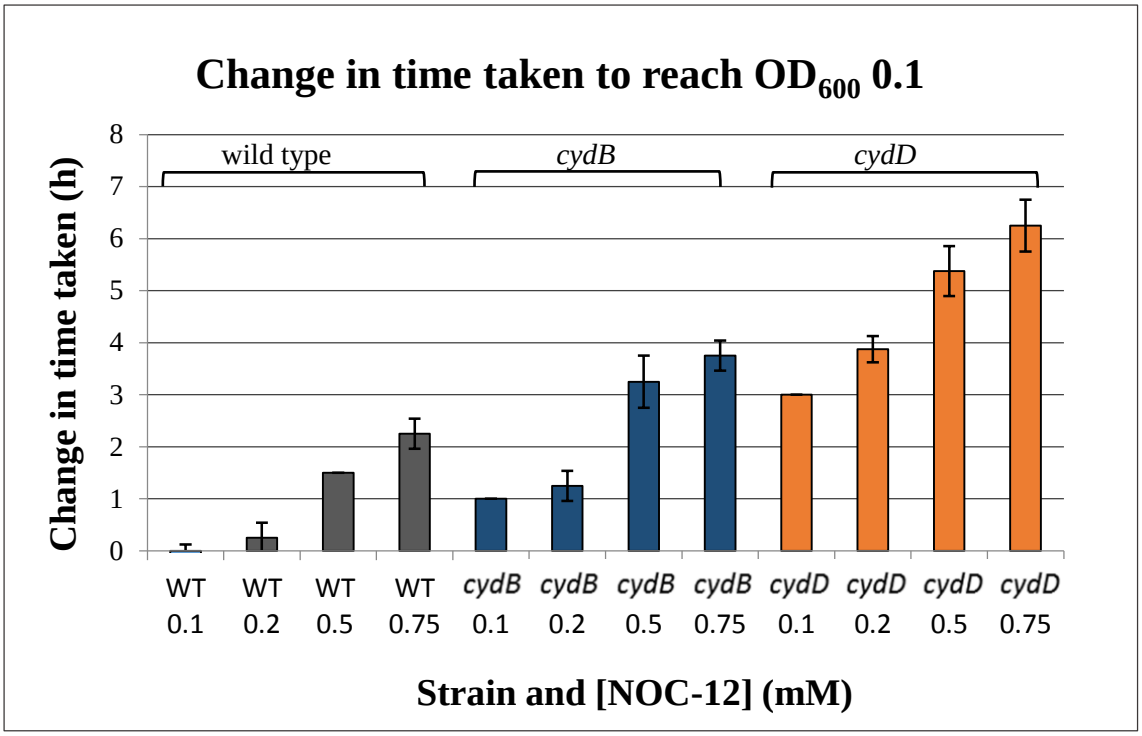

Figure 3-3. Change in time taken to reach an OD_{600} of 0.1 in the presence of the NO donor NOC-12
Cultures of wild type (grey), *cydB* (blue) and *cydD* (orange) *E. coli* Keio strains were grown under aerobic conditions. Various concentrations of NOC-12 were added after 1.5 h of growth. The time taken for cultures to reach an OD_{600} of 0.1 was determined, and data are expressed as the increase in time due to NOC-12 inhibtion (relative to the no NOC-12 control). Error bars represent standard deviations of three technical repeats.

3.2.2 Periplasmic cysteine and glutathione provide additional protection from NO

The finding that a *cydD* mutant is more sensitive to NOC-12 than a *cydB* mutant is interesting, as one might expect that these strains would exhibit a similar level of elevated NO sensitivity (due to loss of cytochrome *bd*-I assembly (Mason *et al.* 2009)). Given that both the known substrates for CydDC contain thiol groups that can react with incoming NO, it was then hypothesised that CydDC-exported thiols can provide additional protection to *E. coli* from NO, beyond the involvement of cytochrome *bd*-I. With a reduction in periplasmic thiols to react with incoming NO, it is likely that a *cydD* mutant is confronted with a larger concentration of NO within the cytoplasm than strains with functional CydDC. To test this hypothesis, reduced glutathione and cysteine were added to growth media during further NOC-12 growth experiments.

As before, the growth of *cydB* and *cydD* Keio mutants was inhibited using the nitric oxide donor NOC-12 at a concentration of 0.75mM. The extent of NO-mediated growth inhibition was compared to when the growth media was supplemented with 1.2

mM cysteine and 2.4 mM GSH. The outer membrane porins allow the diffusion of molecules ~600 Da from the extracellular fluid to the periplasm (Decad and Nikaido 1976). Hence, it is reasonable to assume that extracellular glutathione and cysteine are at equilibrium with the periplasmic space. As before, a plate reader was used to measure OD readings. Defined medium (Flatley *et al.* 2005) with and without additional cysteine and glutathione was inoculated with bacteria and then aliquoted as 200 µl volumes into the wells of 96 well plates. Cells were grown in a plate reader at 37ºC and 200 rpm for an hour and a half before being challenged with 0.75 mM NOC-12. It has previously been shown (Figure 3-2) that addition of NOC-12 at a concentration of 0.75 mM has a large affect upon growth of both *cydB* and *cydD E. coli* Keio strains; this relatively large concentration of NOC-12 (0.75 mM) was used in this experiment as it was assumed that as targets of NO, additional cysteine and glutathione in the media would react with NOC-12 and dampen the observed affects upon growth. Growth curves are shown in Figure 3-4, and the level of inhibition was defined by the time taken to resume growth and reach an OD_{600} of 0.25 (Figure 3-5), which was diminished for the *cydD* mutant when additional cysteine and glutathione was present. This supports the hypothesis that a lack of NO-reactive thiols in the periplasm causes *cydD* mutants to be more sensitive to NO.

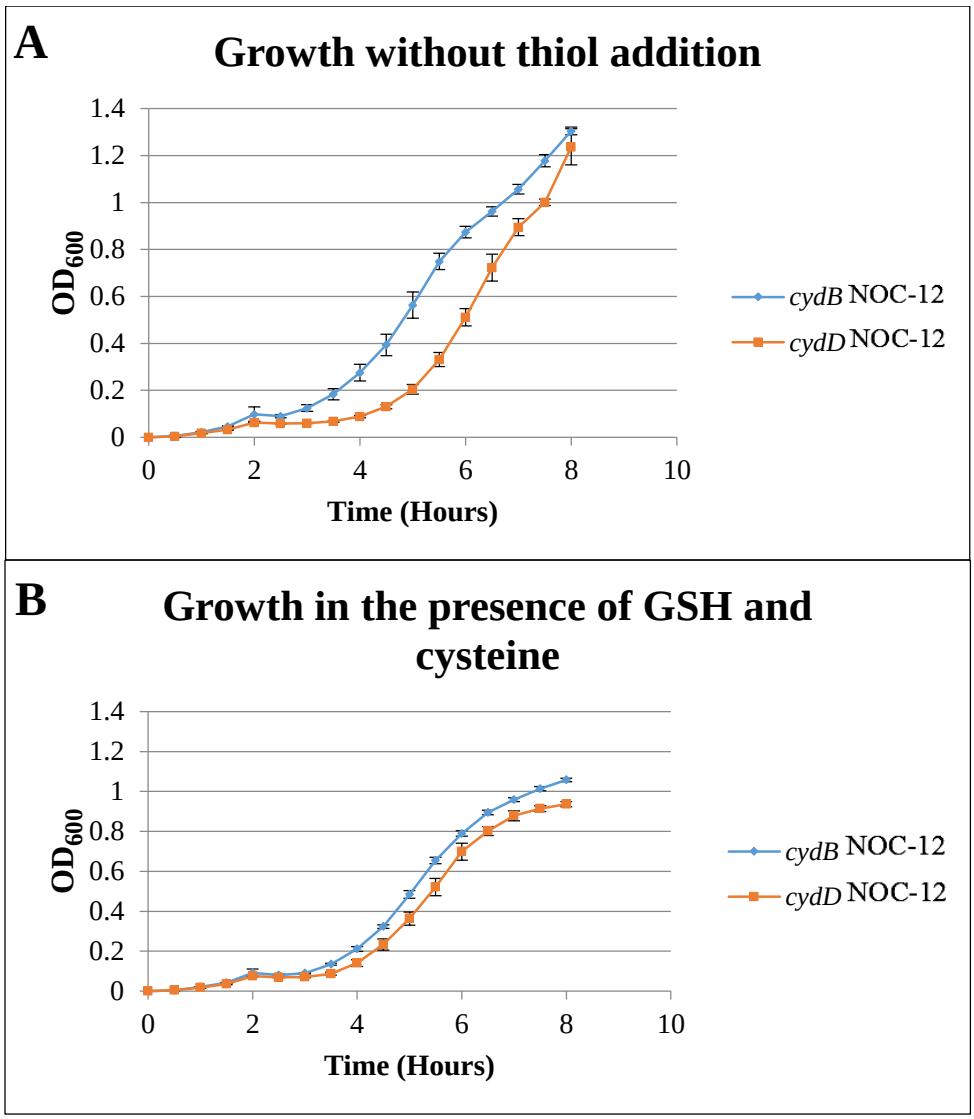

Figure 3-4. Effect of exogenous glutathione and cysteine to NO tolerance of *cydB* and *cydD* mutants

cydB (MS53)(blue) and *cydD* (MS54)(orange) *E. coli* Keio mutants were grown in the presence (B) or absence (A) of 0.75 mM NOC-12 to determine if exogenous addition of cysteine and GSH alleviated NOC-12 growth inhibition. Error bars represent standard deviations of five technical repeats.

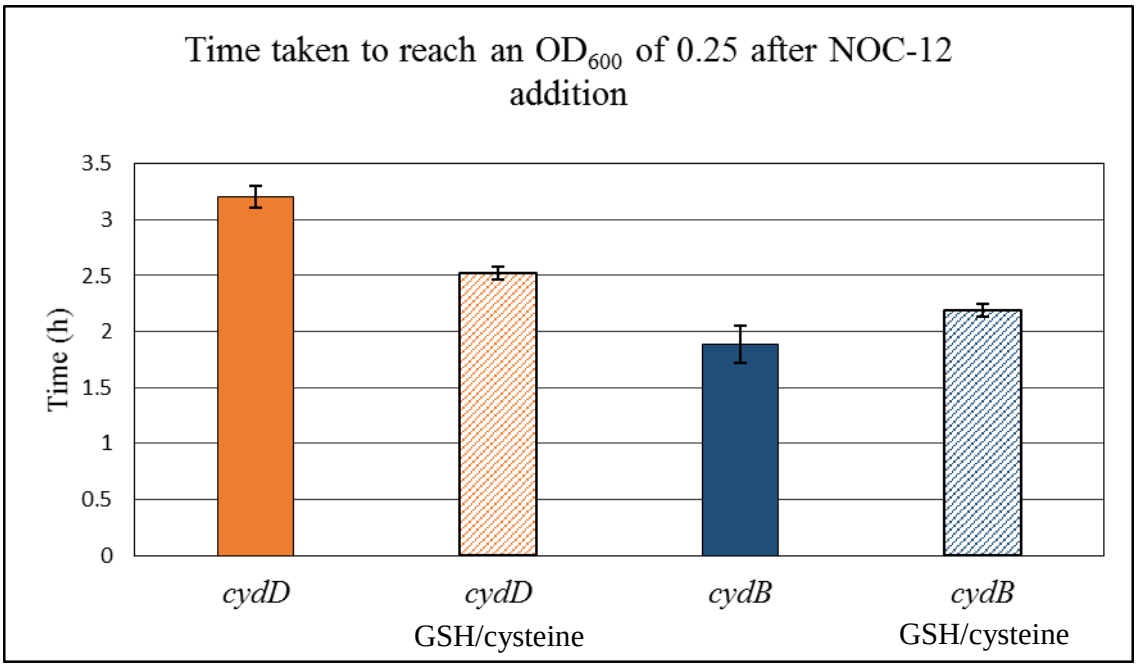

Figure 3-5. Exogenous glutathione and cysteine reduces the inhibitory effects of NOC-12 on a *cydD* mutant

Aerobic growth of *E. coli* Keio strains in a 96 well plate was measured using a plate reader. The time taken for strains to reach OD_{600} 0.25 in the presence of NOC-12 was measured to determine level of growth inhibition. Some of the wells contained medium supplemented with the low-molecular weight thiols cysteine (1.2 mM) and glutathione (2.4 mM). The effect the added thiols have on nitrosative stress can be determined by comparing the time taken to reach OD_{600} of 0.25. Error bars show standard deviation of five technical repeats.

One would expect that addition of GSH and cysteine in general would aid tolerance to NO. It is intriguing that supplementing media with GSH and cysteine does not, however, alleviate NO sensitivity of a *cydB* mutant and actually produces a slight hindrance to growth, possibly due to the toxic effect of cysteine.

3.2.3 Addition of reduced glutathione is more effective at relieving the NO induced growth inhibition of a *cydD* mutant than cysteine

To assess the individual contribution of the two thiols to NO tolerance, growth curves were performed (using a plate reader) with an equal concentration of either cysteine (1 mM) or GSH (1 mM) added separately to the growth medium. As described above, the growth of *cydB* and *cydD* strains is inhibited by addition of NOC-12. The magnitude of this growth inhibition was compared when cultures were grown in defined medium (Flatley *et al.* 2005) containing 0.1 % (w/v) casamino acids supplemented with 1 mM

cysteine or 1 mM GSH. Cells were grown in a plate reader at 37ºC 200 rpm for an hour and a half before being challenged with 0.5 mM NOC-12. A relatively large concentration of NOC-12 was used as it was assumed that as targets of NO, additional cysteine or glutathione in the media would react with NOC-12. Growth curves are shown in Figure 3-6. As seen by the little difference in time taken to reach an OD_{600} of 0.25 (Figure 3-7), adding cysteine at a concentration of 1 mM to the media had very little effect on the NOC-12-mediated growth inhibition of a *cydD* strain. However addition of glutathione (1 mM) noticeably alleviates the growth inhibition of the *cydD* strain caused by NOC-12. The NOC-12-mediated growth inhibition of the *cydB* strain is also diminished by the addition of glutathione.

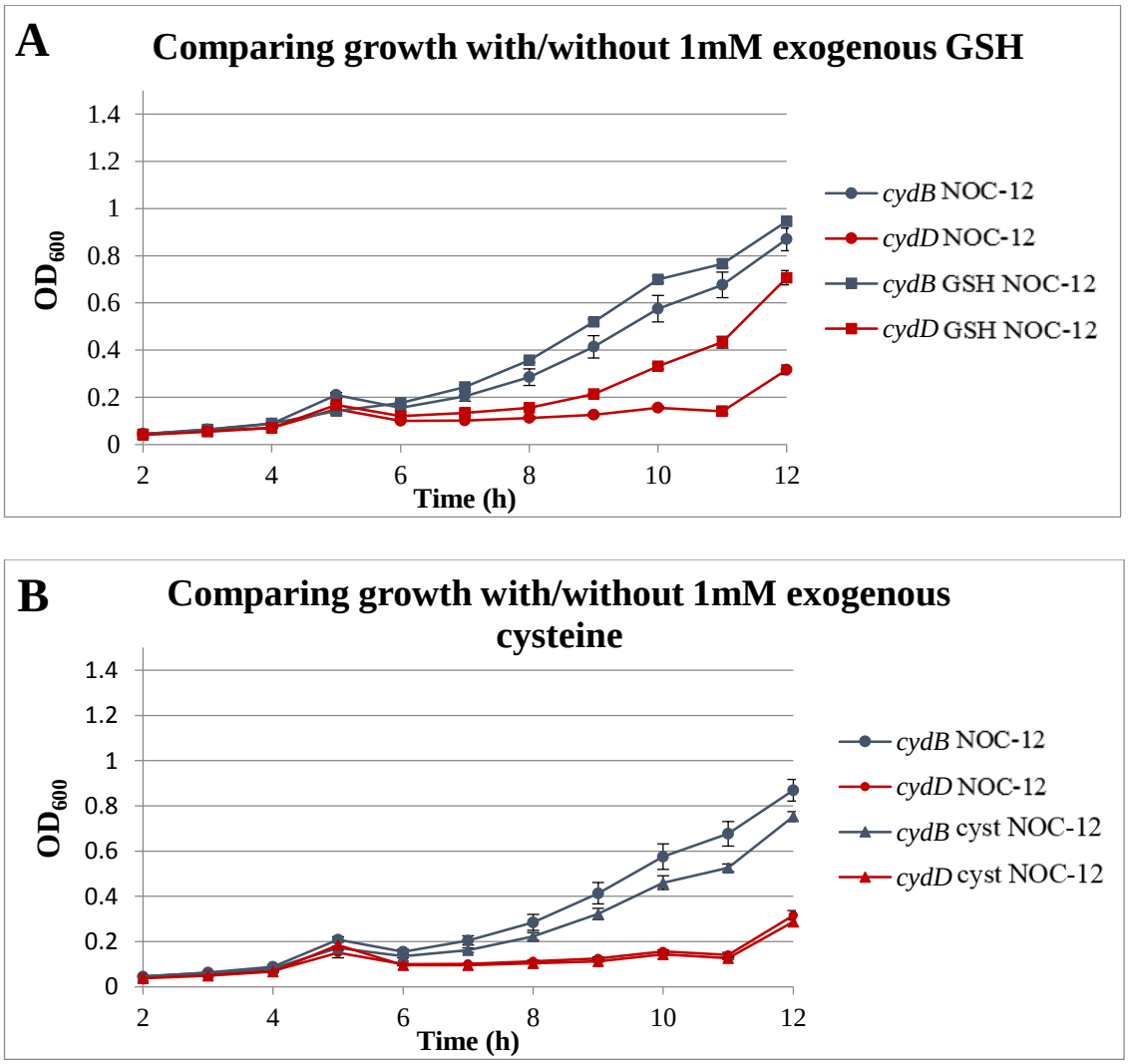

Figure 3-6. Effect of exogenous glutathione or cysteine to NO tolerance of *cydB* and *cydD* mutants

cydB (blue) and *cydD* (red) mutants were grown in the presence of NOC-12 (circles), to determine if exogenous addition of GSH (A) or cysteine (B) alleviated growth inhibition. Error bars show standard deviation of five technical repeats.

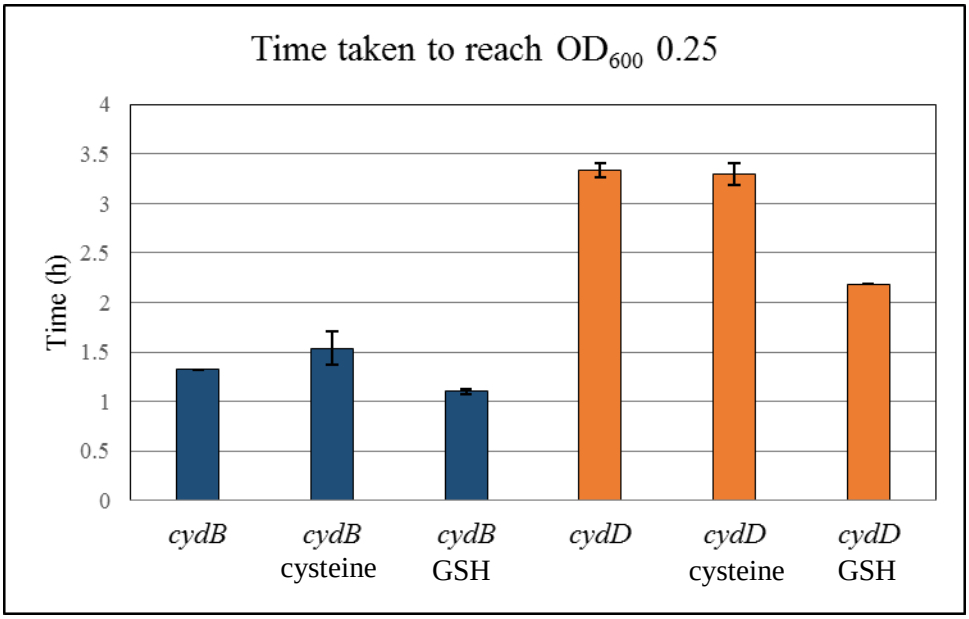

Figure 3-7. Exogenous glutathione is more effective than cysteine at alleviating NO-mediated growth inhibition

Aerobic growth of *E. coli* Keio strains in a 96 well plate was measured using a plate reader. Strains were grown in the presence of 0.5 mM NOC-12 with or without exogenous cysteine (1 mM) or glutathione (1 mM). The effect the added thiols have on nitrosative stress was defined by the time taken to reach an OD_{600} of 0.25. Error bars show standard deviation of five technical repeats.

3.2.4 Exogenous glutathione and cysteine restores cytochrome *bd*-I assembly in a *cydDC* mutant

One of the most important phenotypes of a *cydDC* mutant, is a lack of functional cytochrome *bd*-I (Poole *et al.* 1993; Poole, Gibson and Wu 1994; Bebbington and Williams 1993; Georgiou, Hong and Gennis 1987). In a strain lacking CydDC it has been shown that cytochrome *bd*-I protein polypeptides CydA and CydB are still synthesised and inserted into the cytoplasmic membrane but that the haem cofactors, essential to cytochrome functional are not incorporated within these subunits (Bebbington and Williams 1993). Some phenotypes of a *cydD* mutant such as the loss of motility, the sensitivity to dithiothreitol and benzylpenicillin along with the absence of holocytochrome *c* and periplasmic cytochrome b_{562} can be corrected with the addition of either cysteine or glutathione to the growth media (Pittman *et al.* 2002; Pittman,

Robinson and Poole 2005). However, the restoration of cytochrome *bd*-I has not been observed by the addition of GSH or cysteine alone, so it was of interest to determine whether both CydDC substrates are needed in the periplasm for cytochrome *bd*-I assembly.

As CO binds to different haem groups, giving characteristic spectra, it is possible to use 'CO reduced' *minus* 'reduced' spectra (i.e. CO difference spectra) to detect the presence of fully assembled cytochrome *bd*-I. CO difference spectra of whole wild type cells expressing functional cytochrome *bd*-I have peaks at 420 nm and 642 nm with a trough at 442 nm and 622 nm as seen in the wild type trace (black in Figure 3-8). The α-band peak at 642 nm corresponds to the CO-ligated form of cytochrome *d*. The trough at 622 nm is assigned to the loss of absorbance of the reduced un-ligated cytochrome *d* on binding CO. In the γ (soret) region, the absorption maximum of cytochrome *bd*-I is at 420 nm with a trough at 442 nm (Kalnenieks *et al.* 1998). This is thought to correspond to the haem b_{595} of cytochrome *bd*-I. CydDC mutants lack haem cofactors within cytochrome *bd*-I, which can be observed in the CO difference spectra of *cydD* cells (Figure 3-8, red trace). Whole *cydD* cells, which are deficient in cytochrome *bd*-I assembly, produce CO difference spectra that lack the peak and trough at 642nm and 622nm, respectively. The peak and trough at 420 nm and 442 nm, respectively, are also shifted slightly to the left; in the absence of cytochrome *bd*-I, the CO bound cytochrome *bo′* appears more prominent with a peak around 416 nm and a trough around 430nm (Kita, Konishi and Anraku 1984). This provides a simple assay to detect the presence of fully assembled cytochrome *bd*-I within whole cells. As seen in Figure 3-8 a *cydD* (red line) mutant loses the peaks attributed to cytochrome *bd*-I when compared to a wild type strain (black line).

For these assays, bacterial strains from the Keio collection were grown microaerobically to encourage the production of cytochrome *bd*-I. As described in Section 2.3.1 microaerobic conditions were achieved by increasing the volume within 250 ml conical flasks to 100ml, and reducing the rpm from 180 to 150, to reduce the level of dissolved oxygen. Defined medium as described in Section 2.1.5.2 (Flatley *et al.* 2005) had been used to grow bacteria at first, but when wild type strains were assayed no cytochrome *bd*-I signal could be seen. Growing cells in rich LB media permitted cytochrome *bd*-I to be observed in wild type cells and importantly did not result in the detection of cytochrome *bd*-I spectroscopic signals in a *cydB* or *cydD* mutant.

Previous attempts to restore cytochrome *bd*-I in *cydD* strains did not employ the strategy of adding both CydDC substrates to the growth medium in tandem. CO-difference spectra of whole cells in Figure 3-8 are consistent with previous results that cysteine (green trace) or glutathione (purple trace) alone are unable to restore cytochrome *bd*-I assembly in a *cydD* mutant. Interestingly, here we show that when added together simultaneously cysteine (0.5 mM) and GSH (1 mM) can restore the assembly of cytochrome *bd*-I (blue trace). This spectrum is comparable to that of wild type cells in that the peak at 642nm is seen which corresponds to the CO-ligated form of cytochrome *d*, although the features at 416 nm and 430 nm are poorly defined compared to the wild type trace. We therefore conclude that addition of glutathione and cysteine restores haem insertion into cytochrome *bd*-I.

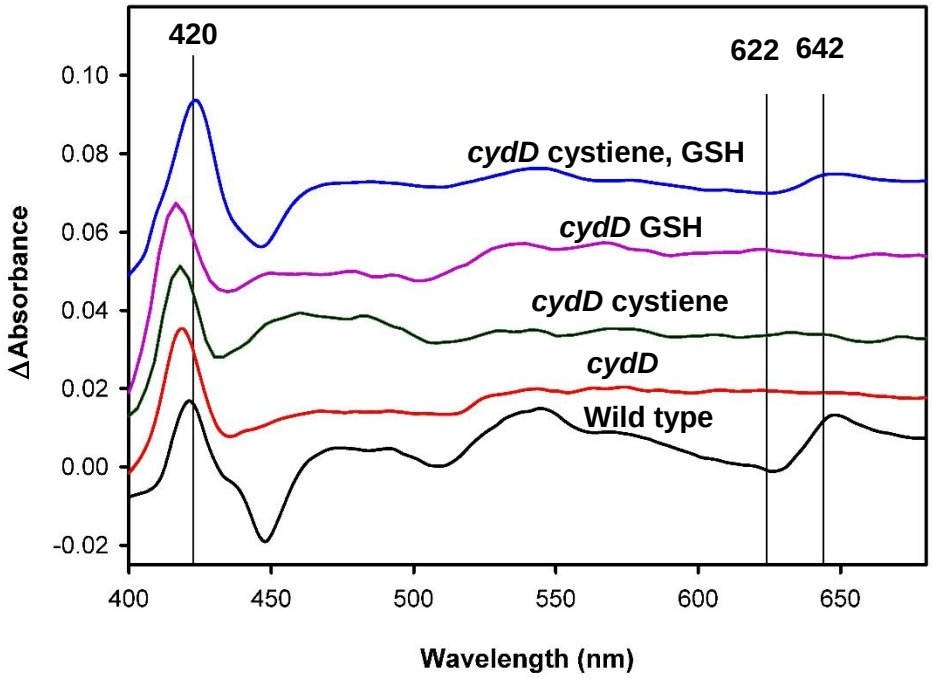

Figure 3-8. Glutathione and cysteine restore cytochrome *bd*-I assembly in a *cydD* mutant

CO difference spectra (400 nm- 700 nm) were collected at room temperature. Whole cell samples (*E. coli* from the Keio collection) were scanned in a custom-built SDB4 dual wavelength spectrophotometer (Kalnenieks *et al.* 1998). Each scan is labelled with the strain and which low-molecular weight thiols were used to supplement the growth medium (LB). Cells were grown microaerobically at 37 ºC overnight, then harvested at 4000 rpm and 4ºC before being re-suspended in 1 ml of 0.1 M potassium phosphate buffer, pH 7.4. Further dilutions were made where required to enable whole cell CO difference spectra to be recorded. The protein concentration of the *cydD* GSH cysteine sample used here was 5.6 mg/ml. Spectra have been normalised to give a common Soret peak magnitude and offset to fit onto the same figure.

3.2.5 Metabolomic perturbations elicited by loss of CydDC

Loss of CydDC elicits a pleiotropic phenotype, so it is expected that a lot of changes occur within cells in response to the absence of the exporter complex. A *cydD vs.* WT microarray experiment has previously been performed by Dr Stuart Hunt (University of Sheffield) and Dr. Mark Shepherd (University of Kent) (Holyoake *et al.* 2015). As expected a large number of genes were shown to be differentially regulated in the absence of CydDC-mediated reduced thiol export; 97 genes were shown to be significantly up-regulated and 41 genes were shown to be significantly down-regulated. Of these, selected genes were mapped onto a metabolic diagram to provide a physiological overview of the loss of *cydD* (Figure 3-9). The diagram highlights the up-regulation of genes involved in protein degradation, *β*-oxidation of fatty acids and respiration. The authors propose that misfolded proteins and fatty acids are broken down to feed into the TCA cycle in order to restore the balance of metabolic flux. Genes encoding the NapGH and NapAB complexes were also shown to be up-regulated in the *cydD* mutant. As NapGH channels electrons from ubiquinol to NapAB, an electron accepting nitrate reductase the authors suggest that the up-regulation of these genes compensates for the loss of cytochrome *bd*-I assembly. Of the genes that are down-regulated, many are involved in thiosulphate transport, nucleotide metabolism and motility.

Transcriptomic studies, however, do not provide information on protein translation nor do they provide an insight into the concentrations of metabolic intermediates in the cell. To complement this microarray data, metabolite extractions (Section 2.4.2) of *cydD* and wild type cells were analysed via 1D-^{1}H NMR spectroscopy as detailed in Section 2.4.3. Six metabolite extractions and NMR analyses were performed for both wild type and *cydD* cultures.

The ^{1}H-NMR spectra were normalised to position the signal for 4,4-dimethyl-4-disilapentane-1-sulfonic acid (DSS) at 0.00 ppm (Figure 3-10). At first glance the NMR spectra of *cydD* metabolites is similar to the spectrum obtained for metabolites extracted from the wild type strain. Indeed, the AMIX global analysis software (Bruker) calculated no significant difference overall between *cydD* and wild type spectra. However, manual inspection of the spectra of *cydD* and wild type cells reveals regions in which peak positions and intensities vary between the two strains. To identify the metabolites that vary in abundance between the two strains the online resource 'The Madison Metabolomics Consortium Database' (MMCD) was used (Cui *et al.* 2008).

Peaks in NMR data collected were assigned to a metabolite by inputting chemical shift values with a tolerance of ±0.05 parts per million (ppm) chemical shift variance into an NMR-based search of metabolites. Published NMR data of metabolites which create peaks at the input chemical shift value were then compared with the peaks in NMR data collected. Corrected intensity signals were then used to create averages, standard deviations and *t*-test data of assigned metabolites (Figure 3-11).

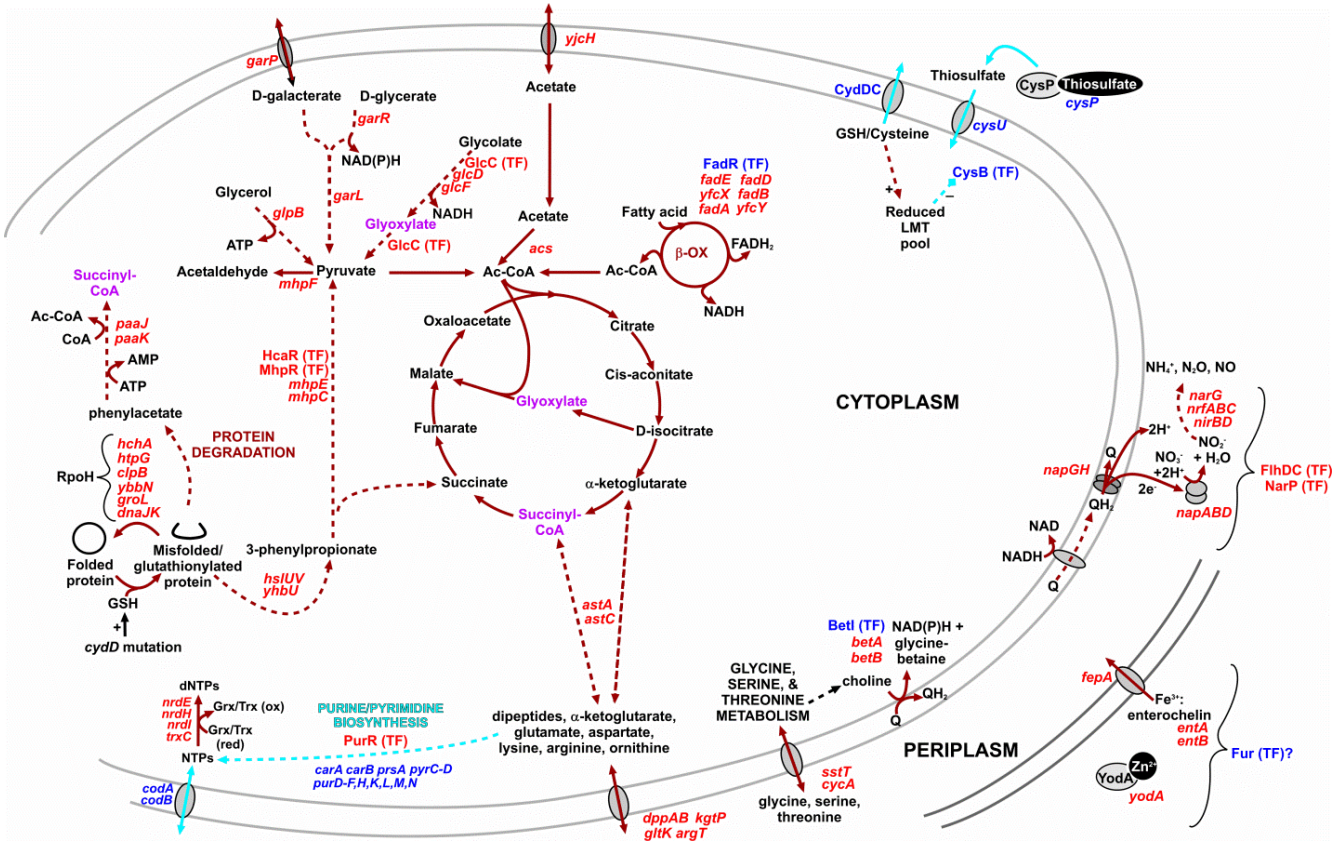

Figure 3-9. Model for the adaptations of a *cydD* strain (Holyoake *et al.* 2015).
The gene transcript levels and transcription factor activities that are up- and down-regulated in the *cydD vs.* wild type transcriptomics are shown in red and blue, respectively. The brown and cyan lines denote processes that are predicted to be up- and down-regulated, respectively. TCA cycle intermediates that are also shown outside the cycle are highlighted in purple. Abbreviations: Ac-CoA, Acetyl CoA; GSH, reduced glutathione; Grx, Glutaredoxin; LMT, low-molecular weight thiol; Trx, Thioredoxin.

3.2.5.1 Deletion of *cydD* results in depletion of intracellular succinate, D-mannitol and NAD

The spectra of metabolites extracted from wild type cells contains a large peak at a chemical shift of 2.4 (Figure 3-10A), but this single peak is missing in the spectra of metabolites extracted from *cydD* cells (Figure 3-10B). To assign this peak to a metabolite the website for the 'Madison metabolite consortium database' (MMCD) was used (Kalnenie*ks et al.* 1998). A chemical shift of 2.4 was entered for an NMR-based search of metabolites. NMR data of each possible metabolite was then compared with the peak at chemical shift 2.4 in Figure 3-10A. The search concluded that the NMR standard for succinate (Appendix A-1) was very similar to the differences in signal intensities at a chemical shift of 2.4 (between the wild type and *cydD* mutant). The 1D-^{1}H NMR spectra of succinate is one single peak at 2.4 which correlates well with the changes seen between wild type and mutant cell derived metabolites. As the peak at 2.4 is missing in a *cydD* mutant this shows that a *cydD* mutant has reduced levels of succinate when compared to wild type. The change in levels of succinate were not shown however, to be significant at the 95% significance level when unpaired *t*-tests were performed (Figure 3-11).

Looking at Figure 3-10 a peak with a chemical shift around 3.8 is also less prevalent in the *cydD* metabolic profile than that of wild type cells. The reference NMR data of D-mannitol shows a large peak at a chemical shift around 3.75 with other smaller peaks surrounding it (Appendix A-2), this is consistent with the changes in peaks between the two strains in collected NMR data (Figure 3-10), and thus shows that D-mannitol is reduced in the absence of CydDC. The levels of D-mannitol were shown to be significant at the 95% significance level (Figure 3-11).

Peaks at 9.35 and 8.42 match peaks assigned to NAD (Appendix A-3) both these peaks are reduced in *cydD* spectra when compared to wild type spectra, and this difference in signal intensities is significant at the 95% level when unpaired *t*-tests are performed.

3.2.5.2 Betaine, fumarate and L-methionine are elevated in a *cydD* strain

As seen in Figure 3-10 the spectra of metabolites extracted from *cydD* cells contains a large peak at a chemical shift of around 3.27, the magnitude of this peak is diminished in the spectra of metabolites extracted from wild type cells. To assign this peak to a

metabolite the website for the 'Madison metabolite consortium database' was again used. A chemical shift of 3.27 was inputted for an NMR-based search of metabolites. NMR reference data of each possible metabolite was then compared with the collected 1D-^{1}H NMR data. For example, although there are alternative metabolites that also include peaks at a chemical shift around 3.27 in their NMR reference data (including L-arginine, L-phenylalanine, coenzyme A, D-Glucuronate and D-cellobiose), the peaks that accompany the peak at 3.27 do not correlate with the differences in peaks seen in the NMR data collected in this thesis. Comparison of the NMR reference data with the data collected (Figure 3-10) showed a good correlation with the NMR reference spectrum of betaine (Appendix A-4). The peak at 3.25 is distinct within the spectra of *cydD* metabolites but not in wild type metabolites, furthermore an unpaired *t*-test showed a significant difference at the 99% level and thus it was concluded that betaine levels are elevated when *cydD* is deleted.

Alongside the peak at 3.27, a peak at chemical shift 2.15 is detected in four of the five NMR spectra for *cydD* cells but only one of the six spectra of wild type metabolite extracts. The reference 1D-^{1}H NMR data of L-methionine (Appendix A-5) matches the changes in peaks between the two strains. Further analysis showed that the level of methionine in the two strains is significantly different at the 95% level. Thus methionine is more abundant in cells lacking CydDC. Reference 1D-^{1}H NMR data for fumarate produces a single peak at a chemical shift around 6.5 (Appendix A-6). Larger peak intensities are seen for *cydD* spectra than wild type spectra, the differences in peak intensities is also shown to be significant at the 95% level in unpaired *t*-tests.

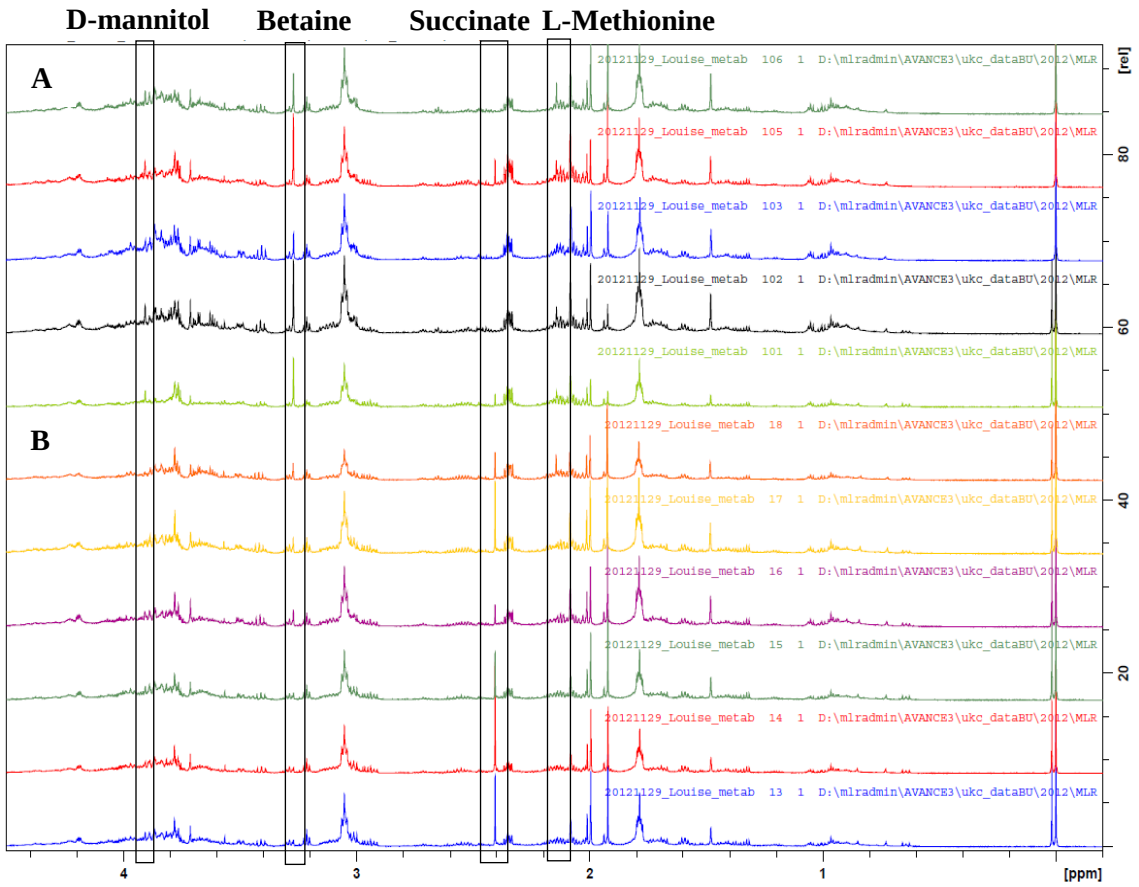

Figure 3-10. 1D-^{1}H NMR metabolite analysis of wild type or *cydD* cells

Metabolite extractions of wild type (A) and *cydD* (B) cells were analysed via 1D-^{1}H NMR spectroscopy, where six metabolite extractions and NMR analyses were performed for both wild type and *cydD* cultures, one of the wild type results was anomalous so this has been removed here. Where spectra differ between extracts from wild type and *cydD* cells, boxes have been drawn and the proposed metabolite labelled at the top of the spectra.

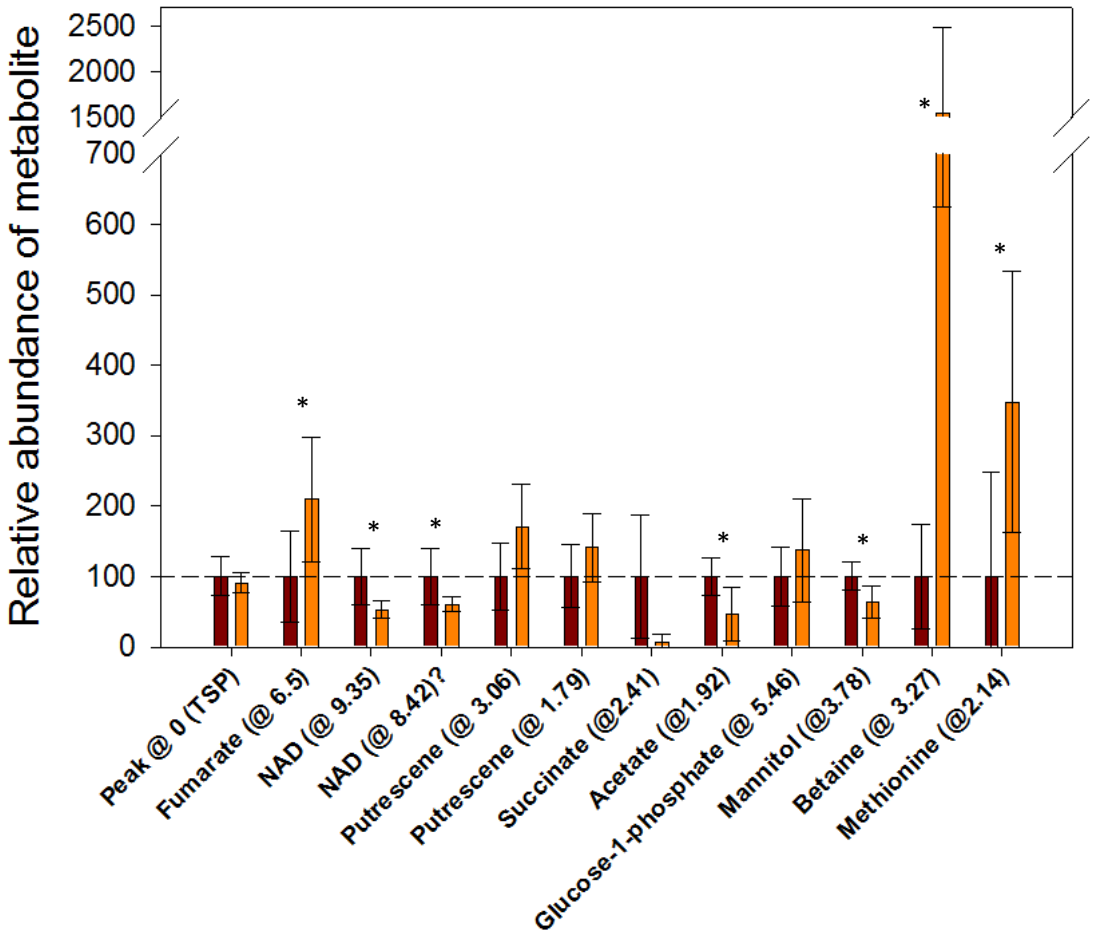

Figure 3-11. Relative abundance of metabolites in *cydD* and wild type *E. coli* cells

Red bars show metabolite levels in wild type (MS52) cells (normalised to an arbitrary value of 100), and yellow bars show metabolite levels in *cydD* (MS54) cells: the magnitude of the *cydD* metabolite data has been scaled relative to the wild type data. Error bars represent standard deviation. Asterisks denote that an unpaired *t*-test has been performed and a significant difference of 95% or above was observed. Only betaine shows a significant difference above the 99% confidence level.

3.3 Discussion

It has previously been shown that cytochrome *bd*-I contributes to the protection of cells against NO (Mason *et al.* 2009). With a fast NO dissociation rate, cytochrome *bd*-I is less sensitive to NO than the alternative terminal oxidase cytochrome *bo′*, thus cytochrome *bd*-I permits aerobic respiration to continue in the presence of NO. Since CydDC is required for the assembly of cytochrome *bd*-I, it was at first anticipated that cells lacking CydDC would exhibit a similar level of NO-mediated growth inhibition to that of cells lacking cytochrome *bd*-I only. To test this hypothesis, NOC-12 was used as a nitric oxide donor and growth was monitored after its addition. This approach demonstrated that growth of a *cydD* Keio mutant is more sensitive than a cytochrome *bd*-I mutant, which indicates an additional contribution to NO tolerance for the exporter complex. We hypothesised that the difference in sensitivity between the two strains is due to the export of thiols to the periplasm. As thiol groups are targets of NO (Ignarro 1989; Stamler *et al.* 1992; Stamler, Singel and Loscalzo 1992), we estimated that loss of export of these thiols to the periplasm would result in a higher concentration of NO being allowed to enter into the cytoplasm, in which NO can reach vunerable targets. To test this hypothesis, glutathione and cysteine were added to the growth medium and then a short time later the cells were challenged with NOC-12. The aim was to replace cysteine and GSH in the periplasm of *cydD* mutant cells to determine the sensitivity to NO. The results showed that exogenous addition of thiols reduces the NO-mediated growth inhibition of the *cydD* strain to a level comparable to a cytochrome *bd*-I mutant. These data are consistent with the hypothesis that CydDC contributes to the protection from NO both by permitting the assembly of cytochrome *bd*-I and via the export of low-molecular weight thiols that react with incoming NO.

After identifying cysteine (2002) and later glutathione (2005) as substrates of CydDC, Pittman *et al.* assayed the restoration of cytochrome *bd*-I in the presence of exogenous reduced glutathione or cysteine. Cysteine was added to the growth medium at final concentrations of 0.2 mM or 2 mM (Pittman *et al.* 2002). Exogenous glutathione was added to the growth medium at concentrations of 0.1, 0.25, 0.5, 1 or 2 mM (Pittman, Robinson and Poole 2005). Restoration of cytochrome *bd*-I assembly was not observed for cysteine nor glutathione at these respective concentrations. This lack of cytochrome *bd*-I restoration and the promiscuous nature of ABC-type transporters in general have led to a proposal that CydDC has additional substrates that are yet to be discovered. In the current study, cytochrome *bd*-I assembly was examined in the presence of both glutathione and cysteine. Since high concentrations of cysteine can be

toxic to cells, a low concentration (0.5 mM) was used so that an appropriate OD_{600} could be reached after overnight growth. A combination of 0.5 mM cysteine and 1 mM reduced glutathione was added to *cydD* cells for overnight growth. The CO difference spectra of these cells displayed spectral characteristics of assembled cytochrome *bd*-I. We therefore concluded that glutathione and cysteine added simultaneously to a *cydD* mutant can restore haem insertion into cytochrome *bd*-I. This result is interesting as it suggests that loss of cytochrome *bd*-I assembly in a strain lacking CydDC is not merely due to loss of a reduced thiol pool in the periplasm, otherwise just one of the thiols would have restored cytochrome *bd*-I assembly. Instead, the requirement of both thiols indicates a process in which both thiols play a part.

The metabolomics data suggests that loss of CydDC may result in a slight increase in L-methionine and fumarate and reduction of succinate, D-mannitol, acetate and NAD (unpaired *t*-test at the 95% level). However, a large increase in betaine levels was observed, and this was the only metabolite detected in *cydD* cells that could be confidently described as having altered abundance: betaine is significantly altered at the 99% level compared to wild type cells (unpaired *t*-test). This observation is consistent with *cydD vs*. wild type microarray data (Holyoake *et al.* 2015, collected by Dr. Mark Shepherd & Dr. Stuart Hunt) in which the betaine synthesis genes *betA* and *betB* are up-regulated and the transcription factor BetI, a repressor of these genes has reduced activity as supported by modelling of transcription factor activities (Holyoake *et al.* 2015). The *betAB* operon is involved in the biosynthesis of betaine, an osmoprotectant also known as glycine betaine. Taken together this would show that in response to loss of CydDC, activity of the transcription factor BetI is decreased, resulting in the up-regulation of *betAB* operon at the transcriptional level which results in an increase in the osmoprotectant betaine (Andresen *et al.* 1988). The *betA* gene encodes a choline dehydrogenase (CHD) that utilises FAD and pyrroloquinoline (PQQ) cofactors. Intriguingly, BetA has been shown to use ubiquinone as an electron acceptor (Barrett and Dawson 1975). It is therefore hypothesised that BetA and BetB permit electrons to feed into the ubiquinol pool (Figure 3-12) while simultaneously providing glycine-betaine to alleviate osmotic perturbations elicited by an accumulation of glutathione and cysteine in *cydD* cells.

The reduction in levels of NAD^+ in the absence of CydDC is likely to be a result of the reducing conditions produced by the loss of thiol export and thus the excessive

amount of reduced thiols in the cytoplasm. Furthermore, BetB utilises NAD during betaine biosynthesis, as levels of this metabolite are significantly increased in *cydD* cells, this could further explain the depletion of NAD. It is unclear why D-mannitol levels are also depleted.

Despite the *cydD vs.* wild type microaray analysis showing an up-regulation of *yjcH* responsible for acetate import, acetate levels were shown to be depleted in *cydD* cells. Microarray analysis however also led to the conclusion that misfolded proteins and fatty acids are broken down in *cydD* cells to feed into the TCA cycle in order to restore the balance of metabolic flux, so it is likely that acetate levels are depleted due to its use in fuelling *β*-oxidation of fatty acids as well as the TCA cycle.

Succinate and fumarate, intermediates of the TCA cycle are both altered in *cydD* cells: levels of succinate are reduced and fumarate is increased, reflecting a potential increase in succinate dehydrogenase activity that catalyses the oxidation of succinate to fumarate with the simultaneous reduction of ubiquinone to ubiquinol (Figure 3-12). This supports the findings of the *cydD vs.* wild type microarray which showed that genes of the TCA cycle are induced (Figure 3-9). This change in energy metabolism may be due, in part, to a requirement for additional electron flux into the quinone pool.

Metabolites were assigned to chemical shift peaks via the comparison of collected NMR data with NMR reference data sets from the 'Madison metabolite consortium database'. The comparison of peaks, however, is problematic for a number of reasons, including the presence of metabolites in biological samples that have yet to be added to the database, changes in the chemical shift of peaks due to variations in pH and salt concentration as well as the crowded nature of the collected 1D-^{1}H data which means that there are peak overlaps, this all culminates in the fact that peaks could be incorrectly assigned. (Cui *et al.* 2008). Mass spectrometry to compare the metabolite extracts from wild type and *cydD* cultures could confirm that the metabolites identified in this chapter are indeed altered by the deletion of *cydD*.

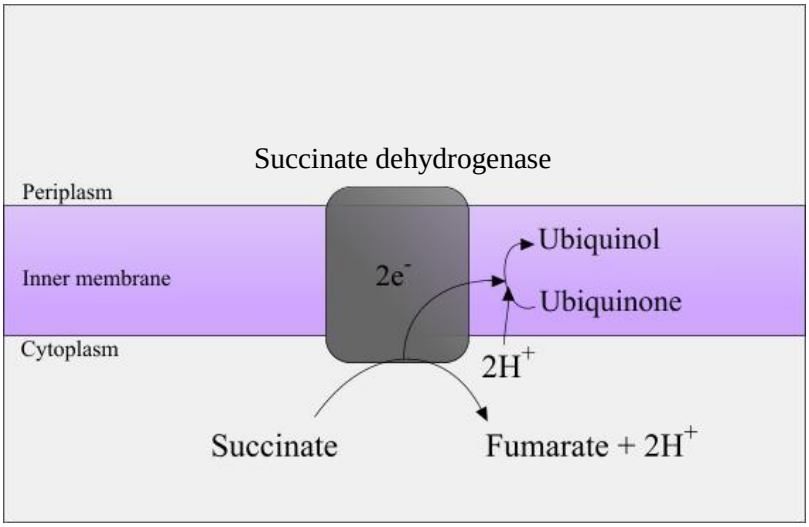

Figure 3-12. Succinate dehydrogenase

Succinate and fumarate levels are affected by the loss of *cydD*; an increase in fumarate and a decrease in succinate levels reflect upon the up-regulation of succinate dehydrogenase seen in previous *cydD vs.* WT microarray analysis. Succinate dehydrogenase catalyses the oxidation of succinate to fumarate with simultaneous reduction of ubiquinone to ubiquinol. An increase in succinate dehydrogenase expression and activity is likely to be the reason for the changes in TCA cycle intermediates, this would also provide additional reducing power to the quinol pool of *cydD* mutants.

Chapter 4

Global adaptations in response to CydDC activity: transcriptomic perturbations resulting from variations in periplasmic cysteine/glutathione levels

Summary

Exogenous cysteine and GSH have previously been shown, to restore cytochrome *bd*-I assembly in a *cydD* mutant, suggesting that the presence of these thiols in the periplasm of cells is crucial for the assembly of cytochrome *bd*-I. Microarray experiments were performed to further probe the role of glutathione and cysteine in the periplasm. In cells lacking CydDC, GSH and cysteine will still be present in the cytoplasm, potentially at higher concentrations than in wild type cells, the periplasm however, is thought to be deficient of these thiols due to a lack of export from the cytoplasm. Exogenous addition of GSH and cysteine should restore their presence in the periplasmic space. As a *cydD vs*. wild type microarray experiment had already been perfomed, a microarray experiment was designed to compare the regulation of genes of a *cydDC* mutant when GSH and cysteine were added exogenously. As it is likely that addition of GSH and cysteine to a *cydDC* mutant would lead to restoration of cytochrome *bd*-I, a *cydDC cydAB* mutant was also used in parallel with the aim to study the effects of transcription caused by the addition of thiols that are independent of cytochrome *bd*-I restoration.

The addition of GSH and cysteine to *cydDC* cells led to an up-regulation of 163 genes and a down-regulation of 173 genes compared to *cydDC* cells alone. Whereas the addition of these thiols to *cydDC cydAB* cells led to an up-regulation of 135 genes and a down-regulation of 220 genes when compared to *cydDC cydAB* cells alone. The large number of genes found to have altered expression in response to the addition of GSH and cysteine to growth media, both in *cydDC* and *cydDC cydAB* cells made it difficult to clearly identify the physiological changes taking place. The activities of transcription factors were modelled to determine which transcription factors have altered activities in response to the exogenous thiols. This gave an insight into the stimuli imposed upon cells and the transcriptional mechanisms underpinning changes to gene expression. Genes controlled by TFs with altered activities formed a subset of genes for ease of interpretation.

Analysis of this subset of genes showed that independently of cytochrome *bd*-I restoration, the addition of GSH and cysteine to growth media resulted in an up-regulation of respiratory genes, including those encoding cytochrome *bd*-II and hydrogenase I. An up-regulation in transcription of genes related to molybdenum cofactor biosynthesis, ion transport and the regulation of intracellular formate levels was also observed. Conversely a down-regulation was simultaneously reported in genes

encoding proteins of the tricarboxylic acid (TCA) cycle, motility genes and genes involved in the biosynthesis and transport of amino acids.

By investigating the stimuli of TFs with altered activities in both *cydDC* and *cydDC cydAB* cells, it was found that cells were potentially responding to changes in the demand for amino acids, as well as osmotic stress, low oxygen conditions, phosphate starvation, and changes in the levels of copper, H_2O_2, dihydroxyacetone and sodium.

In connection with thiol-mediated cytochrome *bd*-I restoration, an increase in expression of genes encoding cytochrome *bd*-I was observed alongside a down-regulation of genes of the methylcitrate cycle (in which propanoate is used as a carbon source to generate to succinate and pyruvate) which respond to changes in available carbon sources.

4.1 Introduction

The ABC-type transporter CydDC is known to export reduced glutathione and cysteine to the periplasm of *E. coli*. Loss of CydDC results in an over-oxidising periplasm and a pleiotropic phenotype which resembles the phenotypes of *dsb* mutants. The low-molecular weight (LMW) thiols exported by CydDC are therefore thought to participate in maintaining the redox environment of the periplasm. Exogenous addition of the known allocrites of CydDC has been shown to restore the survival and temperature-sensitive phenotypes of a *cydC* mutant (Goldman, Gabbert and Kranz 1996a), and it has been shown that exogenous cysteine can also re-establish cell motility, restore resistance to benzylpenicillin and DTT and can partially restore the assembly of *c*-type cytochromes (Pittman *et al.* 2002). In the previous chapter we showed for the first time that cytochrome *bd*-I assembly can be restored in a *cydD* mutant by the addition of cysteine and reduced glutathione to the growth medium. These observations highlight the multiple cellular roles played by reduced thiols within the periplasm, and the importance of their export by CydDC. Furthermore, considering that the exported thiols are thought to help maintain the redox environment of the periplasm, this is of consequence to extracytoplasmic proteins that contain disulphide bonds. As discussed in Section 1.1, disulphide bonds are essential for protein structure and function. It is therefore expected that loss of *cydDC* would lead to problems with functionality of these proteins including proteins related to cell motility, attachment and the secretion of extracellular proteins.

The assembly of cytochrome *bd*-I in a strain lacking CydDC has not been shown to be restored by the addition of glutathione or cysteine alone, but simultaneous addition of the two reduced thiols can permit haem insertion into the polypeptide chains of cytochrome *bd*-I (Chapter 3). This finding highlights the lack of understanding around the relationship between CydDC and cytochrome *bd*-I. This chapter seeks to characterise the transcriptomic adaptations that result from replenishing the periplasm of strains lacking CydDC with glutathione and cysteine, with a view to elucidating mechanistic insights into physiological processes controlled by external reductant.

4.2. Results

4.2.1 The role of CydDC-exported GSH and cysteine

With the discovery that exogenously added GSH and cysteine restores cytochrome *bd*-I assembly in a *cydDC* mutant (Chapter 3), it was of interest to elucidate the transcriptomic adaptations that result from the addition of these low-molecular weight thiols to cultures lacking the CydDC complex. As discussed in Chapter 3, it is reasonable to assume that extracellular glutathione and cysteine are at equilibrium within the periplasmic space (Decad and Nikaido 1976), so extracellular reductant levels are thought to mimic those of the periplasm. A microarray approach was chosen to provide insights into how cells respond to the absence/presence of these thiols within the periplasm: genome-wide transcriptional analysis with microarray technology is a powerful tool for determining how gene expression is affected. Since transcriptional perturbations are usually triggered by changes in the local environment, it was hypothesised that this approach would provide insights into how CydDC-mediated thiol export influences conditions in the cytoplasm. A *cydD vs*. wild type microarray had been previously performed (as discussed in more detail in Section 3.2.5), in consideration of this wild type cells were not included in the following experiments; experimental conditions were replicated to allow comparisons between datasets.

In a *cydDC* mutant, many of the phenotypes are attributable to the loss of *bd*-type oxidase assembly. In a microarray experiment that compares gene expression of a *cydDC* mutant in the presence or absence of GSH and cysteine, one would expect to see a lot of gene changes that are primarily due to the restoration of cytochrome *bd*-I. By using a *cydDC cydAB* double mutant alongside a *cydDC* mutant, it was hypothesised that one could differentiate between transciptomic changes resulting from addition of GSH and cysteine (direct effects) and those that result from the restoration cytochrome *bd*-I assembly (indirect effects). Hence, a microarray experiment was designed (Figure 4-1) in which these thiols would be added exogenously at concentrations to match those used in cytochrome *bd*-I restoration assays (Figure 3-8). Two microarray experiments were planned, with one to use a *cydDC* mutant and the other a *cydDC cydAB* double mutant. Global gene transcription could then be compared between these mutants when 1 mM GSH and 0.5 mM cysteine were added to the growth medium. It was envisaged that this approach would provide insights into the global effects of LMW thiols normally exported by CydDC in *E. coli*.

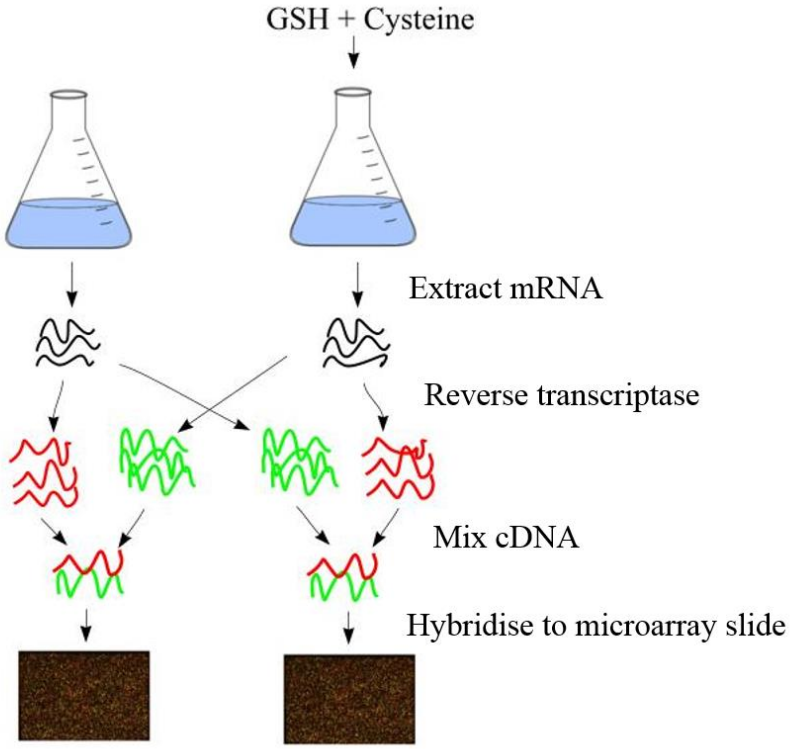

Figure 4-1. Experimental design of the microarray experiment

Example of a microarray experiment designed to investigate the transcriptomic adaptations that arise from the presence of GSH and cysteine in the periplasm. *cydDC* cells (MS14) were grown in the presence or absence of exogenous GSH and cysteine. mRNA was extracted from bacteria and used as the template for a reverse transcription reaction to make labelled complementary DNA (cDNA). A dye swap was utilised to ensure no bias due to dye signal strength. This meant that each mRNA sample was labelled separately with both cy3 (green) and cy5 (red) dyes as depicted with the arrows in the diagram. Dye swaps are seen as technical repeats as they give two sets of results from the same two flasks of cells, to obtain accurate results these dye swap experiments were repeated with bacteria grown in separate flasks to ensure two biological repeats and accumulate a total of four sets of fold-change values for each microarray experiment. As exogenous GSH and cysteine have been shown to restore cytochrome *bd*-I, a *cydDC cydAB* mutant (MS336) was used for a second microarray experiment that is otherwise identical to the experiment shown above. It was envisaged that by comparison of these two array datasets one could distinguish between transcriptional changes resulting from restoration of cytochrome *bd*-I assembly and those that are independent of this complex.

4.2.2 Creating an MG1655 *cydDC cydAB* double mutant

For one of the two microarray experiments performed in this chapter it was necessary to create a *cydDC cydAB* double mutant. A single mutant needed to be cured of the resistance cassette so that the presence of a second deletion could be detected. Removal of the resistance cassette utilised the pCP20 plasmid (Table 2-1) which encodes a flippase enzyme (FLP) for the removal of DNA between repeat sequences.

4.2.2.1 Removal of the resistance cassette in a *cydAB*::Cm MG1655 E. *coli* strain

MS15 cells (*cydAB*::Cm)(Table 2.1) were made competent using the method as described by Brachmann *et al*. 1998 (Section 2.2.6.1), cells were then transformed with plasmid pCP20 (as described in Section 2.2.6.2). To select for transformation cells were spread onto ampicillin Luria Bertani (LB) plates. Ampicillin resistant colonies were then grown in LB at 42^{o}C to remove the temperature sensitive pCP20 plasmid. Colonies were picked and streaked onto LB, LB-ampicillin and LB-kanamycin plates. Colonies that could only grow on LB plates were expected to be cured of the chloramphenicol resistance cassette as well as the pCP20 plasmid. The λ–Red mutagenesis approach (Datsenko and Wanner 2000) was then used to replace the *cydDC* operon with a chloramphenicol resistance cassette, as is described in Section 2.2.4. Briefly, primers pMS35 and pMS36 (Table 2-2) anneal 500 bp either side of the *cydDC* operon, were used to amplify the chloramphenicol resistance cassette from a K-12 *cydDC*::Cm mutant, generating 500 bp flanking regions, homologous to the DNA either side of the genomic *cydDC* operon. The amplified DNA fragment was introduced into cells via electroporation, and recombination was enhanced between the homologous regions by the λ-Red recombinase. Following the mutagenesis protocol, colony PCR was performed to confirm both the replacement of DNA at the *cydDC* locus and the absence of the *cydAB* operon, this was later repeated using the bacterial culture grown for the microarray.

4.2.2.2 PCR verification of MS336 (*cydAB*$^{-}$ *cydDC*::Cm)

As there is no selective pressure to keep the *cydAB* deletion, a PCR was performed on the double mutant liquid culture used in the microarray experiment. This checked both that the *cydDC* operon was replaced by a chloramphenicol cassette (*cydDC*::Cm) and that the *cydAB* operon was not present.

To check the *cydDC* operon, primers pMS3 and pMS4 were used (Table 2-2), when these anneal to the original wild type DNA sequence a fragment of 3,862 bp in length is produced, this corresponds to the band seen in Figure 4 close to the 4 kb marker band. Replacement of the *cydDC* operon with the chloramphenicol resistance cassette is expected to produce DNA fragments of 1,552 bp in length. MS14 (*cydDC*::Cm) was used as a control, and similar bands were seen both for this strain and the newly made double mutant next to the 1,500 bp band in the DNA ladder thus indicating that the operon had been replaced.

To check the *cydAB* locus, primers pMS9 and pMS10 were used (Table 2-2). Colonies of strains MS2 (MG1655 WT) and MS15 (*cydAB*::Cm) were included as controls; use of MS2 as a DNA template resulted in a band inbetween the 3 kb and 4 kb marker bands (Figure 4-2), this corresponds to the expected size of 3,124 bp which includes the *cydAB* genes and 500 bp flanking regions. Use of MS15 (*cydAB*::Cm) as the DNA template resulted in a band at around 1,500 bp (Figure 4-2), this represents the size of the chloramphenicol resistance cassette along with the 500 bp flanking regions; the expected band size was 1,552 bp. MS13 (*cydAB*::Km) was also included in this PCR check, the resulting band around 2,000 bp corresponds to the expected band size (2015 bp). PCR of the *cydDC*::Cm *cydAB* double mutant (MS336) resulted in a much smaller band compared to the other reactions at around 600 bp (Figure 4-2), the expected fragment size was 550 bp, thus indicating that the *cydAB* operon was not present.

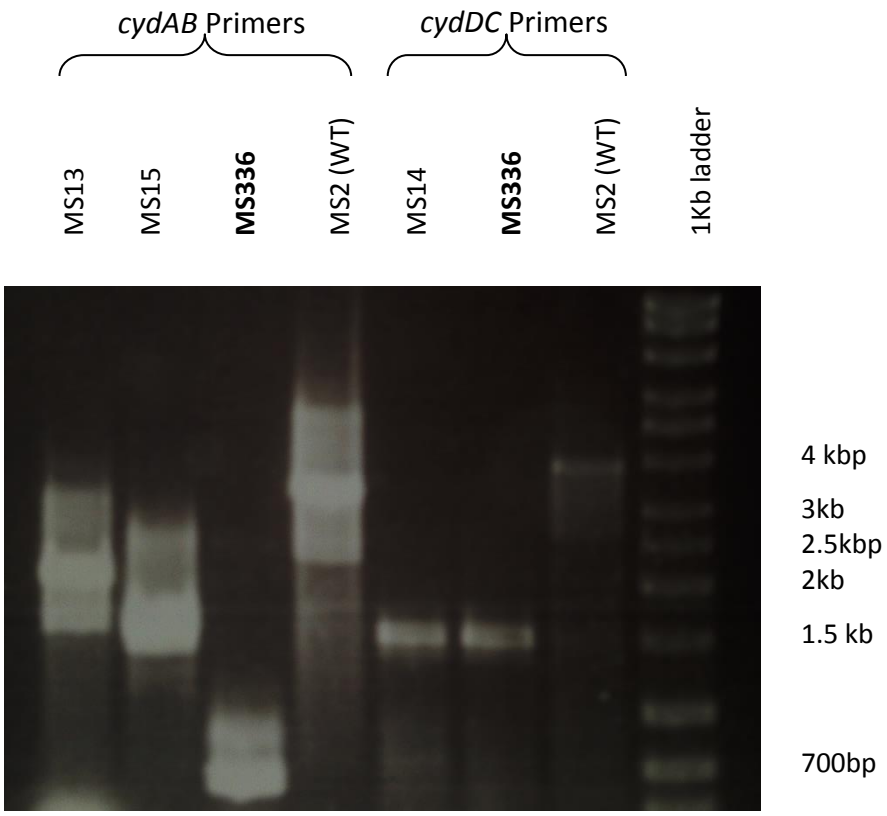

Figure 4-2. PCR verification of double mutant

Colony PCR was performed to ensure the *cydDC* operon was replaced by a chloramphenicol cassette (*cydDC*::Cm) and that the *cydAB* operon was not present. To check the *cydDC* operon primers pMS3 and pMS4 were used (right side of the gel), for the *cydAB* operon, primers pMS9 and pMS10 were used (left side of the gel) (Table 2-2). Colonies of strains MS13 (*cydAB*::Km), MS15 (*cydAB*::Cm) and MS2 (MG1655 WT) were used as positive controls to test that primers pMS9 and pMS10 are working. Colonies of strains MS14 (*cydDC*::Cm) and MS2 (MG1655 WT) were used as controls to test that primers pMS3 and pMS4 are working and to compare band sizes.

PCR of MS336 with primers pMS9 and pMS10 resulted in a band around 600 bp, much smaller than the bands seen when using MS2 (WT), MS13 (*cydAB*::Km) or MS15 (*cydAB*::Cm) as the DNA template, this small band correlates with the expected band size of 550 bp for the flanking regions of the FRT sites thus indicating the absence of the *cydAB* operon.

Using primers pMS3 and pMS4 with MS336 as the DNA template results in a band around 1,500 bp, close to the expect size of 1,552 bp for the chloramphenicol resistance cassette along with the 500 bp flanking regions, this is also seen when using MS14 (*cydDC*::Cm) suggesting that in both these strains a chloramphenicol resistance cassette has replaced the *cydDC* operon.

4.2.3 Global transcriptomic changes that result from exogenous addition of GSH and cysteine

Addition of GSH and cysteine did not affect the rate of growth, so cells were grown in batch culture and it was not necessary to limit growth rates using continuous culture. MG1655 *cydDC*::Cm (MS14) and MG1655 *cydAB cydDC*::Cm (MS336) were grown in 10 ml LB overnight cultures at 37°C 180 rpm. Of these overnights, 500 µl was used to inoculate 50 ml defined media (supplemented with $MgCl_2$ and 10% casamino acids) in 250 ml conical flasks. Where appropriate, freshly prepared and filter sterilised 250 mM GSH and 500 mM cysteine stock solutions were added to give a final concentration of 1 mM GSH and 0.5 mM cysteine. Cultures were then grown at 37°C 180 rpm until an OD_{600} of 0.4 was reached. At this point, 30 ml of culture was removed from the flasks and treated as described in sections 2.2.7.2 and 2.2.7.3. The growth conditions were chosen to mimic those of existing microarray data of *cydB vs.* WT (Shepherd *et al.* 2010) and *cydD vs.* WT (Holyoake *et al.* 2015).

Dye swap experiments were performed to compensate for differences in signal and binding affinities of the two dyes cy3 and cy5 (Figure 4-1). For each microarray experiment, two biological and two technical repeats were used to perform two dye swap experiments. This gave four separate fold-change values per gene (Figure 4-3) which could be averaged. Fold-changes with magnitudes equal to or above 2 (i.e. +/- 2) and with *p*-values equal to or below 0.05 were considered significant. *p*-values were determined using the Benjamini Hochberg FDR (False discovery rate) statistical method (Benjamini and Hochberg 1995), which assumes that randomly 5% of the genes will have a *p*-value of 0.05 or lower just by chance. Benjamini Hochberg reduces the number of genes that are incorrectly rejected as false discoveries. As shown in the volcano plots in Figure 4-4, the spread of the data could be visualised with the aforementioned stringencies. For the *cydDC* + GSH/cysteine *vs. cydDC* comparison, a total of 163 genes were significantly up-regulated, and 173 genes were significantly down-regulated (the spread of the data is shown in Figure 4-4A and gene lists are found on the CD that accompanies the thesis). For the microarray experiment *cydDC cydAB* + GSH/cysteine *vs*. *cydDC cydAB*, a total of 135 genes were significantly up-regulated, and 220 genes were significantly down-regulated (the spread of the data is shown in Figure 4-4B and gene lists are found on the CD that accompanies the thesis).

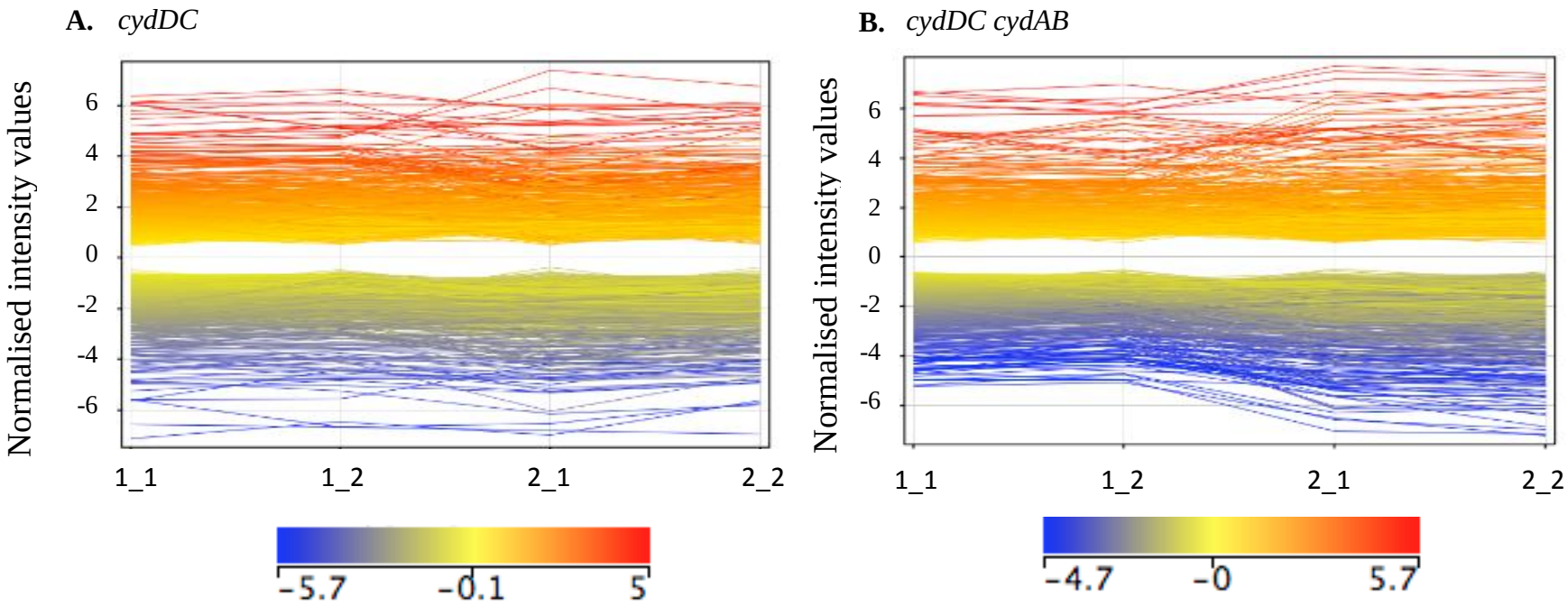

Figure 4-3. Expression profiles showing the magnitude of the effect of reduced glutathione and cysteine on gene regulation
Graphs were generated in GeneSpring (v13.1). The four points along the X-axis represent four scanned array samples: 1_1 and 1_2 are biological repeats, and 2_1 and 2_2 are technical repeats with dyes swapped. Line gradients between 1_1 and 1_2 or 2_1 and 2_2 shows the discrepancy between scanned array repeats, ideally these lines will be straight to represent good reproducibility. Line gradients between 1_2 and 2_1 show changes between dye-swap pairs. Each coloured line represents a gene, only genes which have a fold-change of over 2 or under -2 with a P-value less than 0.05 are shown. As represented in the colour-bar scale, red indicates genes that are up-regulated and blue represents genes that are down-regulated. **A.** Data for the *cydDC* + GSH/cysteine *vs. cydDC* comparison. **B.** Data for the *cydDC cydAB* + GSH/cysteine *vs. cydDC cydAB* comparison.

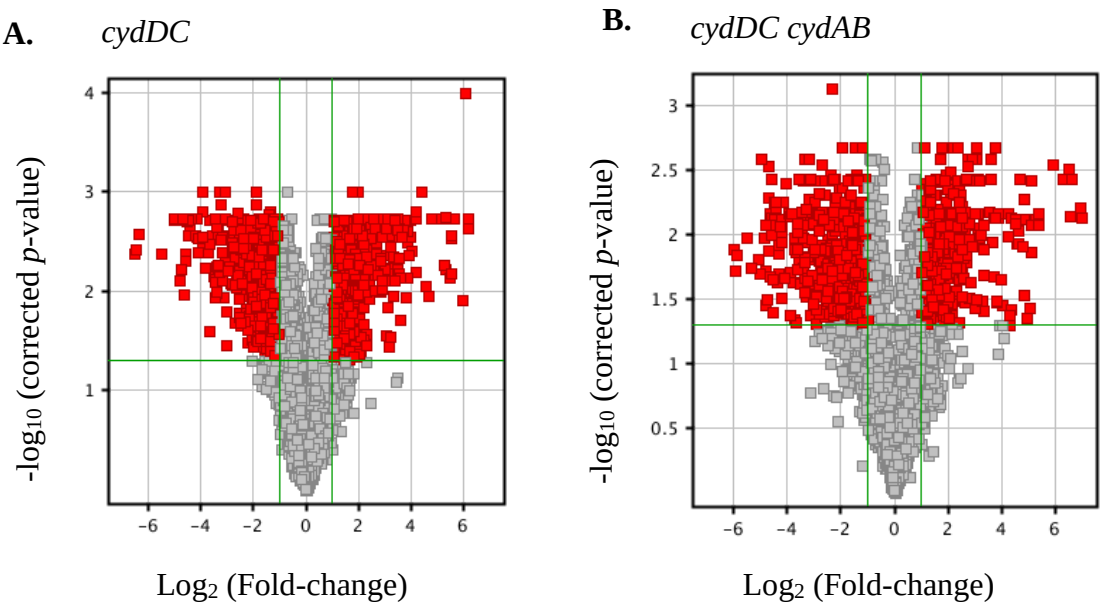

Figure 4-4. Volcano plots showing the cut off of significant gene fold-changes
Figure created in GeneSpring (v13.1) to show the spread of the data and to demonstrate the number of genes included in the 'significant' data sets. Significant data is represented by red squares (with both an average $\log_2$ fold-change over 2 or under -2, and a *p*-value above 0.05), insignificant data is represented by grey squares. **A.** Data for the *cydDC* + GSH/cysteine *vs. cydDC* comparison. **B.** Data for the *cydDC cydAB* + GSH/cysteine *vs. cydDC cydAB* comparison.

4.2.3.1 Exogenous GSH/cysteine controls the activities of key transcription factors

As both microarray experiments identified a large number of differentially regulated genes, it was at first difficult to glean meaningful insights into how the addition of exogenous thiols altered conditions in the cell. To gain an understanding of the physiological changes taking place, activities of transcription factors (TFs) were modelled to investigate the underpinning transcriptional mechanisms in operation that elicit the transcriptomic responses (i.e. a knowledge of TF activities provides information on environmental changes).

Mathematical modelling of the transcription factor activities was carried out using TFinfer version 2.0 (Shahzad Asif *et al.* 2010). The complete transcriptomic data-sets obtained from GeneSpring were used for the analysis; therefore no limitations with regard to gene expression level were enforced prior to the application of TFinfer. For both of the microarray experiments described above, AppY, BirA, ArcA CsgD, GadX, NhaR, PepA, RcsB TrpR are predicted to have an increased activity and CueR, DhaR, FlhDC, LeuO, and OxyS are predicted to have a reduced activity (Figures 4.4. and 4.5).

These changes are predicted in both mutants but at slightly different levels, for example the increase in AppY activity is larger for the *cydDC cydAB* mutant than the increase in activity seen in the *cydDC* mutant. However, major difference in TF activities between the two datasets (shown as red bars in Figures 4-5 and 4-6) are that RstA has a significant increase in activity and MngR, PutA and PrpR have reduced activity after addition of GSH and cysteine only in *cydDC* cells. Furthermore, OmpR and PspF are predicted to have reduced activity only in the *cydDC cydAB* experiment (Figure 4-6). These differences show that the *cydDC* and *cydDC cydAB* mutants are reacting to the addition of the thiols in a slightly different manner. The most obvious difference between the two mutants is the capability for cytochrome *bd*-I restoration in *cydDC* but not *cydDC cydAB* cells. It is therefore predicted that the variation between the datasets of the two microarray experiments is due to cytochrome *bd*-I restoration after thiol addition to *cydDC* cells.

To separate the direct effects of exogenous thiols upon transcription from those elicited by cytochrome *bd*-I restoration, the response of both *cydDC* and *cydDC cydAB* cells to exogenous thiols were compared. Changes to gene regulation (in the same direction) seen in both microarray experiments (Supplementary Table 3) are considered independent of cytochrome *bd*-I, whereas differentially regulated genes found in the *cydDC* strain but not *cydDC cydAB* strain after thiol addition (Supplementary Table 4) are considered dependent upon cytochrome *bd*-I (more direct effects of periplasmic reductants).

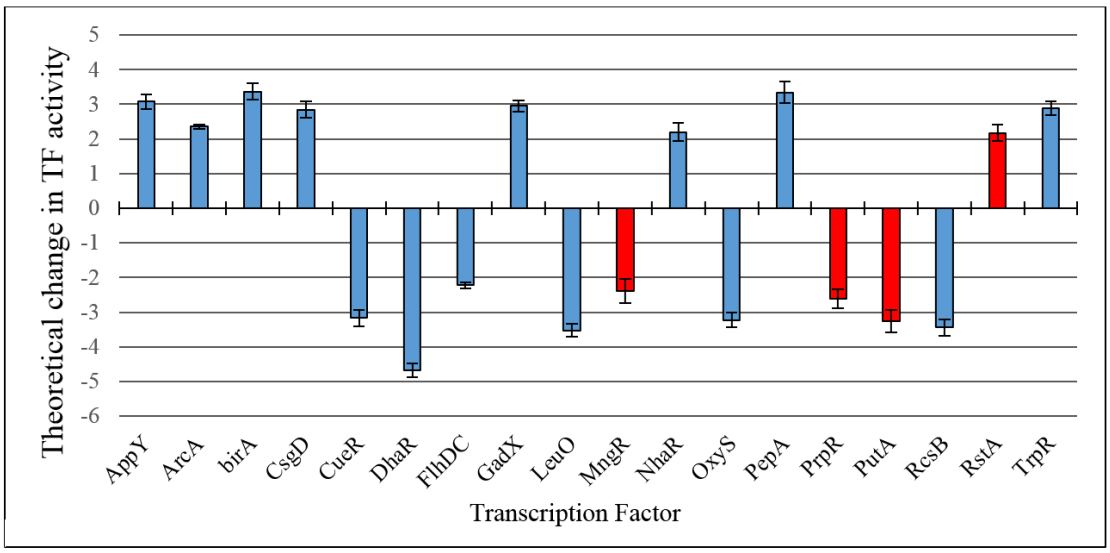

Figure 4-5. Theoretical change in transcription factor activities when cysteine and reduced glutathione are added to a *cydDC* mutant
As determined by TFinfer, changes over 2 are considered significant. All TFs with changes above 2 and below -2 were selected and are displayed here. Red bars denote transcription factor activities that were not observed in the *cydD CcydAB* experiment (Figure 4-6). Error bars represent confidence intervals generated by TFinfer.

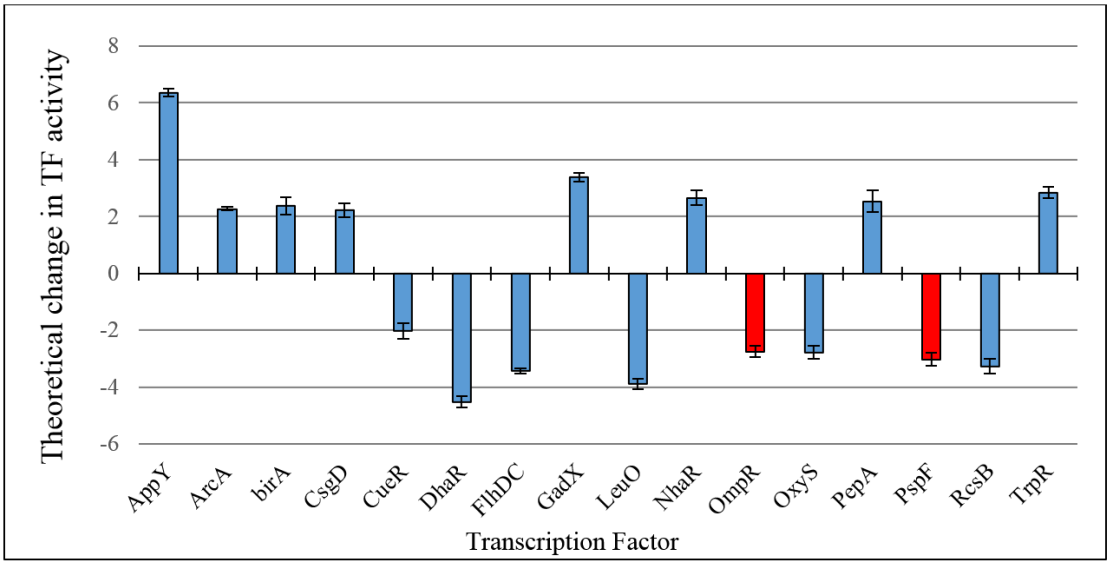

Figure 4-6. Theoretical change in transcription factor activities when cysteine and reduced glutathione are added to a *cydDC cydAB* mutant
As determined by TFinfer, theoretical changes in transcription factor activity over 2 are considered significant, applicable transcription factors are shown here. Red bars denote transcription factor activities that were not observed in the *cydDC* experiment (Figure 4-5). Error bars represent confidence intervals generated by TFinfer.

4.2.3.2 Transcriptional changes elicited by GSH/cysteine, that are independent of cytochrome *bd*-I assembly

To investigate how cells lacking *cydDC* respond to the addition of GSH and cysteine independently of cytochrome *bd*-I assembly, transcription factors with altered activity after the addition of GSH and cysteine in both *cydDC* and *cydD CcydAB* cells were identified using the data from Figures 4-5 and 4-6. The genes affected by those TFs were then compiled to make Table 4-1, which includes a colour scale to aid visualisation of average fold-changes.

Table 4-1. Transcriptional changes resulting from addition of GSH/cysteine that are independent of cytochrome *bd*-I assembly

Changes to transcription factor activities after the addition of GSH and cysteine to both *cydDC* and *cydDC cydAB* strains, include a significant increase in the activities of AppY, ArcA, BirA, CsgD, GadX, NhaR, PepA, RcsB and TrpR while causing a significant decrease in the activities of CueR, DhaR, FlhDC, LeuO and OxyS (Figures 4-5 and 4-6). The mean fold increase or decrease of individual gene expression after the addition of thiols is indicated by the colour scale bar. Functional annotations were taken from the Ecogene (http://www.ecogene.org) and RegulonDB (http://regulondb.ccg.unam.mx) websites.

Repression **Induction**

<-80 -60-80 -60-30 -30-10 -10-2 2-10 10-30 30-60 60-80 >80

Gene name	Description	*cydDC* GSH cysteine *vs.* *cydDC* fold-changes	*cydDC cydAB* GSH cysteine *vs.* *cydDC cydAB* fold-changes	TF
dps	Fe-binding and storage protein	23.34	13.94	*oxyS*
osmB	lipoprotein	21.31	18.51	RcsB
ybaS	predicted glutaminase	15.51	28.18	GadX
pflB	pyruvate formate lyase I	14.16	6.95	ArcA
focA	formate transporter	12.85	5.05	ArcA
ybaT	predicted transporter	12.25	28.7	GadX
nhaA	sodium-proton antiporter	7.49	8.01	NhaR
appC	"cytochrome *bd*-II oxidase, subunit I"	6.17	123.91	AppY/ArcA
appA	phosphoanhydride phosphorylase	5.88	94.83	AppY/ArcA
appB	"cytochrome *bd*-II oxidase, subunit II"	5.49	120.08	AppY/ArcA
hyaC	"hydrogenase 1, *b*-type cytochrome	4.86	32.56	AppY/ArcA

	subunit"			
hyaF	protein involved in nickel incorporation into hydrogenase-1 proteins	4.34	19.59	AppY/ArcA
hyaB	"hydrogenase 1, large subunit"	4.05	33.67	AppY/ArcA
moaA	molybdopterin biosynthesis protein A	3.91	2.35	CueR
hyaA	"hydrogenase 1, small subunit"	3.82	33.88	AppY/ArcA
moaC	"molybdopterin biosynthesis, protein C"	3.72	2.19	CueR
rutB	predicted enzyme	3.6	2.51	ArcA
hyaE	protein involved in processing of HyaA and HyaB proteins	3.37	19.6	AppY/ArcA
moaE	"molybdopterin synthase, large subunit"	3.27	2.67	CueR
moaD	"molybdopterin synthase, small subunit"	3.22	2.16	CueR
copA	copper transporter	2.61	2.87	CueR
yaiA	predicted protein	2.38	3.76	TrpR
yacH	predicted protein	-2.35	-3.05	ArcA
gltI	glutamate and aspartate transporter subunit	-2.42	-7.41	FlhDC
trpD	fused glutamine amidotransferase (component II) of anthranilate synthase/anthranilate phosphoribosyl transferase	-2.63	-4.33	TrpR
flgM	anti-sigma factor for FliA (sigma 28)	-2.9	-2.57	FlhDC
flgA	assembly protein for flagellar basal-body periplasmic P ring	-3.23	-8.24	FlhDC
sucC	"succinyl-CoA synthetase, beta subunit"	-3.24	-10.69	ArcA
flgN	export chaperone for FlgK and FlgL	-3.39	-8.74	FlhDC
oppA	oligopeptide transporter subunit	-3.52	-4.68	ArcA
sucD	"succinyl-CoA synthetase, NAD(P)-binding, alpha subunit"	-3.58	-12.18	ArcA
oppD	oligopeptide transporter subunit	-3.6	-4.25	ArcA
flgG	flagellar component of cell-distal portion of basal-body rod	-3.64	-5.61	FlhDC
sdhB	"succinate dehydrogenase, FeS subunit"	-3.73	-4.54	ArcA
oppB	oligopeptide transporter subunit	-3.9	-5.2	ArcA
trpA	"tryptophan synthase, alpha subunit"	-3.94	-3.16	TrpR
oppC	oligopeptide transporter subunit	-3.98	-4.99	ArcA
acnB	bifunctional aconitate hydratase 2/2-methylisocitrate dehydratase	-4.56	-6.5	CueR
icd	"e14 prophage; isocitrate dehydrogenase, specific for NADP+"	-4.58	-10.33	ArcA
flgF	flagellar component of cell-proximal portion of basal-body rod	-4.58	-9.99	FlhDC
gltL	glutamate and aspartate transporter subunit	-4.61	-5.79	FlhDC
oppF	oligopeptide transporter subunit	-4.69	-5.13	ArcA
flgB	flagellar component of cell-proximal portion of basal-body rod	-4.82	-18.47	FlhDC
gltK	glutamate and aspartate transporter subunit	-5.04	-4.08	FlhDC
flgI	predicted flagellar basal body protein	-5.23	-10.28	FlhDC

gltA	citrate synthase	-5.61	-7.13	ArcA
flgE	flagellar hook protein	-5.76	-23.99	FlhDC
leuD	3-isopropylmalate isomerase subunit	-5.85	-11.03	LeuO
flgC	flagellar component of cell-proximal portion of basal-body rod	-6.04	-24.19	FlhDC
leuC	"3-isopropylmalate isomerase subunit, dehydratase component"	-6.51	-9.07	LeuO
flgD	flagellar hook assembly protein	-6.74	-26.18	FlhDC
trpB	"tryptophan synthase, beta subunit"	-7.01	-4.55	TrpR
flgH	flagellar protein of basal-body outer-membrane L ring	-7.13	-23.66	FlhDC
leuA	2-isopropylmalate synthase	-7.69	-10.15	LeuO
carB	carbamoyl-phosphate synthase large subunit	-9.61	-9.74	PepA
aldA	"aldehyde dehydrogenase A, NAD-linked"	-10.55	-10.89	ArcA
leuB	3-isopropylmalate dehydrogenase	-10.58	-14.79	LeuO
dhaM	fused predicted dihydroxyacetone-specific PTS enzymes: HPr component/EI component	-13.29	-10.74	DhaR
dhaK	"dihydroxyacetone kinase, N-terminal domain"	-20.68	-21.34	DhaR
dhaL	"dihydroxyacetone kinase, C-terminal domain"	-23.37	-23.94	DhaR

Of the genes regulated by the transcription factors with altered activity in both *cydDC* and *cydDC cydAB* cells when GSH and cysteine are added to the medium, a total of 60 genes have significantly altered expression.

Genes that see an increase in transcription include those encoding the acid phosphatase (*appA*) and linked *appBC* genes encoding cytochrome *bd*-II that is discussed in Section 1.5.3. These genes are significantly more up-regulated in *cydDC cydAB* cells than in *cydDC* cells. Genes that are required for the synthesis of hydrogenase-I (*hyaABCDF*), and molybdenum cofactor biosynthesis (*moaACDE*) also see an increase in expression. An increase in expression of *pflB* encoding pyruvate formate lyase, is observed, this enzyme is involved in anaerobic metabolism, and catalyses the Coenzyme A-dependent, non-oxidative cleavage of pyruvate and Coenzyme A to produce acetyl-CoA and formate. An induction of *focA*, which encodes a formate transporter involved in regulating intracellular formate levels by exporting formate produced by pyruvate formate lyase from the cytoplasm is also seen. Other transporters induced by the addition of LMW thiols include, *copA* and *nhaA*; *nhaA* encodes a Na+/H+ antiporter, to expel sodium ions from the cytoplasm to enable

adaptation to high salinity at alkaline pH and *copA* encodes a transmembrane copper efflux protein.

The gene encoding DNA protein from starved cells (*dps*), is the most induced gene of Table 4-1, this protein protects cells from multiple environmental stresses both by binding to and protecting DNA, by sequestering iron and via ferroxidase activity (Zhao *et al.* 2002; Martinez and Kolter 1997). *osmB* is also up-regulated, this gene encodes an outer membrane lipoprotein that responds to hyperosmolarity, suggesting that thiol addition inflicts osmotic stress upon cells. The function of OsmB is however unknown (Jung, Gutierrez and Villarejo 1989).

Alongside genes involved in flagella biosynthesis (*flgABCDEFGHIJMN*) listed in Table 4-1, additional motility genes are also repressed in both *cydDC* and *cydDC cydAB* cells after the addition of GSH and cysteine to the growth media (Supplementary Table 4), this includes chemotaxis and *fli* genes. The repression of motility related genes is stronger in the *cydDC cydAB* cells than *cydDC* cells.

Also repressed are genes of the tricarboxylic acid (TCA) cycle including*; acnB, gltA, sucA, sucB, sucCD, sdhABCD* and *icd* and genes involved in the biosynthesis and transport of amino acids. This includes biosynthesis of tryptophan (*trpABD*), leucine (*leuABCD*) (Figure 4-7) and arginine (*carAB)* as well as the transport of glutamate and aspartate via an ABC-transporter (*gltKL* and *gltI*), and the transport of oligopeptides (of a maximum of 5 amino acids in length) via *oppABCD* encoded ABC-type transporter.

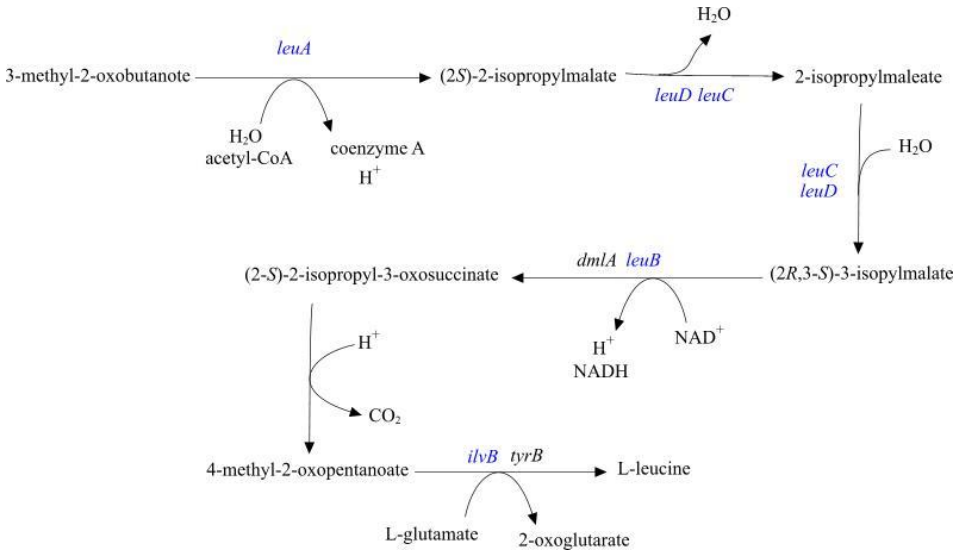

Figure 4-7. Leucine biosynthesis

Blue represents genes of leucine biosynthesis that are repressed by the addition of thiols to *cydDC* and *cydD CcydAB* cells.

Repression of *aldA* is also seen, this gene encodes aldehyde dehydrogenase A which has a broad substrate specificity and is therefore involved in a range of metabolic pathways. One such pathway is the metabolism/degradation of glycol.

4.2.3.3 Transcriptional changes elicited by restoration of cytochrome *bd*-I assembly

To perform a focussed analysis of how the restoration of cytochrome *bd*-I affects transcription, the activity of transcription factors that are only significantly affected by GSH/cysteine addition within *cydDC* cells were listed (i.e. not present in the *cydDC cydAB* array dataset). These were identified by cross-referencing the data in Figures 4-5 and 4-6. The genes affected by those TFs were then compiled to make Table 4-2, which includes a colour scale to aid visualisation of average fold changes.

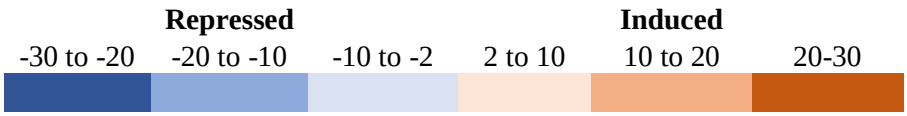

Gene name	Description	*cydDC* GSH cysteine *vs.* *cydDC* fold - changes	*cydDC cydAB* GSH cysteine *vs. cydDC cydAB* fold - changes	TF
prpR	DNA-binding transcriptional activator	4.52	1.47	PrpR
mngB	alpha-mannosidase	3.04	1.65	MngR
prpD	2-methylcitrate dehydratase	-2.77	-1.12	PrpR
prpC	2-methylcitrate synthase	-2.92	1.08	PrpR

Table 4-2. Transcriptional changes resulting from GSH/cysteine-mediated cytochrome *bd*-I assembly

Addition of GSH and cysteine to a *cydDC* strain is hypothesised (via TFinfer) to decrease the activity of the transcription factors MngR, PrpR and PutA. An increase in the activity of RstA is also seen. These transcription factors are however not significantly affected by the addition of GSH and cysteine to a *cydDC cydAB* mutant, suggesting a response to cytochrome *bd*-I restoration. Significant fold-changes of genes controlled by these TFs in a *cydDC* strain after the addition of thiols is indicated by the colour scale bar. Functional annotations were taken from the Ecogene http://www.ecogene.org and RegulonDB http://regulondb.ccg.unam.mx websites.

TFinfer identified four TFs with activities affected by the addition of thiols to *cydDC* cells that were not affected in *cydDC cydAB* cells after thiol addition, indicating that the change in activity of these transcription factors is due to the restoration of cytochrome *bd*-I assembly. Listing the genes controlled by these transcription factors and reducing this list to genes in which a significant change is seen in *cydDC* but not *cydDC cydAB* cells reduces this list to just four genes. These genes are involved in catabolism of propanoate to succinate and pyruvate via the methylcitrate cycle (Brock *et al.* 2002) and the degradation of mannosyl-D-glycerate.

TF modelling via TFinfer is a great way to produce a more focused subset of data, however, genes with large fold changes upon thiol addition are present in the original data and have not been included in the analysis so far. Supplementary data in the CD attached to this thesis lists all genes changes, here some of the largest fold changes seen are for genes involved in acid response, including *gadABCE* and *hdeABD* (Table 4-3). The *gad* acid resistance system includes the glutamate decarboxylase enzymes GadA and GadB, which catalyse the irreversible decarboxylation of glutamate to γ-aminobutyrate (GABA). GadC is an antiporter that exports γ-aminobutyrate in exchange for glutamic acid. It is thought that these proteins protect the cell from acid stress by consuming one cytoplasmic proton to decarboxylate glutamatic acid into γ-aminobutyrate, a neutral compound. GadC-mediated export of γ-aminobutyrate to the outside of the cell would promote neutralisation of the external pH (Capitani *et al.* 2003). *hdeA* and *hdeB* encode periplasmic chaperone proteins. Under neutral pH these proteins are found as dimers that dissociate into monomers at low pH, the monomers bind to acid-denatured proteins to prevent acid-induced aggregation of periplasmic proteins (Kern *et al.* 2007; Hong *et al.* 2005).

Gene name	Description	*cydDC* GSH cysteine *vs.* *cydDC* fold -change	*cydDC* *cydAB* GSH cysteine *vs.* *cydDC* *cydAB* fold -change
gadA	glutamate decarboxylase A, PLP-dependent	72.54	98.12
gadC	predicted glutamate:gamma-aminobutyric acid antiporter	71.57	58.49
gadB	glutamate decarboxylase B, PLP-dependent	67.16	88.67
gadE	DNA-binding transcriptional activator	48.69	41.32
hdeA	acid-resistance protein	45.10	27.66
hdeB	acid-resistance protein	37.79	35.67
hdeD	acid-resistance membrane protein	27.64	41.33

Table 4-3. Transcriptional changes to key genes involved in acid response after the addition of GSH and cystiene

Differential expression of acid tolerance genes resulting from the presence of reduced glutathione (1 mM) and cysteine (0.5 mM) in the growth medium. The mean fold increase or decrease in individual gene expression is indicated by the colour scale bar. Functional annotations were taken from GeneSpring (v13.1) software.

Supplementary Table 4 shows the entire list of genes significantly affected in *cydDC* but not *cydDC cydAB* cells after thiol addition. This list gives more of an insight into which genes are affected by the thiol-mediated restoration of cytochrome *bd*-I. An increase in expression of *cydABX* encoding cytochrome *bd*-I as well as *ybgE* within the same operon is seen. A down-regulation of genes with a role in the arginine degradation pathway (*astABCDE*) is also observed.

4.3. Discussion

The results reported above identify transcriptomic changes that result from the addition of GSH and cysteine to the growth media. Herein, the GSH/cysteine-induced transcriptional adaptations that are cytochrome *bd*-I-independent are analysed in the context of their potential impact upon metabolic processes, followed by a discussion of the cytochrome *bd*-I-dependent adaptations.

To further analyse the environmental changes that could elicit the cytochrome *bd*-I-independent gene regulation in response to GSH/cysteine, environmental stimuli were identified for all the transcription factors (TFs) in Table 4-1 (Table 4-4).

TF analysis gives an insight into the changes of the local environment; by looking at which stimuli TFs respond to, as detailed in Table 4-4. Transcription factors that are affected by the addition of GSH and cysteine in both *cydDC* and *cydDC cydAB* mutants respond to a range of external stimuli which includes; low oxygen and low osmolarity, starvation of phosphate and amino acids, changes to the levels of copper, H_2O_2, dihydroxyacetone (Dha) and sodium, as well as a reduction in the demand for biotin. This culminates in a down-regulation of genes involved in dihydroxyacetone degradation, flagella and amino acid biosynthesis, and genes of the TCA cycle. Changes to TF activities also underpin an up-regulation of respiratory genes, including those that encode cytochrome *bd*-II and hydrogenase I, as well as genes related to the regulation of intracellular formate levels and genes associated with molybdenum cofactor biosynthesis.

In both *cydDC* and *cydDC cydAB* cells, addition of thiols leads to an increase in the activities of CsgD (both a repressor and activator) and RcsB (activator), these transcription factors are induced under low osmolarity, with *osmB*, a lipoprotein regulated by RcsB, being one of the most up-regulated genes in Table 4-1.

ArcA and AppY respond to low oxygen levels, their activities are shown to be up regulated by the addition of reduced glutathione and cysteine in both *cydDC* and *cydDC cydAB* cells. ArcA is the response regulator of the Arc (anoxic redox control) two-component system ArcAB, a global regulator that acts upon many genes involved in respiratory metabolism (Liu and De Wulf, 2004). In the microarrays performed, addition of reduced thiols led to an up-regulation of respiratory genes *appBC* encoding cytochrome *bd*-II and *hyaABCDF* encoding hydrogenase-I (in *cydDC* cells, genes of the *cydABX* operon encoding cytochrome *bd*-I are also up-regulated by these TFs, however

as *cydDC cydAB* cells do not contain the *cydAB* operon, they are not included in Table 4-1). ArcA also acts simultaneously as a repressor, genes of the TCA cycle, including *acnB, gltA, sucA, sucB, sucC, sucD, sdhABCD* and *icd,* were shown to be repressed after thiol addition.

ArcA is transphosphorylated by the sensor kinase ArcB when oxygen is limiting or absent, phosphorylated ArcA simultaneously induces expression of cytochrome *bd*-I and represses the expression of cytochrome *bo*. Membrane anchored ArcB senses respiratory growth conditions via the redox state of the quinone pool using a thiol-based redox switch (Iuchi and Lin, 1988; Malpica *et al.*, 2004; Alvarez *et al.*, 2013). Under aerobic conditions the quinone pool of *E. coli* is mainly made up of ubiquinone, which is maintained in an oxidised stated via the transfer of electrons to oxygen via terminal oxidases, thus electrons flow from the redox active cysteine residues of ArcB to produce disulphide bonds that silence the kinase activity (Malpica *et al.*, 2004). As oxygen becomes limiting the quinone pool becomes more reduced which permits electron transfer to cysteine residues of ArcB, reducing disulphide bonds and activating the ArcB kinase function. We speculate that reduced thiols in the periplasm may reduce the quinone pool and/or the cysteine residues of ArcB directly to cause the observed activation of ArcA activity. ArcA has been shown to induce *appY* gene expression under conditions of anaerobiosis, in consideration of this it is possible to further speculate that thiol induced reduction of ArcB disulphide bonds is also responsible for the increase in AppY TF activity.

None of the other transcription factors mentioned in Tables 4-4 and 4-5 appear to have redox-sensitive cysteines at the cytoplasmic membrane, so it is unlikely that sensor kinase mis-folding is the cause of changes to activity of the remaining TFs. A large up-regulation of genes involved in the acid response, however does suggest that the addition of cysteine and GSH is resulting in acidification of the internal and external environment.

TF	Role	Induced by	References
AppY	Activator	Anaerobiosis, stationary phase, and phosphate starvation	(Brøndsted and Atlung 1996; Atlung *et al.* 1997)
ArcA	Both	Low oxygen conditions	(Georgellis, Lynch and Lin 1997; Iuchi and Lin 1988)
BirA	Repressor	A reduced demand for biotin	(Eisenberg, O and Hsiung 1982; Adikaram and Beckett 2013)
CsgD	Both	Low osmolarity and low growth temperature (<32°C)	(Gu*aldi et al.* 2008; Prigent-Combaret *et al*. 2001)
CueR	Both	Presence of copper	(Stoyanov, Magnani and Solioz 2003; Yamamoto and Ishihama 2005)
DhaR	Both	Presence of dihydroxyacetone	(Bächl*er et al*. 2005)
FlhDC	Both	Inducer unknown	(Stafford, Ogi and Hughes 2005; Claret and Hughes 2002; Lay and Gottesman 2012)
GadX	Both	Inducer unknown- possibly Na+ concentration but not proven	(Richard and Foster 2007)
LeuO	Activator	Amino acid starvation	(*Chen et al*. 2001; Majumder *et al*. 2001)
NhaR	Activator	Na+ concentration	(Rahav-Manor *et al*. 1992; Padan and Schuldiner 1994)
oxyS	Repressor	H_2O_2	(Gonzalez-Flecha and Demple 1999; Altuvia, Weinstein-Fischer and Zhang 1997)
PepA	Repressor	Inducer unknown	(Devroe*de et al.* 2004)
RcsB	Activator	Changes in temperature, overexpression of membrane protein, and osmolarity	(Sledjeski and Gottesman 1996; Majdalani and Gottesman 2005; Mouslim, Latifi and Groisman 2003)
TrpR	repressor	Increase in intracellular levels of tryptophan	(Squires, Lee and Yanofsky 1975; Gunsalus and Yanofsky 1980)

Table 4-4. Identification of GSH/cysteine-mediated environmental changes that are independent of cytochrome *bd*-I assembly

Transcription factors identified in Table 4-1 are listed with environmental stimuli that induce function. It is hypothesised that these environmental changes take place due to the presence of CydDC substrates GSH and cysteine in the periplasm, and are independent of cytochrome *bd*-I assembly.

DhaR is an activator of the *dhaKLM* operon when in the presence of dihydroxyacetone. Here, the activity of DhaR is reduced and the *dhaKLM* genes are the most repressed genes in Table 4-1. The *dhaKLM* genes encode three subunits of the Dha kinase which utilises phosphoenolpyruvate (PEP) as a source of phosphate to phosphorylate dihydroxyacetone.

FlhDC controls motility and chemotaxis by activating genes of flagella biosynthesis. Activity of FlhDC was found to be reduced by the addition of GSH and

cysteine, as the motility genes *flgABCDEFGHIJMN* are repressed. Unfortunately as no inducer of FlhDC has yet been reported, this makes it difficult to understand why these genes are repressed by the addition of thiols to the media.

LeuO (activator) and TrpR (repressor) are induced by changes in the level of amino acids and alter the biosynthesis of amino acids accordingly. Here, the addition of GSH and cysteine leads to an increase in the repression of tryptophan biosynthesis by TrpR and a repression of leucine biosynthesis by a reduction in LeuO activity, implying that the demand for amino acids within cells is reduced.

NhaR (and potentially GadX) respond to changes in sodium ion levels. CueR responds to increases in copper levels, as CueR activity is decreased, it is possible that intracellular copper levels are diminished. The small RNA *oxyS* is induced by H_2O_2, so a repression if *oxyS* activity in the current study indicates a reduction in oxidative stress and H_2O_2 levels.

To further analyse the environmental changes that could elicit the cytochrome *bd*-I-dependent gene regulation in response to GSH/cysteine, environmental stimuli were identified for all the transcription factors in Table 4-2 (Table 4-5).

TF	**Role**	**Induced by**	**References**
MngR	Repressor	Fatty acids levels	(Sam*paio et al*. 2004; Quail, Dempsey and Guest 1994)
PrpR	Both	The absence of glucose or glycerol	(Lee, Newman and Keasling 2005)
PutA	Repressor	Absence of proline	(Deutch *et al.* 1989; Zhou *et al.* 2008)
RstA	repressor and activator	Low Mg^{2+}	(Minagawa *et al.* 2003; K. Yamamoto *et al.* 2005; Ogasawara *et al.* 2007)

Table 4-5. Identification of GSH/cysteine-mediated environmental changes that result from cytochrome *bd*-I assembly

Transcription factors identified in Table 4-2 are listed with environmental stimuli that induce function. It is hypothesised that these environmental changes take place due to the presence of CydDC substrates GSH and cysteine in the periplasm, and are dependent upon cytochrome *bd*-I assembly.

Transcription factors that are affected only by the addition of GSH and cysteine in a *cydDC* mutant but not the *cydDC cydAB* mutant respond to stimuli including, levels of fatty acids and Mg^{2+} as well as the presence of proline, glucose and glycerol (Table 4-5).

The repressor MngR is known to be degraded by fatty acids and is shown here to be down-regulated by thiol addition. This suggests that fatty acid levels are increased. Interestingly, the *mngAB* operon, controlled by MngR is found upstream of the *cydABX* operon.

PutA has two functions that are mutually exclusive of one another. In the absence of proline, PutA is cytoplasmic and acts as a repressor of proline degradation enzymes. In the presence of proline PutA is associated with the inner membrane and catalyses both enzymatic steps in the proline degradative pathway which simultaneously reduces ubiquinone to ubiquinol. Transcription factor activity of PutA is reduced when cytochrome *bd*-I is restored by thiol addition, so proline degradation is presumed to be up-regulated with an increase in reduction of ubiquinone to ubiquinol. PutA activity has also been shown to be reduced by prolonged exposure to osmotic stress, so the reduction in transcription factor activity may be due to this reason rather than changes in proline levels (Deutch *et al.* 1989).

PrpR is an activator of *prpBCD*, the activity of PrpR is reduced as seen by the repression of *prpC* and *prpD*. The *prpBCDE* operon encodes proteins involved in the methylcitrate cycle which utilises propionate as a carbon source, this cycle yields succinate and pyruvate that can feed into the TCA cycle.

4.3.1 The impact of the CydDC substrates upon *E. coli* physiology

In the absence of CydDC, cysteine and GSH are still present in the cytoplasm, but the absence of thiol export to the periplasm leads to a pleiotropic phenotype, including loss of fully assembled cytochrome *bd*-I. This microarray experiment aimed to define the affects that CydDC-mediated thiol export has on gene expression in *E. coli* by replacing thiols in the periplasm. Two microarray experiments were designed to indicate changes in expression of genes caused dependently or independently of cytochrome *bd*-I restoration.

These experiments showed that thiol addition affects the expression of many genes, both in *cydDC* and *cydDC cydAB* cells; which reflects the pleiotropic phenotype of CydDC mutants.

In both *cydDC* and *cydDC cydAB* cells, the transcription of genes related to central metabolism are affected, with genes of the TCA cycle being repressed alongside the biosynthesis and transport of amino acids. Transcription of motility genes were also

down-regulated in the presence of the two LMW thiols. Respiratory genes are up-regulated, including *appBC* which encodes cytochrome *bd*-II and *hyaABCDF* genes that encode hydrogenase-I.

In response to the addition of GSH and cysteine, transcription factors with altered activity respond to a variety of stimuli, including; a sufficient level of intracellular amino acids, low oxygen, changes in osmolarity, phosphate starvation, over-expression of membrane proteins and the reduced levels of dihydroxyacetone.

Chapter 5

Roles of CydDC and cytochrome *bd*-I in the pathogenesis of uropathogenic *E. coli*; colonisation and survival within the host

Summary

In Chapter 3 it was reported that CydDC-mediated reductant export provides tolerance to NO independently of cytochrome *bd*-I. NO is an important tool of the host innate immune system armoury and these findings suggest that cytochrome *bd*-I and CydDC may provide a concerted role in survival within the host environment. Given that the genetic variation between pathogenic and non-pathogenic strains is considerable, an analysis of the gene and protein sequences encoding CydDC and cytochrome *bd*-I from the commensal strain MG1655 were compared with those from two UPEC strains; CFT073 and EC958. This data showed that the protein sequences of cytochrome *bd*-I in all these strains were identical. Amino acid substitutions were shown to exist between the protein sequences of MG1655 CydD and CydC and the corresponding proteins in the pathogenic strains. The location of these amino acids suggests that these variations are unlikely to affect the core function of the exporter complex.

To investigate the contribution of CydDC and cytochrome *bd*-I to nitric oxide tolerance in the context of pathogenic *E. coli*, NOC-12 growth curves were performed using the UPEC strains CFT073 and EC958. Deletion of either CydDC or cytochrome *bd*-I was found to elicit sensitivity to NO in both UPEC strains. When comparing the inhibition of the two CFT073 mutants, a similar inhibition was seen for both mutants after the addition of 0.5 mM NOC-12, increasing the concentration of NOC-12 to 1 mM resulted in a larger growth inhibition for strains lacking CydDC. This suggested that at higher concentrations of NOC-12, CydDC plays a more prominent role in NO-tolerance for the CFT073 strain. In the EC958 background, however, the cytochrome *bd*-I mutant was more sensitive to NO than the *cydDC* mutant.

Prior to infection studies, it seemed prudent to investigate if deletion of cytochrome *bd*-I and CydDC affected the level of type 1 fimbriae (an important adhesin and virulence factor). Yeast agglutination assays demonstrated that aerobically-grown non-pathogenic and CFT073 cells exhibited a low level of fimbriation, and that type 1 fimbriae are not expressed by EC958 cells when grown aerobically. Changing the culture conditions to static growth selected for type 1 fimbriae expression in all three *E. coli* strains, and deletion of CydDC or cytochrome *bd*-I was shown to have no effect upon the level of type 1 fimbriae in UPEC strains under these growth conditions.

The role of cytochrome *bd*-I and CydDC in UPEC strains was studied in the context of the host using a mouse UTI model and macrophage survival assays. The

deletion of cytochrome *bd*-I reduces the survival of UPEC strain EC958 within macrophage cells. However, the deletion of *cydDC* (and consequent loss of functional cytochrome *bd*-I) was shown to have no effect upon the ability of UPEC strain EC958 to survive within macrophage cells or to colonise the mouse model of UTI. Taken together with the observation that the EC958*cydDC* strain is less sensitive to NO than expected (due to previous K-12 data), this intriguing observation highlights how some clinical isolates of the same species can respond differently to the loss of highly conserved membrane proteins.

5.1 Introduction

Uropathogenic *E. coli* (UPEC) are among the most common infectious diseases of humans (Harding and Ronald 1994), causing an estimated 150 million infections a year globally. A major cause of morbidity and mortality, symptomatic UTIs usually start as cystitis, but can ascend into pyelonephritis with potential for bacteria to cross the epithelial cells of the proximal tubule and the endothelial cells of the capillary to gain access to the bloodstream, causing bacteraemia and occasionally sepsis. With a high rate of recurrence and the emergence of antibiotic resistance, it is important to understand the mechanisms that promote survival of pathogens that cause UTI. It is well-known that *E. coli* has several resistance mechanisms that provide tolerance to the toxic effects of host-derived NO that is encountered during infection, including the NO-tolerant cytochrome *bd*-I terminal respiratory oxidase that permits aerobic respiration under the microaerobic conditions encountered during infection (Mason *et al.* 2009). This chapter explores the importance of cytochrome *bd*-I and the CydDC ABC transporter (that is required for cytochrome *bd*-I assembly) during UPEC infection.

We have previously shown (Chapter 3) that deletion of genes encoding cytochrome *bd*-I (*cydB*) and CydDC (*cydD*) in non-pathogenic *E. coli* strains elicits an NO-sensitive phenotype. We further showed that growth of the *cydD* mutant is more sensitive to nitric oxide than the *cydB* mutant. These findings suggest that reductant export by CydDC may provide a significant contribution to the survival of UPEC during infection. However, large pathogenicity islands carrying virulence genes create genetic diversity within UPEC strains (Lloyd *et al.* 2009; Welch *et al.* 2002; Groisman and Ochman 1996), which may explain why uropathogenic *E. coli* have been reported to display greater resistance to nitrosative stress than non-pathogenic *E. coli* (Bower and Mulvey 2006). Given these profound genetic differences between *E. coli* K-12 and UPEC strains, it is essential to assess the importance of CydDC and cytochrome *bd*-I in UPEC genetic backgrounds before assuming that the role of these proteins in NO tolerance remains the same. The well-characterised pyelonephritis-causing CFT073 strain and the multi-drug resistant EC958 isolate (Lau *et al.* 2008) of the sepsis-causing ST131 clonal group were used.

Pyelonephritis is considered the most serious UTI as it is known to cause scarring of the kidneys. *E. coli* CFT073 was first isolated from the blood and urine of a woman being treated for acute pyelonephritis in the USA (Mobley and Green 1990). This highly virulent strain is cytotoxic for cultured human renal cells and causes acute

pyelonephritis in an ascending UTI mouse model (Mobley and Green 1990; Mobley *et al.* 1993). Like other pyelonephritogenic *E. coli* strains, CFT073 cells express P fimbriae, encoded by the pap (pyelonephritis-associated pili) genes, which allow a firm attachment to uroepithelial cells (Källenius *et al.* 1981).

The *E. coli* clonal group sequence type 131 (ST131) has emerged to become a globally dominant cause of human infection (Rogers, Sidjabat and Paterson 2011), and the success of this pathogen is largely attributed to accumulated antibiotic resistance and virulence genes. This multidrug resistant clone carries the CTX-M-15 extended spectrum beta-lactamase enzyme and is fluoroquinolone resistant. EC958 is a single isolate of the ST131 clonal group that was first isolated in 2005 from the urine of a patient with a urinary tract infection in the UK (Woodford *et al.* 2007). EC958 represents the most well-characterised ST131 strain, with a genome sequence published in 2011 (Totsika *et al.* 2011) which was followed by a transposon mutagenesis study that identified genes required for resistance to human serum (Phan *et al.* 2013).

In this chapter, we assess the sensitivity of *cydDC* and *cydAB* mutants of UPEC strains CFT073 and EC958 to NO via *in vitro* growth experiments, then analyse the importance of CydDC and cytochrome *bd*-I in the context of *in vivo* survival via macrophage survival assays and a mouse UTI model.

5.2 Results

5.2.1 Investigating sequence conservation in CydDC and cytochrome *bd*-I

Given the high degree of genetic variability between K-12 and UPEC strains, it was deemed prudent to analyse sequence similarities/differences within CydAB and CydDC protein complexes from the non-pathogenic MG1655 strain and UPEC strains CFT073 and EC958.

5.2.1.1 The sequences of the *cydDC* operon are similar for MG1655, CFT073 and EC958 strains

The nucleotide sequences of *cydDC* from different *E. coli* strains were aligned using Bioedit (v7.2.5) to enable a direct comparison of the nucleotide sequences. Despite a number of single nucleotide polymorphisms (SNPs), the *cydDC* nucleotide sequence of MG1655 has a 98% identity with the *cydDC* sequences of CFT073 and EC958. When comparing the *cydDC* nucleotide sequences of CFT073 and EC958 a 99% identity is seen.

5.2.1.2 Variations in amino acid sequences of CydD and CydC

To determine if the differences in gene sequence were of any significance, the translated amino acid sequences were aligned (Appendix C-1), and SNPs were investigated to decide if they resulted in a change of amino acid. Those that lead to an amino acid change are described in Table 5-1. The majority of amino acid changes seen are shared between the two pathogenic groups. Most of the substitutions result in a non-conservative amino acid substitution (as highlighted with the use of colour in Table 5-1).

Protein	Amino acid Position	*E. coli* MG1655	*E. coli* CFT073	*E. coli* EC958
CydD	70	Valine	Phenylalanine	Phenylalanine
CydD	457	Alanine	Threonine	Threonine
CydD	560	Arginine	Glutamine	Glutamine
CydC	323	Glutamate	Glutamate	Lysine
CydC	360	Serine	Tyrosine	Tyrosine
CydC	385	Glutamine	Leucine	Leucine
CydC	447	Serine	Alanine	Alanine
CydC	522	Arginine	Cysteine	Cysteine

Table 5-1 Amino acid variations in CydD and CydC in *E. coli* strains MG1655, CFT073 and EC958

Colours indicate the nature of amino acid side chains: orange, non-polar; green, polar; blue, basic; purple acidic.

To investigate how these SNPs might affect protein function, amino acid changes were mapped onto their predicted location on membrane topology maps using Protter v1.0 (Omasits *et al.* 2014), an online programme that predicts membrane topology. It was found that the large majority of the variable amino acids are located in the ATP-binding domains (Figure 5-1). The change from valine to phenylalanine at position 70 in CydD maintains a hydrophobic amino acid at that site, which is consistent with the predicted location within a membrane spanning helix (Figure 5-1). This mutation is unlikely to affect protein structure or function as the amino acid is changed to another hydrophobic amino acid side chain. The remaining replacements of amino acids are found at the C-terminus of CydD or CydC, where the ATP-binding domains of each protein are found. These changes are less conservative in amino side chain characteristics, suggesting that they could potentially affect protein function.

The highly conserved Walker-A ATP-binding motif G/AxxxxGKT/S (where x is any amino acid), and the consensus Walker-B motif, zzzzD or zzzzDE, (where z is a hydrophobic amino acid), are integral parts of ATP-binding domains (Hanson and Whiteheart 2005). The P-loop of the Walker-A motif directly binds the phosphates of ATP and the aspartate residue of the Walker-B motif can coordinate a magnesium ion that is required for ATP hydrolysis (Hanson and Whiteheart 2005). Further investigation of the variation in amino acid sequences within CydD and CydC (Figure 5-1) showed that none of the substitutions that differ between pathogenic or non-pathogenic *E. coli* strains occur within the Walker-A or B motifs of the ATP-binding domains. This implies that the variations seen in UPEC CydD and CydC protein sequences are unlikely to affect the core function of CydDC

To further investigate the spatial organisation of these SNPS, a recent model of the structure of CydDC was studied (Shepherd 2015). This model was generated by using a structural homolog, Sav1866 (an ABC transporter of *Staphylococcus aureus*) as a template via the memoir modelling tool (Ebejer *et al.* 2013). The Sav1866 template had been created by crystallisation of Sav1866 in the presence of two bound ADP molecules, despite this the NBDs exhibit an ATP bound conformation which is consistent with the finding that the TMDs are in an outward facing conformation (Dawson and Locher 2006). The bound ADP molecules of the Sav1866 model were shown to into fit the NBDs of CydDC. Labelling the model with the SNPs listed in Table 5-1 identified that these SNPs are dispersed across the dimer complex. None of the amino acids seem to be close to the conserved histidine residues or the nucleotide binding site in the NBDs, instead appearing at the outer edges of the NBDs (Figure 5-2). This further suggests that the core function of CydDC is unlikely to be affected by the SNPs found in UPEC strains.

5.2.1.3 The gene sequences of *cydAB* are similar for MG1655, CFT073 and EC958 *E. coli* strains and lead to no changes in amino acid sequence

The nucleotide sequences of *cydAB* from different *E. coli* strains were aligned using Bioedit (v7.2.5) to enable a direct comparison of the nucleotide sequences. The *cydAB* nucleotide sequence of MG1655, despite a number of single nucleotide polymorphisms (SNPs), has a 99% identity with the *cydAB* sequences of CFT073 and EC958. None of the SNPs within the sequence of *cydAB* cause a substitution of amino acids and therefore the amino acid sequences are identical for all three strains.

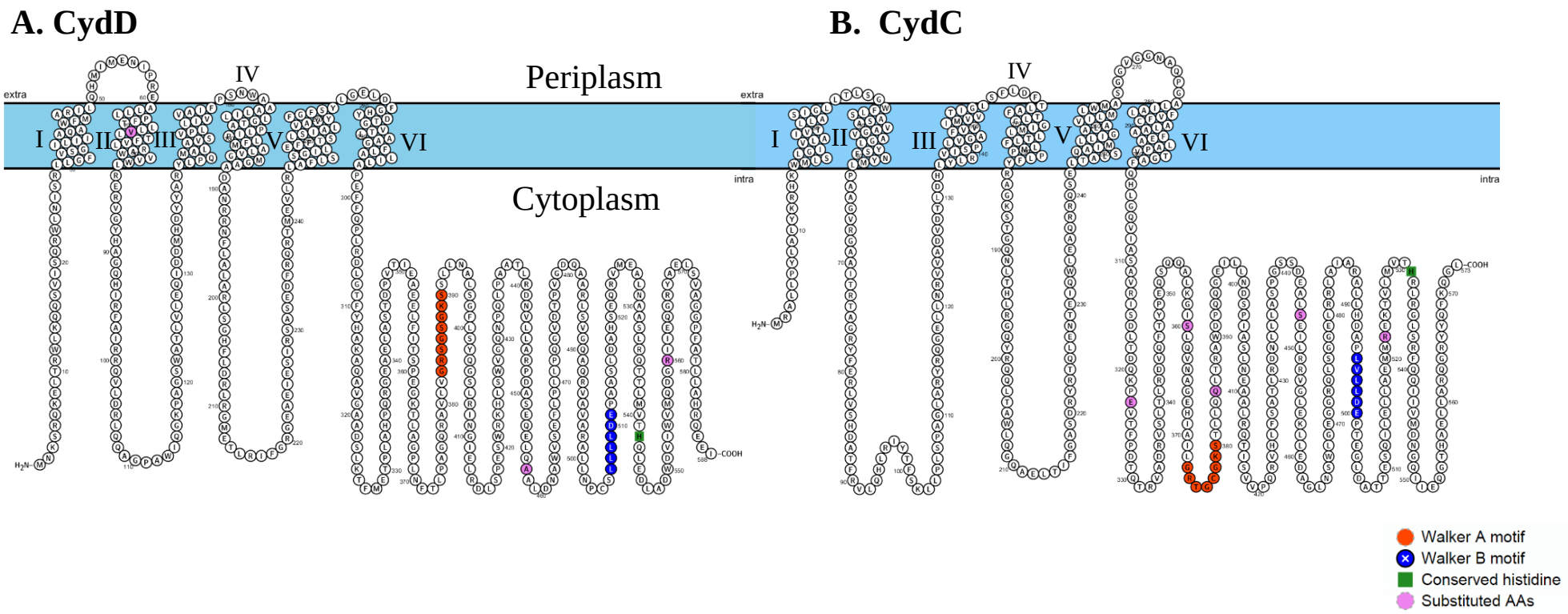

Figure 5-1. Membrane topology of CydD and CydC showing positions at which amino acids vary between MG1655, CFT073 and EC958 *E. coli* strains

Where amino acids in the CFT073 and/or EC958 sequences are different from the MG1655 sequence, these amino acids are coloured pink. The sequences coloured red or blue in the C-terminal ATP-binding domains show the Walker A and B motifs respectively. Most of the amino acid substitutions occur within the ATP-binding domains (an intracellular domain) of CydD and CydC. The conserved histidine residue conserved within ABC transporters is shown in green. One substitution occurs within a membrane helix, but this is a conservative change from valine to phenylalanine both of which have uncharged side chains. Figure was generated using the online Protter (v1.0) tool.

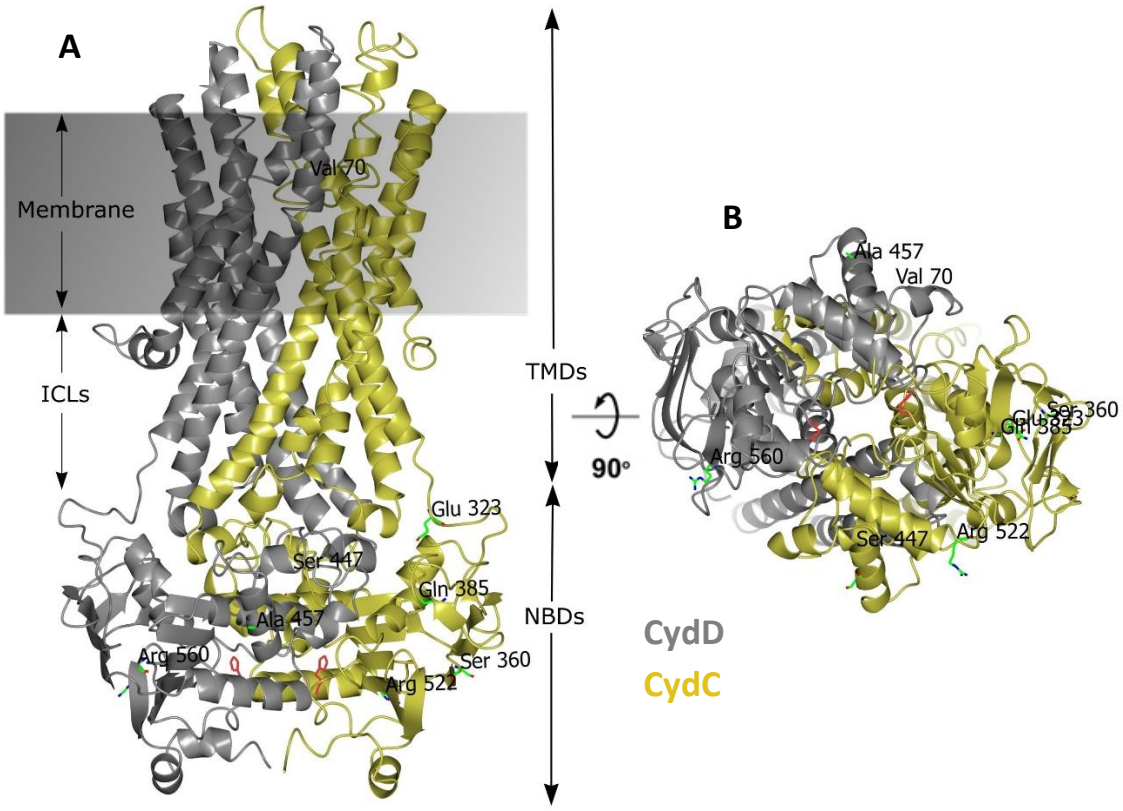

Figure 5-2 Spatial organisation of SNPs within CydDC of *E. coli*

A The CydDC model superimposed on to the structure of Sav1866 by Shepherd, 2015 was used to determine the spatial position of the SNPs listed in Table 5-1 in a bid to determine if SNPs are likely to affect protein function. Conserved histidine residues His542 of CydD and His531 of CydC are highlighted in red, these residues form a hydrogen bond with the γ-phosphate of ATP. **B** 90° rotation shows the view from the cytoplasm and emphasises the lack of SNPs in the area of nucleotide binding. Abbreviations: ICLs, intracytoplasmic loops; TMD, transmembrane domains; NBDs, nucleotide binding domains.

5.2.2 Deletion of the *cydDC* operon in the CFT073 strain

A CFT073*cydAB* strain was available in the Shepherd lab collection (MS17), which had been kindly provided by Prof. Mark Schembri at the University of Queensland. For this chapter it was necessary to generate a CFT073*cydDC* strain (MS115) using the λ–Red mutagenesis approach (Datsenko and Wanner 2000) described in Section 2.2.4. Briefly, primers pMS35 and pMS36 (Table 2-2) that anneal 500 bp either side of the *cydDC* operon, were used to amplify the chloramphenicol resistance cassette from a K-12 *cydDC*::Cm mutant, generating 500 bp flanking regions, homologous to the DNA either side of the genomic *cydDC* operon. The DNA was introduced into cells via

electroporation, and recombination between the homologous regions was enhanced by the λ-Red recombinase. Following the mutagenesis protocol, colony PCR was performed to confirm that the mutation had been introduced. PCR using primers pMS3 and pMS4 (Table 2-2) produces fragments of sizes 3,862 bp when the original DNA sequence was used as a template and 1,552 bp when the chloramphenicol resistance cassette had replaced the *cydDC* operon (Figure 5-3). These data clearly indicate that the *cydDC* operon had been replaced by the resistance cassette. This was later verified via Sanger sequencing, performed as described in Section 2.2.5 and the results are shown in Appendix C-2.

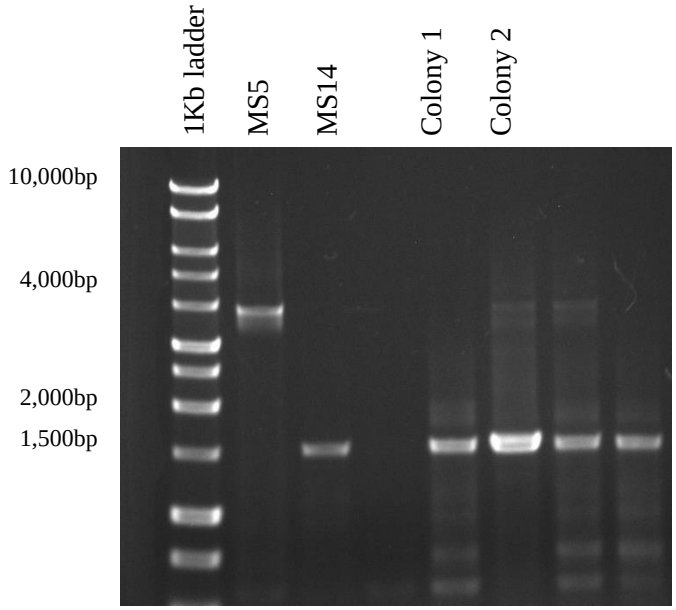

Figure 5-3. PCR verification of electroporation colonies

Colony PCR was performed on colonies resistant to chloramphenicol after electroporation of MS5 (CFT073 pKD46) with *cydDC*::Cm DNA fragment. For the PCR, primers pMS3 and pMS4 (Table 2-2) were used. Colonies of strains MS5 and MS14 (MG1655 *cydDC*::Cm) were tested alongside electroporation colonies as controls. Use of MS5 as a DNA template resulted in a band at around 4,000 bp representing the size of the *cydDC* operon (expected size 3,862 bp) and MS14 showed a band around 1,500 bp representing the size of *cydDC*::Cm (expected size 1552 bp). PCR of the electroporation colonies also resulted in DNA fragments around 1,500 bp in length, indicating that the *cydDC* operon has been replaced by the chloramphenicol resistance cassette. The ladder used was a 1 Kb ladder from Promega.

5.2.3 Nitric oxide tolerance: The contribution of CydDC and cytochrome *bd*-I in the pathogenic strains EC958 and CFT073

In Chapter 3 it was shown that cytochrome *bd*-I and CydDC complexes contribute to NO tolerance in non-pathogenic *E. coli* K-12 strains via growth experiments using NOC-12 as an NO donor. It was therefore of interest to investigate if this holds true for pathogenic strains. Herein, the contribution of CydDC and cytochrome *bd*-I to NO tolerance is investigated in clinical isolates EC958 and CFT073.

5.2.3.1 Loss of functional cytochrome *bd*-I and CydDC in EC958 strains elicits sensitivity to NO.

EC958 strains were kindly provided by Prof. Mark Shembri from the University of Queensland. Initial growth curves demonstrated that deletion of *cydAB* and *cydDC* in EC958 and CFT073 strains increases the lag phase. Since NO is a labile molecule and changes to cell density can have a profound effect upon NO sensitivity, the addition of NOC-12 was performed once cells were no longer in the lag phase at a defined optical density of cell culture. Strains were allowed to grow in flasks to an OD_{600} of 0.5, which ensured that cells were no longer in lag phase. Cultures were then diluted to an OD_{600} of 0.2 before being placed into microplate wells for growth curves to be performed in a plate reader. Higher concentrations of NOC-12 were used than in previous growth curves due to the higher starting optical density. Growth in the presence of NOC-12 shows a similar pattern to that seen using Keio strains (Figure 3-2) Growth is inhibited for a period of time that is dependent upon the concentration of NOC-12 added and strain used, and then growth resumes once cells have adapted to the NO released and/or the level of NO has been depleted (Figure 5-4). The extent of growth inhibition by NO could then be assessed by comparing the duration in which growth is inhibited, for example by comparing the time taken to reach an OD_{600} of 0.5.

In the absence of NOC-12, the growth of all three strains is very similar as shown by the similar amount of time taken for these strains to reach an OD_{600} of 0.5 (Figure 5-5). When NOC-12 is added at a concentration of 0.5 mM there is a drastic difference in growth inhibition when *cydDC* (MS271) and *cydAB* (MS16) are deleted when compared to wild type (MS10) as shown by the extension of the time taken to reach OD_{600} 0.5, wild type growth appears to remain unaffected, with growth comparable to growth without NOC-12 addition. This shows that cells are normally able

to adapt to this level of nitrosative stress, however when cells lose these protein complexes this protection against growth inhibition is lost. Growth of wild type strains is inhibited when the concentration of NOC-12 is increased to 0.75 mM, and the difference in growth inhibition of wild type and mutant cells is diminished, suggesting that at this concentration, CydDC and cytochrome *bd*-I are not able to completely protect cells from the detrimental effects of NO.

Comparison of the inhibitory effect of NOC-12 between EC958*cydAB* and EC958*cydDC* strains indicates that *cydAB* is slightly more sensitive to NO, taking longer to reach an OD_{600} of 0.5 at equivalent NOC-12 concentrations (Figure 5-5), although the *cydDC* strain is also more sensitive to NO than the isogenic wild type.

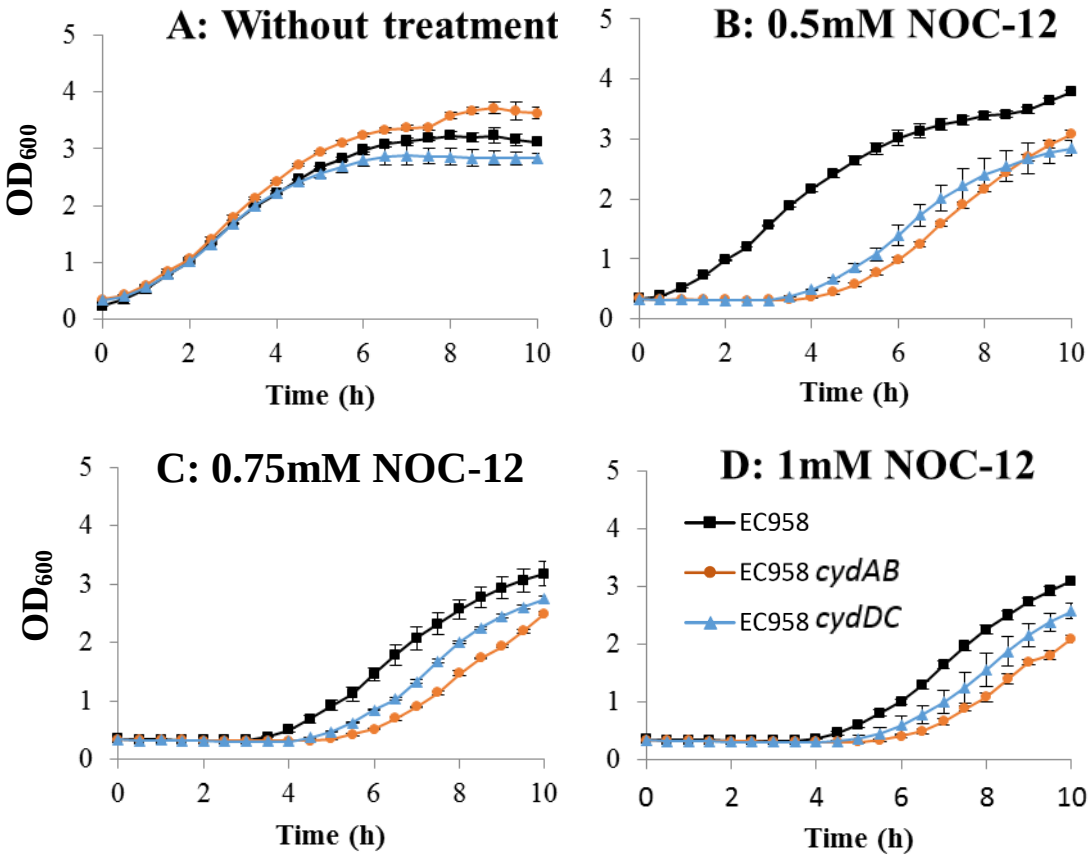

Figure 5-4. Mutation of *cydAB* and *cydDC* in EC958 UPEC strains elicits sensitivity to NO

Cultures were grown shaking in 96 well plates. Bacterial growth was measured using a plate reader. **A** without addition of NOC-12 **B** following the addition of 0.5 mM NOC-12 **C** 0.75 mM NOC-12 and **D** 1 mM NOC-12. All data shown in this figure was collected within the same 96 well plate. Each condition was performed with five technical repeats, standard deviation of these is shown by the error bars.

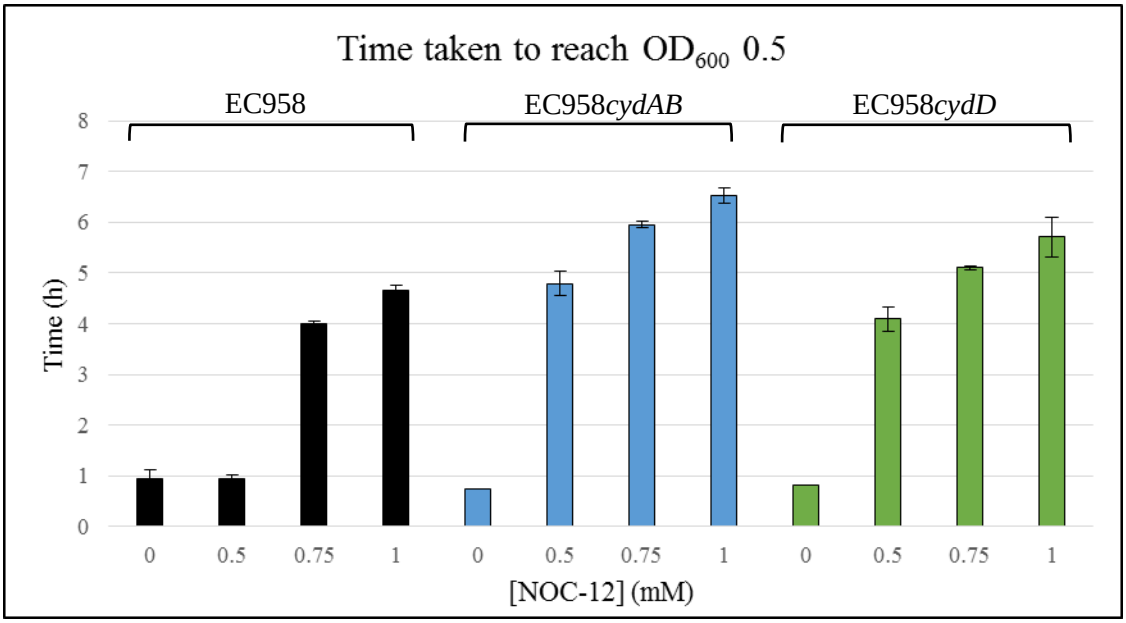

Figure 5-5. Mutation of *cydAB* and *cydDC* in EC958 elicits sensitivity to nitric oxide

The time taken to reach an OD_{600} of 0.5 was used as a measurement of growth inhibition between wild type, *cydAB* and *cydDC* strains of uropathogenic *E. coli* EC958. The more that a strain was inhibited by NO released from NOC-12 the longer these strains took to reach an OD_{600} of 0.5. NOC-12 was added at concentrations of 0.5 mM, 0.75 mM and 1 mM. The error bars show the standard deviation of five technical repeats.

The extent of growth inhibition by NO was assessed for *E. coli* CFT073 *cydAB* and *cydDC* mutants, as previously performed for *E. coli* EC958 (Section 5.3.1), growth curves are shown in Figure 5-6. The extent of inhibition was compared between the strains by analysing the length of time in which growth is inhibited after NOC-12 addition (Figure 5-7). Unlike the EC958 strain, growth of wild type CFT073 (MS1) was inhibited by NOC-12 added at a concentration of 0.5 mM, suggesting that CFT073 strains are more sensitive to nitrosative stress than EC958. Despite this, mutation of *cydAB* (MS17) and *cydDC* (MS115) did elicit additional sensitivity to 0.5 mM NOC-12 as shown by the prolonged time taken to reach OD_{600} 0.5. This suggests that CydDC and cytochrome *bd*-I do have a role in protection against nitrosative stress in *E. coli* CFT073. A similar level of growth inhibition is observed for CFT073*cydAB* (blue) and CFT073*cydDC* (orange) at a NOC-12 concentration of 0.5 mM. Increasing the concentration of NOC-12 to 1 mM however, elicits a larger sensitivity of growth for

strains lacking CydDC than those lacking cytochrome *bd*-I. This suggests that at higher doses of NO, CydDC has a more influential role in protection from nitrosative stress.

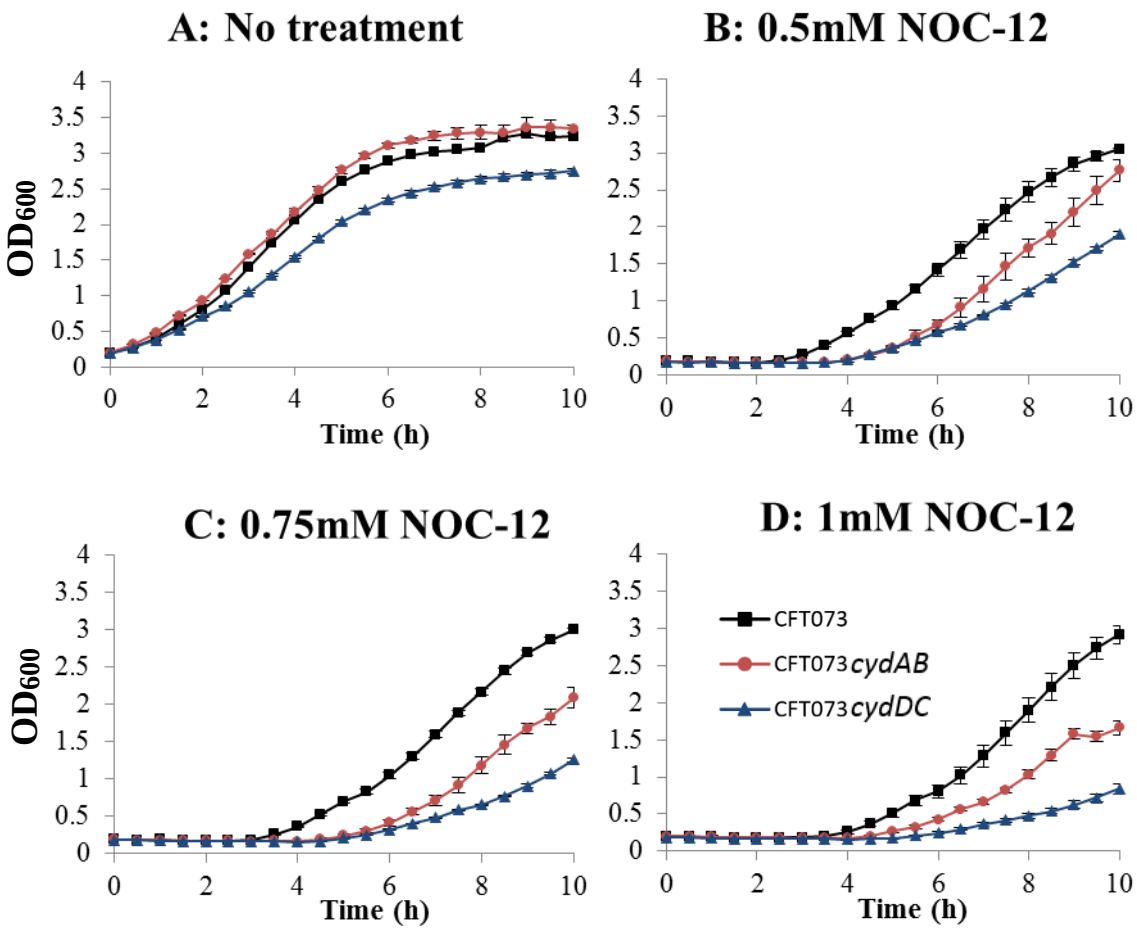

Figure 5-6. Growth of CFT073 UPEC strains in the presence of NOC-12

Cultures were grown shaking in 96 well plates. Bacterial growth was measured using a plate reader. **A** without addition of NOC-12 **B** following the addition of 0.5 mM NOC-12 **C** 0.75 mM NOC-12 and **D** 1 mM NOC-12. All data shown in this figure was collected within the same 96 well plate. Each condition was performed with five technical repeats, standard deviation of these is shown by the error bars.

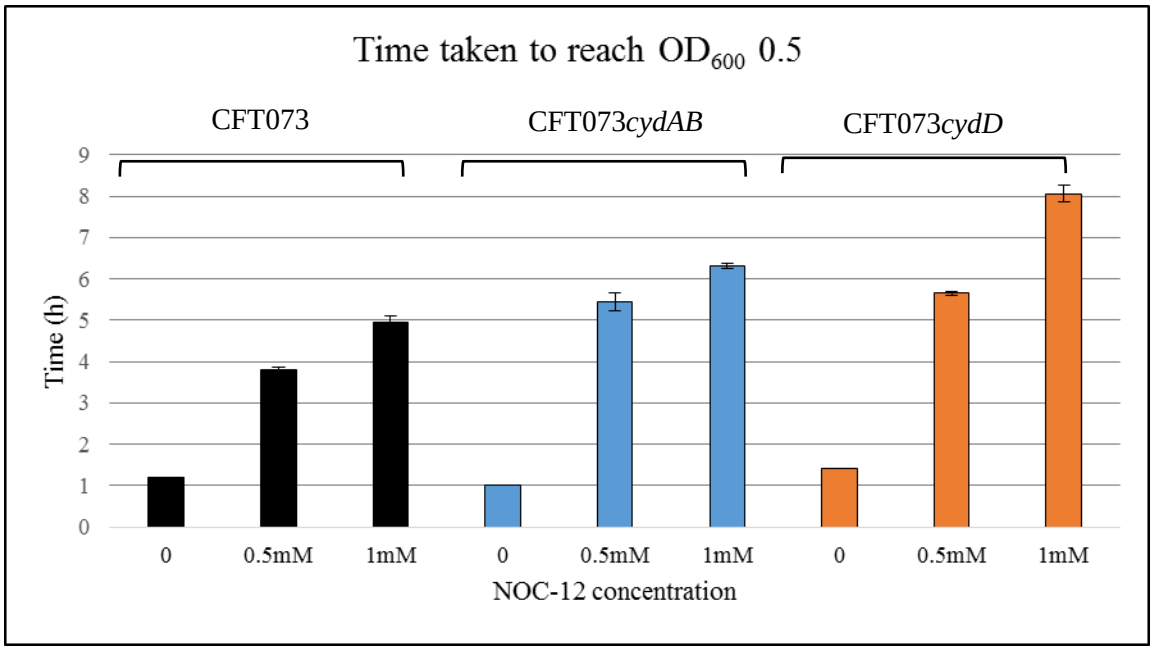

Figure 5-7. Loss of CydDC and cytochrome *bd*-I leads to NO sensitivity in CFT073 UPEC

Wild type, *cydAB* and *cydDC* mutants of *E. coli* CFT073 were grown at 37ºC, 200 rpm in 96 well plates. Following the addition of NOC-12 (0.5 mM and 1 mM) bacterial growth was measured at OD_{600}. Growth inhibition after the addition of NOC-12 was assessed by comparing the time taken for growth to reach an OD_{600} of 0.5. Five technical repeats were performed for each growth condition and the error bars represent standard deviation between these.

5.2.4 Cytochrome *bd*-I and CydDC influence type 1 fimbriation

To colonise the urinary tract, UPEC strains need to tightly adhere to uroepithelial cells to prevent being flushed out by the shearing force of urine flow. Type 1 (or mannose-sensitive) fimbriae are one of the few virulence factors shown to satisfy Molecular Koch's Postulates in acute UTI (Connell and Agace 1996; Bahrani-Mougeot *et al.* 2002). It has been demonstrated through use of a fimbrial adhesin inhibitor that type 1 fimbriae are crucial for *E. coli* EC958 to establish infection within the bladders of mice (Totsika *et al.* 2013).

The structural subunits of type 1 fimbriae are homologous proteins sharing an invariant disulphide bridge (Crespo *et al.* 2012), it has been shown in CFT073 cells, that functional assembly of type 1 fimbriae can occur independently of the DsbAB and DsbLI disulphide folding machineries (Totsika *et al.* 2009), suggesting an alternative mechanism is involved. Since CydDC regulates the redox environment of the periplasm

and is therefore likely to influence disulphide folding (Pittman *et al.* 2002; Pittman, Robinson and Poole 2005), deletion of *cydDC* is hypothesised to perturb disulphide formation in type 1 fimbriae, preventing these mutants from being able to successfully adhere to host cells. To determine the level of type 1 fimbriation, a yeast agglutination assay (Section 2.1.9) was used; *Saccharomyces cerevisiae* cells were mixed with bacterial cells and this mixture was viewed under a light microscope. Bacterial fimbriae attach to mannoside-containing receptors on the surface of yeast cells which can be visualised as agglutination due to yeast cells being larger than bacterial cells. The theory is that, the more fimbriae present on each bacterial cell, the more yeast cells are bound to the bacterial cell to elicit a larger amount of agglutination. If little or no fimbriae are present on the bacterial cells, yeast and bacteria will continue to be freely diffused throughout the mixture. This is a quick and easy way of assessing functional fimbriae but is limited in sensitivity, as exact fimbriae levels cannot be determined.

5.2.4.1 Loss of CydDC and cytochrome *bd*-I elicits loss of type 1 fimbriae in CFT073 and Keio strains in agitated cultures

Wild type Keio and CFT073 strains exhibit agglutination (Figure 5-8), indicating the presence of type 1 fimbriae on these cells that is manifested as clumping under the light microscope. In addition to wild type and *cydDC* experiments, strains lacking cytochrome *bd*-I were also included as a control, and it was hypothesised that loss of this operon would not inhibit fimbrial assembly. All of the EC958 strains appear very similar to the afimbriate (Afim) control strain, showing no agglutination when mixed with the yeast solution. This is possibly due to a 1,895bp insertion that was identified in the *fimB* gene of EC958, inactivating a recombinase that activates expression of type 1 fimbriae (Totsika *et al.* 2011).

Mutation of *cydAB* and *cydDC* in the Keio and CFT073 background diminishes the amount of agglutination seen (Figure 5-8), and suggests that deletion of these genes diminishes assembly of type 1 fimbriae. Gene deletions in the Keio background appears to completely inhibit agglutination with the yeast cells, whereas the CFT073 mutants display a very small amount of agglutination but this is significantly diminished compared to the wild type. The lack of resolution in this experimental approach precludes a quantitative assessment of the contributions of cytochrome *bd*-I and

CydDC. However, the surprising finding is that loss of cytochrome *bd*-I assembly diminishes the assembly of type 1 fimbriae.

A strain which is locked in the 'on' position at the *fim* switch (AAEC554) (McClain *et al.* 1993) was used as a positive control, and none of the other *E. coli* strains tested showed the same level of agglutination as this 'locked on strain'. This suggests that the test cultures exhibiting agglutination comprise populations of cells that have some *fim* switches in the 'on' position, and some in the 'off' orientation.

5.2.4.2 Loss of cytochrome *bd*-I or CydDC does not diminish type 1 fimbriation in static aerated liquid cultures

Fimbriae are crucial for UPEC to colonise the urinary tract and it is likely that their expression will be induced by an environmental cue during host colonisation. Inside the urinary tract, bacterial pathogens will encounter oxygen limiting conditions, so it was of interest to investigate the impact of CydDC and cytochrome *bd*-I upon the assembly of type 1 fimbriae under conditions found inside the host.

Expression of functional type 1 fimbriae is known to be enhanced when cultures are grown statically (Totsika *et al.* 2011). Hence, decreasing the dissolved oxygen concentrations was undertaken to allow the influence of CydDC and cytochrome *bd*-I on fimbriae levels to be investigated under conditions found during infection. Yeast agglutination in all test strains was improved when grown statically (Figure 5-9) compared to when cultures are agitated (Figure 5-8), which is consistent with the model that static growth strongly selects for type 1 fimbriae expression. Agglutination in pathogenic strains CFT073 and EC958 was unaffected by deletion of the *cydAB* or *cydDC* operons, suggesting that expression of type 1 fimbriae is not influenced by these systems under conditions of diminished aeration.

In the Keio background, mutation of *cydB* does not completely abolish the expression of type 1 fimbriae as agglutination is still observed, however the level of type 1 fimbriae appears to be reduced as the amount of agglutination seen after 5 minutes is diminished. Interestingly, the *cydD* mutant, which is also unable to assemble cytochrome *bd*-I, exhibits similar agglutination properties to the isogenic wild type strain.

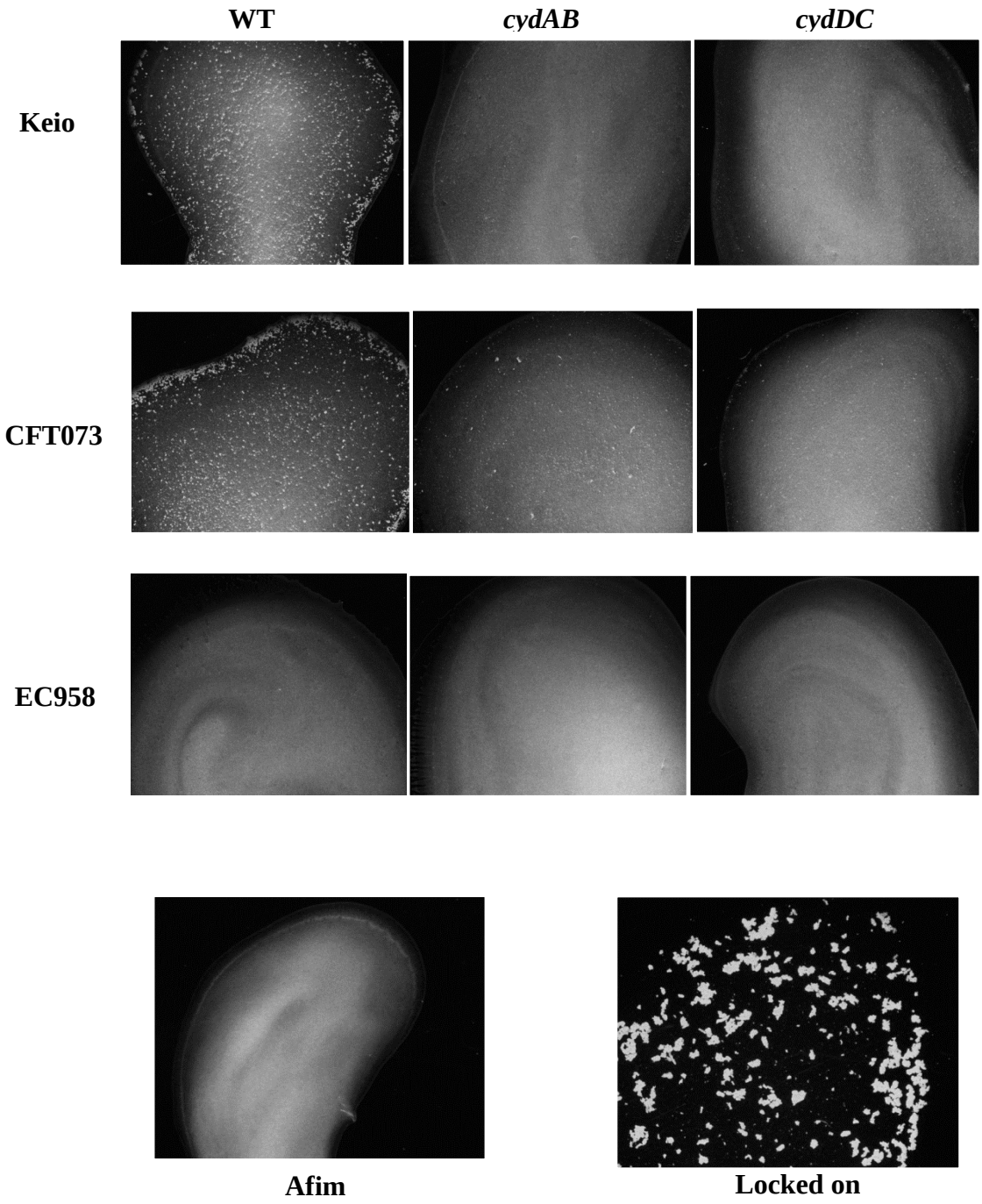

Figure 5-8. Loss of type 1 fimbriae is seen in CFT073 and Keio strains lacking CydDC or cytochrome *bd*-I

Yeast agglutination assay showing the levels of expression of type 1 fimbriae on *E. coli* cells of Keio, CFT073 and EC958 strains when grown in agitated cultures. A strain in which the *fim* switch is locked in the 'on' position (AAEC554) (McClain *et al*. 1993) was used as a positive control, and an afimbriate strain (Afim) was used as an agglutination negative control (BGEC487) (Kulasekara and Blomfield 1999).

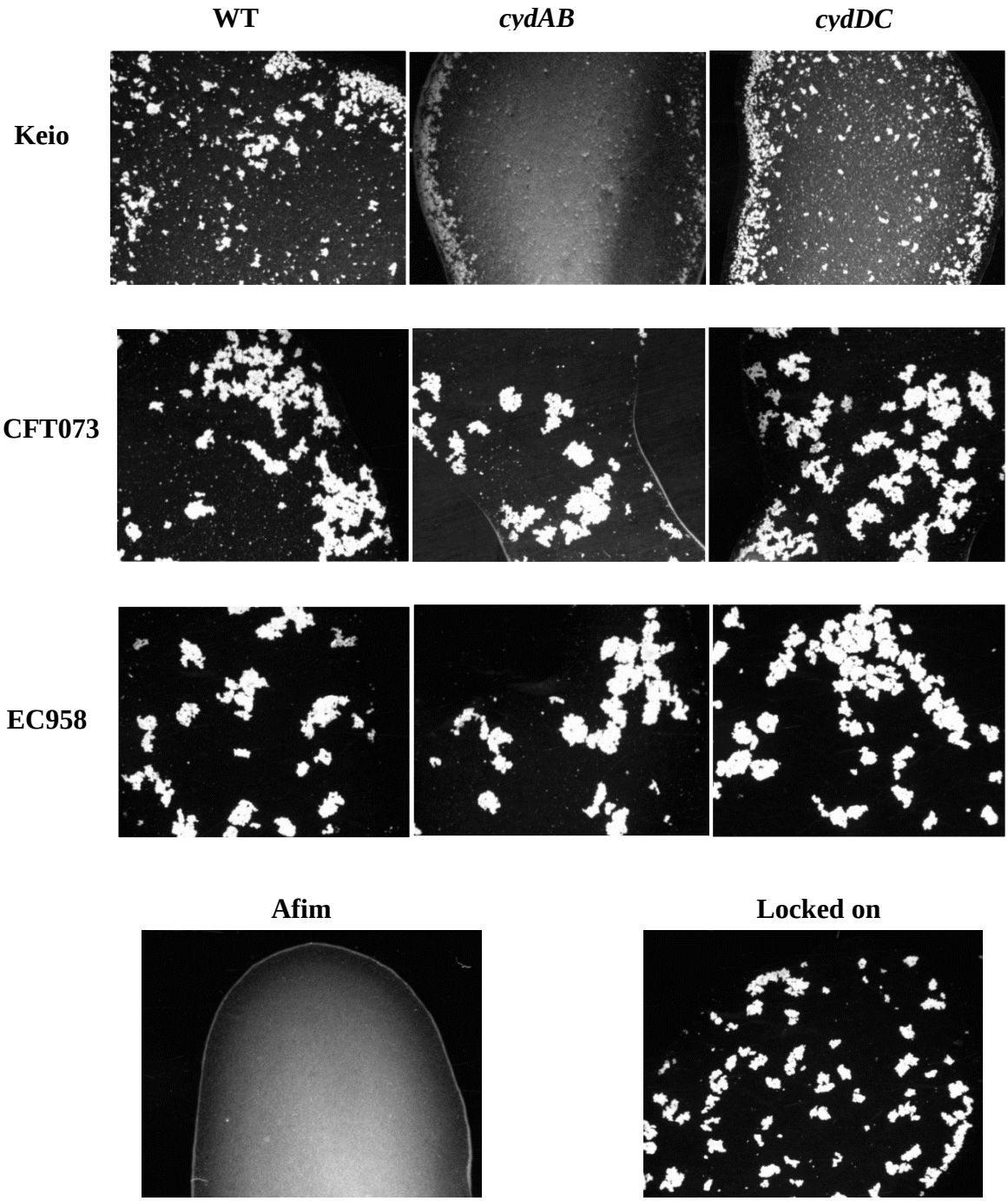

Figure 5-9. Loss of type 1 fimbriae is not observed in UPEC strains lacking CydDC or cytochrome *bd*-I when grown statically

Yeast agglutination assay showing the levels of type 1 fimbriae of various *E. coli* strains (Keio, CFT073 and EC958) when grown statically at 37°C. A strain in which the *fim* switch is locked in the 'on' orientation (AAEC554) (McClain *et al*. 1993) was used as a positive control, and an afimbriate strain (Afim) was used as an agglutination negative control (BGEC487) (Kulasekara and Blomfield 1999).

5.2.5 Macrophage survival assays

During infection pathogenic strains of *E. coli* are engulfed by macrophages, which expose the pathogen to nitrosative stress. Previous chapters and sections within this chapter have demonstrated the importance of CydDC and cytochrome *bd*-I for the tolerance of *E. coli* to nitrosative stress. It was therefore of interest to investigate the ability of *cydDC* and *cydAB* strains to survive exposure to macrophages that have been primed to produce NO.

It is well-known that innate immunity plays a major role in defence against UPEC. In mice, it has been shown that UPEC infection results in the recruitment of macrophage cells to the bladder (Ingersoll and Cohen 2008; Engel *et al.* 2008), indicating that macrophages participate in the innate immune response against UPEC. Furthermore, given that macrophages utilise nitric oxide as a defence against invading bacteria, it was of interest to investigate the contribution of CydDC and cytochrome *bd*-I to survival within macrophage cells. The exact role that intra-macrophage survival plays in the virulence of UPEC strains is still uncertain but it is thought that intracellular bacterial communities (IBCs) within epithelial cells provide a constant supply of bacteria for reinfection of macrophage cells, if UPEC are able to survive within macrophage cells it is possible that the bacteria may be transported within macrophage cells to other sites within the host (Bokil *et al.* 2011).

5.2.5.1 Loss of cytochrome *bd*-I but not CydDC elicits reduced survival of *E. coli* EC958 within murine macrophage.

Macrophage survival assays were performed as described in Section 2.5.2 at the University of Queensland. EC958 has previously shown elevated bacterial loads in bone marrow derived macrophage (BMM) at 24 hours post infection when compared to CFT073, showing that they are adapted to growth within macrophage cells (Bokil *et al.* 2011). Wild type, *cydAB* and *cydDC* mutants of EC958 background were used in these experiments. As discussed in Section 5.2.4, the virulence of UPEC strains relies heavily upon adhesion through type 1 fimbriae. EC958 strains were used in macrophage and mouse model experiments, and to ensure that differential fimbriae expression did not interfere with these experiments strains were subjected to multiple passages of static growth to select for expression of fimbriae and therefore create ‘Fim enriched’ strains.

Once grown to stationary phase, Fim enrichment was confirmed by a quick yeast agglutination assay (Section 2.1.9).

Cultures were diluted to achieve equivalent OD_{600} readings for all strains and were used to infect BMMs in 24-well plates. A multiplicity of infection of 10 was used (10 bacterial cells to every 1 macrophage cell) and this was checked by plating out the bacteria used to infect macrophage cells and counting the resulting number of CFU (Figure 5-10). After 30 minutes of BMM infection, extracellular bacteria were removed by washing with 200 μg gentamycin, this prevented any more uptake of bacteria in macrophage cells. The number of intra-macrophage bacteria after 2 and 24 hours of infection of macrophage cells were used as a measure of survival within macrophage cells. The results show that the survival of EC958*cydAB* is dramatically reduced when compared to wild type and EC958*cydDC* strains (Figure-11).

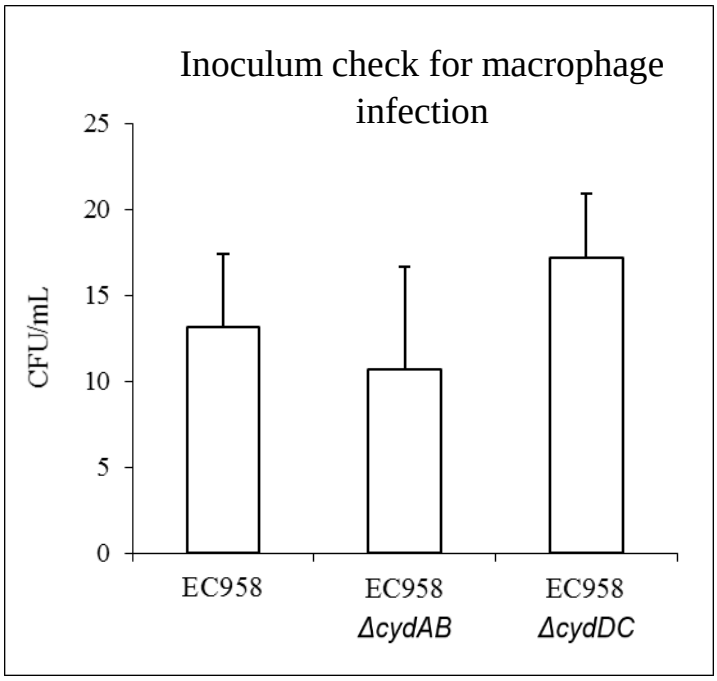

Figure 5-10. Inoculum check for macrophage survival assay
The number of bacterial cells added to macrophage cells for each strain of uropathogenic *E. coli* EC958. Error bars are based upon three CFU bacterial counts of inoculum added to macrophage cells.

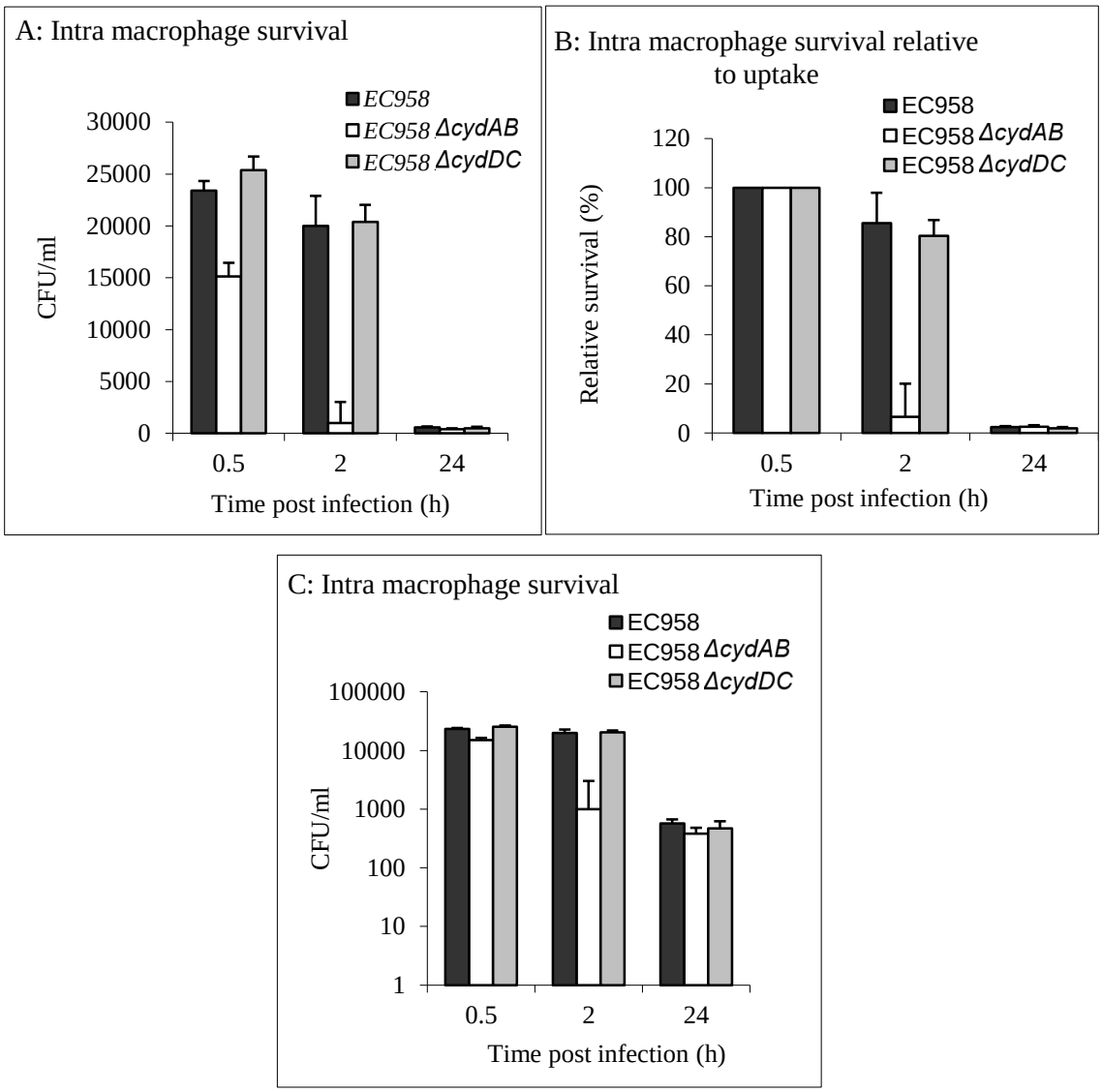

Figure 5-11. Loss of cytochrome *bd*-I reduces UPEC survival within macrophages

A. Intracellular colony counts after 30 min, 2 h and 24 h post-infection. The number of bacteria 30 minutes post infection is considered as the number of cells taken up by macrophage, two hours post infection is thought of as a good time point to see how well bacteria are able to survive within macrophages. At 24 hours post infection it is expected that most of the bacteria will be killed. **B.** The number of bacteria as a proportion of the number of bacteria taken up by macrophage cells. **C.** The number of bacterial cells inside macrophage cells 30 minutes, 2 hours and 24 hours post infection, on a log scale.

5.2.6 Mouse model of UTI

Previous work has demonstrated that loss of cytochrome *bd*-I elicits a diminished ability to colonise the mouse urinary tract (Dr Mark Shepherd, personal communication). It was hypothesised that loss of CydDC would have a dramatic effect on host colonisation, so the ability of UPEC to establish infection of the mouse urinary tract was studied. Competition experiments (described in Section 2.5.1) were performed to ensure larger, more significant datasets. A total of 15 mice were infected with an equal number of wild type (MS6016) and EC958*cydDC*::Gm (MS6110) strains, and colony counts were measured from the urine, bladder and kidneys. To permit the enumeration of both wild type and mutant strains taken from the same source, the wild type EC958 strain was *lac*$^{-}$ and chloramphenicol resistant. Therefore wild type CFUs could be distinguished from those of mutant strains on chloramphenicol plates and MacConkey agar plates. On MacConkey agar plates EC958*lac*::*mkate* (wild type) colonies would appear white, and mutant colonies would appear pink/red.

As with the macrophage survival experiments, stationary phase cultures to be used in the mouse experiments were confirmed positive for expression of type 1 fimbriae by the yeast agglutination assay (Section 2.1.9)

5.2.6.1 Loss of CydDC has no significant effect upon EC958 colonisation of lower urinary tract in mice.

The colony counts from the urine, bladder and kidneys of mice infected with EC958 and EC958*cydDC* were measured (Figure 5-12). In this model of infection and time frame we would not expect to see bacteria within the kidneys and this was verified experimentally (Appendix C-3). Each circle (EC958) and square (EC958*cydDC*) represents a mouse and indicates the CFUs isolated from each sample. Colonisation of the urine and bladder was very similar for both strains, with the mean value for each strain appearing to be almost identical. The wilcoxon matched-pairs signed rank test shows that there is no significant difference in the number of wild type and mutant bacteria isolated from urine and bladder tissue samples. As a precaution, CFU/ml of the inoculum was measured for each infection and used to calculate the fitness index, removing any potential bias from variations in initial culture density (Figure 5-13).

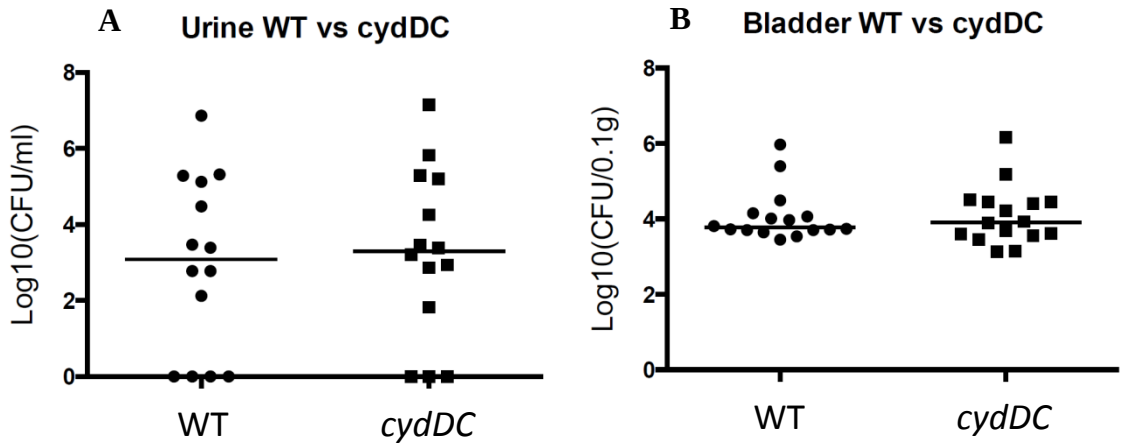

Figure 5-12. Loss of CydDC has no effect upon bacterial load isolated from urine or bladder of mice

Each circle or square represents a mouse and the CFU isolated from **A** urine or **B** homogenised bladder samples. Lines through the dots shows mean of values. Figures were created in Prism.

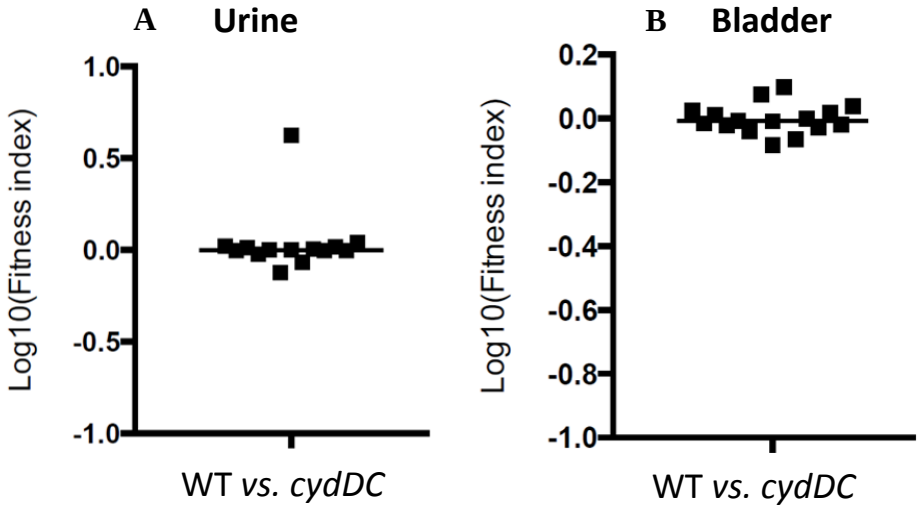

Figure 5-13. Fitness index: Loss of CydDC has no significant affect upon bacterial load in the bladder of mice infected with EC958

Log fitness index of bacterial loads in mouse **A** urine and **B** bladder tissue. Fitness index takes into account the nature of a competition experiment, the number of wild type cells introduced to mice will not be exactly the same as mutant cells. So to remove bias a fitness index is determined which compares the ratio of wild type: mutant at the start and end of the experiment. A fitness index of 1 means that the number of CFU isolated of both strains is equal. The same is true for a $\log_{10}$ fitness value of 0.

5. 3 Discussion

This chapter explored the variation in the roles played by CydDC and cytochrome *bd*-I in either non-pathogenic *E. coli* or UPEC strains. Previous experiments showed that non-pathogenic *E. coli* rely upon cytochrome *bd*-I and CydDC for protection from NO. This finding is of importance in the context of *E. coli* pathogenesis. However, as pathogenic strains vary genetically from laboratory strains, it remained to be determined whether NO protection by cytochrome *bd*-I and CydDC is as significant within strains of UPEC. To start with, the gene and protein sequences of both CydDC and cytochrome *bd*-I complexes were compared between the laboratory strain MG1655 and two UPEC strains CFT073 and EC958. As no significant differences between cytochrome *bd*-I protein sequences were observed it was assumed that cytochrome *bd*-I is fully functional and should perform the same role as in non-pathogenic *E. coli*.

Despite UPEC and non-pathogenic strains being of the same species, variations in gene content could result in UPEC strains responding differently to NO exposure. Indeed, UPEC are thought to be more tolerant of NO, possibly due to the vertical acquirement of DNA elements containing multiple genes such as pathogenicity islands (Groisman and Ochman 1996). Hence, it was anticipated that UPEC strains might not rely upon cytochrome *bd*-I or CydDC for NO tolerance as heavily as non-pathogenic strains. To test this, NOC-12 experiments previously performed on Keio collection strains (Chapter 3), were repeated with UPEC strains to determine the contribution of CydDC and cytochrome *bd*-I to the protection against NO in UPEC strains. These experiments showed that loss of cytochrome *bd*-I and CydDC in CFT073 and EC958 UPEC strains still elicited sensitivity to NO. The relative sensitivity, however, when compared between CydDC and cytochrome *bd*-1 mutants was inconsistent with data collected on the non-pathogenic K-12 strain. For example, in the EC958 background, mutants of cytochrome *bd*-I were more sensitive to NO than an EC958 *cydDC* mutant. In the CFT073 background, *cydAB* and *cydDC* mutants showed a very similar level of growth inhibition at a concentration of 0.5 mM NOC-12 but a greater sensitivity of strains lacking CydDC at a NOC-12 concentration of 1 mM when compared to mutants of cytochrome *bd*-I. The similar level of inhibition elicited by the addition of 0.5 mM NOC-12 for CFT073 strains lacking either CydDC or cytochrome *bd*-I might suggest

that the sensitivity of CFT073*cydDC* may be attributed solely to the loss of cytochrome *bd*-I. It is possible that the presence of exported thiols in the periplasm is not as important for defence against a NOC-12 concentration of 0.5 mM: at this concentration other NO detoxification systems in the cell (e.g. Hmp), could be sufficient to deal with incoming NO. The increase to 1 mM NOC-12 would then require LMW thiols in combination with Hmp to diminish the level of NO in the cytoplasm.

In the EC958 experiments, the data unexpectedly showed that EC958*cydDC* was less sensitive to NO than EC958*cydAB* but still more sensitive than the isogenic wild type. Considering that CydDC is necessary for cytochrome *bd*-I function this finding cannot be easily explained. It was originally thought that a UPEC strain without CydDC would not be able to assemble cytochrome *bd*-I, and that a *cydDC* mutant would be equally or more sensitive to NO than a cytochrome *bd*-I mutant. As *bd*-I assembly has not been measured in the EC958*cydDC* strain it could be possible that a small amount of cytochrome *bd*-I in UPEC strains is still functional in the absence of CydDC. The EC958 genome could potentially encode more than one copy of CydDC, with the release of the EC958 genome in 2014 (Forde *et al.* 2014), it is now possible to search the genome for sequences similar to *cydDC*. The mega BLAST tool on the NCBI website (http://blast.ncbi.nlm.nih.gov) can be used to search for highly similar sequences; the gene sequences of *cydD* and *cydC* from EC958 were used as a query to search the entire *E. coli* ST131 EC958 genome for closely related sequences, with an aim to determine if alternative *cydD* and *cydC* genes are encoded by the pathogen. Only one hit, the original *cydDC* operon was found, thus demonstrating that the ST131 genome encodes only one copy of CydDC.

Alternaively, it is possible that glutathione and/or cysteine may be exported into the periplasm by another route that is independent of CydDC. Indeed, glutathione has previously been shown to be present in the periplasm of a *cydDC* mutant (Eser *et al.* 2009). Another possibility is that additional thioredoxin-like proteins in the periplasm of EC958 (as seen in other pathogenic bacteria, (Heras *et al.* 2009) that are not present in lab strains of *E. coli* may help to maintain the redox environment of the periplasm, making the export of thiols by CydDC less important for the assembly of cytochrome *bd*-I. As performed above, the BLAST tool was again used, this time *dsbL* and *dsbI* gene sequences were used as a query to search the entire *E. coli* ST131 EC958 genome for closely related sequences, highly similar sequences were indeed found within the genome, coding DNA sequences (CDS) EC958_3442 and EC958_3443 were shown to

correspond to *dsbL* and *dsbI* respectively. The difference in sensitivity between the *cydDC* mutant and isogenic wild type is still relatively large, suggesting that cytochrome *bd*-I assembly in EC958 remains largely reliant upon CydDC, but possibly not to the same extent as for Keio *E. coli*.

Despite the variation of NO inhibition between *cydDC* and cytochrome *bd*-I mutants among UPEC strains, it was nevertheless, still shown that cytochrome *bd*-I and CydDC both contribute to the protection of UPEC strains against NO. The results imply that these protein complexes have a role in the survival of EC958 and CFT073 UPEC strains within the host. In addition to NO tolerance, CydDC may influence survival during infection through facilitating the folding of extracytoplasmic virulence factors that contain disulphide bonds (as mentioned in Section 1.1 and depicted in Figure 5-14); ensuring that conditions are maintained for correct protein folding and assembly. For bacteria colonising the urinary tract, it is important to be able to adhere tightly to epithelial cells and to resist the shearing force of urine flow. To accomplish this, UPEC utilise fimbriae including the mannose-sensitive type 1 fimbriae. It was hypothesised that the level of functional type 1 fimbriae would be affected by loss of the CydDC exporter complex due to the absence of disulphide bonding. To test this hypothesis the yeast agglutination assay was used with cytochrome *bd*-I mutants as controls. Deletion of cytochrome *bd*-I and CydDC in Keio or CFT073 backgrounds was shown to diminish the level of type 1 fimbriae expressed in aerobically grown cells, although type 1 fimbriae were not expressed by EC958 cells when grown aerobically. Changing the culture conditions to static growth selected for type 1 fimbriae expression in all three *E. coli* backgrounds. Static growth relates to pathogenesis, as bacteria experience reduced oxygen availability when inside the host. Apart from a slight reduction in the level of agglutination seen for the cytochrome *bd*-I mutant of the Keio collection, under static growth conditions, deletion of CydDC or cytochrome *bd*-I was not shown to have an effect upon the expression of type 1 fimbriae. This was unexpected, with the prediction being that loss of CydDC would affect redox poise within the periplasm and thus prevent disulphide folding of fimbrial proteins. Considering this finding, one would expect that adhesion to host cells by type 1 fimbriae would not be affected by the loss of CydDC during pathogenesis. UPEC, however, do possess alternative adhesins which could be affected by the loss of CydDC, including P fimbriae, that require correct disulphide bonding for folding of both pilus subunits and the PapD chaperone (Jacob-dubuisson *et al.* 1994).

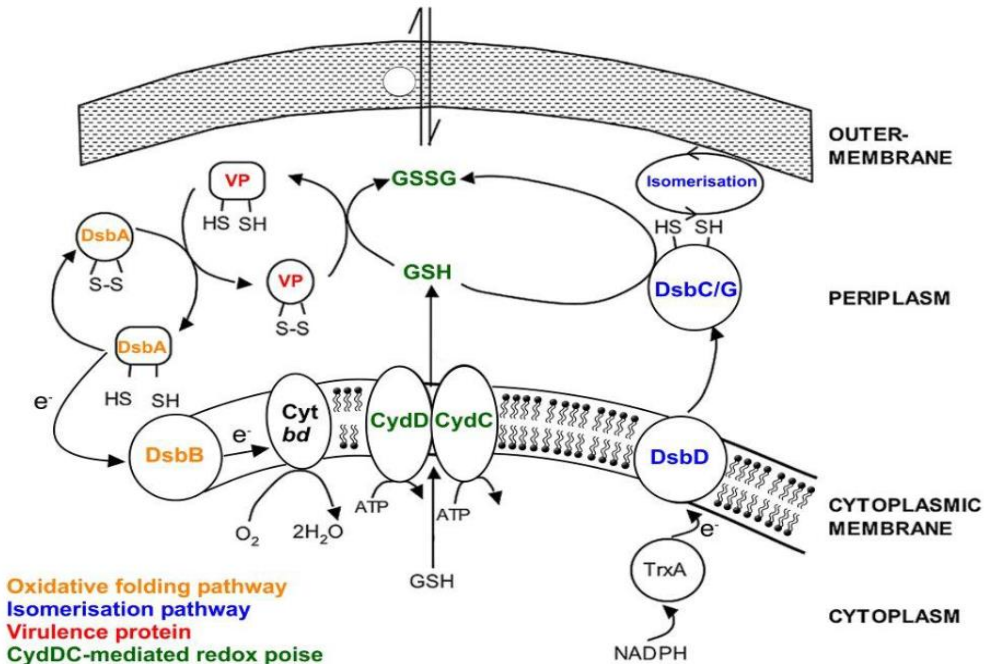

Figure 5-14. Disulphide folding within the *E. coli* periplasm

The oxidative folding pathway (DsbAB) and disulphide bond isomerisation pathway (DsbCD) work to ensure that proteins in the periplasm are correctly folded. Glutathione (GSH) and cysteine exported to the periplasm via the ABC transporter CydDC collaborate in balancing the redox environment of the periplasm and are thus thought to influence disulphide bonding. The *bd*-type oxidases require CydDC for assembly and act as an electron sink for electrons released to form disulphide bonds. Figure adapted from Pittman *et al*. 2005

In vivo experiments allow the interaction between the host and virulence factors to be studied. Experiments were performed to directly determine the contribution of CydDC and cytochrome *bd*-I to the survival of EC958 within macrophage cells, and the contribution of CydDC to the colonisation of the mouse lower urinary tract. The results of the macrophage survival assay were striking, in that they showed an EC958*cydDC* mutant survives much better than an EC958*cydAB* mutant. Again, it would be expected that bacteria without CydDC would also lack cytochrome *bd*-I and that a similar effect upon survival within mouse macrophages would be observed as for the cytochrome *bd*-I mutant. A similar result was seen in the mouse UTI model, where colonisation of the mouse bladder was shown to be unaffected by the loss of CydDC. The discrepancy seen between *cydDC* and cytochrome *bd*-I mutants in NOC-12 growth curves of EC958 was therefore also mirrored in the *in vivo* experiments, although the difference between the mutant strains was much more pronounced in the macrophage

work. For the mouse UTI experiments, no significant difference was seen between the number of wild type and *cydDC* mutant bacteria harvested from mouse urine and bladders after 24 hours. Taken together, these observations suggest that CydDC does not facilitate the colonisation of the mouse lower urinary tract nor to survival within macrophage cells. It further shows that the results of the yeast agglutination assay, in which we concluded that CydDC is not required for correct folding of type 1 fimbriae holds true for other extracytoplasmic virulence factors which are used by UPEC to colonise the urinary tract within the first 24 hours of infection. This result does not however provide information on the role of CydDC during UPEC pathogenesis after this time point.

Messens *et al.* (2007) demonstrated that loss of periplasmic GSH increases the redox potential of the *E .coli* periplasm from -165 mV to -125 mV, despite this, RNase I activity is not affected. As RNase I requires the formation of correct disulphide bonds, the group concluded that the role played by DsbA and DsbC in the formation of correct disulphide bonds in RNase I is much larger than that of the redox environment of the periplasm. The findings shown in this chapter are in agreement with this concept and suggest that thiol export by CydDC has less of an affect on disulphide bonding than originally proposed.

Chapter 6

Final Discussion

6.1 Background

Before embarking on this work, CydDC had been shown to export the low-molecular weight thiols GSH and cysteine from the cytoplasm to the periplasm of *E. coli* cells (Pittman *et al*., 2002, 2005). These findings placed CydDC with a role in periplasmic redox homeostasis. Mutants of CydDC display a pleiotropic phenotype, with the most important phenotype being the loss of cytochrome *bd*-I assembly. Despite most of the phenotypes of *cydDC* mutants having been shown to be complemented by the exogenous addition of either GSH or cysteine, this was not the case with cytochrome *bd*-I assembly which remained elusive, and had led to speculation of additional substrates of CydDC.

In this work, it was shown for the first time, that the simultaneous addition of GSH and cysteine to the growth medium of a *cydD* mutant allows the restoration of cytochrome *bd*-I, despite previous demonstrations that exogenous addition of neither cysteine (0.2-2mM) nor GSH (0.1-2mM) could restore assembly. Thus contrasting the reasoning behind the search for additional substrates of CydDC. In consideration of previous reports of CydDC-independent GSH export to the periplasm (Eser *et al.*, 2009), this finding demonstrates that any alternative GSH export methods do not provide a sufficient rate of GSH export to permit assembly when cysteine alone is added exogenously, instead both cysteine and GSH must be provided exogenously for cytochrome assembly. This requirement for both reduced thiols raises questions about the relationship between CydDC export and cytochrome *bd*-I assembly. DTT, a strong reducing agent was shown to be unable to restore cytochrome *bd*-I assembly when added exogenously to *cydD* cells, emphasising that loss of cytochrome assembly is not merely due to a need for reducing power in the periplasm. Ultimately this finding hints at a complex process in which both thiols play a role in cytochrome *bd*-I assembly.

As discussed is Section 1.1.3 *c*-type cytochrome maturation requires the reduction of both the CXXCH haem binding motif and the haem cofactor. Considering that both *c*-type cytochromes and cytochrome *bd*-I assembly are vulnerable to the loss of CydDC, it is possible that cysteine and GSH play a specialised redox role in these processes. It is important to note however that *c*-type cytochrome assembly can be partially restored with the exogenous addition of cysteine; it may be of interest therefore to study

assembly of *c*-type cytochromes in the presence of both GSH and cysteine, to determine if further restoration is observed.

The di-haem active of cytochrome *bd*-I is only detectable in the presence of *cydX*, encoding a single transmembrane helix of the quinol oxidase. In the absence of CydDC, CydAB polypeptides are still inserted into the membrane, yet it is unknown whether CydX would still be incorporated (Georgiou *et al.*, 1987). If the absence of CydDC does affect CydX incorporation, haem cofactor stability would be affected and further investigation may help to explain the necessity of two different reduced thiols.

A microarray analysis was performed to investigate the effects of exogenous GSH and cysteine upon cells lacking CydDC with the hope of understanding the significance of both LMW thiols in the assembly of cytochrome *bd*-I. Therein activity of the ArcAB two-component system was shown to be increased upon the addition of cysteine and GSH, ArcB senses the redox status of the quinone pool and ultimately adapts transcriptional regulation of respiratory genes. This reflects upon the up-regulation of the *cydABX* genes when thiols were added to the growth medium of the *cydDC* mutant. Taken together with reports of significant cytochrome *bd*-I restoration in a *cydC* mutant in response to the overexpression of the *cydAB* genes (Goldman *et al.*, 1996) it is possible that changes to gene expression in response to changes of the redox environment may have a partial role to play in cytochrome *bd*-I assembly.

Another key finding was the demonstration that CydDC provides *E. coli* cells with tolerance to nitric oxide and the conclusion that CydDC of K-12 strains provides addition NO protection to cells beyond permitting the assembly of cytochrome *bd*-I. This finding, alongside the perceived role of CydDC in periplasmic redox homeostasis led to the hypothesis that CydDC plays a role in virulence of pathogenic *E. coli*. *In vivo* experiments tested the ability of *cydDC* and *cydAB* uropathogenic *E. coli* (UPEC) mutants to survive within NO-producing macrophage cells. A mouse model of UTI was also used, this tested the ability of *cydDC* mutants to colonise the lower urinary tract of mice. The results of these were disappointing, showing that loss of CydDC had little/no affect upon colonisation of the urinary tract or for survival within macrophage cells. Herein, these and other findings shown within this work will be examined critically in the context of the previous state of knowledge surrounding CydDC.

6.1.1 A dual role for CydDC in NO tolerance

Previous work had shown that cytochrome *bd*-I contributes to the tolerance of *E. coli* to nitric oxide by virtue of a fast NO dissociate rate, that permits binding of oxygen to the terminal oxidase in the presence of NO (Mason *et al*. 2009). Considering that CydDC is required for the assembly of cytochrome *bd*-I, it was hypothesised that loss of CydDC would result in NO sensitivity. In Chapter 3, a donor of NO, NOC-12, was used to test the contribution of CydDC to NO tolerance alongside a wild type and cytochrome *bd*-I mutant. The data presented and discussed in Chapter 3 demonstrated that CydDC has a role in NO tolerance beyond permitting the assembly of cytochrome *bd*-I. It was predicted that the NO reactive thiols GSH and cysteine exported to the periplasm by CydDC could intercept incoming NO at the periplasm, to reduce the concentration of reactive NO that reaches vulnerable targets within the cytoplasm. This hypothesis is depicted in Figure 6-1. To test this, NOC-12 growth curves were performed, in which glutathione and cysteine were added to the growth medium to represent thiols normally present in the periplasm of cytochrome *bd*-I mutant cells; the aim was to show that the additional protection provided by CydDC beyond facilitating cytochrome *bd*-I assembly is due to these thiols. The additional thiols reduced the NO sensitivity of *cydD* cells to a level similar to *cydB* cells and it was thus concluded that CydDC has a dual role in tolerance to NO; enabling cytochrome *bd*-I assembly and export of thiols to shield against incoming NO.

The NO growth curves performed in this thesis were done so under aerobic conditions, it would be interesting to have also performed these under microaerobic conditions in which cytochrome *bd*-I is maximally expressed. As discussed in Section 1.5.4.1 the ratio of cytochrome *bd*-I to cytochrome *bo′* changes as oxygen tension changes, cells become much more reliant upon cytochrome *bd*-I under microaerobic conditions, whether this would affect NO sensitivity of *cydB* and *cydD* strains would need to be determined. CydDC though not under control of ArcA and FNR like cytochrome *bd*-I, is still shown to be regulated by oxygen concentration, with maximal expression under aerobic conditions, expression is 5-fold lower under anaerobic conditions. Anaerobic expression of *cydD* is elevated in the presence of nitrate or nitrite and deletion of CydDC results in loss of *c*-type cytochromes, which includes cytochrome *c* nitrite reductase NrfA. As discussed in Section 1.6.3 periplasmic NrfA consumes NO under anaerobic conditions and its loss induces a much greater sensitivity to NO (Poock *et al.*

2002). Considering this, it would be assumed that under anaerobiosis, loss of CydDC would also result in an increase in NO sensitivity. However NorV and Hmp would also be expressed under these conditions.

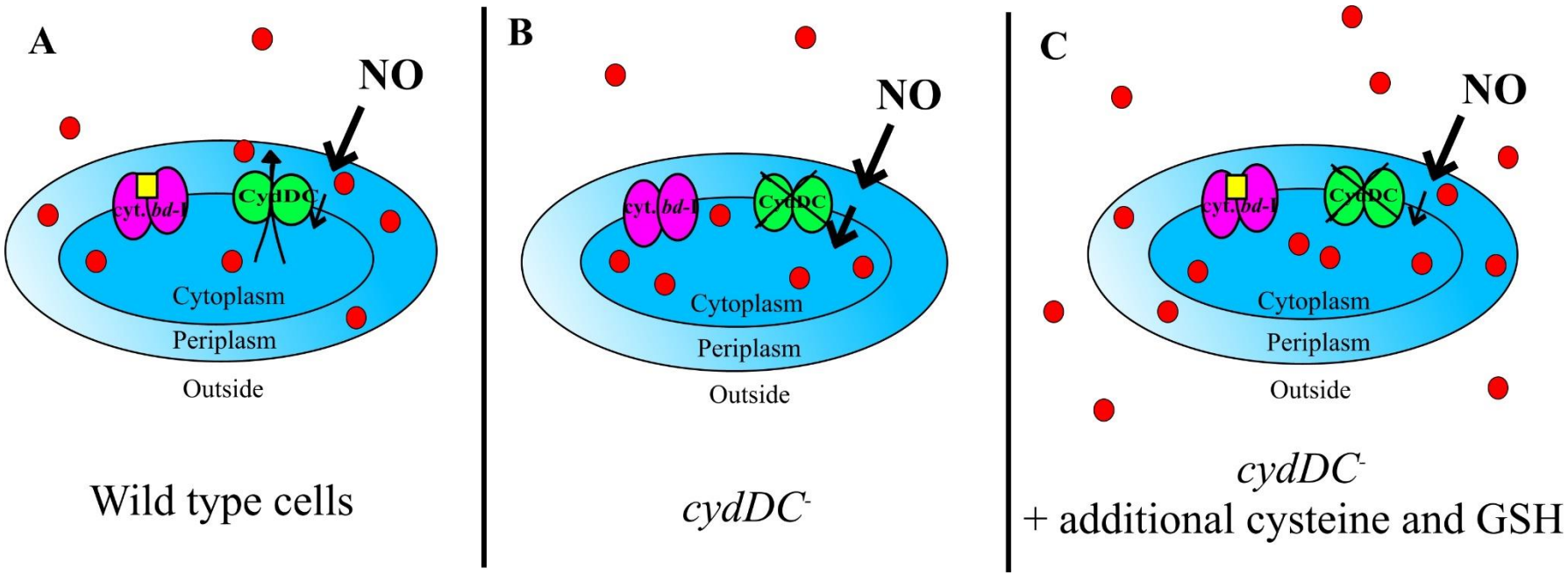

Figure 6-1 Model describing the role of CydDC mediated cysteine/glutathione export: incoming NO is intercepted and cytochrome *bd*-I assembly is enabled

A) Wild type cells express CydDC (green) which exports cysteine and reduced glutathione (depicted as red circles) to the periplasm, there thiols can then intercept incoming NO to reduce the affects within the cytoplasm (as signified by a reduced arrow from the periplasm to the cytoplasm). B) Deletion of *cydDC* prevents the export of thiols to the periplasm, so higher levels of NO can reach the cytoplasm (as represented by the larger arrow). C) Exogenous addition of cysteine and reduced glutathione re-creates the affect of CydDC export in a mutant lacking CydDC, permitting assembly of cytochrome *bd*-I and reducing the level of NO that can enter the cytoplasm, which explains the observed reduction in growth inhibition in NOC-12 growth curves.

6.1.2 The impact of CydDC substrates upon *E. coli* physiology: insights from a transcriptomic study

With an aim to study what happens within cells when the two known thiol substrates of CydDC are exogenously added to cells lacking CydDC (as in the cytochrome *bd*-I restoration experiments), transcriptional analysis of *cydDC* cells were performed with the addition of GSH and cysteine to the growth medium. In this situation, cytochrome *bd*-I restoration is expected, and a large number of changes to gene expression are likely to be due to a gain of function of the oxidase. For this reason, transcriptional changes in a *cydDC cydAB* mutant with the addition of GSH and cysteine were also studied.

As a large number of genes were identified, the results of the two microarray experiments were processed to produce a more focused subset of genes. This was achieved first by using TFinfer to deduce which transcription factors have activities that are significantly affected by the thiols. This permitted an understanding of the environmental stimuli imposed on cells by thiol addition. A major aim of this study was to examine the effects of thiol addition beyond the restoration of cytochrome *bd*-I, so transcription factors were grouped; TFs affected in both *cydDC* and *cydDC cydAB* cells (considered to be independent of cytochrome *bd*-I restoration), and TFs that were only significantly affected in *cydDC* cells but not *cydDC cydAB* cells (considered to be cytochrome *bd*-I restoration dependent). Lists of genes that are controlled by these two groups of TFs were listed in Tables 4-1 and 4-2, only genes that were shown to be significantly up- or down- regulated were included. These two tables were then used to create a metabolic map (Figure 6-2).

Changes in gene expression that were independent of cytochrome *bd*-I restoration included a repression of genes involved in motility, the TCA cycle, dihydroxyacetone degradation, as well as amino acid biosynthesis and transport. An induction of genes related to respiration was observed including *appBC* that encodes cytochrome *bd*-II and *hyaABCDF* genes that encode hydrogenase-I. Placing these changes in gene expression on a metabolic map (Figure 6-2), showed that the repression of genes encoding enzymes of the TCA cycle are accompanied by a repression of genes encoding enzymes that feed into the TCA cycle too.

Addition of thiols repressed expression of TCA cycle genes via the ArcA transcription factor. The same genes were up-regulated in the *cydD vs*. wild type

microarray, the authors of the latter study proposed that misfolded proteins and fatty acids are broken down to feed into the TCA cycle in order to restore the balance of metabolic flux (Holyoake *et al.*, 2016). NMR metabolomic data showed that in the absence of *cydD*, levels of succinate were elevated while those of fumarate were simultaneously depleted, which suggested an increase in succinate dehydrogenase activity. Succinate dehydrogenase catalyses the oxidation of succinate to fumarate and simultaneously reduces ubiquinone to ubiquinol (Figure 3-12). Taken together this indicates that loss of CydDC-exported thiols affects the redox status of the quinone pool and that TCA cycle genes are up-regulated to aid in re-balancing of the redox status. This is interesting as ArcB senses respiratory growth conditions via the redox state of the quinone pool using a thiol-based redox switch (Iuchi and Lin, 1988; Malpica *et al.*, 2004; Alvarez *et al.*, 2013) and ArcA, the corresponding response regulator controls expression of *cydABX* genes encoding cytochrome *bd*-I, it suggests that in wild type cells, CydDC-mediated thiol export affects the transcription of the genes encoding cytochrome *bd*-I, adding a new level to the relationship between the two protein complexes. Previously it had been shown that the regulation of *cydDC* and *cydABX* operons are not coordinated (Section 1.2), these results however suggest some form of relationship between the level of activity of CydDC and transcription of *cydABX*.

The repression of motility genes suggests that swarming motility is reduced by the addition of thiols. Which is surprising considering that Pittman *et al.* 2002 showed that exogenous cysteine restores motility defects of a *cydD* mutant, (most likely by permitting the correct disulphide folding of FlgI). It had been expected that addition of both cysteine and GSH would restore assembly of the flagella suprastructure by balancing the redox environment of the periplasm. It is therefore possible that contrary to a re-balancing of the periplasmic redox environment, the amount of thiols added is surplus to requirement and instead the periplasm is becoming more reduced than is observed in wild type cells. It would be of interest to observe the motility of *cydDC* cells in the presence of exogenous thiols to determine the actual effect of both thiols.

A larger repression of motility genes was observed after the addition of thiols to *cydDC cydAB* cells when compared to *cydDC* cells. Looking at the previously performed *cydB vs*. wild type microarray data, flagella genes were repressed and accompanied by a reduced swarming motility (Shepherd *et al.*, 2010). The authors suggest that repression

of motility genes is an energy conserving mechanism in the face of reduced energetic efficiency of cytochrome *bd*-II. It is thus likely that the difference between repression of motility genes is due to the lack of cytochrome *bd*-I restoration in the *cydDC cydAB* double mutant and the larger reliance upon cytochrome *bd*-II as shown by the increased regulation of *appBC* in the *cydDC cydAB* background.

Changes in gene expression that are considered dependent upon the restoration of cytochrome *bd*-I include a repression of genes of the 2-methylcitrate cycle, this cycle overlaps with the TCA cycle and utilises propionate to produces pyruvate. Northern-blot analysis has shown than unlike *acnB*, *prpD* is exclusively transcribed during growth on propionate (Brock *et al.* 2002). This suggests that in the absence of exogenous glutathione and cysteine, *cydDC* cells utilise propionate as a carbon source.

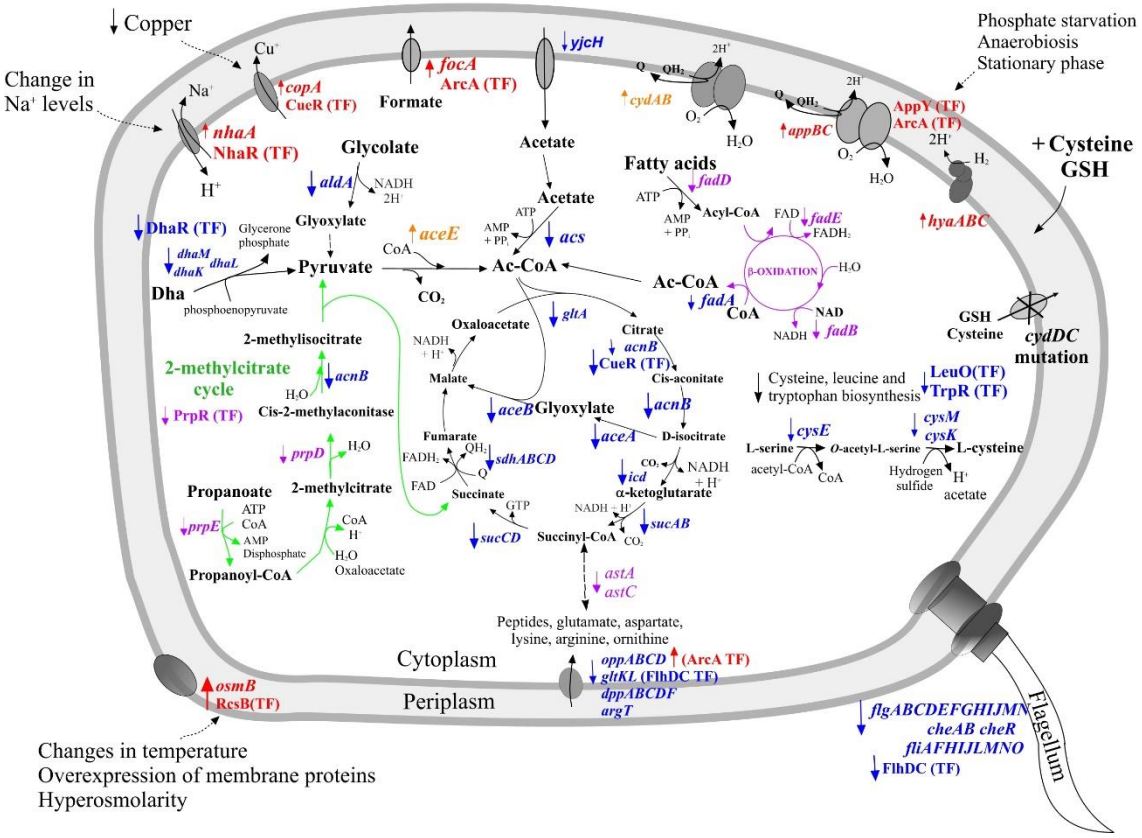

Figure 6-2. Model for the processes influenced by CydDC substrates in the periplasm: environmental signals and downstream effects

The gene transcript levels and transcription factor activities that are up- and down-regulated in the *cydDC* GSH/cysteine *vs. cydDC* and *cydDC cydAB* GSH/cysteine *vs. cydDC cydAB* are shown in red and blue, respectively. The gene transcript levels and transcription factor activities that are up- and down-regulated only in the *cydDC* GSH/cysteine *vs. cydDC* microarray are shown in orange and purple, respectively. The green and purple lines denote steps in the 2-methylcitrate cycle and *β*-oxidative of fatty acids. Dotted lines show potential environmental stimuli responded to. Abbreviations: Ac-CoA, Acetyl CoA; Dha, dihydroxyacetone; GSH, reduced glutathione; TF, transcription factor.

6.1.3 *In vivo* model for CydDC

The role of cytochrome *bd*-I (Mason *et al*. 2009) in NO tolerance of K-12 strains had already been shown. Considering that the function of cytochrome *bd*-I is reliant upon CydDC, it was expected that mutants of CydDC would be equally as sensitive as cytochrome *bd*-I mutants. Growth curves utilising the nitric oxide (NO) donor, NOC-12 showed that CydDC provides protection to cells from NO, beyond the role of cytochrome *bd*-I assembly.

NO is an important defence in the armoury of the host innate immune system. These findings suggested that cytochrome *bd*-I and CydDC may provide a concerted role in survival within the host environment. Therefore, the contribution of CydDC and cytochrome *bd*-I of UPEC strains, CFT073 and EC958, to NO tolerance were tested. The results showed that loss of either of the two complexes resulted in NO sensitivity in both CFT073 and EC958. Comparisons between the two mutants were however inconsistent with non-pathogenic K-12 strain data. For example, an EC958 cytochrome *bd*-I mutant was shown to be more sensitive to NO than the EC958 *cydDC* mutant. CydDC and cytochrome *bd*-I mutants of CFT073 were shown to have a similar level of growth inhibition after the addition of lower concentrations of NOC-12, yet a greater sensitivity of *cydDC* mutants were seen at higher NOC-12 concentrations when compared to cytochrome *bd*-I mutants. Despite this inconsistency, CydDC and cytochrome *bd*-I were still shown to be more sensitive to NO when compared to wild type cells. These results were promising, suggesting that loss of CydDC would result in a loss of NO tolerance and potentially the loss of other functions requiring disulphide bonding in the periplasm as CydDC is known to participate in redox homeostasis of the periplasm.

In vivo studies were used to test the ability of EC958 CydDC and cytochrome *bd*-I mutants to colonise the urinary tract via the UTI mouse model, and the ability to survive within macrophage cells of the immune system via macrophage survival assays.

Results of macrophage survival assays were striking, in that they showed that loss of CydDC had no effect upon the survival of EC958 cells within macrophage cells. Yet the EC958*cydAB* mutant showed a reduced survival when compared to the isogenic wild type and EC958*cydDC* cells. Considering that bacteria without CydDC should also lack functional cytochrome *bd*-I, a similar level of survival was expected when comparing

that of EC958*cydDC* and EC958*cydAB* cells. The discrepancy between the two mutants suggests that cytochrome *bd*-I assembly is restored in the *cydDC* mutant, potentially via thiols provided by the RPMI medium used to culture the macrophage cells or the macrophage cells themselves (Figure 6-3). Taken together macrophage survival assays showed that the results of NOC-12 growth curves do not always directly translate into the context of survival *in vivo*.

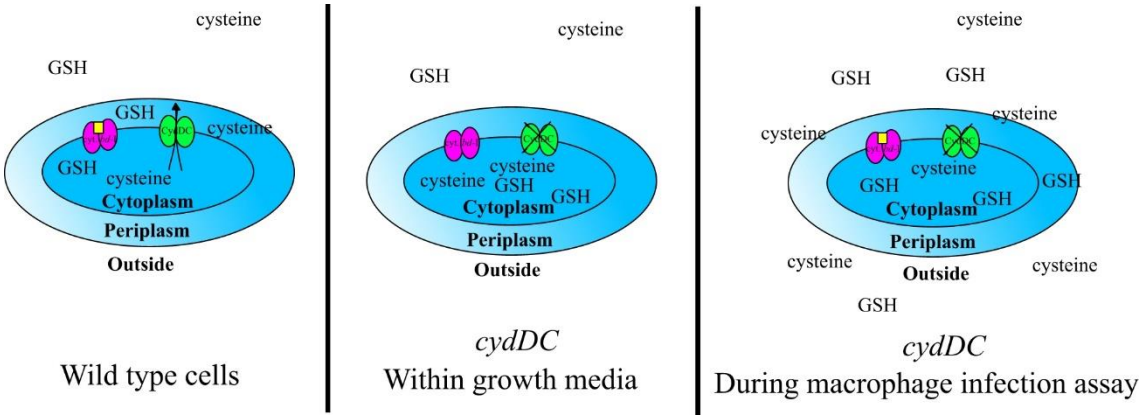

Figure 6-3. Mechanism for cytochrome *bd*-I restoration in *cydDC* mutant cells during macrophage infection assays

A wild type cells express CydDC (green) which permits haem (yellow) insertion into cytochrome *bd*-I (pink). **B** deletion of *cydDC* causes a pleiotropic phenotype including loss of haem insertion into cytochrome *bd*-I. **C** During macrophage infection assays, we hypothesise that host derived thiols are imported into the periplasm of *cydDC* mutant cells to permit the assembly of cytochrome *bd*-I.

In the mouse UTI model wild type/*cydDC* competition experiment, no significant difference was seen between the number of wild type (EC958) and EC958*cydDC* mutant CFU harvested from mouse urine and bladders after 24 hours of infection. Thus disappointingly, CydDC was not shown to facilitate the colonisation of the mouse lower urinary tract. This finding mirrors the results of the yeast agglutination assay, in which it was concluded that CydDC is not required for the correct folding of type 1 fimbriae. That the loss of CydDC does not affect colonisation of the mouse urinary tract is indicative that other extracytoplasmic virulence factors which UPEC rely upon to colonise the urinary tract within the first 24 hours of infection are also unaffected by the loss of CydDC. The result of the mouse model experiment does not however provide

information on the role of CydDC during UPEC pathogenesis after 24 hours of infection.

Previously performed mouse UTI model competition experiments showed that loss of cytochrome *bd*-I was detrimental to the colonisation of the mouse urinary tract (Dr Mark Shepherd, personal communication). Therefore a discrepancy between the EC958 mutants of CydDC and cytochrome *bd*-I was again observed, suggesting that restoration of cytochrome *bd*-I in the EC958*cydDC* mutant occurs during the experiment. There is no evidence for high concentrations of cysteine and glutathione in mouse urine, however, due to the nature of the experiment, in which wild type and *cydDC* mutants were combined before being introduced to the mouse urinary tract, it is possible that wild type cells, capable of exporting GSH and cysteine to the periplasm of cells may have complemented neighbouring *cydDC* mutants as porins of the outer membrane allow the diffusion of molecules >600 Da from the periplasm to the extracellular fluid (Decad and Nikaido 1976).

The differences in results between the *cydDC* and cytochrome *bd*-I mutants were much more pronounced in the *in vivo* experiments, whereas NO sensitivity of the two mutants had been relatively similar in the NOC-12 growth curve experiments. This could be due to static growth imposed upon bacteria to enrich for type 1 fimbriae before use in *in vivo* experiments. Under these conditions we would expect differential expression of *cydDC* and *cydAB* (cytochrome *bd*-I); as discussed in Section 1.5.4.1, *cydAB* of *E. coli* is maximally expressed under microaerobic conditions and at high cell densities, *cydAB* is regulated by FNR and ArcA (Tseng *et al.* 1996). As discussed in Section 1.2, however, CydDC shows a decrease in expression when grown anaerobically or at high cell densities, furthermore *cydDC* shows no significant regulation by FNR or ArcA (Cook, Membrillo-hernández and Poole 1997).

In conclusion, despite the importance of CydDC in cytochrome *bd*-I assembly, *in vivo* findings suggest that CydDC would not be an appropriate target to combat infections caused by uropathogenic *E. coli*. Cytochrome *bd*-I, however, which was shown to contribute to the survival within macrophage cells and has been shown in the work of others to reduce the ability of UPEC to colonise the urinary tract, would be a more sensible target.

6.1.4 The role of CydDC in Gram-positive organisms

The role of CydDC appears to be clear in the context of Gram-negative cells. However, CydDC is also known to be expressed by some Gram-positive bacteria which vary in the structure of their cell wall when compared to Gram-negative strains. The cell envelope of Gram-positive organisms is made up of a thick layer of peptidoglycan surrounding the cytoplasmic membrane and lacks the outer membrane of Gram-negative cells. In the past it has been assumed that Gram-positive organisms do not have a periplasmic space. This presents the question of why CydDC, a transporter of reduced thiols from the cytoplasm to the periplasm of *E. coli* and with a role in maintaining the periplasmic redox status is still encoded by Gram-positive organisms? It is becoming accepted, however, that Gram-positive cells do contain a space between the inner membrane and the thick layer of peptidoglycan that resembles the periplasm of Gram-negatives. The role of CydDC and its expression in Gram-positive bacteria still requires investigation, yet it is possible that CydDC plays a role in maintaining redox poise in this periplasm-like compartment. Further to this, it would be interesting to determine if cytochrome *bd*-I assembly is still lost in Gram-positive *cydDC* mutants. Considering that *cydDC* and *cydAB* operons are separated in the genomes of Gram-negative species, yet in Gram-positive bacteria, are arranged as a *cydABCD* gene cluster, it is intuitive to suggest that the two encoded protein complexes would be functionally related.

M. tuberculosis has an unusual Gram stain result due to its unusual cell wall which possesses features of both Gram-positive and negative bacteria (Fu and Fu-Liu, 2002), the cell wall of *M. tuberculosis* possesses a pseudo-lipid bilayer that resembles the outer membrane of Gram-negative cells. Earlier, in Section 1.8, it was mentioned that the expression of both *cydA* and *cydC* genes transiently increases during *Mycobacterium tuberculosis* infection of the mouse lung and furthermore that mutation of *cydC* impairs growth of *M. tuberculosis* in mice. The correlation between *cydA* and *cydC* gene expression suggests that CydDC is involved in cytochrome *bd*-I assembly yet the exact function of CydDC in *Mycobacterium tuberculosis* infection remains to be determined (Aung *et al.*, 2014).

6.2 Further experiments

In Chapter 5, the results of *in vivo* studies did not reflect the expectations drawn from NOC-12 growth curves. Cells had been grown statically to induce expression of type 1 fimbriae, this however is not how cells were grown during NOC-12 growth curves. This could account for the discrepancy as expression of *cydDC* and *cydAB* are affected by changes to oxygen availability. For this reason it would be interesting to test the NO sensitivity of statically grown *cydDC* and cytochrome *bd*-I mutants.

In the CO difference spectra performed in Chapter 3, growth of a *cydD* mutant in the presence of additional GSH and cysteine was shown to result in cytochrome *bd*-I restoration. The restoration of peaks within the spectral data is however, not a direct indication that the oxidase is functional, just that the haems required for function are present. This could be tested by growing *cydD* cells in a similar way to that of restoration assays, with reduced aeration, overnight with additional cysteine and GSH in the growth medium before performing a NOC-12 growth curve, if cytochrome *bd*-I is functional, a large decrease in the sensitivity of the *cydD* mutant would be expected.

In Chapter 5, the gene and protein sequences of cytochrome *bd*-I and CydDC from non-pathogenic and UPEC strains were compared. This concluded that no amino acid changes are present within the UPEC proteins that are likely to affect function. Nevertheless, in light of the conflicting *cydDC* and cytochrome *bd*-I mutant results in the studies using UPEC strains, it would be important to check that cytochrome *bd*-I assembly is in fact prevented in mutants of CydDC, to do this, CO difference spectroscopy (as performed in Chapter 3) would be performed on whole cells of EC958*cydDC* and CFT073*cydDC*.

References

Abramson, J., Riistama, S., Larsson, G., Jasaitis, A., Svensson-Ek, M., Laakkonen, L., Puustinen, A., Iwata, S., Wikström, M. (2000) The structure of the ubiquinol oxidase from *Escherichia coli* and its ubiquinone binding site. *Nat Struct Biol* **7**: 910–917.

Adikaram, P., and Beckett, D. (2013) Protein:Protein interactions in control of a transcriptional switch. *J Mol Biol* **425**: 4584–4594.

Aga, R.G., and Hughes, M.N. (2008) Globins and other nitric oxide-reactive proteins, part a. In *Methods in Enzymology*. Poole, R.K. (ed.). Academic Press, pp. 35–46.

Altuvia, S., Weinstein-Fischer, D., and Zhang, A. (1997) A small, stable RNA induced by oxidative stress: role as a pleiotropic regulator and antimutator. *Cell* **90**: 43–53.

Alvarez, A.F., Rodriguez, C., and Georgellis, D. (2013) Ubiquinone and menaquinone electron carriers represent the yin and yang in the redox regulation of the ArcB sensor kinase. *J Bacteriol* **195**: 3054–61.

Andresen, P.A., Kaasen, I., Styrvold, O.B., Boulnois, G., and Strøm, A.R. (1988) Molecular cloning, physical mapping and expression of the bet genes governing the osmoregulatory choline-glycine betaine pathway of *Escherichia coli. J Gen Microbiol* **134**: 1737–1746.

Anraku, Y. (1988) Bacterial electron transport chains. *Annu Rev Biochem* **57**: 101–132.

Armine V Avetisyan, Pavel A Dibrov, Anna L Semeykina, Vladimir P Skulachev, M.V.S. (1991) Adaptation of *Bacillus FTU* and *Escherichia coli* to alkaline conditions: the Na^+-motive respiration. *Biochim Biophys Acta* **1098**: 95–104.

Arutyunyan, A.M., Borisov, V.B., Novoderezhkin, V.I., Ghaim, J., Zhang, J., Gennis, R.B., and Konstantinov, A.A. (2008) Strong excitonic interactions in the oxygen-reducing site of *bd*-type oxidase : the Fe-to-Fe distance between hemes *d* and *b595* is 10 Å. *Biochemistry* **47**: 1752–1759.

Atlung, T., Knudsen, K., Heerfordt, L., and Brøndsted, L. (1997) Effects of sigmaS and the transcriptional activator AppY on induction of the *Escherichia coli hya* and *cbdAB-appA* operons in response to carbon and phosphate starvation. *J Bacteriol* **179**: 2141–2146.

Aung, H.L., Berney, M., and Cook, M. (2014) Hypoxia-activated cytochrome *bd* expression in *Mycobacterium smegmatis* s cyclic AMP receptor protein dependent. *J Bacteriol* **196**: 3091–3097.

Baba, T., Ara, T., Hasegawa, M., Takai, Y., Okumura, Y., Baba, M., Datsenko, K. A., Tomita, M., Wanner, B. L. Mori, H. (2006) Construction of *Escherichia coli* K-12 in-frame, single-gene knockout mutants: the Keio collection. *Mol Syst Biol* **2**: 1–11.

Bächler, C., Schneider, P., Bähler, P., Lustig, A., and Erni, B. (2005) *Escherichia coli* dihydroxyacetone kinase controls gene expression by binding to transcription factor DhaR. *EMBO J* **24**: 283–93.

Bachmann, B.J. (1990) Linkage map of *Escherichia coli* K-12 , Edition 8. *Microbiol Rev* **54**: 130–197.

Bachmann, B.J. (1996) Derivations and Genotypes of Some Mutant Derivatives of *Escherichia coli* K-12. In *Escherichia coli and Salmonella: Cellular and Molecular Biology*. Neidhardt, F.C., Curtiss, R., Ingraham, J. l., Lin, E.C.C., Low, K.B., Magasanik, B., *et al.* (Eds). ASM Press, pp. 2460–2488.

Bader, M., Muse, W., Ballou, D.P., Gassner, C., and Bardwell, J.C.A. (1999) Oxidative protein folding is driven by the electron transport system. *Cell* **98**: 217–227.

Bader, M.W., Hiniker, A., Regeimbal, J., Goldstone, D., Haebel, P.W., Riemer, J., Metcalf, P., Bardwell, J. C. (2001) Turning a disulfide isomerase into an oxidase: DsbC mutants that imitate DsbA. *EMBO J* **20**: 1555–1562.

Bahrani-Mougeot, F., Buckles, E., Lockatell, C.V., Hebel, J.R., Johnson, D., Tang, C., and Donnenberg, M.S. (2002) Type 1 fimbriae and extracellular polysaccharides are preeminent uropathogenic *Escherichia coli* virulence determinants in the murine urinary tract. *Mol Microbiol* **45**: 1079–1093.

Bang, I.-S., Liu, L., Vazquez-Torres, A., Crouch, M.-L., Stamler, J.S., and Fang, F.C. (2006) Maintenance of nitric oxide and redox homeostasis by the *Salmonella* flavohemoglobin *hmp*. *J Biol Chem* **281**: 28039–47.

Baptista, J.M., Justino, M.C., Melo, A.M.P., Teixeira, M., and Saraiva, L.M. (2012) Oxidative stress modulates the nitric oxide defense promoted by *Escherichia coli* flavorubredoxin. *J Bacteriol* **194**: 3611–7.

Barker, P.D., Nerou, E.P., Freund, S.M. V., and Fearnley, I.M. (1995) Conversion of Cytochrome *b562* to *c*-type cytochromes. *Biochemistry* **34**: 15191–15203.

Barrett, M.C., and Dawson, A.P. (1975) The reaction of choline dehydrogenase with some electron acceptors. *Biochem J* **151**: 677–683.

Baughn, A., and Malamy, M. (2004) The strict anaerobe *Bacteroides fragilis* grows in and benefits from nanomolar concentrations of oxygen. *Lett to Nat* **427**: 162–165.

Bebbington, K.J., and Williams, H.. (1993) Investigation of the role of the *cydD* gene product in production of a functional cytochrome *d* oxidase in *Escherichia coli*. *FEMS Microbiol Lett* **112**: 19–24.

Becker, S., Holighaus, G., Gabrielczyk, T., and Unden, G. (1996) O^2 as the regulatory signal for FNR-dependent gene regulation in *Escherichia coli*. *J Bacteriol* **178**: 4515–4521.

Beinert, H., and Kiley, P. (1999) Fe-S proteins in sensing and regulatory functions. *Curr Opin Chem Biol* **3**: 152–157.

Bekker, M., Vries, S. de, Beek, A. Ter, Hellingwerf, K.J., and Mattos, M.J.T. de (2009) Respiration of *Escherichia coli* can be fully uncoupled via the nonelectrogenic terminal cytochrome *bd*-II oxidase. *J Bacteriol* **191**: 5510–5517.

Benjamini, Y., and Hochberg, Y. (1995) Controlling the false discovery rate: a practical and powerful approach to multiple testing. *J R Stat Soc Ser B* **57**: 289–300.

Bloch, D. a, Borisov, V.B., Mogi, T., and Verkhovsky, M.I. (2009) Heme/heme redox interaction and resolution of individual optical absorption spectra of the hemes in cytochrome *bd* from *Escherichia coli*. *Biochim Biophys Acta* **1787**: 1246–53.

Bogachev, A. V, Murtazina, R.A., and Skulachev, V.P. (1993) Cytochrome *d* induction

in *Escherichia coli* growing under unfavorable conditions. *FEBS J* **336**: 75–78.

Bogachev, A. V., Murtazina, R.A., Shestopalov, A.I., and Vladimir P. Skulachev (1995) Induction of the *Escherichia coli* cytochrome *d* by low $\Delta\mu_H$,+ and by sodium ions. *Eur J Biochem* **232**: 304–308.

Bokil, N.J., Totsika, M., Carey, A.J., Stacey, K.J., Hancock, V., Saunders, B.M., Ravasi, T.
Ulett, G. C., Schembri, M. A., Sweet, M. J. (2011) Intramacrophage survival of uropathogenic *Escherichia coli*: differences between diverse clinical isolates and between mouse and human macrophages. *Immunobiology* **216**: 1164–71.

Borisov, V., Liebl, U., and Rappaport, F. (2002) Interactions between heme *d* and heme *b595* in quinol oxidase *bd* from *Escherichia coli*: a photoselection study using femtosecond spectroscopy. *Biochemistry* **41**: 1654–1662.

Borisov, V.B., Forte, E., Konstantinov, A. a., Poole, R.K., Sarti, P., and Giuffrè, A. (2004) Interaction of the bacterial terminal oxidase cytochrome *bd* with nitric oxide. *FEBS Lett* **576**: 201–204.

Borisov, V.B., Forte, E., Sarti, P., Brunori, M., Konstantinov, A. a, and Giuffrè, A. (2007) Redox control of fast ligand dissociation from *Escherichia coli* cytochrome *bd*. *Biochem Biophys Res Commun* **355**: 97–102.

Borisov, V.B., Forte, E., Siletsky, S. a, Sarti, P., and Giuffrè, A. (2015) Cytochrome *bd* from *Escherichia coli* catalyzes peroxynitrite decomposition. *Biochim Biophys Acta* **1847**: 182–8.

Borisov, V.B., Gennis, R.B., Hemp, J., and Verkhovsky, M.I. (2011) The cytochrome *bd* respiratory oxygen reductases. *Biochim Biophys Acta* **1807**: 1398–1413.

Borisov, V.B., and Verkhovsky, M.I. (2013) Accommodation of CO in the di-heme active site of cytochrome *bd* terminal oxidase from *Escherichia coli*. *J Inorg Biochem* **118**: 65–67.

Bouwman, C.W., Kohli, M., Killoran, A., Touchie, G. a., Kadner, R.J., and Martin, N.L. (2003) Characterization of SrgA, a *Salmonella enterica serovar Typhimurium* virulence plasmid-encoded paralogue of the disulfide oxidoreductase DsbA, essential for biogenesis of plasmid-encoded fimbriae. *J Bacteriol* **185**: 991–1000.

Bower, J.M., and Mulvey, M.A. (2006) Polyamine-mediated resistance of uropathogenic *Escherichia coli* to nitrosative stress. *J Bacteriol* **188**: 928–33.

Brachmann, C., Davies, A., Cost, G., Caputo, E., Li, J., Hieter, P., and Boeke, J. (1998) Designer deletion strains derived from *Saccharomyces cerevisiae* S288C: a useful set of strains and plasmids for PCR-mediated gene disruption and other applications. *Yeast* **14**: 115–132.

Brock, M., Maerker, C., Schütz, A., Völker, U., and Buckel, W. (2002) Oxidation of propionate to pyruvate in *Escherichia coli*. *Eur J Biochem* **269**: 6184–6194.

Brøndsted, L., and Atlung, T. (1996) Effect of growth conditions on expression of the acid phosphatase (*cyx-appA*) operon and the *appY* gene, which encodes a transcriptional activator of *Escherichia coli*. *J Bacteriol* **178**: 1556–1564.

Burall, L.S., Harro, J.M., Li, X., Lockatell, C.V., Himpsl, S.D., Hebel, J.R., Lockatell, C.V.,

Himpsl, S. D., Hebel, J. R., Johnson, D. E., Mobley, H. L. T. (2004) *Proteus mirabilis* genes that contribute to pathogenesis of urinary tract infection: identification of 25 signature-tagged mutants attenuated at least 100-Fold. *Infect Immun* **72**: 2922–2938.

Butler, A.R., Glidewell, C., and Li, M.S. (1988) *Nitrosyl complexes of iron-sulfur clusters*. Academic London, .

Calhoun, M., Newton, G., and Gennis, R. (1991) *E. coli* map. Physical map locations of genes encoding components of the aerobic respiratory chain of *Escherichia coli*. *J Bacteriol* **173**: 1569–1570.

Capitani, G., Biase, D. De, Aurizi, C., Gut, H., Bossa, F., and Grutter, M.G. (2003) Crystal structure and functional analysis of *Escherichia coli* glutamate decarboxylase. *EMBO J* **22**: 4027–4037.

Chaveroche, M., Ghigo, J., and D'Enfert, C. (2000) A rapid method for efficient gene replacement in the filamentous fungus *Aspergillus nidulans*. *Nucleic Acids Res* **28**: 1–6.

Chen, C.C., Fang, M., Majumder, A., and Wu, H.Y. (2001) A 72-base pair AT-rich DNA sequence element functions as a bacterial gene silencer. *J Biol Chem* **276**: 9478–85.

Claret, L., and Hughes, C. (2002) Interaction of the atypical prokaryotic transcription activator FlhD2C2 with early promoters of the flagellar gene hierarchy. *J Mol Biol* **321**: 185–199.

Collet, J., and Bardwell, J.C.A. (2002) Oxidative protein folding in bacteria. *Mol Microbiol* **44**: 1–8.

Connell, I., and Agace, W. (1996) Type 1 fimbrial expression enhances *Escherichia coli* virulence for the urinary tract. *Proc Natl Acad Sci USA* **93**: 9827–9832.

Cook, G.M., Cruz-Ramos, H., Moir, A.J.G., and Poole, R.K. (2002) A novel haem compound accumulated in *Escherichia coli* overexpressing the *cydDC* operon, encoding an ABC-type transporter required for cytochrome assembly. *Arch Microbiol* **178**: 358–69.

Cook, G.M., Membrillo-hernández, J., and Poole, R.K. (1997) Transcriptional regulation of the *cydDC* operon, encoding a heterodimeric ABC transporter required for assembly of cytochromes *c* and *bd* in *Escherichia coli* K-12: regulation by oxygen and alternative electron acceptors. *J Bacteriol* **179**: 6525–6530.

Cooper, C. (1999) Nitric oxide and iron proteins. *Biochim Biophys Acta (BBA)-Bioenergetics* **1411**: 290–309.

Cotter, P. a, Chepuri, V., Gennis, R.B., and Gunsalus, R.P. (1990) Cytochrome *o* (*cyoABCDE*) and *d* (*cydAB*) oxidase gene expression in *Escherichia coli* is regulated by oxygen, pH, and the *fnr* gene product. *J Bacteriol* **172**: 6333–6338.

Crespo, M.D., Puorger, C., Schärer, M. a, Eidam, O., Grütter, M.G., Capitani, G., and Glockshuber, R. (2012) Quality control of disulfide bond formation in pilus subunits by the chaperone FimC. *Nat Chem Biol* **8**: 707–13.

Crooke, H., and Cole, J. (1995) The biogenesis of *c*-type cytochromes in *Escherichia coli* requires a membrane-bound protein, DipZ, with a protein disulphide isomerase-like domain. *Mol Microbiol* **15**: 1139–1150.

Cruz-Ramos, H., Cook, G.M., Wu, G., Cleeter, M.W., and Poole, R.K. (2004a) Membrane topology and mutational analysis of *Escherichia coli* CydDC, an ABC-type cysteine exporter required for cytochrome assembly. *Microbiology* **150**: 3415–3427.

Cruz-Ramos, H., Cook, G.M., Wu, G., Cleeter, M.W., and Poole, R.K. (2004b) Membrane topology and mutational analysis of *Escherichia coli* CydDC, an ABC-type cysteine exporter required for cytochrome assembly. *Microbiology* **150**: 3415–27.

Cui, Q., Lewis, I., Hegeman, A., and Anderson, M. (2008) Metabolite identification via the madison metabolomics consortium database. *Nat Biotechnol* **26**: 162–165.

Cutruzzola, F. (1999) Bacterial nitric oxide synthesis. *Biochim Biophys Acta* **1411**: 231–249.

D'Autréaux, B., Tucker, N.P., Dixon, R., and Spiro, S. (2005) A non-haem iron centre in the transcription factor NorR senses nitric oxide. *Nature* **437**: 769–72.

D'Mello, R., Hill, S., and Poole, R. (1995) Affinity of cytochrome *bo*'in *Escherichia coli* determined by the deoxygenation of oxyleghemoglobin and oxymyoglobin: Km values for oxygen are in the submicromolar. *J Bacteriol* **177**: 867–870.

D'mello, R., Hill, S., and Poole, R.K. (1996) The cytochrome *bd* quinol oxidase in *Escherichia coli* has an extremely high oxygen affinity and two oxygen-binding haems: implications for regulation of activity *in vivo* by oxygen inhibition. *Microbiology* **142**: 755–763.

Daltrop, O., Stevens, J.M., Higham, C.W., and Ferguson, S.J. (2002) The CcmE protein of the *c*-type cytochrome biogenesis system: unusual *in vitro* heme incorporation into apo-CcmE and transfer from holo-CcmE to apocytochrome. *Proc Natl Acad Sci U S A* **99**: 9703–9708.

Darby, N.J., and Creighton, T.E. (1995) Catalytic mechanism of DsbA and its comparison with that of protein disulfide isomerase. *Biochemistry* **34**: 3576–3587.

Darwin, A., Hussain, H., Griffiths, L., Grove, J., Sambongi, Y., Busby, S., and Cole, J. (1993) Regulation and sequence of the structural gene for cytochrome *C552* from *Escherichia coli:* not a hexahaem but a 50kDa tetrahaem nitrite reductase. *Mol Microbiol* **9**: 1255–1265.

Dassa, J., Fsihi, H., Marck, C., Dion, M., Kieffer-Bontemps, M., and Boquet, P.L. (1991) A new oxygen-regulated operon in *Escherichia coli* comprises the genes for a putative third cytochrome oxidase and for pH 2.5 acid phosphatase (*appA*). *Mol Gen Genet* **229**: 341–352.

Daßler, T., Maier, T., Winterhalter, C., and Böck, A. (2000) Identification of a major facilitator protein from *Escherichia coli* involved in efflux of metabolites of the cysteine pathway. *Mol Microbiol* **36**: 1101–1112.

Datsenko, K., and Wanner, B. (2000) One-step inactivation of chromosomal genes in *Escherichia coli* K-12 using PCR products. *Proc Natl Acad Sci* **97**: 6640–6645.

Dawson, R.J.P., and Locher, K.P. (2006) Structure of a bacterial multidrug ABC transporter. *Nature* **443**: 180–185.

Decad, G., and Nikaido, H. (1976) The outer membrane of Gram-negative bacteria. *J Bacteriol* **128**: 325–336.

Delaney, J.M., Ang, D., and Georgopoulos, C. (1992) Isolation and characterization of the *Escherichia coli htrD* gene, whose product is required for growth at high temperatures. *J Bacteriol* **174**: 1240–1247.

Deutch, C.E., Hasler, J.M., Houston, R., Sharma, M., and Stone, V.J. (1989) Nonspecific inhibition of proline dehydrogenase synthesis in E*scherichia coli* during osmotic stress. *Can J Microbiol* **35**: 779–785.

Devroede, N., Thia-Toong, T.-L., Gigot, D., Maes, D., and Charlier, D. (2004) Purine and pyrimidine-specific repression of the *Escherichia coli carAB* operon are functionally and structurally coupled. *J Mol Biol* **336**: 25–42.

Drapier, J.-C. (1997) Interplay between NO and [Fe-S] clusters: relevance to biological systems. *Methods* **11**: 319–29.

Dueweket, T.J., and Gennis, R.B. (1991) Proteolysis of the cytochrome d complex with trypsin and chymotrypsin localizes a quinol oxidase domain. *Biochemistry* **30**: 3401–3406.

Ebejer, J.P., Hill, J.R., Kelm, S., Shi, J., and Deane, C.M. (2013) Memoir: template-based structure prediction for membrane proteins. *Nucleic Acids Res* **41**: 379–383.

Eisenberg, M., O, P., and Hsiung, S. (1982) Purification and properties of the biotin repressor. *J Biol Chem* **257**: 15167–15173.

Elfering, S.L., Sarkela, T.M., and Giulivi, C. (2002) Biochemistry of mitochondrial nitric-oxide synthase. *J Biol Chem* **277**: 38079–86.

Endley, S., Murray, D.M.C., and Ficht, T.A. (2001) Interruption of the *cydB* locus in *Brucella abortus* attenuates intracellular survival and virulence in the mouse model of infection. **183**: 2454–2462.

Engel, D.R., Maurer, J., Tittel, a. P., Weisheit, C., Cavlar, T., Schumak, B., Limmer, A., Van Rooijen, N., Trautwein, C., Tacke, F., Kurts, C.. (2008) CCR2 mediates homeostatic and inflammatory release of Gr1 high monocytes from the bone marrow, but is dispensable for bladder infiltration in bacterial urinary tract infection. *J Immunol* **181**: 5579–5586.

Eser, M., Masip, L., Kadokura, H., Georgiou, G., and Beckwith, J. (2009) Disulfide bond formation by exported glutaredoxin indicates glutathione's presence in the *E. coli* periplasm. *Proc Natl Acad Sci USA* **106**: 1572–7.

Fabianek, R., Huber-Wunderlich, M., Glockshuber, R., Nzler, Kunzler, P., Hennecke, H., and Thony-Meyer, L. (1997) Characterization of the *Bradyrhizobium japonicum* CycY protein, a membrane-anchored periplasmic thioredoxin that may play a role as a reductant in the biogenesis of *c*-type cytochromes. *J Biol Chem* **272**: 4467–4473.

Fabianek, R.A., Hennecke, H., and Thony-meyer, L. (2000) Periplasmic protein thiol : disulphde oxidoreductases of *Escherichia coli*. *FEMS Microbiol Rev* **24**: 303–316.

Fang, F.C. (2004) Antimicrobial reactive oxygen and nitrogen species: concepts and controversies. *Nat Rev Microbiol* **2**: 820–32.

Fang, H., Lin, R., and Gennis, R. (1989) Location of heme axial ligands in the cytochrome *d* terminal oxidase complex of *Escherichia coli* determined by site-directed mutagenesis. *J Biol Chem* **264**: 8026–8032.

Flatley, J., Barrett, J., Pullan, S.T., Hughes, M.N., Green, J., and Poole, R.K. (2005) Transcriptional responses of *Escherichia coli* to S-nitrosoglutathione under defined chemostat conditions reveal major changes in methionine biosynthesis. *J Biol Chem* **280**: 10065–72.

Forde, B.M., Zakour, N.L., Stanton-Cook, M., Phan, M.D., Totsika, M., Peters, K.M., Chan, K. G., Schembri, M. A., Upton, M., Beatson, S. A. (2014) The complete genome sequence of *Escherichia coli* EC958: A high quality reference sequence for the globally disseminated multidrug resistant *E. coli* O25b:H4-ST131 clone. *PLoS One* **9**.

Franke, I., Resch, A., Daßler, T., Maier, T., and Böck, A. (2003) YfiK from *Escherichia*

coli promotes export of o-acetylserine and cysteine. *J Bacteriol* **185**: 1161–1166.

Frech, C., Wunderlich, M., Glockshuber, R., and Schmid, F.X. (1996) Preferential binding of an unfolded protein to DsbA. *EMBO J* **15**: 392–98.

Fronzes, R., Remaut, H., and Waksman, G. (2008) Architectures and biogenesis of non-flagellar protein appendages in Gram-negative bacteria. *EMBO J* **27**: 2271–80.

Fu, H., Iuchi, S., and Lin, E.C.C. (1991) The requirement of ArcA and Fnr for peak expression of the *cyd* operon in *Escherichia coli* under microaerobic conditions. *Mol Gen Genet* **226**: 209–213.

Fu, L.M., and Fu-Liu, C.S. (2002) Is *Mycobacterium tuberculosis* a closer relative to Gram-positive or Gram– negative bacterial pathogens? *Tuberculosis* **82**: 85–90.

Gardner, A.M., Gessner, C.R., and Gardner, P.R. (2003) Regulation of the nitric oxide reduction operon (*norRVW*) in *Escherichia coli*. Role of NorR and sigma54 in the nitric oxide stress response. *J Biol Chem* **278**: 10081–6.

Gardner, A.M., Helmick, R. a, and Gardner, P.R. (2002) Flavorubredoxin, an inducible catalyst for nitric oxide reduction and detoxification in *Escherichia coli. J Biol Chem* **277**: 8172–7.

Gardner, P.R., Gardner, A.M., Martin, L.A., and Salzman, A.L. (1998) Nitric oxide dioxygenase: an enzymic function for flavohemoglobin. *Proc Natl Acad Sci* **95**: 10378–10383.

Georgellis, D., Lynch, A., and Lin, E. (1997) *In vitro* phosphorylation study of the *arc* two-component signal transduction system of *Escherichia coli. J Bacteriol* **179**: 5429–5435.

Georgiou, C.D., Hong, F., and Gennis, R.B. (1987) Identification of the *cydC* locus required for expression of the functional form of the cytochrome *d* terminal oxidase complex in *Escherichia coli*. *J Bacteriol* **169**: 2107–2112.

Gohlke, U., Warne, A., and Saraste, M. (1997) Projection structure of the cytochrome *bo* ubiquinol oxidase from *Escherichia coli* at 6 Å resolution. *EMBO J* **16**: 1181–1188.

Goldman, B.S., Gabbert, K.K., and Kranz, R.G. (1996a) Use of heme reporters for studies of cytochrome biosynthesis and heme transport. *J Bacteriol* **178**: 6338–6347.

Goldman, B.S., Gabbert, K.K., and Kranz, R.G. (1996b) The temperature-sensitive growth and survival phenotypes of *Escherichia coli cydDC* and *cydAB* strains are due to deficiencies in cytochrome *bd* and are corrected by exogenous catalase and reducing agents. *J Bacteriol* **178**: 6348–6351.

Gomes, C., Vicente, J., Wasserfallen, A., and Teixeira, M. (2000) Spectroscopic studies and characterization of a novel electron-transfer chain from *Escherichia coli* involving a flavorubredoxin and its flavoprotein reductase partner. *Biochemistry* **39**: 16230–16237.

Gomes, C.M., Giuffrè, A., Forte, E., Vicente, J.B., Saraiva, L.M., Brunori, M., and Teixeira, M. (2002) A novel type of nitric-oxide reductase. *Escherichia coli* flavorubredoxin. *J Biol Chem* **277**: 25273–6.

Gonzalez-Flecha, B., and Demple, B. (1999) Role for the *oxyS* gene in regulation of intracellular hydrogen peroxide in *Escherichia coli*. *J Bacteriol* **181**: 3833–3836.

Green, G., Fang, H., Lin, R., Newton, G., Mather, M., Georgious, C., and Gennis, R. (1988) The nucleotide sequence of the *cyd* locus encoding the two subunits of the cytochrome *d* terminal oxidase complex of *Escherichia coli. J Biol Chem* **263**: 13138–

13143.

Green, J., Irvine, a. S., Meng, W., and Guest, J.R. (1996) FNR-DNA interactions at natural and semi-synthetic promoters. *Mol Microbiol* **19**: 125–137.

Grimshaw, J.P. a, Stirnimann, C.U., Brozzo, M.S., Malojcic, G., Grütter, M.G., Capitani, G., and Glockshuber, R. (2008) DsbL and DsbI form a specific dithiol oxidase system for periplasmic arylsulfate sulfotransferase in uropathogenic *Escherichia coli*. *J Mol Biol* **380**: 667–80.

Groisman, E., and Ochman, H. (1996) Pathogenicity islands: bacterial evolution in quantum leaps. *Cell* **87**: 791–794.

Gualdi, L., Tagliabue, L., Bertagnoli, S., Ieranò, T., Castro, C. De, and Landini, P. (2008) Cellulose modulates biofilm formation by counteracting curli-mediated colonization of solid surfaces in *Escherichia coli*. *Microbiology* **154**: 2017–2024.

Gunsalus, R. (1992) Control of electron flow in *Escherichia coli*: coordinated transcription of respiratory pathway genes. *J Bacteriol* **174**: 7069–7074.

Gunsalus, R.P., and Yanofsky, C. (1980) Nucleotide sequence and expression of *Escherichia coli trpR*, the structural gene for the *trp* aporepressor. *Proc Natl Acad Sci* **77**: 7117–7121.

Ha, U.-H., Wang, Y., and Jin, S. (2003) DsbA of *Pseudomonas aeruginosa* is essential for multiple virulence factors. *Infect Immun* **71**: 1590–1595.

Hanson, P.I., and Whiteheart, S.W. (2005) AAA+ proteins: have engine, will work. *Nat Rev Mol Cell Biol* **6**: 519–29.

Harborne, N.R., Griffiths, L., Busby, S.J., and Cole, J.A. (1992) Transcriptional control, translation and function of the products of the five open reading frames of the *Escherichia coli nir* operon. *Mol Microbiol* **6**: 2805–2813.

Harding, G.K.M., and Ronald, A.R. (1994) The management of urinary infections: what have we learned in the past decade? *Int J Antimicrob Agents* **4**: 83–88.

Heras, B., Shouldice, S.R., Totsika, M., Scanlon, M.J., Schembri, M. a, and Martin, J.L. (2009) DSB proteins and bacterial pathogenicity. *Nat Rev Microbiol* **7**: 215–25.

Hill, J.J., Alben, J., and Gennist, R.B. (1993) Spectroscopic evidence for a heme-heme binuclear center in the cytochrome *bd* ubiquinol oxidase from *Escherichia coli*. *Proc Natl Acad Sci* **90**: 5863–5867.

Hoeser, J., Hong, S., Gehmann, G., Gennis, R.B., and Friedrich, T. (2014) Subunit CydX of *Escherichia coli* cytochrome *bd* ubiquinol oxidase is essential for assembly and stability of the di-heme active site. *FEBS Lett* **588**: 1537–41.

Holyoake, L. V., Hunt, S., Sanguinetti, G., Cook, G.M., Howard, M.J., Rowe, M.L., Poole, R. K., Shepherd, M., (2016) CydDC-mediated reductant export in *Escherichia coli* controls the transcriptional wiring of energy metabolism and combats nitrosative stress. *Biochem J* **473**: 693–701.

Hong, W., Jiao, W., Hu, J., Zhang, J., Liu, C., Fu, X., Shen, D., Xia, B., Chang, Z. (2005) Periplasmic protein HdeA exhibits chaperone-like activity exclusively within stomach pH range by transforming into disordered conformation. *J Biol Chem* **280**: 27029–27034.

Hosie, A., and Poole, P. (2001) Bacterial ABC transporters of amino acids. *Res Microbiol* **152**: 259–270.

Hrabie, J.A., Klose, J.R., Wink, D.A., and Keefer, L.K. (1993) New nitric oxide-releasing Zwitterions derived from polyamines. *J Org Chem* **58**: 1472–1476.

Ignarro, L.J. (1989) Biological actions and properties of endothelium-derived nitric oxide formed and released from artery and vein. *Circ Res* **65**: 1–21.

Inaba, K. (2008) Protein disulfide bond generation in *Escherichia coli* DsbB-DsbA. *J Synchrotron Radiat* **15**: 199–201.

Ingersoll, K.S., and Cohen, J. (2008) The impact of medication regimen factors on adherence to chronic treatment: a review of literature. *J Behav Med* **31**: 213–24.

Ingledew, W., and Poole, R. (1984) The respiratory chains of *Escherichia coli*. *Microbiol Rev* **48**: 222–271.

Iuchi, S., Chepuri, V., Fu, H., Gennis, R., and Lin, E. (1990) Requirement for terminal cytochromes in generation of the aerobic signal for the arc regulatory system in *Escherichia coli*: study utilizing deletions and *lac* fusions of. *J Bacteriol* **172**: 6020–6025.

Iuchi, S., and Lin, E. (1988) *arcA* (dye), a global regulatory gene in *Escherichia coli* mediating repression of enzymes in aerobic pathways. *Proc Natl Acad Sci* **85**: 1888–1892.

Iuchi, S., and Lin, E. (1992) Purification and phosphorylation of the Arc regulatory components of *Escherichia coli*. *J Bacteriol* **174**: 5617–5623.

Jacob-dubuisson, F., Pinkner, J., Xu, Z., Striker, R., Padmanhaban, A., and Hultgren, S.J. (1994) PapD chaperone function in pilus biogenesis depends on oxidant and chaperone-like activities of DsbA. *Biochemistry* **91**: 11552–11556.

James, P.E., Grinberg, O.Y., Michaels, G., and Harold M. Swartz (1995) Intraphagosomal oxygen in stimulated macrophages. *J Cell Physiol* **163**: 241–247.

Jones, P.M., and George, A.M. (2004) The ABC transporter structure and mechanism: Perspectives on recent research. *Cell Mol Life Sci* **61**: 682–699.

Junemann, S. (1997) Cytochrome *bd* terminal oxidase. *Biochim Biophys Acta* **1321**: 107–127.

Jung, J., Gutierrez, C., and Villarejo, M. (1989) Sequence of an osmotically inducible lipoprotein gene. *J Bacteriol* **171**: 511–520.

Justino, M.C., Almeida, C.C., Gonçalves, V.L., Teixeira, M., and Saraiva, L.M. (2006) *Escherichia coli* YtfE is a di-iron protein with an important function in assembly of iron-sulphur clusters. *FEMS Microbiol Lett* **257**: 278–84.

Justino, M.C., Almeida, C.C., Teixeira, M., and Saraiva, L.M. (2007) *Escherichia coli* di-iron YtfE protein is necessary for the repair of stress-damaged iron-sulfur clusters. *J Biol Chem* **282**: 10352–9.

Justino, M.C., Vicente, J.B., Teixeira, M., and Saraiva, L.M. (2005) New genes implicated in the protection of anaerobically grown *Escherichia coli* against nitric oxide. *J Biol Chem* **280**: 2636–43.

Källenius, G., Svenson, S., Hultberg, H., and Möllby, R. (1981) Occurrence of P-fimbriated *Escherichia coli* in urinary tract infections. *Lancet* **318**: 1369–1372.

Kalnenieks, U., Galinina, N., Bringer-Meyer, S., and Poole, R.K. (1998) Membrane D-lactate oxidase in Zymomonas mobilis: evidence for a branched respiratory chain. *FEMS Microbiol Lett* **168**: 91–97.

Katzen, F., and Beckwith, J. (2000) Transmembrane electron transfer by the membrane protein DsbD occurs via a disulfide bond cascade. *Cell* **103**: 769–779.

Kaysser, T., Ghaim, J., Georgiou, C., and Gennis, R. (1995) Methionine-393 is an axial ligand of the heme *b558* component of the cytochrome *bd* ubiquinol oxidase from *Escherichia coli. Biochemistry* **34**: 13491–13501.

Kern, R., Malki, A., Abdallah, J., Tagourti, J., and Richarme, G. (2007) *Escherichia coli* HdeB is an acid stress chaperone. *J Bacteriol* **189**: 603–610.

Kita, K., Konishi, K., and Anraku, Y. (1984) Terminal oxidases of *Escherichia coli* aerobic respiratory chain. II. Purification and properties of cytochrome *b558-d* complex from cells grown with limited oxygen and evidence of branched electron-carrying systems. *J Biol Chem* **259**: 3375–3381.

Korshunov, S., and Imlay, J.A. (2010) Two sources of endogenous hydrogen peroxide in *Escherichia coli. Mol Microbiol* **75**: 1389–1401.

Kranz, R.G., and Gennis, R.B. (1983) Immunological Characterization of the cytochrome. *J Biol Chem* **258**: 10614–10621.

Kulasekara, H.D., and Blomfield, I.C. (1999) The molecular basis for the specificity of *fimE* in the phase variation of type 1 fimbriae of *Escherichia coli* K-12. *Mol Microbiol* **31**: 1171–1181.

Larsen, M.H., Kallipolitis, B.H., Christiansen, J.K., Olsen, J.E., and Ingmer, H. (2006) The response regulator ResD modulates virulence gene expression in response to carbohydrates in *Listeria monocytogenes*. *Mol Microbiol* **61**: 1622–1635.

Łasica, A.M., and Jagusztyn-Krynicka, E.K. (2007) The role of Dsb proteins of Gram-negative bacteria in the process of pathogenesis. *FEMS Microbiol Rev* **31**: 626–36.

Lau, S.H., Kaufmann, M.E., Livermore, D.M., Woodford, N., Willshaw, G. a, Cheasty, T., Stamper, K., Reddy, S., Cheesbrough, J., Bolton, F. J., Fox, A. J., Upton, M. (2008) UK epidemic *Escherichia coli* strains A-E, with CTX-M-15 beta-lactamase, all belong to the international O25:H4-ST131 clone. *J Antimicrob Chemother* **62**: 1241–4.

Lay, N. De, and Gottesman, S. (2012) A complex network of small non-coding RNAs regulate motility in *Escherichia coli. Mol Microbiol* **86**: 524–538.

Lazazzera, B., and Beinert, H. (1996) DNA binding and dimerization of the Fe− S-containing FNR protein from *Escherichia coli* are regulated by oxygen. *J Biol Chem* **271**: 2762–2768.

Lee, S.K., Newman, J.D., and Keasling, J.D. (2005) Catabolite repression of the propionate catabolic genes in *Escherichia coli* and *Salmonella enterica:* evidence for involvement of the cyclic AMP receptor protein. *J Bacteriol* **187**: 2793–800.

Lemieux, L., Calhoun, M., Thomas, J.W., Ingledew, W.J., and Gennisl, R.B. (1992) Determination of the ligands of the low spin heme of the cytochrome *o* ubiquinol oxidase complex using site-directed mutagenesis. *J Biol Chem* **267**: 2105–2113.

Linton, K.J., and Higgins, C.F. (1998) The *Escherichia coli* ATP-binding cassette (ABC) proteins. *Mol Microbiol* **28**: 5–13.

Liu, X., and Wulf, P. De (2004) Probing the ArcA-P modulon of *Escherichia coli* by whole genome transcriptional analysis and sequence recognition profiling. *J Biol Chem* **279**: 12588–12597.

Lloyd, A.L., Smith, S.N., Eaton, K., and Mobley, H.L.T. (2009) Uropathogenic

Escherichia coli suppresses the host inflammatory response via pathogenicity island genes *sisA* and *sisB*. *Infect Immun* **77**: 5322–33.

Loisel-Meyer, S., Jimenez de Bagues, M.P., Kohler, S., Liautard, J., and V, J.-M. (2005) Differential use of the two high-oxygen-affinity terminal oxidases of *Brucella suis* for *in vitro* and intramacrophagic multiplication. *Infect Immun* **73**: 7768–7771.

Lund, B., Lindberg, F., Marklund, B., and Normark, S. (1987) Galactopyranose-binding adhesin of uropathogenic *Escherichia coli*. *Proc Natl Acad Sci* **84**: 5898–5902.

Lundberg, J.O., Weitzberg, E., Cole, J.A., and Benjamin, N. (2004) Nitrate, bacteria and human health. *Nat Rev Microbiol* **2**: 593–602.

Majdalani, N., and Gottesman, S. (2005) The Rcs phosphorelay: a complex signal transduction system. *Annu Rev Microbiol* **59**: 379–405.

Majumder, A., Fang, M., Tsai, K.J., Ueguchi, C., Mizuno, T., and Wu, H.Y. (2001) LeuO expression in response to starvation for branched-chain amino acids. *J Biol Chem* **276**: 19046–51.

Malpica, R., Franco, B., Rodriguez, C., Kwon, O., and Georgellis, D. (2004) Identification of a quinone-sensitive redox switch in the ArcB sensor kinase. *Proceedings of the National Academy of Sciences of the United States of Americ*a **101**: 13318-13323.

Martinez, A., and Kolter, R. (1997) Protection of DNA during oxidative stress by the nonspecific DNA-binding protein Dps. *J Bacteriol* **179**: 5188–5194.

Mason, M.G., Shepherd, M., Nicholls, P., Dobbin, P.S., Dodsworth, K.S., Poole, R.K., and Cooper, C.E. (2009) Cytochrome *bd* confers nitric oxide resistance to *Escherichia coli*. *Nat Chem Biol* **5**: 94–6.

Matsumoto, Y., Murai, M., Fujita, D., Sakamoto, K., Miyoshi, H., Yoshida, M., and Mogi, T. (2006) Mass spectrometric analysis of the ubiquinol-binding site in cytochrome *bd* from *Escherichia coli*. *J Biol Chem* **281**: 1905–12.

McClain, M., Blomfield, I., Eberhardt, K., and Eisenstein, B. (1993) Inversion-independent phase variation of type 1 fimbriae in *Escherichia coli*. *J Bacteriol* **175**: 4335–4344.

Ménard, R., Sansonetti, P., and Parsot, C. (1993) Nonpolar mutagenesis of the *ipa* genes defines IpaB, IpaC, and IpaD as effectors of *Shigella flexneri* entry into epithelial cells. *J Bacteriol* **175**: 5899–5906.

Messens, J., Collet, J.F., Belle, K. Van, Brosens, E., Loris, R., and Wyns, L. (2007) The oxidase DsbA folds a protein with a nonconsecutive disulfide. *J Biol Chem* **282**: 31302–31307.

Minagawa, S., Ogasawara, H., Kato, A., Yamamoto, K., Eguchi, Y., Oshima, T., Mori, H., Ishihama, A., Utsumi, R. (2003) Identification and molecular characterization of the Mg^{2+} stimulon of *Escherichia coli*. *J Bacteriol* **185**: 3696–3702.

Minghetti, K., Goswitz, V., and Gabriel, N. (1992) Modified, large-scale purification of the cytochrome *o* complex (*bo*-type oxidase) of *Escherichia coli* yields a two heme/one copper terminal oxidase with high specific. *Biochemistry* **31**: 6917–6924.

Missiakas, D., Georgopoulos, C., and Raina, S. (1993) Identification and characterization of the *Escherichia coli* gene *dsbB* , whose product is involved in the formation of disulfide bonds *in vivo*. *Proc Natl Acad Sci* **90**: 7084–7088.

Mobley, H., Jarvis, K., Elwood, J., Whittle, D., Lockate, C., Russell, R., Johnson, D. E., Donnenberg, M. S., Warren, J. W. (1993) Isogenic P-fimbrial deletion mutants of pyelonephritogenic *Escherichia coli* - the role of alpha-Gal(1-4)beta-Gal binding in virulence of a wild-type strain. *Mol Microbiol* **10**: 143–155.

Mobley, H.L., and Green, D. (1990) Pyelonephritogenic *Escherichia coli* and killing of cultured human renal proximal tubular epithelial cells: role of hemolysin in some strains. *Infect Immun* **58**: 1281–1289.

Mogi, T., Akimoto, S., Endou, S., Watanabe-nakayama, T., Mizuochi-asai, E., and Miyoshi, H. (2006) Probing the ubiquinol-binding site in cytochrome *bd* by site-directed mutagenesis. *Biochemistry* **45**: 7924–7930.

Mogi, T., Endou, S., and Akimoto, S. (2006) Glutamates 99 and 107 in transmembrane helix III of subunit I of cytochrome *bd* are critical for binding of the heme b_{595}-*d* binuclear center and enzyme activity. *Biochemistry* **45**: 15785–15792.

Monika, E.M., Goldman, B.S., Beckman, D.L., and Kranz, R.G. (1997) A thioreduction pathway tethered to the membrane for periplasmic cytochromes *c* biogenesis; *in vitro* and *in vivo* studies. *J Mol Biol* **271**: 679–92.

Mouslim, C., Latifi, T., and Groisman, E. (2003) Signal-dependent requirement for the co-activator protein RcsA in transcription of the RcsB-regulated *ugd* gene. *J Biol Chem* **278**: 50588–95.

Moussatova, A., Kandt, C., O'Mara, M.L., and Tieleman, D.P. (2008) ATP-binding cassette transporters in *Escherichia coli*. *Biochim Biophys Acta - Biomembranes* **1778**: 1757–1771.

Muller, M., and Webster, R. (1997) Characterization of the *tol-pal* and *cyd* region of *Escherichia coli* K-12: transcript analysis and identification of two new proteins encoded by the *cyd* operon. *J Bacteriol* **179**: 2077–2080.

Neidhardt, F.C., Bloch, P.L., and Smith, D.F. (1974) Culture Medium for Enterobacteria. *J Bacteriol* **119**: 736–747.

Nicholson, D., and Neupert, W. (1989) Import of cytochrome *c* into mitochondria: reduction of heme, mediated by NADH and flavin nucleotides, is obligatory for its covalent linkage to apocytochrome *c*. *Proc Natl Acad Sci USA* **86**: 4340–4344.

Ogasawara, H., Hasegawa, A., Kanda, E., Miki, T., Yamamoto, K., and Ishihama, A. (2007) Genomic SELEX search for target promoters under the control of the PhoQP-RstBA signal relay cascade. *J Bacteriol* **189**: 4791–4799.

Okamoto, K., Nomura, T., Fujii, Y., and Yamanaka, H. (1998) Contribution of the disulfide bond of the A subunit to the action of *Escherichia coli* heat-labile enterotoxin. *J Bacteriol* **180**: 1368–1374.

Omasits, U., Ahrens, C.H., Müller, S., and Wollscheid, B. (2014) Protter: interactive protein feature visualization and integration with experimental proteomic data. *Bioinformatics* **30**: 884–886.

Osborne, J., and Gennis, R. (1999) Sequence analysis of cytochrome *bd* oxidase suggests a revised topology for subunit I. *Biochim Biophys Acta - Bioenerg* **1410**: 32–50.

Owens, R.A., and Hartman, P.E. (1986) Export of glutathione by some widely used *Salmonella typhimurium* and *Escherichia coli* strains. *J Bacteriol* **168**: 109–114.

Pacher, P., Beckman, J., and Liaudet, L. (2007) Nitric oxide and peroxynitrite in health

and disease. *Physiol Rev* **87**: 315–424.

Padan, E., and Schuldiner, S. (1994) Molecular physiology of the Na^+/H^+ antiporter in *Escherichia coli*. *J Exp Biol* **196**: 443–456.

Pallen, M., and Matzke, N. (2006) From The origin of species to the origin of bacterial flagella. *Nat Rev Microbiol* **4**: 784–790.

Peek, J.A., and Taylor, R.K. (1992) Characterization of a periplasmic thiol:disulfide interchange protein required for the functional maturation of secreted virulence factors of *Vibrio cholerae*. *Microbiology* **89**: 6210–6214.

Phan, M.D., Peters, K.M., Sarkar, S., Lukowski, S.W., Allsopp, L.P., Gomes Moriel, D., Achard, M. E. S., Totsika, M., Marshall, V. M., Upton, M., Beatson, S., Schembri, M. A. (2013) The serum resistome of a globally disseminated multidrug resistant uropathogenic *Escherichia coli* clone. *PLoS Genet* **9**: 1–18.

Pittman, M.S., Corker, H., Wu, G., Binet, M.B., Moir, A.J.G., and Poole, R.K. (2002) Cysteine is exported from the *Escherichia coli* cytoplasm by CydDC, an ATP-binding cassette-type transporter required for cytochrome assembly. *J Biol Chem* **277**: 49841–9.

Pittman, M.S., Robinson, H.C., and Poole, R.K. (2005) A bacterial glutathione transporter (*Escherichia coli* CydDC) exports reductant to the periplasm. *J Biol Chem* **280**: 32254–61.

Poock, S.R., Leach, E.R., Moir, J.W.B., Cole, J.A., and Richardson, D.J. (2002) Respiratory detoxification of nitric oxide by the cytochrome *c* nitrite reductase of *Escherichia coli*. *J Biol Chem* **277**: 23664–9.

Poole, R., and Hughes, M. (2000) New functions for the ancient globin family: bacterial responses to nitric oxide and nitrosative stress. *Mol Microbiol* **36**: 775–783.

Poole, R. k, Gibson, F., and Wu, G. (1994) The *cydD* gene product, component of a heterodimeric ABC transporter, is required for assembly of periplasmic cytochrome *c* and of cytochrome *bd* in *Escherichia coli*. *FEMS Microbiol Lett* **117**: 217–223.

Poole, R., Williams, H., Downie, A., and Gibson, F. (1989) Mutations affecting the cytochrome *d*-containing oxidase complex of *Escherichia coli* K12: identification and mapping of a fourth locus, *cydD*. *J Gen Microbiol* **135**: 1865–1874.

Poole, R.K., Anjum, M.F., Membrillo-Hernández, J., Kim, S. O., Hughes, M.N., and Stewart, V. (1996) Nitric oxide, nitrite, and Fnr regulation of *hmp* (flavohemoglobin) gene expression in *Escherichia coli* K-12. *J Bacteriol* **178**: 5487–5492.

Poole, R.K., Hatch, L.J., Cleeter, M., Gibson, G., Cox, G., and Wu, G. (1993) Cytochrome *bd* biosynthesis in *Escherichia coli*: the sequences of the *cydC* and *cydD* genes suggest that they encode the components of an ABC membrane transporter. *Mol Microbiol* **10**: 421–430.

Prigent-Combaret, C., Brombacher, E., Vidal, O., Ambert, A., Lejeune, P., Landini, P., and Dorel, C. (2001) Complex regulatory network controls initial adhesion and biofilm formation in *Escherichia coli* via regulation of the *csgD* gene. *J Bacteriol* **183**: 7213–23.

Pullan, S.T., Gidley, M.D., Jones, R. a, Barrett, J., Stevanin, T.M., Read, R.C., Gidley, M. D.,
Jones, R., Barrett, J., Stevanin, T. M., Read, R. C., Green, J., Poole, R. K. (2007) Nitric oxide in chemostat-cultured *Escherichia coli* is sensed by Fnr and other global

regulators: unaltered methionine biosynthesis indicates lack of S-nitrosation. *J Bacteriol* **189**: 1845–55.

Puustinen, A., Finel, M., and Haltia, T. (1991) Properties of the two terminal oxidases of *Escherichia coli*. *Biochemistry* **3**: 3936–3942.

Puustinen, A., and Wikstrom, M. (1991) The heme groups of cytochrome *o* from *Escherichia coli*. **88**: 6122–6126.

Quail, M. a., Dempsey, C.E., and Guest, J.R. (1994) Identification of a fatty acyl responsive regulator (FarR) in *Escherichia coli*. *FEBS Lett* **356**: 183–187.

Rabin, R., and Stewart, V. (1993) Dual response regulators (NarL and NarP) interact with dual sensors (NarX and NarQ) to control nitrate-and nitrite-regulated gene expression in *Escherichia coli* K-12. *J Bacteriol* **175**: 3259–3268.

Rahav-Manor, O., Karpel, R., Taglicht, D., Glaserz, G., Schuldiner, S., and Padan, E. (1992) NhaR, a protein homologous to a family of bacterial regulatory proteins (LysR), regulates *nhaA*, the sodium proton antiporter gene in *Escherichia coli*. *J Biol Chem* **267**: 10433–10438.

Raina, S., and Missiakas, D. (1997) Making and breaking disulfide bonds. *Annu Rev Microbiol* **51**: 179–202.

Rappaport, F., Zhang, J., Vos, M.H., Gennis, R.B., and Borisov, V.B. (2010) Heme-heme and heme-ligand interactions in the di-heme oxygen-reducing site of cytochrome *bd* from *Escherichia coli* revealed by nanosecond absorption spectroscopy. *Biochim Biophys Acta* **1797**: 1657–64.

Rezaïki, L., Cesselin, B., Yamamoto, Y., Vido, K., West, E. van, Gaudu, P., and Gruss, A. (2004) Respiration metabolism reduces oxidative and acid stress to improve long-term survival of *Lactococcus lactis*. *Mol Microbiol* **53**: 1331–42.

Richard, H., and Foster, J.W. (2007) Sodium regulates *Escherichia coli* acid resistance, and influences GadX- and GadW-dependent activation of *gadE*. *Microbiology* **153**: 3154–61.

Riddles, P.W., Blakeley, R.L., and Zerner., B. (1979) Ellman's reagent: 5,59-dithio-(2-nitrobenzoic acid)—a reexamination. *Anal Biochem* **94**: 75–81.

Rietsch, A., and Beckwith, J. (1998) The genetics of disulfide bond metabolism. *Annu Rev Genet* **32**: 163–84.

Rogers, B., Sidjabat, H.E., and Paterson, D.L. (2011) *Escherichia coli* O25b-ST131: a pandemic, multiresistant, community-associated strain. *J Antimicrob Chemother* **66**: 1–14.

Roos, V., Ulett, G.C., Schembri, M.A., and Klemm, P. (2006) The asymptomatic bacteriuria *Escherichia coli* strain 83972 outcompetes uropathogenic *E. coli* strains in human urine. *Infect Immun* **74**: 615–24.

Rothery, R.A., and Ingledew, W.J. (1989) The cytochromes of anaerobically *Escherichia coli*. *J Biochem* **261**: 437–443.

Saiki, K., Mogi, T., and Anraku, Y. (1992) Heme *o* biosynthesis in *Escherichia coli:* the *cyoE* gene in the cytochrome *bo* operon encodes a protoheme IX farnesyltransferase. *Biochem Biophys Res Commun* **189**: 1491–1497.

Salerno, J., Bolgiano, B., and Poole, R. (1990) Heme-copper and heme-heme interactions in the cytochrome *bo*-containing quinol oxidase of *Escherichia coli*. *J Biol*

265: 4364–4368.

Salmond, G.P.C., and Reeves, P.J. (1993) Membrance traffic wardens and protein secretion in Gram-negative bacteria. *Trends Biochem Sci* **18**: 7–12.

Sambrook, J., Fritsch, E.F., and Maniatis., T. (1989) *Molecular cloning: A laboratory manual. Second edition. Volumes 1, 2, and 3. Current protocols in molecular biology. Volumes 1 and 2*. .

Sampaio, M.-M., Chevance, F., Dippel, R., Eppler, T., Schlegel, A., Boos, W., Lu, Y-J., Rock, C. O. (2004) Phosphotransferase-mediated transport of the osmolyte 2-O-alpha-mannosyl-D-glycerate in *Escherichia coli* occurs by the product of the *mngA* (*hrsA*) gene and is regulated by the *mngR* (*farR*) gene product acting as repressor. *J Biol Chem* **279**: 5537–48.

Sansonetti, P.J., Arondel, J., Fontaine, A., D'Hauteville, H., and Bernardini, M.L. (1991) OmpB (osmo-regulation) and *icsA* (cell-to-cell spread) mutants of Shigella flexneri: vaccine candidates and probes to study the pathogenesis of shigellosis. *Vaccine* **9**: 416–422.

Saraste, M., Sibbalda, P.R., and Wittinghoferb, A. (1988) Cytochrome oxidase: Structure, function, and physiopathology. *Ann N Y Acad Sci* **550**: 314–324.

Sarti, P., Giuffré, A., Forte, E., Mastronicola, D., Barone, M.C., and Brunori, M. (2000) Nitric oxide and cytochrome *c* oxidase: mechanisms of inhibition and NO degradation. *Biochem Biophys Res Commun* **274**: 183–7.

Shahzad Asif, H.M., Rolfe, M.D., Green, J., Lawrence, N.D., Rattray, M., and Sanguinetti, G. (2010) TFInfer: A tool for probabilistic inference of transcription factor activities. *Bioinformatics* **26**: 2635–2636.

Shepherd, M. (2015) The CydDC ABC transporter of *Escherichia coli*: new roles for a reductant efflux pump. *Biochem Soc Trans* **43**: 908–912.

Shepherd, M., Heath, M.D., and Poole, R.K. (2007) NikA binds heme : A new role for an *Escherichia coli* periplasmic. *Biochemistry* **46**: 5030–5037.

Shepherd, M., Sanguinetti, G., Cook, G.M., and Poole, R.K. (2010) Compensations for diminished terminal oxidase activity in *Escherichia coli:* cytochrome *bd*-II-mediated respiration and glutamate metabolism. *J Biol Chem* **285**: 18464–72.

Shi, L., Sohaskey, C.D., Kana, B.D., Dawes, S., North, R.J., Mizrahi, V., and Gennaro, M.L. (2005) Changes in energy metabolism of *Mycobacterium tuberculosis* in mouse lung and under *in vitro* conditions affecting aerobic respiration. *Proc Natl Acad Sci* **102**: 15629–15634.

Shimizu, T., Tsutsuki, H., Matsumoto, A., Nakaya, H., and Noda, M. (2012) The nitric oxide reductase of enterohaemorrhagic *Escherichia coli* plays an important role for the survival within macrophages. *Mol Microbiol* **85**: 492–512.

Siegele, D.A., Imlay, K.R.C., and Imlay, J.A. (1996) The stationary phase exit defect of *cydC* (*surB*) mutants is due to the lack of a functional terminal cytochrome oxidase. *J Bacteriol* **178**: 6091–6096.

Sinha, S., Langford, P.R., and Kroll, J.S. (2004) Functional diversity of three different DsbA proteins from Neisseria meningitidis. *Microbiology* **150**: 2993–3000.

Sledjeski, D., and Gottesman, S. (1996) Osmotic shock induction of capsule synthesis in *Escherichia coli* K-12. *J Bacteriol* **178**: 1204–1206.

Smirnova, G., Muzyka, N., and Oktyabrsky, O. (2012) Transmembrane glutathione cycling in growing *Escherichia coli* cells. *Microbiol Res* **167**: 166–72.

Sørensen, M.A., and Pedersen, S. (1991) Cysteine, even in low concentrations, induces transient amino acid starvation in *Escherichia coli*. *J Bacteriol* **173**: 5244–5246.

Spinner, F., Cheesman, M., Thomson, A., Kaysser, T., Gennis, R., Peng, Q., and Peterson, J. (1995) The haem *b558* component of the cytochrome *bd* quinol oxidase complex from *Escherichia coli* has histidine-methionine axial ligation. *J Biochem* **308**: 641–644.

Spiro, S. (2006) Nitric oxide-sensing mechanisms in *Escherichia coli*. *Biochem Soc Trans* **34**: 200–202.

Squires, C., Lee, F., and Yanofsky, C. (1975) Interaction of the trp repressor and RNA polymerase with the *trp* operon. *J Mol Biol* **92**: 93–111.

Stafford, G.P., Ogi, T., and Hughes, C. (2005) Binding and transcriptional activation of non-flagellar genes by the *Escherichia coli* flagellar master regulator FlhD2C2. *Microbiology* **151**: 1779–1788.

Stafford, S.J., Humphreys, D.P., and Lund, P.A. (1999) Mutations in *dsbA* and *dsbB*, but not dsbC, lead to an enhanced sensitivity of *Escherichia coli* to Hg^{2+} and Cd^{2+}. *FEMS Microbiol Lett* **174**: 179–184.

Stamler, J.S., Simon, D.I., Osborne, J.A., Mullins, M.E., Jarakit, O., Michel, T., Singel, D. J.

Loscalzo, J. (1992) S-Nitrosylation of proteins with nitric oxide : Synthesis and characterization of biologically active compounds. *Proc Natl Acad Sci USA* **89**: 444–448.

Stamler, J.S., Singel, D.J., and Loscalzo, J. (1992) Biochemistry of nitric oxide and redox-activated forms. *Science (80-)* **258**: 1898–1902.

Stenberg, F., Heijne, G. von, and Daley, D.O. (2007) Assembly of the cytochrome *bo3* complex. *J Mol Biol* **371**: 765–73.

Stoyanov, J. V, Magnani, D., and Solioz, M. (2003) Measurement of cytoplasmic copper, silver, and gold with a lux biosensor shows copper and silver, but not gold, efflux by the CopA ATPase of *Escherichia coli*. *FEBS Lett* **546**: 391–394.

Stuehr, D.J. (1999) Mammalian nitric oxide synthases. *Biochim Biophys Acta - Bioenerg* **1411**: 217–230.

Sturr, M.G., Krulwich, T.A., and Hicks, D.B. (1996) Purification of a cytochrome *bd* terminal oxidase encoded by the *Escherichia coli app* locus from a delta *cyo* delta *cyd* strain complemented by genes from *Bacillus firmus* OF4. *J Bacteriol* **178**: 1742–1749.

Sun, J., Kahlow, M., Kaysser, T., and Osborne, J. (1996) Resonance Raman spectroscopic identification of a histidine ligand of *b595* and the nature of the ligation of chlorin *d* in the fully reduced *Escherichia coli* cytochrome. *Biochemistry* **35**: 2403–2412.

Suzuki, H., Hashimoto, W., and Kumagai, H. (1993) *Escherichia coli* K-12 can utilize an exogenous gamma-glutamyl peptide as an amino acid source, for which gamma-glutamyltranspeptidase is essential. *J Bacteriol* **175**: 6038–6040.

Suzuki, H., Kamatani, S., Kim, E.S., and Kumagai, H. (2001) Aminopeptidases A, B, and N and dipeptidase D are the four cysteinylglycinases of *Escherichia coli* K-12. *J*

Bacteriol **183**: 1489–1490.

Suzuki, H., Koyanagi, T., Izuka, S., Onishi, A., and Kumagai, H. (2005) The *yliA, -B, -C,* and *-D* genes of *Escherichia coli* K-12 encode a novel glutathione importer with an ATP-binding cassette. *J Bacteriol* **187**: 5861–7.

Suzuki, H., Kumagai, H., and Tochikura, T. (1987) Isolation, genetic mapping, and characterization of *Escherichia coli* K-12 mutants lacking gamma-glutamyltranspeptidase. *J Bacteriol* **169**: 3926–3931.

Tamegai, H., Kawano, H., Ishii, A., Chikuma, S., Nakasone, K., and Kato, C. (2005) Pressure-regulated biosynthesis of cytochrome *bd* in piezo- and psychrophilic deep-sea bacterium *Shewanella violacea* DSS12. *Extremophiles* **9**: 247–53.

Thanassi, D.G., and Hultgren, S.J. (2000) Assembly of complex organelles: pilus biogenesis in Gram-negative bacteria as a model system. *Methods* **20**: 111–126.

Thony-meyer, L., and Kunzler, P. (1997) Translocation to the periplasm and signal sequence cleavage of preapocytochrome *c* depend on *sec* and *lep*, but not on the *ccm* gene products. *Eur J Biochem* **246**: 794–799.

Todorovic, S., Justino, M.C., Wellenreuther, G., Hildebrandt, P., Murgida, D.H., Meyer-Klaucke, W., and Saraiva, L.M. (2008) Iron-sulfur repair YtfE protein from *Escherichia coli*: structural characterization of the di-iron center. *J Biol Inorg Chem* **13**: 765–70.

Totsika, M., Beatson, S. a, Sarkar, S., Phan, M.-D., Petty, N.K., Bachmann, N., Szubert, M., Sidjabat, H. E., Paterson, D. L., Upton, M., Schembri, M. (2011) Insights into a multidrug resistant *Escherichia coli* pathogen of the globally disseminated ST131 lineage: genome analysis and virulence mechanisms. *PLoS One* **6**: 1–11.

Totsika, M., Heras, B., Wurpel, D.J., and Schembri, M.A. (2009) Characterization of two homologous disulfide bond systems involved in virulence factor biogenesis in uropathogenic *Escherichia coli* CFT073. *J Bacteriol* **191**: 3901–3908.

Totsika, M., Kostakioti, M., Hannan, T.J., Upton, M., Beatson, S. a, Janetka, J.W., Hultgren, S. J., Schembri, M. A. (2013) A FimH inhibitor prevents acute bladder infection and treats chronic cystitis caused by multidrug-resistant uropathogenic *Escherichia coli* ST131. *J Infect Dis* **208**: 921–8.

Truong, Q.L., Cho, Y., Barate, A.K., Kim, S., and Hahn, T.-W. (2014) Characterization and protective property of *Brucella abortus cydC* and *looP* mutants. *Clin vaccine Immunol* **21**: 1573–80.

Tseng, C.P., Albrecht, J., Gunsalus, R.P., Tseng, C., and Albrecht, J. (1996) Effect of microaerophilic cell growth conditions on expression of the aerobic (*cyoABCDE* and *cydAB*) and anaerobic (*narGHJI*, *frdABCD*, and *dmsABC*) respiratory pathway genes in *Escherichia coli*. *J Bacteriol* **178**: 1094–1098.

Tucker, N., and D'autreaux, B. (2004) DNA binding activity of the *Escherichia coli* nitric oxide sensor NorR suggests a conserved target sequence in diverse proteobacteria. *J Bacteriol* **186**: 6656–6660.

Turner, a. K., Barber, L.Z., Wigley, P., Muhammad, S., Jones, M. a., Lovell, M. A., Hulme, S., Barrow, P. A. (2003) Contribution of proton-translocating proteins to the virulence of *Salmonella enterica Serovars Typhimurium, Gallinarum*, and *Dublin* in chickens and mice. *Infect Immun* **71**: 3392–3401.

Ueguchil, C., and Mizuno, T. (1993) The *Escherichia coli* nucleoid protein H-NS

functions directly as a transcriptional repressor. *EMBO J* **12**: 1039–1046.

Unden, G., Becker, S., Bongaerts, J., and Six, S. (1995) O2-sensing and O2-dependent gene-regulation in facultatively anaerobic bacteria. *Arch Microbiol* **164**: 81–90.

VanOrsdel, C.E., Bhatt, S., Allen, R.J., Brenner, E.P., Hobson, J.J., Jamil, A., Haynes, B. M.
Genson, A. M., Hemm, M. R. (2013) The *Escherichia coli* CydX protein is a member of the CydAB cytochrome *bd* oxidase complex and is required for cytochrome *bd* oxidase activity. *J Bacteriol* **195**: 3640–50.

Vicente, J.B., Scandurra, F.M., Rodrigues, J. V, Brunori, M., Sarti, P., Teixeira, M., and Giuffrè, A. (2007) Kinetics of electron transfer from NADH to the *Escherichia coli* nitric oxide reductase flavorubredoxin. *FEBS J* **274**: 677–86.

Vicente, J.B., and Teixeira, M. (2005) Redox and spectroscopic properties of the *Escherichia coli* nitric oxide-detoxifying system involving flavorubredoxin and its NADH-oxidizing redox partner. *J Biol Chem* **280**: 34599–608.

Vine, C.E., and Cole, J.A. (2011) Nitrosative stress in *Escherichia coli:* reduction of nitric oxide. *Biochem Soc Trans* **39**: 213–5.

Vos, M., Borisov, V., Liebl, U., Martin, J., and Konstantinov, A. (2000) Femtosecond resolution of ligand-heme interactions in the high-affinity quinol oxidase *bd*: A di-heme active site? *Proc Natl Acad Sci* **97**: 1554–1559.

Ward, A., Reyes, C.L., Yu, J., Roth, C.B., and Chang, G. (2007) Flexibility in the ABC transporter MsbA: Alternating access with a twist. *Proc Natl Acad Sci U S A* **104**: 19005–10.

Watmough, N.J., Butland, G., Cheesman, M.R., Moir, J.W.B., Richardson, D.J., and Spiro, S. (1999) Nitric oxide in bacteria: synthesis and consumption. *Biochim Biophys Acta - Bioenerg* **1411**: 456–474.

Way, S.S., Borczuk, A.C., and Goldberg, M. (1999) Adaptive immune response to *Shigella flexneri* 2a *cydC* in Immunocompetent mice and mice lacking immunoglobulin A. *Infect Immun* **67**: 2001–2004.

Way, S.S., Sallustio, S., Magliozzo, R.S., and Goldberg, M.B. (1999) Impact of either elevated or decreased levels of cytochrome *bd* expression on *Shigella flexneri* virulence. *J Bacteriol* **181**: 1229–1237.

Welch, R.A., Burland, V., Iii, G.P., Redford, P., Roesch, P., Rasko, D., Redford, P., Buckles, E. L., Liou, S., Boutin, A., Hackett, J., Stroud, D., Mayhew, G F., Rose, D J., Zhou, S., Schwartz, D. C., Perna, N. T., Mobley, H. L. T. (2002) Extensive mosaic structure revealed by the complete genome sequence of uropathogenic *Escherichia coli. Proc Natl Acad Sci* **99**: 17020–17024.

Wiriyathanawudhiwong, N., Ohtsu, I., Li, Z.-D., Mori, H., and Takagi, H. (2009) The outer membrane TolC is involved in cysteine tolerance and overproduction in *Escherichia coli. Appl Microbiol Biotechnol* **81**: 903–913.

Wonderen, J.H. van, Burlat, B., Richardson, D.J., Cheesman, M.R., and Butt, J.N. (2008) The nitric oxide reductase activity of cytochrome *c* nitrite reductase from *Escherichia coli*. *J Biol Chem* **283**: 9587–94.

Woodford, N., Reddy, S., Fagan, E.J., Hill, R.L.R., Hopkins, K.L., Kaufmann, M.E., Kistler, J., Palepou, M-F. I., Pike, R., Ward, M. E., Cheesbrough, J., Livermore, D. M. (2007) Wide geographic spread of diverse acquired AmpC beta-lactamases among

Escherichia coli and *Klebsiella spp.* in the UK and Ireland. *J Antimicrob Chemother* **59**: 102–5.

Wullt, B., Bergsten, G., Connell, H., Röllano, P., Gebretsadik, N., Hull, R., and Svanborg, C. (2000) P fimbriae enhance the early establishment of *Escherichia coli* in the human urinary tract. *Mol Microbiol* **38**: 456–464.

Yamada, S., Awano, N., Inubushi, K., Maeda, E., Nakamori, S., Nishino, K., Yamaguchi, A., Takagi, H. (2006) Effect of drug transporter genes on cysteine export and overproduction in *Escherichia coli*. *Appl Environ Microbiol* **72**: 4735–4742.

Yamamoto, K., Hirao, K., Oshima, T., Aiba, H., Utsumi, R., and Ishihama, A. (2005) Functional characterization *in vitro* of all two-component signal transduction systems from *Escherichia coli*. *J Biol Chem* **280**: 1448–56.

Yamamoto, K., and Ishihama, A. (2005) Transcriptional response of *Escherichia coli* to external copper. *Mol Microbiol* **56**: 215–27.

Yamamoto, Y., Poyart, C., Trieu-Cuot, P., Lamberet, G., Gruss, A., and Gaudu, P. (2005) Respiration metabolism of Group B Streptococcus is activated by environmental haem and quinone and contributes to virulence. *Mol Microbiol* **56**: 525–34.

Yamashita, M., Shepherd, M., Booth, W.I., Xie, H., Postis, V., Nyathi, Y., Tzokov, S. B., Poole, R. K., Baldwin, S., Bullough, P. (2014) Structure and function of the bacterial heterodimeric ABC transporter CydDC: stimulation of ATPase activity by thiol and heme compounds. *J Biol Chem* **289**: 23177–88.

Yu, H., Sato, E.F., Nagata, K., Nishikawa, M., Kashiba, M., Arakawa, T., Kobayashi, K., Tamura, T., Inoue, M. (1997) Oxygen-dependent regulation of the respiration and growth of *Escherichia coli* by nitric oxide. *FEBS Lett* **409**: 161–165.

Yu, J., Edwards-Jones, B., Neyrolles, O., and Kroll, J.S. (2000) Key role for DsbA in cell-to-cell spread of *Shigella flexneri*, permitting secretion of Ipa proteins into interepithelial protrusions. *Infect Immun* **68**: 6449–6456.

Yu, J., Webb, H., and Hirst, T. (1992) A homologue of the *Escherichia coli* DsbA protein involved in disulphide bond formation is required for enterotoxin biogenesis in *Vibrio cholerae*. *Mol Microbiol* **6**: 1949 –1958.

Zhang, J., Hellwig, P., Osborne, J.P., and Gennis, R.B. (2004) Arginine 391 in subunit I of the cytochrome *bd* quinol oxidase from *Escherichia coli* stabilizes the reduced form of the hemes and is essential for quinol oxidase activity. *J Biol Chem* **279**: 53980–7.

Zhang, H. Z. & Donnenberg, M.S. (1996) DsbA is required for stability of the type IV pilin of enteropathogenic *Escherichia coli*. *Mol Microbiol* **21**: 787–797.

Zhao, G., Ceci, P., Ilari, A., Giangiacomo, L., Laue, T.M., Chiancone, E., and Chasteen, N.D. (2002) Iron and hydrogen peroxide detoxification properties of DNA-binding protein from starved cells. A ferritin-like DNA-binding protein of *Escherichia coli*. *J Biol Chem* **277**: 27689–96.

Zhou, Y., Larson, J.D., Bottoms, C. a, Arturo, E.C., Henzl, M.T., Jenkins, J.L., Nix, J. C.,
Becker, D. F.,Tanner, J. J. (2008) Structural basis of the transcriptional regulation of the proline utilization regulon by multifunctional PutA. *J Mol Biol* **381**: 174–88.

Zhou, Z., White, K. a., Polissi, A., Georgopoulos, C., and Raetz, C.R.H. (1998) Function of *Escherichia coli* MsbA, an essential ABC family transporter, in lipid A and phospholipid Biosynthesis. *J Biol Chem* **273**: 12466–12475.

Zumft, W. (1997) Cell biology and molecular basis of denitrification. *Microbiol Mol Biol Rev* **61**: 533–616.

Appendix

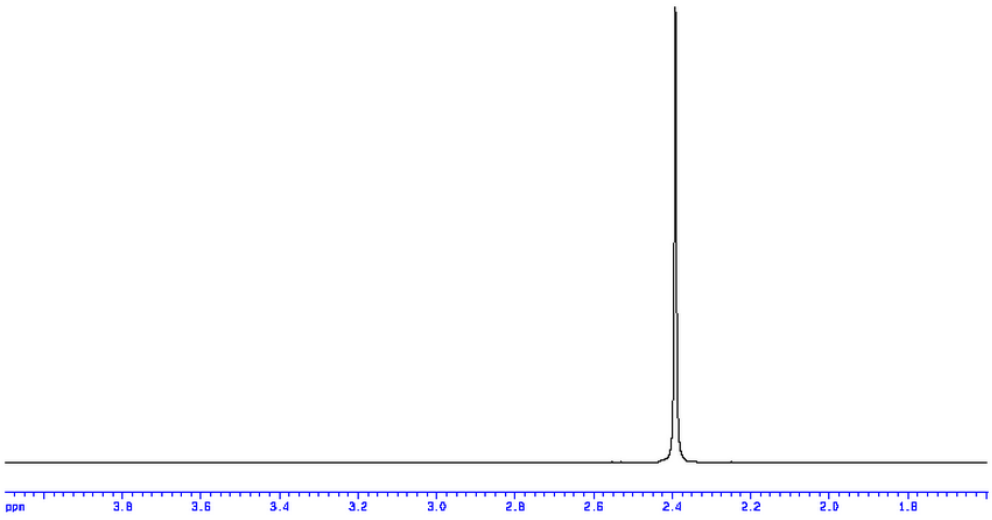

Appendix A-1. Reference 1D-^{1}H NMR data for succinate

Taken from the Madison metabolite consortium database website. The 1D-^{1}H NMR data for succinate standard produces a single peak at a chemical shift of 2.4, similar to that seen in NMR data for wild type but not *cydD* derived metabolites.

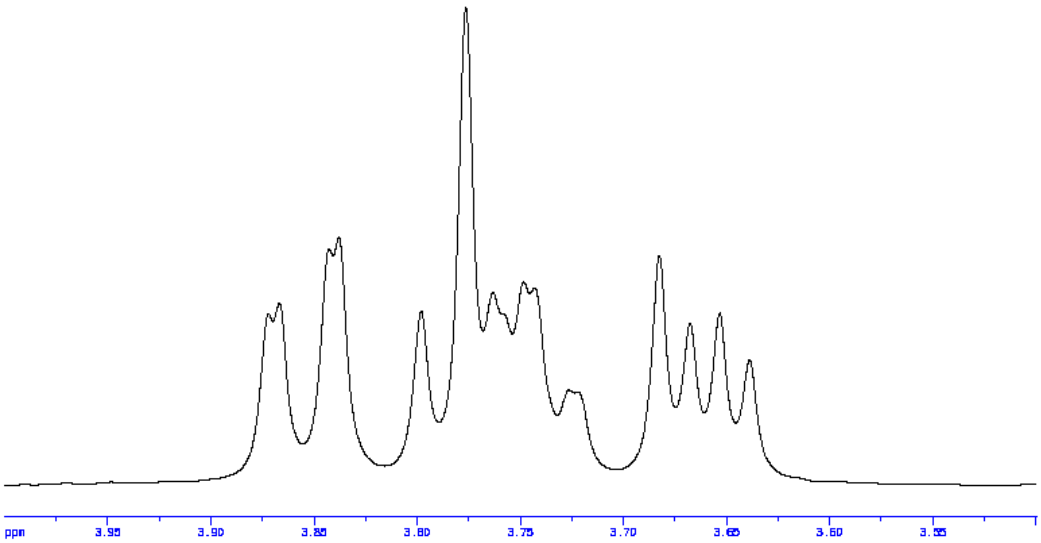

Appendix A-2. Reference 1D-^{1}H NMR data for D-mannitol

Taken from the Madison metabolite consortium database website. The 1D-^{1}H NMR data for D-mannitol produces a large peak at a chemical shift around 3.75 with other smaller peaks surrounding it, this is similar to that seen in NMR data for wild type but not *cydD* derived metabolites.

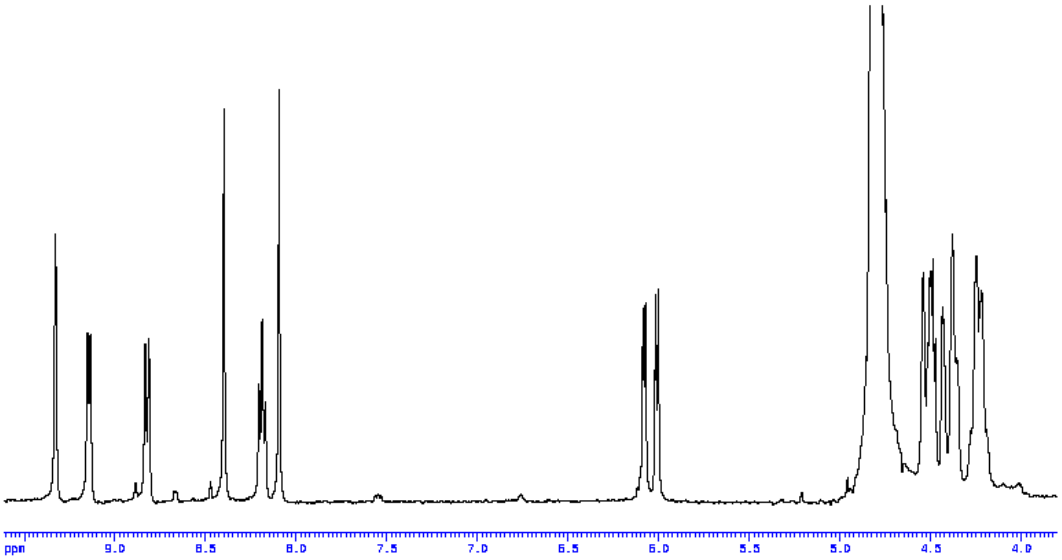

Appendix A-3. Reference 1D-^{1}H NMR data for NAD

Taken from the Madison metabolite consortium database website.

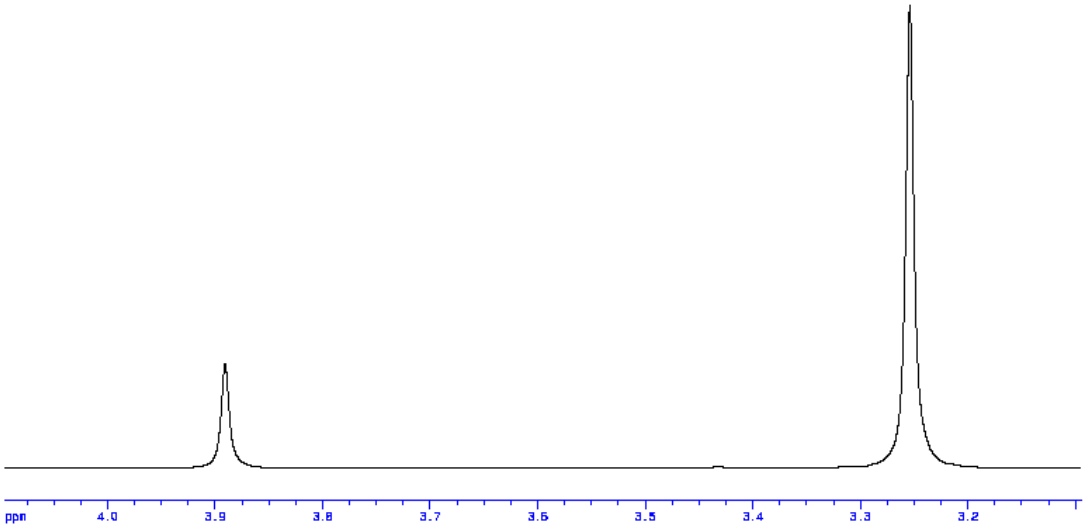

Appendix A-4 Reference 1D-^{1}H NMR data for betaine

Taken from the Madison metabolite consortium database website. The 1D-^{1}H NMR data for betaine standard produces a large peak at a chemical shift of around 3.27, similar to that seen in NMR data for *cydD* but not wild type derived metabolites.

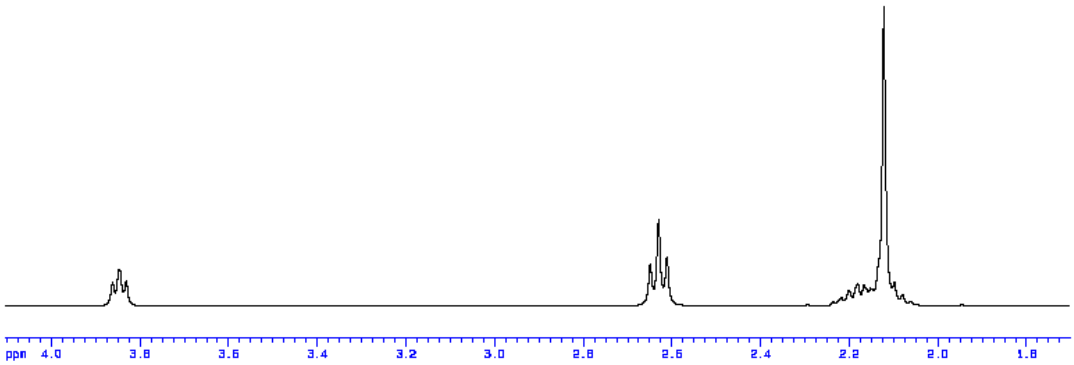

Appendix A-5. Reference 1D-^{1}H NMR data for L-methionine

The 1D-^{1}H NMR data for methionine standard produces a large peak at a chemical shift of around 2.15, similar to that seen in NMR data for *cydD* but not wild type derived metabolites. Taken from the Madison metabolite consortium database website.

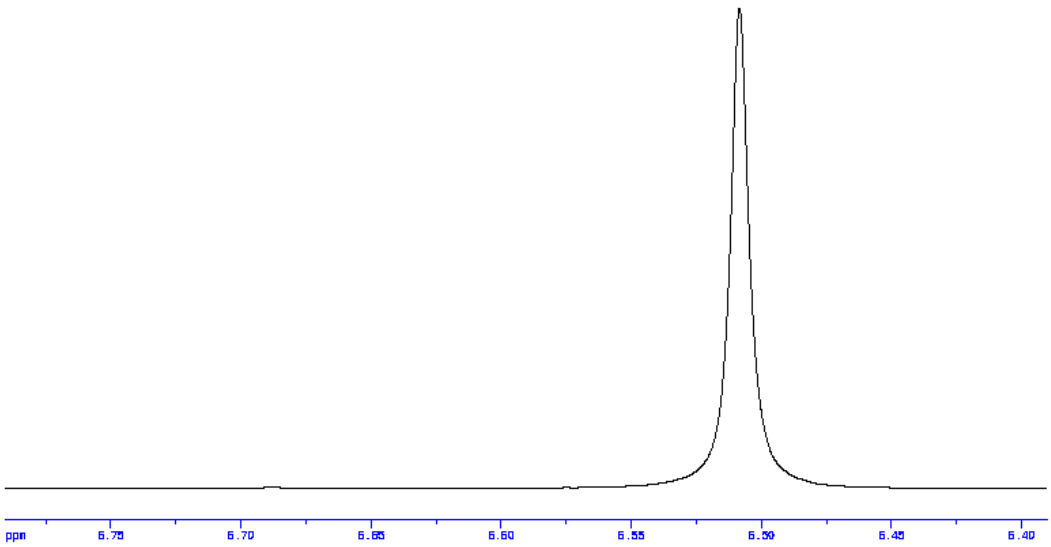

Appendix A-6 Reference 1D-^{1}H NMR data for fumarate

Taken from the Madison metabolite consortium database website. The 1D-^{1}H NMR data for fumarate standard produces a single peak at a chemical shift around 6.5.

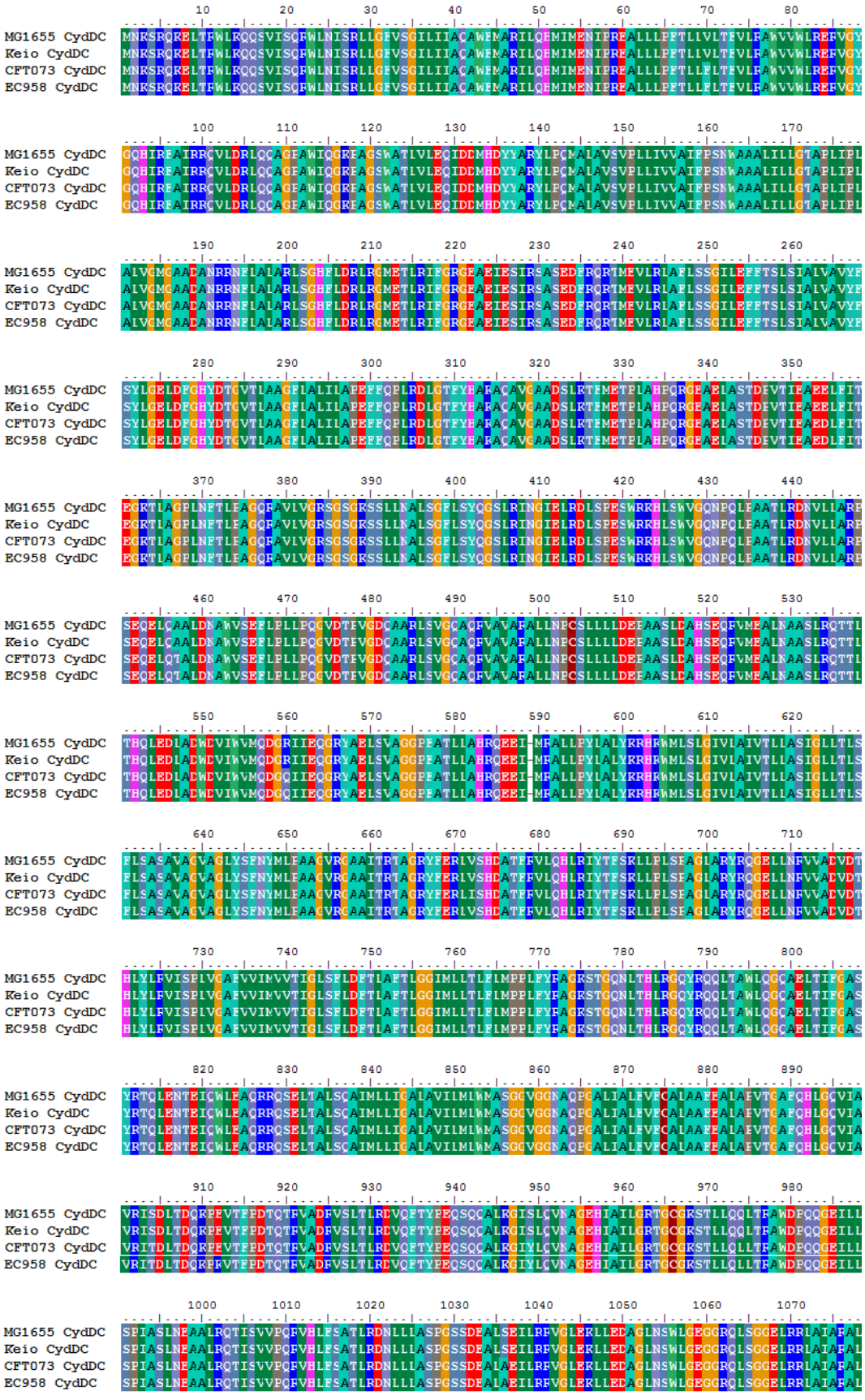
MG1655 CydDC
Keio CydDC
CFT073 CydDC
EC958 CydDC

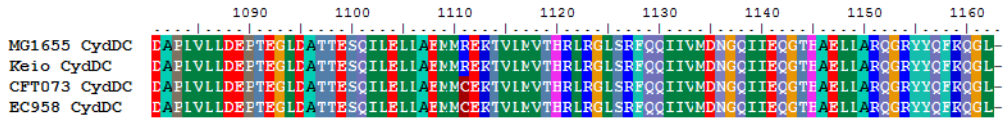

Appendix C-1. CydD and CydC amino acids sequences compared between non-pathogenic *E. coli* and two UPEC strains

Alignment of CydD and CydC amino acid sequences taken from non-pathogenic MG1655 and Keio strains, compared to UPEC strains EC958 and CFT073. Sequences were aligned using Bioedit free software (v7.2.5). Amino acids are coloured to allow differences in amino acid sequence to be easily visualised.

A

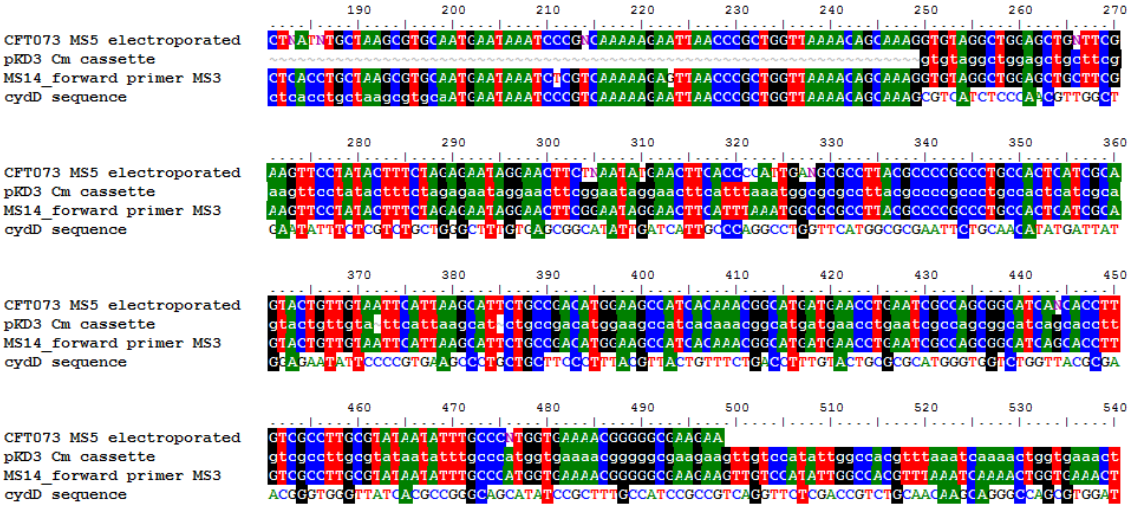

B

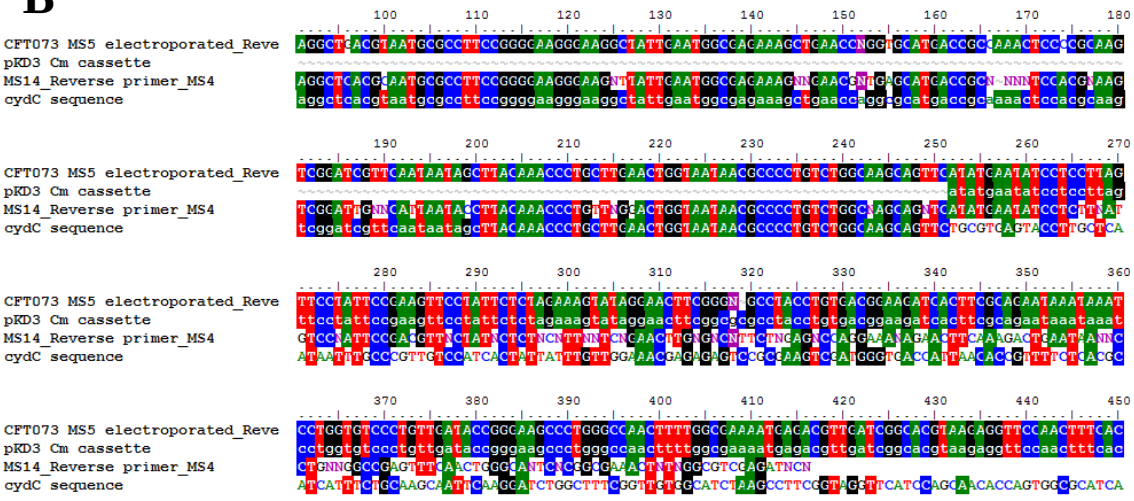

Appendix C-2. Sequencing data for CFT073 *cydDC*

After λ-Red mutagenesis of a wild type CFT073 strain (MS5) to replace the *cydDC* operon with a chloramphenicol cassette, a resultant colony was sent for sequencing to confirm the replacement. Here the sequences in order show that of sequencing data for the resultant CFT073 electroporation colony to be tested (CFT073 MS5 electroporated), the sequence of pKD3, the original source of the chloramphenicol resistance cassette, the sequencing data of MG1655 *cydDC*::Cm (MS14) and the start of *cydD* or end of *cydC*. Sequencing data that used **A** primer 3 (forward) or **B** primer 4 (reverse) was aligned (using Bioedit v7.2.5) to show that 50bp into the *cydD* gene of the electroporation strain (position 250 **A**), the chloramphenicol gene starts and 50bp inwards from the end of *cydC* (position 250 **B**) the Cm cassette ends. This data concludes that in the electroporated strain designated MS115, the *cydDC* operon has successfully been replaced by the Cm resistance cassette creating a *cydDC* knockout mutation in a CFT073 background.

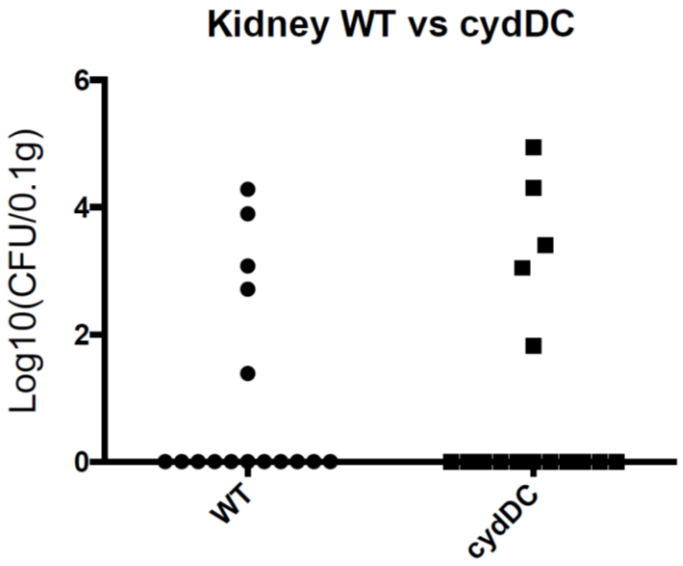

Appendix C-3. CFU isolated from mouse kidney

In this model of infection and the time frame used, we would not expect to see bacteria within the kidneys, and the presence of bacteria is likely to suggest that the catheter had been placed too far into the urethra. The presence of bacteria was tested by counting CFU isolated from the kidneys of infected mice. Here the Log_{10} number of wild type (circles) and *cydDC* mutant (squares) CFU for each mouse is represented.